Deciphering *Staphylococcus aureus* WTA interactions

Dissertation

der Mathematisch-Naturwissenschaftlichen Fakultät
der Eberhard Karls Universität Tübingen
zur Erlangung des Grades eines
Doktors der Naturwissenschaften
(Dr. rer. nat.)

vorgelegt von
Esther Lehmann
aus Heilbronn

Tübingen
2023

Gedruckt mit Genehmigung der Mathematisch-Naturwissenschaftlichen Fakultät der Eberhard Karls Universität Tübingen.

Tag der mündlichen Qualifikation:	14.06.2023
Dekan:	Prof. Dr. Thilo Stehle
1. Berichterstatter/-in:	Prof. Dr. Andreas Peschel
2. Berichterstatter/-in:	Prof. Dr. Friedrich Götz

Meiner Herde

"Mischief Managed!" – Harry Potter; J.K. Rowling

Table of Contents

TABLE OF CONTENTS

Summary

The opportunistic pathogen *Staphylococcus aureus* is highly prevalent in the human population. Due to frequent development of antimicrobial resistance, *S. aureus* infections become increasingly hard to treat. Furthermore, all efforts to develop a protective *S. aureus*-vaccine have failed so far. *S. aureus* secondary cell wall glycopolymers (SCWGs), namely wall teichoic acid (WTA) and capsular polysaccharide (CP), are known virulence factors. Both contribute to host adaptation and antimicrobial resistance and have been investigated as potential vaccine candidates.

As such, this thesis focusses mainly on the role of *S. aureus* WTA as virulence factor and the impact of CP expression on WTA functions. We demonstrated that expression of an *S. aureus*-type WTA by a several *Staphylococcus epidermidis* lineages allows for phage-mediated horizontal gene transfer between the two species, highlighting the central role of the *S. aureus* phage-receptor WTA for cross-species interaction. Interestingly, by this extend WTA not only potentially shapes phage-mediated microbiome interactions but also *S. aureus* host adaptation, as phage acquisition has been implicated in host jump and adaptation from livestock to humans.

Both colonization and infection by *S. aureus* depend on bacterial adhesion to the respective tissue, and *S. aureus* WTA was previously shown to act as a glycopolymer adhesin. We describe LOX-1 as novel receptor for *S. aureus* WTA on endothelial cells, and thereby add to a small but growing number of molecular interaction partners of *S. aureus* WTA on the human host. We present evidence that the impact of WTA on cell adhesion has so far been underestimated relative to the influence of proteinaceous adhesion factors. As such, we are only beginning to understand the multiple roles of *S. aureus* WTA in host colonization and pathogenicity during infections.

Based on their biosynthetic pathways and function in pathogenesis, it has long been proposed that there might be a necessity to coordinate the expression of the two SCWGs WTA and CP. Until now, this coordinated expression was only speculated to take place, based on the opposing virulence mechanisms of WTA and CP. We collected evidence for indirect functional interaction in the form of WTA masking through expression of CP. Therefore, WTA-CP interaction might have implications for all aspects of WTA-mediated virulence.

This thesis provides fundamental insights into *S. aureus* SCWG biology and highlights a gap in our understanding of glycan-glycan interactions that might underlie our still lacking comprehension of the behavior and adaptability of this important pathogen.

Zusammenfassung

Der opportunistische Krankheitserreger *Staphylococcus aureus* ist sehr prävalent innerhalb der menschlichen Bevölkerung und aufgrund zunehmender Antibiotikaresistenzen sind Infektionen mit *S. aureus* zunehmend schwerer zu behandeln. Erschwerend kommt hinzu, dass bislang alle Bemühungen einen wirksamen Impfstoff gegen *S. aureus* zu entwickeln gescheitert sind. Die sekundären Zellwandglykopolymere (SZWG) von *S. aureus*, die Wandteichosäure (WTA) und das Kapselpolysaccharid (KP), sind wichtige Virulenzfaktoren von *S. aureus*. Beide tragen zur Wirtsanpassung und antimikrobiellen Resistenz bei und wurden als potenzielle Impfstoffkandidaten untersucht.

Die vorliegende Arbeit konzentriert sich hauptsächlich auf die Rolle von *S. aureus* WTA als Virulenzfaktor und die Auswirkungen der KP-Expression auf WTA-Funktionen. Wir konnten zeigen, dass die Expression von *S. aureus*-typischer WTA, durch verschiedene *Staphylococcus epidermidis* Stämme, Phagen vermittelten horizontalen Gentransfer zwischen den beiden Spezies ermöglicht. Dies verdeutlicht die zentrale Rolle des *S. aureus* Phagenrezeptors WTA, für die speziesübergreifende Interaktion. Interessanterweise beeinflusst WTA nicht nur die durch Phagen vermittelten Interaktion zwischen *S. aureus* und dem Microbiom, sondern auch die Anpassung von *S. aureus* an den Wirt. Der Erwerb von Phagen trägt in vielen Fällen zur Wirtsanpassung wie z.B. der Übertragung von *S. aureus* zwischen Vieh und dem Menschen bei.

Des Weiteren hängen sowohl die Kolonisierung als auch die Infektion durch *S. aureus* von der Adhäsion der Bakterien an das jeweilige Gewebe ab. Es wurde bereits gezeigt, dass *S. aureus* WTA als Glykopolymer-Adhäsin fungiert. Mit LOX-1 haben wir einen neuen Witrszellrezeptor für *S. aureus* WTA auf Endothelzellen und somit einen neuen molekularen Interaktionspartnern der *S. aureus* WTA beschrieben. Wir legen Beweise dafür vor, dass der Einfluss von WTA auf die Zelladhäsion im Vergleich zum Einfluss proteinartiger Adhäsionsfaktoren bisher unterschätzt wurde. Dies unterstreicht, dass die vielfältigen Rollen von *S. aureus* WTA bei der Kolonisierung des Wirts sowie der Pathogenitätsentwicklung noch nicht hinreichend verstanden sind.

Auf der Grundlage ihrer Biosynthesewege und ihrer teilweise gegensätzlichen Funktion für die Pathogenese wurde eine mögliche Koordination der Expression von WTA und KP vermutet. Wir haben zum ersten Mal systematisch den Einfluss der KP-Expression auf WTA abhängige Prozesse untersucht und konnten zeigen, dass die Funktionalität der WTA negativ mit der KP-Expression korreliert. Somit hat die funktionelle Interaction von WTA und KP potenziell Auswirkungen auf alle Aspekte der WTA-vermittelten Virulenz.

Diese Arbeit bietet grundlegende Einblicke in die Biologie von *S. aureus* SZWG und offenbart eine Lücke in unserem Verständnis der Interaktionen von Polysacchariden. Wissen über diese

Grundlegenden Zusammenhänge ist maßgebend, da es uns Einblicke in die Anpassungsfähigkeit dieses wichtigen Erregers ermöglicht und somit potenziell neue Behandlungsmöglichkeiten eröffnet.

List of publications

Chapter I

***Staphylococcus epidermidis* clones express *Staphylococcus aureus*-type wall teichoic acid to shift from a commensal to pathogen lifestyle.**

Du X, Larsen J, Li M, Walter A, Slavetinsky C, Both A, Sanchez Carballo PM, Stegger M, Lehmann E, Liu Y, Liu J, Slavetinsky J, Duda KA, Krismer B, Heilbronner S, Weidenmaier C, Mayer C, Rohde H, Winstel V, Peschel A.

Nat Microbiol. 2021 Jun;6(6):757-768. doi: 10.1038/s41564-021-00913-z.
Epub 2021 May 24. PMID: 34031577.

Chapter II

Influence of *Staphylococcus aureus* Strain Background on Sa3int Phage Life Cycle Switches.

Rohmer C, Dobritz R, Tuncbilek-Dere D, Lehmann E, Gerlach D, George SE, Bae T, Nieselt K, Wolz C.

Viruses. 2022 Nov 8;14(11):2471. doi: 10.3390/v14112471.
PMID: 36366569; PMCID: PMC9694928.

Chapter III

Wall teichoic acids mediate *Staphylococcus aureus* binding to scavenger receptor LOX-1 on endothelial cells.

Slavetinsky J, Lehmann E, Slavetinsky C, Gritsch L, van Dalen R, Bleul L, Kretschmer D, Wolz C, Weidenmaier C, Peschel A.

Manuscript ready for submission

Chapter IV

Capsular polysaccharides obstruct the function of wall-teichoic acid in *Staphylococcus aureus*

Lehmann E, van Dalen R, Gritsch L, Slavetinsky C, Korn N, Rohmer C, Peschel A, Weidenmaier C, Wolz C.

Manuscript ready for submission

Personal contribution to publications

Accepted publications

***Staphylococcus epidermidis* clones express *Staphylococcus aureus*-type wall teichoic acid to shift from a commensal to pathogen lifestyle.**

I contributed by performing cell culture experiments and microscopic analysis.

Influence of *Staphylococcus aureus* Strain Background on Sa3int Phage Life Cycle Switches.

I contributed to methodology and performed assays to analyse differential phage adsorption.

Manuscripts ready for submission

Wall teichoic acids mediate *Staphylococcus aureus* binding to scavenger receptor LOX-1 on endothelial cells.

I contributed to conception and design of experiment as well as analysis and interpretation of the data. I generated the complementation USA300 JE2 Δ*tagO* p*tagO* and performed adhesion experiments in CHO-k1 and CHO-LOX-1. I supervised adhesion experiments in HUVECs and contributed to manuscript writing and editing. I designed the figures.

Capsular polysaccharides obstruct the function of wall-teichoic acid in *Staphylococcus aureus*

I conceptualized the project. I designed and analysed the experiments and interpreted the data. In addition to pre-experiments for the phage adsorption and cell adhesion experiments, I performed antibody deposition assays, and the mouse skin abscess formation model and generated the USA300 JE2 srtA::erm mutant. I supervised and analysed all experiments not directly performed by myself. I wrote the ethical application for the performed animal experiments in consultation with C. Wolz and S. Heilbronner. The manuscript was written and edited by me in consultation with C. Wolz. I designed the figures.

I conceptualized this project as basis for my application for a "Promotionsstipendium nach Landesgraduiertenförderungsgesetz" to fund the first two-years of my PhD (and of this project).

General Introduction

Staphylococcus aureus, a member of the ESKAPE group

The discovery of antibiotics to treat bacterial infections in 1928 lead to a sharp decrease in lethality worldwide and kickstarted the “golden age” of antibiotics (Sakai and Morimoto 2022). They became essential to modern medicine in their use to prevent or treat bacterial infections. However, antibiotic use is challenged by the emergence of antibiotic-resistant bacteria (Mulani et al. 2019; Ventola 2015). To still be able to treat bacterial infections in the future, modern medical research must find new strategies to combat and overcome antibiotic resistance.

The so-called ESKAPE group is comprised of the six highly virulent and antibiotic resistant bacterial pathogens: *Enterococcus faecium*, *Staphylococcus aureus*, *Klebsiella pneumoniae*, *Acinetobacter baumannii*, *Pseudomonas aeruginosa*, and *Enterobacter spp* (Rice 2008). All ESKAPE members are highly clinically relevant as they ‘escape’ or evade classical antimicrobial treatment due to frequent development of multi-drug resistance (MDR) (Navidinia 2016; David M. P. De Oliveira 2020; WHO-ECDC 2022).

Aside from the search for new antibiotics, there are other important measures to combat hard-to-treat infections by MDR pathogens in the future (Wojcik-Bojek, Rozalska, and Sadowska 2022; Mulani et al. 2019; Ma et al. 2020). These measures can be assigned to the two main categories of disease prevention and immune prophylaxis (Wojcik-Bojek, Rozalska, and Sadowska 2022). This introduction will focus on the ESKAPE pathogen *S. aureus*.

S. aureus is an asymptomatic colonizer of approximately 30% of the human population (Williams 1963; Lowy 1998; Wertheim et al. 2005), with the nares (Noble 1967; Melissa D. Sanford 1994) and the gut (Acton et al. 2009; Senn et al. 2016; Gipson et al. 2020) being considered the primary reservoirs. At the same time, as an opportunistic pathogen, *S. aureus* is one of the most ubiquitously found ESKAPE members in nosocomial infections (Sabat et al. 2021).

S. aureus is the most prevalent isolate from patients with endovascular infections (Kourtis 2019; van Hal et al. 2012). These blood stream infections frequently disseminate into other organs, causing subsequent acute or chronic infections of any organ system. High incidence of treatment failure and lethality can partially be assigned to fast MDR development as well as an unprecedented array of virulence factors. These virulence factors render *S. aureus* highly adaptive, especially in the fast-changing environments encountered during infection. Understanding the molecular mechanisms of *S. aureus* virulence as well as risk factors for the host are of major importance for the development of novel strategies to combat hard-to-treat *S. aureus* infections.

Disease prevention and immune prophylaxis

According to the World Health Organization (WHO 2023) disease, prevention comprises “specific, population-based and individual-based interventions for [prevention and early detection], aiming to minimize the burden of diseases and associated risk factors.” *S. aureus* is highly prevalent in the human population and most invasive *S. aureus* infections are caused by the patient’s own colonizing strain. Thus, the carrier status is a major risk factor for *S. aureus* infections. Screening and decolonization have therefore become the two most important tools for disease prevention (Saraswat et al. 2017; Ribau et al. 2021; Sun et al. 2022).

A third measure falling within disease prevention is vaccine development to convey antibody-mediated immunity against the pathogen. So far there are no effective, licensed vaccines against *S. aureus* or any other ESKAPE group pathogen. Vaccination, while aiming for disease prevention, is a form of immune prophylaxis.

Immune prophylaxis describes the artificial establishment of specific immunity. Within immune prophylaxis, vaccination achieves active immunization against a specific pathogen through activation of immune cells (B-cells and T-cells) and induction of antibody production. In contrast, in passive immunization immunity is conveyed through administration of antibodies against toxins, secreted virulence factors and viral particles (Xiao and Dimitrov 2007; Pantaleo et al. 2022).

The benefits of disease prevention and immune prophylaxis are additive, since a reduction in numbers and severity of infections lowers the use of antimicrobial compounds in general. This reduces the selection for resistant isolates, not only in the target species but also in closely related or niche-associated species. Thereby not only the individual patient but even the population as a whole, including associated fields like animal husbandry benefit from lowered MDR (Wojcik-Bojek, Rozalska, and Sadowska 2022).

The identification of new targets for antimicrobial as well as alternative treatments (e.g. use of probiotics and antibodies) and preventative measures are highly dependent on the identification of effective and conserved target structures. An important target for antimicrobial compounds of *S. aureus* is the *S. aureus* cell envelope. It represents the first line of interaction between the bacterium and its environment (Schneider and Sahl 2010).It consists of peptidoglycan (PG), secondary cell wall polysaccharides (sCWGs), lipoteichoic aids (LTA) and cell wall-linked proteins (figure 1).

The group of the sCWGs consists of the capsular polysaccharides (CP) and the wall teichoic acids. In contrast to the cell membrane (CM) -anchored LTA, the sCWGs are anchored to the PG (van Dalen 2020).

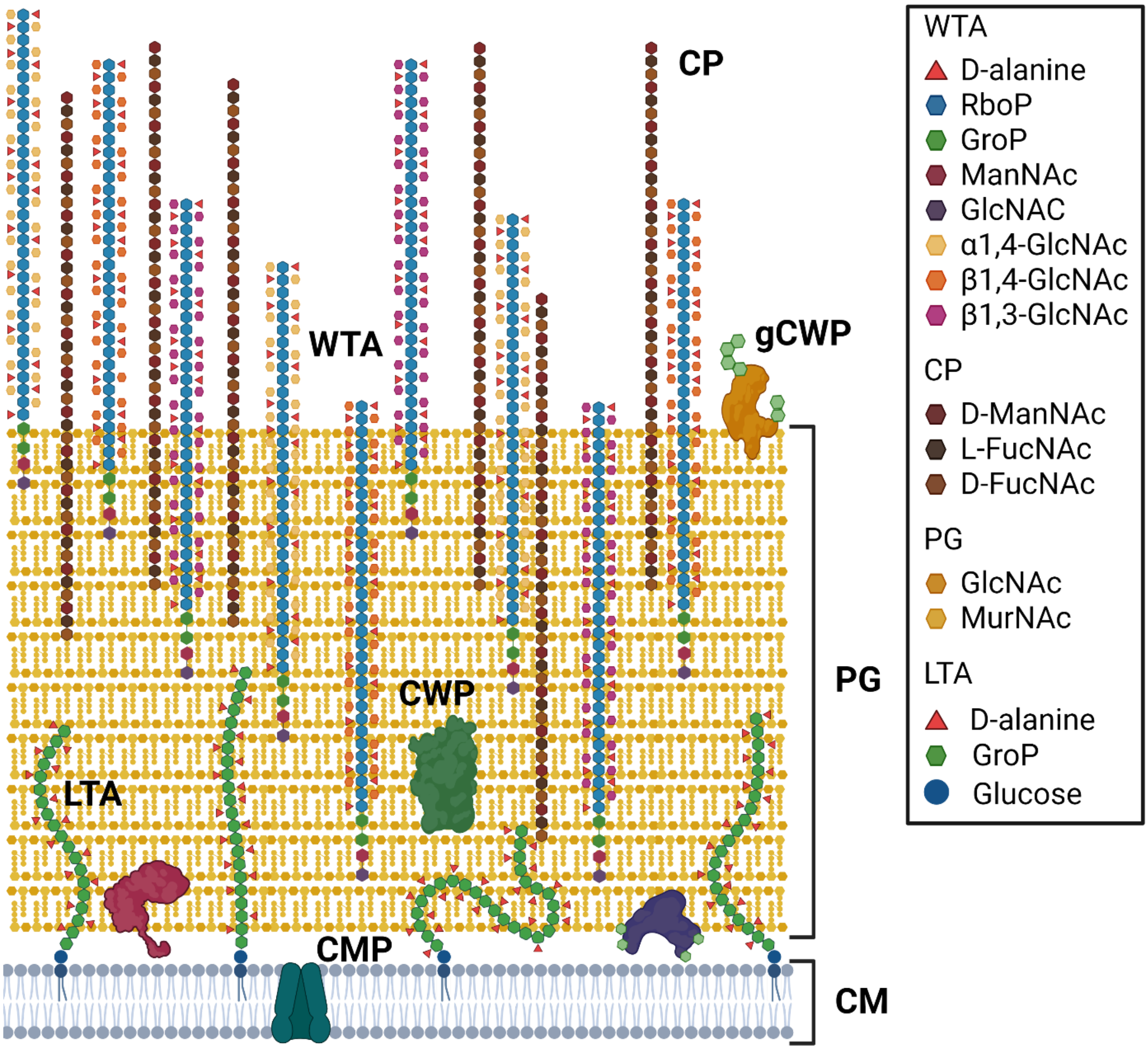

Figure 1. Schematic overview of the *S. aureus* cell wall. The cell membrane (CM) is surrounded by a thick, crosslinked peptidoglycan (PG) layer. Lipoteichoic acids (LTA) and cell membrane proteins (CMP) are linked to the CM, whereas the secondary cell wall glycopolymers wall teichoic acid (WTA) and the capsular polysaccharide (CP), as well as glycosylated or non-glycosylated cell wall proteins (CWP/gCWP), are linked to the PG. (Created with BioRender.com)

It has become evident that the *S. aureus* cell wall is largely comprised of polysaccharides and glycosylated molecules. Thus, glycans shape the initial interaction between *S. aureus* and its environment. They play an important role in bacterial physiology and adaptation (Weidenmaier and Lee 2016; van Dalen 2020).

The thesis in hand focuses on the *S. aureus* sCWGs WTA and CP, and will review their leading role in virulence, their potential as therapeutic and anti-infective targets, and their interaction with one another.

Biosynthesis, regulation, and structure of *S. aureus* WTA vs. CP

The biosynthesis and regulation of CP and WTA have been reviewed in detail (O'Riordan and Lee 2004; Xia and Peschel 2008; Swoboda et al. 2010; Brown 2013; Weidenmaier and Lee

2016; Keinhörster, George, et al. 2019; van Dalen 2020). The following introduction will summarize the findings in a comparative overview.

On a structural level: Both WTA and the CP are linked to *N*-acetylmuramic acid (MurNac) residues of peptidoglycan (PG) at the C-6 hydroxyl by LytR-CspA-Psr (LCP) enzymes (Chan et al. 2014). While linkage of WTA to PG relies on the PG disaccharide linker unit, consisting of *N*-acetylmannosamine-1,4-*N*-acetylglucosamine (ManNAc-GlcNAc) and two glycerol-phosphate (GroP) moieties (Brown 2013; Weidenmaier and Lee 2016), linkage of CP to PG depends on formation of undecaprenyl-PP-*N*-acetylfucosamine (FucNAc) by CapM (Chan et al. 2014). Structurally, WTA is comprised of a ribitol-phosphate (RboP) backbone that is secondarily modified with D-alanine and GlcNAc. The GlcNAc modification can be attached in α-GlcNAc or β-GlcNAc conformation at the RboP C4 hydroxyl (by glycosyltrasferase enzymes TarM or TarS, respectively) or in β-GlcNAc conformation at RboP C3 hydroxyl (by TarP), while D-alanine is attached at RboP C2 by the DltABCD enzyme family (Xia et al. 2010; Brown et al. 2012; Gerlach et al. 2018). The clinically relevant CP types CP5 and CP8 are made of the trisaccharide repeating units D-*N*-acetyl-mannosaminuronic acid, L-FucNAc, and D-FucNAc. The CP serotypes differ in their linkages between the sugars and the site of *O*-acetylation of the mannosaminuronic acid residues (Jones 2005). Of note, *S. aureus* WTA and CP are not branched or crosslinked as is the case for PG, or for WTA and CP of many other gram-positive bacteria (Sumrall et al. 2020; Llull, Garcia, and Lopez 2001).

On a genetic biosynthetic level: While genes involved in WTA biosynthesis and modification are dispersed across the genome (Xia and Peschel 2008; Keinhörster, George, et al. 2019), genes encoding for biosynthesis of the clinically relevant capsule serotypes CP5 and CP8 are allelic and encoded in a single operon made up of sixteen genes (Keinhörster, George, et al. 2019). Of the thirteen capsule serotypes, serotypes CP1, CP2, CP3, CP4, CP5 and CP7 have been confirmed to carry a biosynthetic gene cluster highly homologous to the CP8 gene cluster, with the CP1 strain *S. aureus* M containing an additional non-allelic CP1 gene cluster (Sau 1996) on a non-mobile Staphylococcal Cassette Chromosome Genetic Element (SCC*mec*) called SCC*cap1* (Luong et al. 2002). The genes necessary for WTA biosynthesis and modification are divided over nine to eleven operons, depending on the number of glycosyltransferases present in the stain. The gene clusters *tarAH, tarGBXD, tagO*, *tarI'J'K, tarF, tarIJLS* and *mnaA* are attributed to WTA biosynthesis and translocation, while the gene clusters *dltX, dltABCD*, *tarM* and *tarP* are attributed to WTA modification. The exception to this is *tarS*, which is encoded in the biosynthesis cluster *tarIJLS* but responsible for secondary glycosylation of the WTA. The gene clusters *tarM* and *tarP* are not present in all *S. aureus* stains. While *tarM* is part of the core genome of many pathogenic *S. aureus* strains (Winstel, Xia, and Peschel 2014), *tarP* is encoded on a prophage and only present in select lineages (Gerlach et al. 2018; Gerlach et al. 2022; Tamminga et al. 2022). The genetic organization, regulation and function of the genes involved in WTA biosynthesis are summarized in table 1. Conserved gene clusters homologous to the WTA gene clusters in *S. aureus* have been identified in a variety of especially pathogenic Gram-positive bacteria (Weidenmaier and Peschel 2008). The sixteen CP8-like biosynthesis genes, on the other hand, are encoded in the single operon *capA-P* (Rausch et al. 2019). The genetic organization, regulation and function of the genes involved in CP8-like biosynthesis are summarized in table 2. *cap* genes homologous to those of *S. aureus* can be found in both Gram-positives and Gram-negatives (Rausch et al. 2019). While the enzymes required for polymerization and modification of WTA and CP are unique to the respective polysaccharides, both depend on the gene products of *lcpC* (and redundantly *lcpA* and *lcpB*) to catalyze the ligation to the lipid II_{PG} (Rausch et al. 2019) and, together with LcpA, LcpB and penicillin binding proteins (PBPs), facilitate attachment to the PG.

On the level of regulation: Regulation of the cap operon has been studied extensively, while regulation of WTA biosynthesis remains understudied. This fact may partially be attributed to the dispersion of WTA biosynthesis and modification genes across the genome rather than in a single operon (Keinhörster, George, et al. 2019). The accessory gene regulator (agr) global quorum sensing system of *S. aureus* partially regulates the biosynthesis of both glycopolymers mainly through repression of the repressor of toxins rot, leading to de-repression of *tarH* and P_{cap} (Meredith, Swoboda, and Walker 2008; George et al. 2015). Of note, *cap* expression follows a unique expression pattern that is linked to growth phase. Reverse for what is known for surface proteins, *cap* is repressed during exponential growth. Expression of *cap* starts together with most secreted proteins in post-exponential phase and reaches its maximum during stationary phase. Adding another layer of complexity, CP expression is heterogeneous, as not all cells of the same population will undergo CP expression at any given moment (Poutrel, Rainard, and Sarradin 1997; George et al. 2015; Keinhörster, George, et al. 2019). Interestingly, for surface protein expression this phenotype could be assigned to the agr system and shown to be mediated by its main effector molecule RNAIII (Said-Salim et al. 2003). This mechanism also contributes to the growth phase dependency of CP expression but did not explain the heterogeneous expression pattern (George et al. 2015). Modification of the sigma factor B (sigB) binding motif within P_{cap} results in strains with increased and mostly homogenous CP expression. Thereby, *S*igB acts as repressor for cap expression (Keinhörster, Salzer, et al. 2019). High salt concentrations as well as pH influence CP expression and secondary WTA D-alanylation, with high salt concentrations additionally affecting WTA glycosylation (Dassy 1991; Pöhlmann-Dietze et al. 2000; Neuhaus and Baddiley 2003; Koprivnjak et al. 2006; George et al. 2015; Mistretta et al. 2019)

Table 1. WTA biosynthesis of *S. aureus*: organization, regulation, and function of the involved gene products.

Operon	Gene	Protein	Function in Biosynthesis	Regulation	Reference
tagO	*tagO*	Undecaprenyl-phosphate *N*-acetylglucosaminyl1-phosphate transferase	Initiation of biosynthesis, transfer of GlcNAc–phosphate to lipid II		(Weidenmaier et al. 2004; Soldo, Lazarevic, and Karamata 2002)
mnaA	*mnaA*	UDP-GlcNAc 2-epimerase	Interconversion of UDP-GlcNAc and UDP-ManNAc, providing substrates for TagO and TarA		(Soldo et al. 2002; Mann et al. 2016)
tarAH	*tarA*	Putative *N*-acetyl-mannosaminyltransferase	ManNAc incorporation into the linkage unit		(Ginsberg et al. 2006; Zhang et al. 2006; Qian et al. 2006)
	tarH	ATPase subunit of TarG/H	WTA export, rate limiting factor for WTA quantity	Rot (repression)/ agr (derepression)	(Wanner 2017; Lazarevic and Karamata 1995)
tarGBXD	*tarG*	ABC transporter	WTA export		(Lazarevic and Karamata 1995)
	tarB	Glycerophosphotransferase	Incorporation of the first GroP into the linkage unit		(Bhavsar, Truant, and Brown 2005; Ginsberg et al. 2006; Qian et al. 2006)
	tarX	Glycosyltransferase	Function unknown		
	tarD	Cytidylyltransferase	CDP-glycerol generation		(Badurina, Zolli-Juran, and Brown 2003; Qian et al. 2006)
tarI'J'K	*tarI'*	Cytidylyltransferase	CDP-ribitol generation		(Qian et al. 2006)
	tarJ'	Dehydrogenase	CDP-ribitol generation		(Qian et al. 2006)
	tarK	RboP polymerase/ glycerophosphotransferase	Short-backbone polymerization	Agr (repression)	(Qian et al. 2006; Bae et al. 2004; Meredith, Swoboda, and Walker 2008)

tarF	*tarF*	Glycerophosphotransferase	Incorporation of the second GroP into the linkage unit		(Fitzgerald Stephen N.; Foster 2000; Brown et al. 2010; Qian et al. 2006)
tarIJLS	*tarI*	Cytidylyltransferase	CDP-ribitol generation		(Pereira and Brown 2004; Qian et al. 2006)
	tarJ	Dehydrogenase	CDP-ribitol generation		(Pereira and Brown 2004; Qian et al. 2006)
	tarL	RboP polymerase/ glycerophosphotransferase	Long-backbone polymerization	TarK (repression)	(Qian et al. 2006; Pereira et al. 2008; Meredith, Swoboda, and Walker 2008; Brown, Zhang, and Walker 2008)
	tarS	Glycosyltransferase	β1,4-GlcNAc modification		(Brown et al. 2012)
tarM	*tarM*	Glycosyltransferase	α1,4-GlcNAc modification		(Xia et al. 2010)
tarP	*tarP*	Glycosyltransferase	β1,3-GlcNAc modification		(Gerlach et al. 2018)
dltX	*dltX*		D-Ala incorporation-associated protein		(Wood et al. 2018)
dltABCD	*dltA*	D-alanyl carrier protein ligase	Adenylation of D-alanine, transfer of activated D-alanyl		(Osman et al. 2009; Perego et al. 1995)
	dltB	D-alanyl-lipoteichoic acid biosynthesis protein	putative membrane transport of DltC-D-alanyl		(Perego et al. 1995; Osman et al. 2009)
	dltC	Ligase	D-alanine:D-alanyl carrier protein ligase		(Perego et al. 1995; May et al. 2005)
	dltD	D-alanine transfer protein (glycerophosphate chain)	putative membrane transport of DltC-D-alanyl		(Perego et al. 1995; Osman et al. 2009)

Genes involved in: initiation of synthesis, precursor synthesis, linkage unit synthesis, main polymer synthesis, membrane transport, secondary glycosylation, secondary D-alanylation.

Table 2. CP8-like biosynthesis of *S. aureus*: organisation, regulation, and function of the involved gene products

Operon	Gene	Protein	Function in Biosynthesis	Regulation	Reference
capA-P	*capA*	Dual-function kinase activator/ phosphodiesterase protein	cleavage/release of lipid II	XdrA via CodY (repression), PknB (repression)	(Weidenmaier and Lee 2016; O'Riordan and Lee 2004; Lei and Lee 2018; Rausch et al. 2019)
	capB	Tyrosine kinase complex	regulation of precursor consumption	PknB (repression), capC (modulation)	(Soulat et al. 2006; Gruszczyk et al. 2013; Lei and Lee 2018; Rausch et al. 2019)
	capC	Putative phosphatase	dephosphorylation CapB modulates CP production	Putatively Manganese dependent	(Morona et al. 2002)
	capD	Dehydratase	Generation of UDP-2-acetamido-2,6-dideoxy-D-xylo-4-hexulose		(Li et al. 2014)
	capE	Bifunctional dehydrogenase/epimerase	generation soluble precursor UDP-L-FucNAc		(Kneidinger et al. 2003)
	capF	Epimerase/Reductase	generation soluble precursor UDP-L-FucNAc		(Kneidinger et al. 2003)
	capG	Epimerase	generation soluble precursor UDP-L-FucNAc		(Kneidinger et al. 2003)
	capH	*O*-acetyltransferase	modification, *O*-acetylation		(Bhasin et al. 1998)
	capI	Glycosyltransferase	Transfer of ManNAcA to lipid II_{CP}		(O'Riordan and Lee 2004; Weidenmaier and Lee 2016)
	capJ	Putative polymerase			(Sau 1997; O'Riordan and Lee 2004)
	capK	Putative flipase			(Sau 1997; O'Riordan and Lee 2004)

capL	Transferase	Attachment of L-FucNAc to lipid I_{CP}		(Weidenmaier and Lee 2016; O'Riordan and Lee 2004)
capM	Transferase	Attachment of UDP-D-FucNAc to lipid II to lipid I_{CP}	CapAB (repression indirectly via PknB)	(O'Riordan and Lee 2004; Weidenmaier and Lee 2016)
capN	Reductase	Synthesis of first soluble precursor UDP-D-FucNAc		(Weidenmaier and Lee 2016; O'Riordan and Lee 2004)
capO	Dehydrogenase	Generation of UDP-D-ManNAcA	CapAB (activation)	(Kiser, Cantey-Kiser, and Lee 1999; Portoles et al. 2001; Morona et al. 2002)
capP	Epimerase	Generation of UDP-D-ManNAcA		(Mann et al. 2016; Kiser, Cantey-Kiser, and Lee 1999; Portoles et al. 2001)

Genes involved in: regulation, initiation of synthesis, precursor synthesis, linkage unit synthesis, main polymer synthesis, membrane transport, *O*-acetylation (modification). Regulation of CP expression is mainly achieved on transcriptional level by regulation of P_{cap} (Keinhörster, Salzer, et al. 2019).

Function of *S. aureus* WTA vs CP

The bacterial cell wall comprises the first line of interaction between the bacterium and its environment or host. The multiple roles of WTA in *S. aureus* virulence have been reviewed in great detail (van Dalen 2020; Wu et al. 2021). The role of CP in *S. aureus* virulence, on the other hand, is mostly restricted to correlations in clinical or observations in epidemiological studies and its widely accepted antiphagocytic properties (Weidenmaier and Lee 2016).

Function for *S. aureus* virulence:

Host interaction: Immune evasion/recognition and host defence

The human host is a dynamic and hostile environment in which *S. aureus* is confronted with immune recognition, nutrient limitation, and chemical and physical stresses such as oxygen limitation and shear stresses. For the human immune system to function properly, it relies on discrimination not only between “self” and “foreign”, but among the “foreign” also between “friend” and “foe”. Immune recognition of bacteria is achieved by several means. Receptors of the innate immune system, the so-called pattern recognition receptors (PRRs) like the Toll-like receptor (TLR) family, recognize general bacterial structures such as flagellin, lipoproteins and LPS. TLR binding mediates host defence via immune cell activation and the induction of antimicrobial defence molecules.

While CP expression is wildly accepted to contribute to immune evasion, WTA has been implicated as both a target as well as an evasion mechanism for immune recognition.

WTA is involved in evasion of TLR-activated macrophages secrete cationic antimicrobial peptides (CAMPs), which represent an important defence mechanism of the innate immune system that damages the bacterial membrane, thereby killing invading pathogens. WTA helps to evade this mode of defence, since the positively charged D-alanine residues protect *S. aureus* from most CAMPs through repulsion (Kristian et al. 2003; Zecconi and Scali 2013; Pidwill et al. 2020). As a result, strains lacking D-alanine modifications of teichoic acids are highly susceptible to neutrophil killing (Collins et al. 2002). Although WTA plays an important role in the protection from CAMPs, it renders *S. aureus* susceptible to detection by another family of PRRs, namely the glycan-recognizing C-type lectins (CLRs) (Lebeer, Vanderleyden, and De Keersmaecker 2010). The CLRs langerin, macrophage galactose-type lectin (MGL) and mannose-binding lectin (MBL) detect *S. aureus* WTA (Park et al. 2010; van Dalen, De La Cruz Diaz, et al. 2019; Mnich et al. 2019). MBL is a soluble CLR present in serum. Bacterial opsonization by MBL triggers the lectin pathway of complement activation, facilitating immune cell recruitment and bacterial clearance. Langerin and MGL are instead cellular immune receptors that facilitate bacterial uptake and activation of the immune cell, thereby mediating downstream immune responses. Most interactions between WTA and CLRs result in the recruitment of immune cells, particularly of polymorphonuclear leukocytes (PMNs).

Opsonophagocytic killing (OPK) by PMNs is the primary mechanism by which the host immune system combats *S. aureus* infections (Nanra et al. 2013). For this mechanism to be efficient, opsonization of the bacteria with antibodies and/or complement effectors is a prerequisite (Lu et al. 2014; Dunkelberger and Song 2010). About 70% of *S. aureus*-reactive human IgG antibodies are directed towards the secondary GlcNAc modifications of WTA (Lehar et al. 2015). These antibodies are able to induce complement activation (Jung et al. 2012) and phagocytosis by neutrophils (Lehar et al. 2015; Dalen et al. 2019). Antibodies directed against WTA are predominantly of the IgG2 subclass. Mechanistically, this speaks for direct T-cell-independent B-cell activation by WTA, through crosslinking of B-cell receptors (Jung et al. 2012). However, T-cell-dependent B-cell activation happens in parallel, too. In skin infections, WTA was shown to be presented in major histocompatibility complex II (MHCII) to CD4+ T cells, inducing CD4+ T cell proliferation. Presentation in MHCII depends on the zwitterionic charge of WTA (Weidenmaier, McLoughlin, and Lee 2010). In addition, Kolata et al. identified WTA-specific T-memory cells in human skin, supporting that *S. aureus* skin immunity involves MHC-II presentation of WTA (Kolata et al. 2015; van Dalen 2020).

The CP, on the other hand, is known for its antiphagocytic properties (Thakker 1998; Nanra et al. 2013; Liu 2009) through shielding of opsonins (Kuipers et al. 2016). While this is widely accepted to be the main function of the capsule in *S. aureus* virulence, CP expression does not completely block opsonization by antibodies or complement effectors (de Vor, Rooijakkers, and van Strijp 2020). Interestingly, antibodies raised specifically against CP induce OPK in *in vitro* assays but are often nonprotective *in vivo* (or only against the exact strain used for antibody induction) (Cook et al. 2009; Liu et al. 2017). The CP *in vivo* seems to partially contribute to epitope masking while being only mildly immunostimulatory itself. Additionally, *S. aureus* is specialized in immune evasion by means of secreted proteins (de Vor, Rooijakkers, and van Strijp 2020), which are mostly co-expressed with the CP in later stages of growth (Said-Salim et al. 2003). Therefore, *S. aureus* does not seem to rely solely on CP production for immune evasion. This may also be reflected in the emergence of highly virulent CP-deficient lineages such as USA300 (Weidenmaier and Lee 2016). Interestingly, classical diagnostics and epidemiological classifications in the pre-genomic era relied on serological typing of bacterial strains. CP typing was performed using specific CP antisera commonly produced in rabbits. Here, agglutination in the presence of anti-teichoic acid sera was used as control for acapsular strains (Fournier 1984). Cultivation methods that ensured CP production for specific antisera preparation and WTA-free CP-preparations of the tested isolates were considered crucial for reliable CP typing (Karakawa 1985). While immunization of mice for anti-CP sera production yields predominantly antibodies of the IgG1 subclass (Liu et al. 2017), natural antibodies directed against CP in humans are poorly characterized. Typing-sera against different CP variants are not cross-reactive, but studies about natural antibodies against different CP types are dated and fragmented. So far, evidence for cross-protection of natural antibodies directed against different CP types is lacking.

In addition, we are only starting to understand how the secondary WTA-glycosylation impacts the immunogenicity of the molecule. The glycosyltransferase TarS can be found in all *S. aureus* strains and seems to be dominant *in vivo* (Gerlach et al. 2019; Mistretta et al. 2019; Tamminga et al. 2022). Studies suggested that glycosylation by TarM and TarP reduce the immunogenicity of *S. aureus* (Gerlach et al. 2019). There is some evidence regarding the cross protection of antibodies against different glycosylation variants. Gerlach et al. found significantly reduced cross-protection of mice immunized with TarS glycosylated *S. aureus*, against subsequent infection by TarP glycosylated *S. aureus*. They touched upon the concept of a glyco-switch mechanism by which *S. aureus* might evade immune-recognition by means of differential WTA glycosylation (Gerlach et al. 2018). In contrast to this finding, other studies found cross-reactivity between antibodies against TarS and TarP WTA (Takahashi et al. 2013; van Dalen, Molendijk, et al. 2019; Shen et al. 2023). We can conclude, that while GlcNAc-RboP is an important immunogenic structure (van Dalen 2020) the impact of the individual glycosylation variants on WTA immunogenicity and immune evasion are only partially understood.

While subverting phagocytosis by CP shielding is one way *S. aureus* ensures its survival, the “trojan horse hypothesis” argues that intracellular survival in professional phagocytes poses a mechanism by which *S. aureus* gains access to underlying tissues (Lehar et al. 2015). Once recognized and taken up by professional phagocytes, *S. aureus* is known to survive intracellularly, resist phagosomal killing, and even multiply within the phagosome (Münzenmayer et al. 2016). While capsule production has been implicated in phagosomal escape and survival for other bacteria, like *Bacillus anthracis* (Tonello and Zornetta 2012), *S. aureus* escape relies on effector proteins of the Sae two-component system as well as on the positive cell surface charge introduced by D-alanylation of WTA (Münzenmayer et al. 2016).

Host interaction: biofilm formation, adhesion, antimicrobial resistance, and phage interaction

S. aureus is strongly associated with medical implant-related infections. While most *S. aureus* isolates form protein-dependent biofilms (de Vor, Rooijakkers, and van Strijp 2020), production of polysaccharide intercellular adhesin (PIA) (Cramton et al. 1999), has proven to be crucial for biofilm formation and maturation. In addition, adhesion inorganic surfaces is a prerequisite to initiate biofilm formation. This initiation of biofilm formation highly depends on D-alanylation of WTA (Gross et al. 2001), since the charge of teichoic acids modulates electrostatic interactions between bacteria and inorganic surfaces, which are often negatively charged (Gross et al. 2001; Fabretti et al. 2006). While CP has been implicated in biofilm formation by the Gram-negative pathogen *Klebsiella pneumoniae* (Wang et al. 2015; Huang et al. 2014), no link between CP expression and biofilm formation has been found in *S. aureus*.

S. aureus is the most prevalent isolate from patients with endovascular infections (Wojcik-Bojek, Rozalska, and Sadowska 2022). Mechanistically, adhesion to the endothelial cells is the first crucial step for the onset and progression of endovascular infections. The key role of protein adhesins in the bacterial binding to the vascular lining has been widely demonstrated. Regarding CWGs, WTA was identified as a glycopolymer adhesin that contributes to binding to human cells through interaction with the host scavenger receptors (SRs). SRs are yet another group of PRRs that interact with *S. aureus* surface determinants. SR binding contributes to increased macrophage phagocytosis in an opsonin-independent manner (Pidwill et al. 2020). The SRs SREC-1 (Baur et al. 2014) and LOX-1 (this work) recognize *S. aureus* WTA. SREC-1 binds to WTA in a charge dependent manner and was shown to be crucial for initial epithelial adhesion as well as stable nasal colonization in a cotton rat nasal colonization model (Baur et al. 2014). The role of CP in adhesion, however, remains unclear. Soell et al. showed that purified CP adheres to human epithelial cells, human endothelial cells and monocytes (Soell et al. 1995), while Pöhlmann-Dietze et al. showed in whole-bacteria adhesion assays with different CP mutants inhibited adhesion to human umbilical vein endothelial cells (HUVECs). In this instance, CP expression inhibited adhesion of *S. aureus*, supposedly by masking of the major cell wall adhesins (Pöhlmann-Dietze et al. 2000). While interference of the capsule with adhesion has been widely reported, the evidence supporting masking of classical proteinaceous MSCRAMMs is inconclusive. The interaction of CP with WTA has only recently been investigated (this work).

S. aureus MDR is in major parts attributed to *S. aureus* cell wall composition. The bacterial cell wall is targeted by numerous antibiotics like the β-lactams, bacitracin, glycopeptide antibiotics (e.g. vancomycin), polymyxin B and daptomycin. Therefore, it comes to no surprise that alteration of cell wall composition and modification is an important bacterial resistance mechanism. MRSA poses a huge challenge to health care worldwide. Methicillin resistance was initially solely assigned to carriage of *mecA*, coding for the alternative penicillin binding protein PBP2a that has a lower affinity for β-lactams (Stapleton and Taylor 2002) However, WTA composition also plays an important role in this, since β-1,4-glycosylated WTA is a prerequisite for full β-lactam resistance in MRSA (Brown et al. 2012). Mutants lacking WTA are sensitized to β-lactam-induced cell lysis, a phenotype that has been attributed to mislocalisation of the major autolysin Atl in absence of WTA (Campbell et al. 2011; Schlag et al. 2010; Heilmann et al. 1997). Apart from methicillin resistance, WTA is involved in resistance against vancomycin and daptomycin, both antibiotics of last resort. The mode of action of vancomycin lies in binding of the C-terminal D-Ala–D-Ala residues of the oligopeptide chain of the MurNAc precursor. By binding of the lipid II-attached peptidoglycan precursor, vancomycin prevents release of the universal flippase lipid II and in addition inhibits cross-linking of PG (Hu, Peng, and Rao 2016). Daptomycin acts by insertion into the bacterial cell membrane

(CM), causing leakage of ions and thus depolarization of the CM (Pogliano, Pogliano, and Silverman 2012). Resistance to vancomycin (VR) and for a large part daptomycin (DR) coincides with an increase in cell wall thickness (Bertsche et al. 2013; Foster 2017). For VR this phenotype is assigned to several mutations, one of which affects MsrR, which controls attachment of WTA and CP to PG (Foster 2017). Interestingly, downregulation of WTA biosynthesis decreases cell wall autolysis, specifically by reducing recruitment of autolysins to the septum during cell division, resulting in increased cell size and cell wall thickness. WTA deletion, on the other hand, leads to misplacement of PBPs, thereby reducing cell wall integrity and increasing vancomycin susceptibility. Taken together, downregulation but not deletion of WTA increases vancomycin resistance (Hu, Peng, and Rao 2016). Effects of MsrR mutations on CP attachment to the PG have neither been linked nor addressed in the context of VR development so far. In addition to cell wall thickness, the zwitterionic surface charge introduced by WTA and LTA D-alanylation is implicated in vancomycin and daptomycin resistance via charge-based repulsion (Bertsche et al. 2013; Hu, Peng, and Rao 2016; Kuroda et al. 2019). While for other ESKAPE pathogens, like *A. baumannii*, the CP has been shown to convey antibiotic resistance (Singh, Adams, and Brown 2018), the CP of *S. aureus* does not play a role in antibiotic resistance (Seaman et al. 2004). In contrast to the clinically relevant *S. aureus* CP-types CP5 and CP8, the mucoid CP-types CP1 and CP2 have been implicated in resistance to disinfectants, presumably due to delayed penetration of the mucoid layer. But also for these mucoid CP types there was no difference in antibiotic killing between encapsulated and unencapsulated strains (Kolawole 1984).

Interestingly, CP5 and CP8 seem to lack the pronounced barrier function described for example for the capsule of *A. baumannii* (Tipton et al. 2018; Singh, Adams, and Brown 2018), or *K. pneumoniae* (Campos et al. 2004). While *S. aureus* encapsulation does not protect from antimicrobial compounds like AMPs, antibiotics (Seaman et al. 2004), bile salts (Misawa et al. 2015) or lysostaphin (King, Biel, and Wilkinson 1980), WTA expression conveys these protective functions (Kuroda et al. 2019; Misawa et al. 2015; Ulluwishewa et al. 2016; Wu et al. 2018; Pidwill et al. 2020; Gipson et al. 2020).

Another aspect of sCWGs that shapes the interaction between *S. aureus* and its environment is bacteria-phage interaction. WTA acts as the major phage receptor for *S. aureus* (Xia et al. 2011). In general, phages interact with the bacteria they target in two main ways. On the one hand, the so-called lytic phages use the bacterial host for their propagation, finally lysing it to release progeny virions. This process of killing bacteria by phages shapes microbial communities and offers huge potential for the development of novel anti-infectiva. On the other hand, the lysogenic (also referred to as temperate) phages can additionally co-exist with their host in a symbiotic way, thereby providing the bacteria with accessory genes. During this so-called lysogeny, the phage either integrates into the bacterial chromosome or resides as extrachromosomal plasmid (lysogenic conversion), thereby passively propagating together with the host during cell division (Casjens 2003). The phages of *S. aureus* belong to the order *Caudovirales*. These are double-stranded DNA phages with an icosahedral head and a tail. The *Caudovirales* can be further classified into three families based on tail morphology: 1) *Podoviridae*, with a short tail; 2) *Siphoviridae*, with a long, noncontractile tail; and 3) *Myoviridae* with a long, double-sheathed, contractile tail (Ackermann 2009). The genome plasticity of *S. aureus* relies predominantly on horizontal gene transfer (HGT) of mobile genetic elements (MGEs) (Lindsay 2010). About 15-20% of the *S. aureus* genome is made up of MGEs, such as *S. aureus* pathogenicity islands (SaPIs), plasmids, transposons, and prophages (Haaber et al. 2016). Transduction is the main mode of HGT in *S. aureus*, in which foreign DNA gets transferred by a bacteriophage as a result miss-packaging of the phage head with host instead of phage DNA. In this process, genes encoding antibiotic resistance markers (Sscmec), toxins (PVL) and immune evasion factors (CHIPS, SCIN, SAK) are mobilized by phages (Haaber et al. 2016; Lindsay 2010). The importance of phages for *S. aureus* biology is further highlighted as all isolates carry at least one but up to four prophages in their genome (Lindsay 2010). In addition, host-jump and host-adaptation of *S. aureus* are closely linked to lysogenisation (Ingmer, Gerlach, and Wolz 2019; Rohmer and Wolz 2021). Phage adsorption to its receptor, the WTA of *S. aureus* (Xia et al. 2011), is prerequisite for phage infection. The exact binding epitope on the WTA varies, with a general tendency for GlcNAc-dependent adsorption in *sipho*- and *podoviridae* and backbone-dependent adsorption in *myoviridae* (Ingmer, Gerlach, and Wolz 2019; Azam and Tanji 2019). By this extend, the WTA and its modification play a key role in bacterial acquisition of DNA, resistance development and mobilization of virulence genes. While lysogenisation comes with a lot of benefits to the bacterium, these must be weighed against the risk of phage killing. There are three mechanisms by which bacteria acquire adsorption resistance to resist phage killing 1) blocking of phage receptors, 2) production of CP or 3) production of competitive inhibitors (Labrie, Samson, and Moineau 2010). While in some bacteria there are phages recognizing CP as receptor (Bertozzi Silva, Storms, and Sauvageau 2016), CP production inhibits phage adsorption in *Bacillus anthracis* (Negus et al. 2013) and *S. aureus* (this work).

Function for Therapeutic use:

Phage therapy

When it comes to strategies to combat *S. aureus* infections that target sCWGs, phage therapy is one of the first that comes to mind. Phage therapy hinges on the host specificity and lytic activity of bacteriophages. This therapeutic strategy predates the discovery of antibiotics and while widely used to treat bacterial infections during World War Two, the focus in western medicine shifted to the development and use of antibiotics soon afterwards. With the rise in MDR pathogens, phages are being reconsidered as potential tools in the fight against hard-to-treat infections (Casey, van Sinderen, and Mahony 2018). Potential phages for therapeutic use must meet three main criteria: 1) they need to be strictly lytic and non-transducing, 2) have a broad activity against the target pathogen but no other species, 3) do not carry any known resistance or virulence genes. Additional concerns are synergy with other phages to allow for application of phage cocktails to minimize risk of phage resistance development, and quality-controlled endotoxin-free and host cell-free production of high titer lysates (Lehman et al. 2019). Adsorption of the phage to the bacterial host is a prerequisite for phage infection and, by extend, of phage killing (Azam and Tanji 2019). As the primary phage receptor of *S. aureus*, WTA and its modifications are crucial determinants for susceptibility to phage infection. When it comes to *S. aureus*, strictly lytic phages can be found predominantly among the podo- and myoviruses, while *S. aureus* syphoviruses are commonly among the temperate (and therefore possibly transducing) phages. Concerning the broad host range, *myoviridae* are likely the best candidates for phage therapy of *S. aureus* infections, as they recognize the WTA backbone regardless of GlcNAc modifications (Azam and Tanji 2019). Recent data suggest that the number of phages carrying accessory virulence genes has previously been overestimated (Enault et al. 2017). Regardless, sequencing of candidate phages, to avoid known antibiotic resistance or bacterial virulence genes is needed to assess suitability for phage therapy (Lehman et al. 2019). Phages have also been proven effective in the treatment of biofilms (Dvorackova et al. 2019) and localized human infections (Morozova, Vlassov, and Tikunova 2018). Recent studies identified an immunogenic potential of phages during prolonged, high-dose administration. The major capsid protein as well as the tail morphogenetic protein of the phage elicited a T-cell dependent antibody response that led to inactivation of the phage. The less abundantly present baseplate protein, which contains the receptor binding protein (RBP) recognizing the bacterial host, was not immunogenic (Majewska et al. 2019). Therefore, use of phage-RBP-coupled phage lysins is a promising alternative to the use of intact phages, which has been reviewed extensively (Fischetti 2010). Development of chimeric phage lysins and artilysins in the form of phage-receptor-bound lyso-probes allows to harness the potential of phages without the need to use potentially immunogenic or transducing phages (Casey, van Sinderen, and Mahony 2018; Clegg et al. 2021). The history of phage therapy, including prophylactic phage therapy in animals and humans and combination of phage therapy and antibiotic treatment, has been reviewed in detail and shows promising results for future applications to target *S. aureus* infections (Casey, van Sinderen, and Mahony 2018; Almeida et al. 2019; Azam and Tanji 2019; Lehman et al. 2019).

Phages have additional uses in diagnostics and epidemiology, by using phage typing as a method to group *S. aureus* isolates (Blair and Williams 1961). The glycans that are recognized by phage RBPs are not encoded on the bacterial genome, but are instead enzymatically synthesized in multiple steps (Drula et al. 2022). Therefore, the expression and composition of glycans rely not only on the presence of biosynthesis genes but also the regulation of multiple different enzymes in the environmental context. This makes glycans very diverse and hard to predict using genetic or proteomic tools (Burkholz, Quackenbush, and Bojar 2021). Phages, but also antibodies (as described for the CP antisera) and potentially even CLRs, could be used as glyco-probes to identify virulence determinants like WTA modifications and CP types of *S. aureus* and other bacteria, and thus find application in diagnostics and epidemiology.

Vaccine development

The challenges of *S. aureus* vaccine development as well as the progress made in this field so far have been reviewed in detail (Parker 2018; van Dalen, Molendijk, et al. 2019; Adamo 2021; Clegg et al. 2021; Teymournejad and Montgomery 2021; Jahantigh et al. 2022; Wojcik-Bojek, Rozalska, and Sadowska 2022). Recent studies strongly suggest that key to the failure of all candidate vaccines studied so far is prior exposure to colonizing *S. aureus*, which seems to attenuate the effectivity of vaccines (Ye and Chen 2022). Differences in immunogenicity between the strain with the original vaccine antigen and the actual strains that cause the infection may partially result from differences in WTA glycosylation as discussed above (Gerlach et al. 2018). Through these mechanisms, *S. aureus* inhibits the development of T-cell-dependent B-cell memory, as well as opsonophagocytic antibody responses that are a prerequisite for successful vaccine-induced immunity (Jansen et al. 2013; Pollard 2009). T-cell activation is more potently induced by proteinaceous antigens than by glycans. However, through the use of so-called glycoconjugate vaccines, potent immune memory can also be generated to glycans, such as WTA and CP. Thereby, they are promising candidates for *S. aureus* vaccines, as they are highly immunogenic and have shown promising results in mice (van Dalen, Molendijk, et al. 2019; Parker 2018; Jahantigh et al. 2022). Most *S. aureus* vaccine candidates that have been tested so far include CP and/or WTA (Jansen et al. 2013). The only live vaccine candidate, which is currently being tested in mice, is auxotrophic for D-alanine. It is therefore severely lacking in cell wall integrity and attenuated in growth and pursued as potential living vaccination strain (Moscoso et al. 2018; Parker 2018). The use of this strain as a potential live attenuated vaccine underlines the importance of cell surface charge, specifically the LTA and WTA D-alanylation, for *S. aureus* survival *in vivo*. Quality control in whole-cell vaccines is difficult to assure when it comes to modern days standards (Clegg et al. 2021) but they still find application in veterinary medicine (Lysigin® and Startvac® or TopVac®), where *S. aureus* plays a crucial role in the establishment of bovine mastitis (Reyher et al. 2011). Vaccination of livestock is an important strategy in the fight against MDR *S. aureus*, by decreasing the need to use antibiotics for veterinary applications. Thereby, it decreases the chance of the development of antibiotic resistance and subsequent transfer of antibiotic resistant strains to humans.

Immune prophylaxis

While passive immunization with monoclonal antibodies (mAbs) targeting *S. aureus* surface antigens such as the CP or LTA were largely non-effective, mAbs targeting secreted toxins and immune evasion proteins show mixed but partially promising results and currently undergoing clinical testing (Clegg et al. 2021). While targeting pathogens or secreted virulence factors with effective opsonic antibodies induces phagocytosis and therefore their clearing, another mode of action by which mAbs help to clear infections is blocking of virulence factors like toxins or adhesins, preventing their mode of action (Bennett et al. 2019). Passive immunization has been regarded mostly as a prophylactic strategy since it does not stimulate B-cell immunity. Interestingly, it has been suggested recently that passive immunization with mAbs may actually result in development of long-term B-cell immunity. Mechanistically, successful antibody coating of the targeted antigens by mAbs leads to formation of immune complexes. Phagocytosis of these immune complexes by APCs leading to presentation of the targeted antigens supposedly drives the development of B-cell immunity (Pelegrin, Naranjo-Gomez, and Piechaczyk 2015).

Antimicrobial treatment

Apart from advances in phage therapy, vaccine development and identification of protective mAbs, treatment of *S. aureus* still relies heavily on antibiotics. As described earlier, conserved bacterial surface structures are attractive targets for established antibiotics as well as for the development of new classes of antibiotics (Clegg et al. 2021). Historically, the first target for antibiotic treatment was bacterial cell wall biosynthesis, which has been further exploited during the following “golden age” of antibiotics. Still, to this day, many antibiotic classes target the cell wall and new drug development has not abandoned the cell wall as promising target (Schneider and Sahl 2010).

The glycopeptide antibiotic targocil directly targets WTA biosynthesis via TarG (Tiwari et al. 2018). Interestingly, even though targocil resistance was observed *in vitro*, mediated by mutations in *tarA* or *tarG*, these mutants exhibited aberrant WTA representations in the cell wall and were highly attenuated in virulence (Suzuki 2011). On the downside, targocil is not yet registered for human or veterinary application and potentially only applicable for topical treatment due to low tissue penetration in its current form (Suzuki 2011).

The identification of the peptide-like teixobactin (Ling et al. 2015) added a new class of cell wall-targeting antibiotics to our repertoire. Teixobactin inhibits cell wall biosynthesis through binding to multiple lipid II-coupled cell wall precursors. The bactericidal activity of teixobactin was linked to synergistic inhibition of both lipid II_{PG} and lipid II_{WTA}, resulting in delocalization of autolysins, cell wall damage and subsequent lysis. In contrast to vancomycin, teixobactin does not bind to mature PG, presumably circumventing classical vancomycin resistance mechanisms based on increased cell wall thickness (Homma et al. 2016). Alteration of lipid II as possible resistance mechanism was originally considered unlikely (Foster 2017), but *S. aureus* as well as multiple *Enterococcus* isolates developed vancomycin resistance based on this mechanism (Stogios and Savchenko 2020).

Another branch of drug development focuses on improving and altering of existing antibacterial compounds. The glycopeptide antibiotic oritavancin is a derived from vancomycin. Oritavancin has a dual mode of action, combining inhibition of WTA as well as PG biosynthesis (Singh et al. 2017). Until now there have been no incidences of oritavancin resistance in *S. aureus* (Daum 2018).

Novel antibiotic delivery systems like antibody-antibiotic conjugates show promising results in preclinical and phase one clinical trials. For example, DSTA4637S is a novel rifamycin-class antibiotic that is coupled to a mAb targeting *S. aureus* WTA. Intracellularly, fusion of phago- and lysosome initiates cleavage and thereby activation of the coupled antibiotic, where it promotes killing of the bacteria (Clegg et al. 2021; Lehar et al. 2015). Some critics suggest that future considerations for antibody-delivery-systems should put more emphasis on both effective opsonophagocytic killing as well as enhanced antibiotic sensitization (Ye and Chen 2022).

Outline and Aim

As highlighted above, the identification of new targets for antimicrobial and alternative treatments as well as preventative measures like vaccination are highly dependent on the identification of effective target structures.

Secondary cell wall polysaccharides are highly abundant repetitive structures and important virulence factors of *S. aureus*. The thesis in hand, investigates 1) how the sCWGs WTA and CP shape the interaction between *S. aureus* and its host receptors as well as bacteriophages, and 2) how the interaction of WTA with CP in turn influences bacterial virulence. I strongly believe that insights into the molecular interactions between *S. aureus* and its host, as well as fundamental understanding of (cell wall) physiology, are key to the development of future strategies to target this important pathogen.

Ackermann, Hans- W. 2009. 'Phage Classification and Characterization.' in Martha R. J. Clokie and Andrew M. Kropinski (eds.), *Bacteriophages: Methods and Protocols, Volume 1: Isolation, Characterization, and Interactions* (Humana Press: Totowa, NJ).

Acton, D. S., M. J. Plat-Sinnige, W. van Wamel, N. de Groot, and A. van Belkum. 2009. 'Intestinal carriage of *Staphylococcus aureus*: how does its frequency compare with that of nasal carriage and what is its clinical impact?', *Eur J Clin Microbiol Infect Dis*, 28: 115-27.

Adamo, R. 2021. 'Glycoconjugate vaccines: classic and novel approaches', *Glycoconj J*, 38: 397-98.

Almeida, Gabriel M. F., Elina Laanto, Roghaieh Ashrafi, and Lotta-Riina Sundberg. 2019. 'Bacteriophage Adherence to Mucus Mediates Preventive Protection against Pathogenic Bacteria', *MBio*, 10: e01984-19.

Azam, Aa Haeruman, and Yasunori Tanji. 2019. 'Peculiarities of *Staphylococcus aureus* phages and their possible application in phage therapy', *Applied Microbiology and Biotechnology*, 103: 4279-89.

Badurina, D. S., M. Zolli-Juran, and E. D. Brown. 2003. 'CTP:glycerol 3-phosphate cytidylyltransferase (TarD) from *Staphylococcus aureus* catalyzes the cytidylyl transfer via an ordered Bi-Bi reaction mechanism with micromolar K(m) values', *Biochim Biophys Acta*, 1646: 196-206.

Bae, T., A. K. Banger, A. Wallace, E. M. Glass, F. Aslund, O. Schneewind, and D. M. Missiakas. 2004. '*Staphylococcus aureus* virulence genes identified by bursa aurealis mutagenesis and nematode killing', *Proc Natl Acad Sci U S A*, 101: 12312-7.

Baur, S., M. Rautenberg, M. Faulstich, T. Grau, Y. Severin, C. Unger, W. H. Hoffmann, T. Rudel, I. B. Autenrieth, and C. Weidenmaier. 2014. 'A nasal epithelial receptor for *Staphylococcus aureus* WTA governs adhesion to epithelial cells and modulates nasal colonization', *PLoS Pathog*, 10: e1004089.

Bennett, M. R., R. G. Bombardi, N. Kose, E. H. Parrish, M. B. Nagel, R. A. Petit, T. D. Read, K. L. Schey, I. P. Thomsen, E. P. Skaar, and J. E. Crowe. 2019. 'Human mAbs to *Staphylococcus aureus* IsdA Provide Protection Through Both Heme-Blocking and Fc-Mediated Mechanisms', *J Infect Dis*, 219: 1264-73.

Bertozzi Silva, J., Z. Storms, and D. Sauvageau. 2016. 'Host receptors for bacteriophage adsorption', *FEMS Microbiol Lett*, 363.

Bertsche, U.; Weidenmaier C; Kuehner, Daniel Fau; , Soo-Jin Kuehner D Fau - Yang, Stefanie Yang Sj Fau - Baur, Stefanie Baur S Fau - Wanner, Patrice Wanner S Fau - Francois, Jacques Francois P Fau - Schrenzel, Michael R. Schrenzel J Fau - Yeaman, Arnold S. Yeaman Mr Fau - Bayer, and A. S. Bayer. 2013. 'Correlation of daptomycin resistance

in a clinical *Staphylococcus aureus* strain with increased cell wall teichoic acid production and D-alanylation'.
Bhasin, Navneet, Anne Albus, Francis Michon, Paul J. Livolsi, Jin-Sir Park, and Jean C. Lee. 1998. 'Identification of a gene essential for O-acetylation of the*Staphylococcus aureus*type 5 capsular polysaccharide', *Mol Microbiol*, 27: 9-21.
Bhavsar, A. P., R. Truant, and E. D. Brown. 2005. 'The TagB protein in Bacillus subtilis 168 is an intracellular peripheral membrane protein that can incorporate glycerol phosphate onto a membrane-bound acceptor in vitro', *J Biol Chem*, 280: 36691-700.
Blair, J. E., and R. E. Williams. 1961. 'Phage typing of staphylococci', *Bulletin of the World Health Organization*, 24: 771-84.
Brown, S., T. Meredith, J. Swoboda, and S. Walker. 2010. '*Staphylococcus aureus* and Bacillus subtilis W23 make polyribitol wall teichoic acids using different enzymatic pathways', *Chem Biol*, 17: 1101-10.
Brown, S., G. Xia, L. G. Luhachack, J. Campbell, T. C. Meredith, C. Chen, V. Winstel, C. Gekeler, J. E. Irazoqui, A. Peschel, and S. Walker. 2012. 'Methicillin resistance in *Staphylococcus aureus* requires glycosylated wall teichoic acids', *Proc Natl Acad Sci U S A*, 109: 18909-14.
Brown, S., Y. H. Zhang, and S. Walker. 2008. 'A revised pathway proposed for *Staphylococcus aureus* wall teichoic acid biosynthesis based on in vitro reconstitution of the intracellular steps', *Chem Biol*, 15: 12-21.
Brown, Stephanie.; Santa Maria, John P. Jr.; Walker, Suzanne. 2013. 'Wall teichoic acids of gram-positive bacteria', *Annual review of microbiology*, 67: 313-36.
Burkholz, R., J. Quackenbush, and D. Bojar. 2021. 'Using graph convolutional neural networks to learn a representation for glycans', *Cell Rep*, 35: 109251.
Campbell, Jennifer, Atul K. Singh, John P. Santa Maria, Jr., Younghoon Kim, Stephanie Brown, Jonathan G. Swoboda, Eleftherios Mylonakis, Brian J. Wilkinson, and Suzanne Walker. 2011. 'Synthetic Lethal Compound Combinations Reveal a Fundamental Connection between Wall Teichoic Acid and Peptidoglycan Biosyntheses in *Staphylococcus aureus*', *ACS Chemical Biology*, 6: 106-16.
Campos, M. A., M. A. Vargas, V. Regueiro, C. M. Llompart, S. Alberti, and J. A. Bengoechea. 2004. 'Capsule polysaccharide mediates bacterial resistance to antimicrobial peptides', *Infect Immun*, 72: 7107-14.
Casey, Eoghan, Douwe van Sinderen, and Jennifer Mahony. 2018. 'In Vitro Characteristics of Phages to Guide 'Real Life' Phage Therapy Suitability', *Viruses*, 10: 163.
Casjens, S. 2003. 'Prophages and bacterial genomics: what have we learned so far?', *Mol Microbiol*, 49: 277-300.
Chan, Y. G., H. K. Kim, O. Schneewind, and D. Missiakas. 2014. 'The capsular polysaccharide of *Staphylococcus aureus* is attached to peptidoglycan by the LytR-CpsA-Psr (LCP) family of enzymes', *J Biol Chem*, 289: 15680-90.
Clegg, J., E. Soldaini, R. M. McLoughlin, S. Rittenhouse, F. Bagnoli, and S. Phogat. 2021. '*Staphylococcus aureus* Vaccine Research and Development: The Past, Present and Future, Including Novel Therapeutic Strategies', *Front Immunol*, 12: 705360.
Collins, L. V., S. A. Kristian, C. Weidenmaier, M. Faigle, K. P. Van Kessel, J. A. Van Strijp, F. Götz, B. Neumeister, and A. Peschel. 2002. '*Staphylococcus aureus* strains lacking D-alanine modifications of teichoic acids are highly susceptible to human neutrophil killing and are virulence attenuated in mice', *J Infect Dis*, 186: 214-9.
Cook, J., R. Hepler, G. Pancari, N. Kuklin, H. Fan, X. M. Wang, L. Cope, C. Tan, J. Joyce, J. Onishi, D. Montgomery, A. Anderson, and T. McNeely. 2009. '*Staphylococcus aureus* capsule type 8 antibodies provide inconsistent efficacy in murine models of staphylococcal infection', *Hum Vaccin*, 5: 254-63.
Cramton, S. E., C. Gerke, N. F. Schnell, W. W. Nichols, and F. Gotz. 1999. 'The intercellular adhesion (ica) locus is present in *Staphylococcus aureus* and is required for biofilm formation', *Infect Immun*, 67: 5427-33.
Dalen, Rob van, Jacinto S. De La Cruz Diaz, Matevž Rumpret, Felix F. Fuchsberger, Nienke H. van Teijlingen, Jonas Hanske, Christoph Rademacher, Teunis B. H. Geijtenbeek, Jos A. G. van Strijp, Christopher Weidenmaier, Andreas Peschel, Daniel H. Kaplan,

Nina M. van Sorge, Angelika Gründling, and Tarek Msadek. 2019. 'Langerhans Cells Sense <i>*Staphylococcus aureus*</i> Wall Teichoic Acid through Langerin To Induce Inflammatory Responses', *MBio*, 10: e00330-19.

Dassy, B.; Stringfellow, W. T.; Lieb, M.; Fourni, J.M. 1991. 'Production of type 5 capsular polysaccharide by *Staphylococcus aureus* grown in a semi-synthetic medium', *J Gen Microbiol*.

Daum, Robert S. 2018. '*Staphylococcus aureus*.' in Sarah S. Long, Charles G. Prober and Marc Fischer (eds.), *Principles and Practice of Pediatric Infectious Diseases (Fifth Edition)* (Elsevier).

David M. P. De Oliveira, Brian M. Forde, Timothy J. Kidd, Patrick N. A. Harris, Mark A. Schembri, Scott A. Beatson, David L. Paterson, Mark J. Walker. 2020. 'Antimicrobial Resistance in ESKAPE Pathogens', *Clin Micobiol Review*.

de Vor, L., S. H. M. Rooijakkers, and J. A. G. van Strijp. 2020. 'Staphylococci evade the innate immune response by disarming neutrophils and forming biofilms', *FEBS Lett*, 594: 2556-69.

Drula, E., M. L. Garron, S. Dogan, V. Lombard, B. Henrissat, and N. Terrapon. 2022. 'The carbohydrate-active enzyme database: functions and literature', *Nucleic Acids Res*, 50: D571-D77.

Dunkelberger, J. R., and W. C. Song. 2010. 'Complement and its role in innate and adaptive immune responses', *Cell Res*, 20: 34-50.

Dvorackova, M., F. Ruzicka, M. Benesik, R. Pantucek, and M. Dvorakova-Heroldova. 2019. 'Antimicrobial effect of commercial phage preparation Stafal(R) on biofilm and planktonic forms of methicillin-resistant *Staphylococcus aureus*', *Folia Microbiol (Praha)*, 64: 121-26.

Enault, F., A. Briet, L. Bouteille, S. Roux, M. B. Sullivan, and M. A. Petit. 2017. 'Phages rarely encode antibiotic resistance genes: a cautionary tale for virome analyses', *ISME J*, 11: 237-47.

Fabretti, Francesca, Christian Theilacker, Lucilla Baldassarri, Zbigniew Kaczynski, Andrea Kropec, Otto Holst, and Johannes Huebner. 2006. 'Alanine esters of enterococcal lipoteichoic acid play a role in biofilm formation and resistance to antimicrobial peptides', *Infect Immun*, 74: 4164-71.

Fischetti, V. A. 2010. 'Bacteriophage endolysins: a novel anti-infective to control Gram-positive pathogens', *Int J Med Microbiol*, 300: 357-62.

Fitzgerald Stephen N.; Foster, Thimothy J. 2000. 'Molecular Analysis of the tagF Gene, Encoding CDP-Glycerol: Poly(glycerophosphate) Glycerophosphotransferase of Staphylococcus epidermidis ATCC 14990', *Jurnal of Bacteriology*.

Foster, T. J. 2017. 'Antibiotic resistance in *Staphylococcus aureus*. Current status and future prospects', *FEMS Microbiol Rev*, 41: 430-49.

Fournier, Jean. Michel.; Vann, Willie. F.; and Karakawa, Walter. W. 1984. 'Purification and Characterization of *Staphylococcus aureus* Type 8 Capsular Polysaccharide', *Infect Immun*.

George, S. E., T. Nguyen, T. Geiger, C. Weidenmaier, J. C. Lee, J. Liese, and C. Wolz. 2015. 'Phenotypic heterogeneity and temporal expression of the capsular polysaccharide in *Staphylococcus aureus*', *Mol Microbiol*, 98: 1073-88.

Gerlach, D., Y. Guo, C. De Castro, S. H. Kim, K. Schlatterer, F. F. Xu, C. Pereira, P. H. Seeberger, S. Ali, J. Codée, W. Sirisarn, B. Schulte, C. Wolz, J. Larsen, A. Molinaro, B. L. Lee, G. Xia, T. Stehle, and A. Peschel. 2018. 'Methicillin-resistant *Staphylococcus aureus* alters cell wall glycosylation to evade immunity', *Nature*, 563: 705-09.

Gerlach, David, Yinglan Guo, Thilo Stehle, and Andreas Peschel. 2019. 'Reply to: Do not discard *Staphylococcus aureus* WTA as a vaccine antigen', *Nature*, 572: E3-E4.

Gerlach, David, Raphael N. Sieber, Jesper Larsen, Janes Krusche, Cristina De Castro, Juliane Baumann, Antonio Molinaro, and Andreas Peschel. 2022. 'Horizontal transfer and phylogenetic distribution of the immune evasion factor tarP', *Front Microbiol*, 13.

Ginsberg, Cynthia, Yu-Hui Zhang, Yanqiu Yuan, and Suzanne Walker. 2006. 'In Vitro Reconstitution of Two Essential Steps in Wall Teichoic Acid Biosynthesis', *ACS Chemical Biology*, 1: 25-28.

Gipson, K. S., K. P. Nickerson, E. Drenkard, A. Llanos-Chea, S. K. Dogiparthi, B. B. Lanter, R. M. Hibbler, L. M. Yonker, B. P. Hurley, and C. S. Faherty. 2020. 'The Great ESKAPE: Exploring the Crossroads of Bile and Antibiotic Resistance in Bacterial Pathogens', *Infect Immun*, 88.

Gross, M., S. E. Cramton, F. Gotz, and A. Peschel. 2001. 'Key role of teichoic acid net charge in *Staphylococcus aureus* colonization of artificial surfaces', *Infect Immun*, 69: 3423-6.

Gruszczyk, J., V. Olivares-Illana, J. Nourikyan, A. Fleurie, E. Bechet, V. Gueguen-Chaignon, C. Freton, M. Aumont-Nicaise, S. Morera, C. Grangeasse, and S. Nessler. 2013. 'Comparative analysis of the Tyr-kinases CapB1 and CapB2 fused to their cognate modulators CapA1 and CapA2 from *Staphylococcus aureus*', *PLoS One*, 8: e75958.

Haaber, J., J. J. Leisner, M. T. Cohn, A. Catalan-Moreno, J. B. Nielsen, H. Westh, J. R. Penades, and H. Ingmer. 2016. 'Bacterial viruses enable their host to acquire antibiotic resistance genes from neighbouring cells', *Nat Commun*, 7: 13333.

Heilmann, Christine, Muzaffar Hussain, Georg Peters, and Friedrich Götz. 1997. 'Evidence for autolysin-mediated primary attachment of Staphylococcus epidermidis to a polystyrene surface', *Mol Microbiol*, 24: 1013-24.

Homma, T., A. Nuxoll, A. B. Gandt, P. Ebner, I. Engels, T. Schneider, F. Gotz, K. Lewis, and B. P. Conlon. 2016. 'Dual Targeting of Cell Wall Precursors by Teixobactin Leads to Cell Lysis', *Antimicrob Agents Chemother*, 60: 6510-17.

Hu, Q., H. Peng, and X. Rao. 2016. 'Molecular Events for Promotion of Vancomycin Resistance in Vancomycin Intermediate *Staphylococcus aureus*', *Front Microbiol*, 7: 1601.

Huang, T. W., I. Lam, H. Y. Chang, S. F. Tsai, B. O. Palsson, and P. Charusanti. 2014. 'Capsule deletion via a λ-Red knockout system perturbs biofilm formation and fimbriae expression in Klebsiella pneumoniae MGH 78578', *BMC Res Notes*, 7: 13.

Ingmer, H., D. Gerlach, and C. Wolz. 2019. 'Temperate Phages of *Staphylococcus aureus*', *Microbiol Spectr*, 7.

Jahantigh, H. R., S. Faezi, M. Habibi, M. Mahdavi, A. Stufano, P. Lovreglio, and K. Ahmadi. 2022. 'The Candidate Antigens to Achieving an Effective Vaccine against *Staphylococcus aureus*', *Vaccines (Basel)*, 10.

Jansen, K. U., D. Q. Girgenti, I. L. Scully, and A. S. Anderson. 2013. 'Vaccine review: "Staphyloccocus aureus vaccines: problems and prospects"', *Vaccine*, 31: 2723-30.

Jones, C. 2005. 'Revised structures for the capsular polysaccharides from *Staphylococcus aureus* Types 5 and 8, components of novel glycoconjugate vaccines', *Carbohydr Res*, 340: 1097-106.

Jung, D. J., J. H. An, K. Kurokawa, Y. C. Jung, M. J. Kim, Y. Aoyagi, M. Matsushita, S. Takahashi, H. S. Lee, K. Takahashi, and B. L. Lee. 2012. 'Specific serum Ig recognizing staphylococcal wall teichoic acid induces complement-mediated opsonophagocytosis against *Staphylococcus aureus*', *J Immunol*, 189: 4951-9.

Karakawa, W. W.; Fournier, J. M.; Vann, W. F.; Arbeit, R.; Schneerson, R. S.; Robbins, J. B. 1985. 'Method for the Serological Typing of the Capsular Polysaccharides of *Staphylococcus aureus*', *J Clin Microbiol*.

Keinhörster, D., A. Salzer, A. Duque-Jaramillo, S. E. George, G. Marincola, J. C. Lee, C. Weidenmaier, and C. Wolz. 2019. 'Revisiting the regulation of the capsular polysaccharide biosynthesis gene cluster in *Staphylococcus aureus*', *Mol Microbiol*, 112: 1083-99.

Keinhörster, Daniela, Shilpa Elizabeth George, Christopher Weidenmaier, and Christiane Wolz. 2019. 'Function and regulation of *Staphylococcus aureus* wall teichoic acids and capsular polysaccharides', *Int J Med Microbiol*: 151333.

King, B. F., M. L. Biel, and B. J. Wilkinson. 1980. 'Facile penetration of the *Staphylococcus aureus* capsule by lysostaphin', *Infect Immun*, 29: 892-6.

Kiser, K. B., J. M. Cantey-Kiser, and J. C. Lee. 1999. 'Development and characterization of a *Staphylococcus aureus* nasal colonization model in mice', *Infect Immun*, 67: 5001-6.

Kneidinger, B., K. O'Riordan, J. Li, J. R. Brisson, J. C. Lee, and J. S. Lam. 2003. 'Three highly conserved proteins catalyze the conversion of UDP-N-acetyl-D-glucosamine to precursors for the biosynthesis of O antigen in Pseudomonas aeruginosa O11 and capsule in *Staphylococcus aureus* type 5. Implications for the UDP-N-acetyl-L-fucosamine biosynthetic pathway', *J Biol Chem*, 278: 3615-27.

Kolata, J. B., I. Kuhbandner, C. Link, N. Normann, C. H. Vu, L. Steil, C. Weidenmaier, and B. M. Broker. 2015. 'The Fall of a Dogma? Unexpected High T-Cell Memory Response to *Staphylococcus aureus* in Humans', *J Infect Dis*, 212: 830-8.

Kolawole, Deboye O. 1984. 'Resistance mechanisms of mucoid-grown *Staphylococcus aureus* to the antibacterial action of some disinfectants and antiseptics', *FEMS Microbiology Letters*, 25: 205-09.

Koprivnjak, T., V. Mlakar, L. Swanson, B. Fournier, A. Peschel, and J. P. Weiss. 2006. 'Cation-induced transcriptional regulation of the dlt operon of *Staphylococcus aureus*', *J Bacteriol*, 188: 3622-30.

Kourtis, Athena P. ; Kelly Hatfield; James Baggs; Yi Mu; Isaac See; Erin Epson; Joelle Nadle; Marion A. Kainer; Ghinwa Dumyati; Susan Petit; Susan M. Ray; David Ham; Catherine Capers; Heather Ewing; Nicole Coffin; L. Clifford McDonald; John Jernigan; Denise Cardo. 2019. 'Vital Signs: Epidemiology and Recent Trends in Methicillin-Resistant and in Methicillin-Susceptible *Staphylococcus aureus* Bloodstream Infections — United States'.

Kristian, S. A., X. Lauth, V. Nizet, F. Goetz, B. Neumeister, A. Peschel, and R. Landmann. 2003. 'Alanylation of teichoic acids protects *Staphylococcus aureus* against Toll-like receptor 2-dependent host defense in a mouse tissue cage infection model', *J Infect Dis*, 188: 414-23.

Kuipers, A., D. A. C. Stapels, L. T. Weerwind, Y. P. Ko, M. Ruyken, J. C. Lee, K. P. M. van Kessel, and S. H. M. Rooijakkers. 2016. 'The *Staphylococcus aureus* polysaccharide capsule and Efb-dependent fibrinogen shield act in concert to protect against phagocytosis', *Microbiology (Reading)*, 162: 1185-94.

Kuroda, M., T. Sekizuka, H. Matsui, J. Ohsuga, T. Ohshima, and H. Hanaki. 2019. 'IS256-Mediated Overexpression of the WalKR Two-Component System Regulon Contributes to Reduced Vancomycin Susceptibility in a *Staphylococcus aureus* Clinical Isolate', *Front Microbiol*, 10: 1882.

Labrie, S. J., J. E. Samson, and S. Moineau. 2010. 'Bacteriophage resistance mechanisms', *Nat Rev Microbiol*, 8: 317-27.

Lazarevic, V., and D. Karamata. 1995. 'The tagGH operon of Bacillus subtilis 168 encodes a two-component ABC transporter involved in the metabolism of two wall teichoic acids', *Mol Microbiol*, 16: 345-55.

Lebeer, S., J. Vanderleyden, and S. C. De Keersmaecker. 2010. 'Host interactions of probiotic bacterial surface molecules: comparison with commensals and pathogens', *Nat Rev Microbiol*, 8: 171-84.

Lehar, S. M., T. Pillow, M. Xu, L. Staben, K. K. Kajihara, R. Vandlen, L. DePalatis, H. Raab, W. L. Hazenbos, J. H. Morisaki, J. Kim, S. Park, M. Darwish, B. C. Lee, H. Hernandez, K. M. Loyet, P. Lupardus, R. Fong, D. Yan, C. Chalouni, E. Luis, Y. Khalfin, E. Plise, J. Cheong, J. P. Lyssikatos, M. Strandh, K. Koefoed, P. S. Andersen, J. A. Flygare, M. Wah Tan, E. J. Brown, and S. Mariathasan. 2015. 'Novel antibody-antibiotic conjugate eliminates intracellular *S. aureus*', *Nature*, 527: 323-8.

Lehman, Susan M., Gillian Mearns, Deborah Rankin, Robert A. Cole, Frenk Smrekar, Steven D. Branston, and Sandra Morales. 2019. 'Design and Preclinical Development of a Phage Product for the Treatment of Antibiotic-Resistant *Staphylococcus aureus* Infections', *Viruses*, 11: 88.

Lei, M. G., and C. Y. Lee. 2018. 'Repression of Capsule Production by XdrA and CodY in *Staphylococcus aureus*', *J Bacteriol*, 200.

Li, W., H. Ulm, M. Rausch, X. Li, K. O'Riordan, J. C. Lee, T. Schneider, and C. E. Muller. 2014. 'Analysis of the *Staphylococcus aureus* capsule biosynthesis pathway in vitro: characterization of the UDP-GlcNAc C6 dehydratases CapD and CapE and identification of enzyme inhibitors', *Int J Med Microbiol*, 304: 958-69.

Lindsay, J. A. 2010. 'Genomic variation and evolution of *Staphylococcus aureus*', *Int J Med Microbiol*, 300: 98-103.

REFERENCES

Ling, L. L., T. Schneider, A. J. Peoples, A. L. Spoering, I. Engels, B. P. Conlon, A. Mueller, T. F. Schaberle, D. E. Hughes, S. Epstein, M. Jones, L. Lazarides, V. A. Steadman, D. R. Cohen, C. R. Felix, K. A. Fetterman, W. P. Millett, A. G. Nitti, A. M. Zullo, C. Chen, and K. Lewis. 2015. 'A new antibiotic kills pathogens without detectable resistance', *Nature*, 517: 455-9.

Liu, B., S. Park, C. D. Thompson, X. Li, and J. C. Lee. 2017. 'Antibodies to *Staphylococcus aureus* capsular polysaccharides 5 and 8 perform similarly in vitro but are functionally distinct in vivo', *Virulence*, 8: 859-74.

Liu, G. Y. 2009. 'Molecular pathogenesis of *Staphylococcus aureus* infection', *Pediatr Res*, 65: 71R-77R.

Llull, D., E. Garcia, and R. Lopez. 2001. 'Tts, a processive beta-glucosyltransferase of Streptococcus pneumoniae, directs the synthesis of the branched type 37 capsular polysaccharide in Pneumococcus and other gram-positive species', *J Biol Chem*, 276: 21053-61.

Lowy, Franklin D. 1998. '*Staphylococcus aureus* infections', *The New England Jurnal of Medicine*.

Lu, T., A. R. Porter, A. D. Kennedy, S. D. Kobayashi, and F. R. DeLeo. 2014. 'Phagocytosis and killing of *Staphylococcus aureus* by human neutrophils', *J Innate Immun*, 6: 639-49.

Luong, Thanh T., Shu Ouyang, Kelly Bush, and Chia Y. Lee. 2002. 'Type 1 Capsule Genes of *Staphylococcus aureus* are Carried in a Staphylococcal Cassette Chromosome Genetic Element', *J Bacteriol*, 184: 3623-29.

Ma, Y. X., C. Y. Wang, Y. Y. Li, J. Li, Q. Q. Wan, J. H. Chen, F. R. Tay, and L. N. Niu. 2020. 'Considerations and Caveats in Combating ESKAPE Pathogens against Nosocomial Infections', *Adv Sci (Weinh)*, 7: 1901872.

Majewska, Joanna, Zuzanna Kaźmierczak, Karolina Lahutta, Dorota Lecion, Aleksander Szymczak, Paulina Miernikiewicz, Jarosław Drapała, Marek Harhala, Karolina Marek-Bukowiec, Natalia Jędruchniewicz, Barbara Owczarek, Andrzej Górski, and Krystyna Dąbrowska. 2019. 'Induction of Phage-Specific Antibodies by Two Therapeutic Staphylococcal Bacteriophages Administered per os', *Frontiers in immunology*, 10: 2607-07.

Mann, P. A., A. Muller, K. A. Wolff, T. Fischmann, H. Wang, P. Reed, Y. Hou, W. Li, C. E. Muller, J. Xiao, N. Murgolo, X. Sher, T. Mayhood, P. R. Sheth, A. Mirza, M. Labroli, L. Xiao, M. McCoy, C. J. Gill, M. G. Pinho, T. Schneider, and T. Roemer. 2016. 'Chemical Genetic Analysis and Functional Characterization of Staphylococcal Wall Teichoic Acid 2-Epimerases Reveals Unconventional Antibiotic Drug Targets', *PLoS Pathog*, 12: e1005585.

May, J. J., R. Finking, F. Wiegeshoff, T. T. Weber, N. Bandur, U. Koert, and M. A. Marahiel. 2005. 'Inhibition of the D-alanine:D-alanyl carrier protein ligase from Bacillus subtilis increases the bacterium's susceptibility to antibiotics that target the cell wall', *FEBS J*, 272: 2993-3003.

Melissa D. Sanford, Andreas F. Widmer, Martha J. Bale, Ronald N. Jones, and Richard P. Wenzel. 1994. 'Efficient Detection and Long-Term Persistence of the Carriage of MethicillinResistant *Staphylococcus aureus*'.

Meredith, T. C., J. G. Swoboda, and S. Walker. 2008. 'Late-stage polyribitol phosphate wall teichoic acid biosynthesis in *Staphylococcus aureus*', *J Bacteriol*, 190: 3046-56.

Misawa, Y., K. A. Kelley, X. Wang, L. Wang, W. B. Park, J. Birtel, D. Saslowsky, and J. C. Lee. 2015. '*Staphylococcus aureus* Colonization of the Mouse Gastrointestinal Tract Is Modulated by Wall Teichoic Acid, Capsule, and Surface Proteins', *PLoS Pathog*, 11: e1005061.

Mistretta, N., M. Brossaud, F. Telles, V. Sanchez, P. Talaga, and B. Rokbi. 2019. 'Glycosylation of *Staphylococcus aureus* cell wall teichoic acid is influenced by environmental conditions', *Sci Rep*, 9: 3212.

Mnich, Malgorzata E., Rob van Dalen, David Gerlach, Astrid Hendriks, Guoqing Xia, Andreas Peschel, Jos A. G. van Strijp, and Nina M. van Sorge. 2019. 'The C-Type Lectin

Receptor MGL senses N-acetylgalactosamine on the unique *Staphylococcus aureus* ST395 Wall Teichoic Acid', *Cellular Microbiology*: e13072.

Morona, Judy K., Renato Morona, David C. Miller, and James C. Paton. 2002. 'Streptococcus pneumoniae
Capsule Biosynthesis Protein CpsB Is a Novel Manganese-Dependent Phosphotyrosine-Protein Phosphatase', *J Bacteriol*, 184: 577-83.

Morozova, V. V., V. V. Vlassov, and N. V. Tikunova. 2018. 'Applications of Bacteriophages in the Treatment of Localized Infections in Humans', *Front Microbiol*, 9: 1696.

Moscoso, M., P. Garcia, M. P. Cabral, C. Rumbo, and G. Bou. 2018. 'A D-Alanine auxotrophic live vaccine is effective against lethal infection caused by *Staphylococcus aureus*', *Virulence*, 9: 604-20.

Mulani, M. S., E. E. Kamble, S. N. Kumkar, M. S. Tawre, and K. R. Pardesi. 2019. 'Emerging Strategies to Combat ESKAPE Pathogens in the Era of Antimicrobial Resistance: A Review', *Front Microbiol*, 10: 539.

Münzenmayer, L., T. Geiger, E. Daiber, B. Schulte, S. E. Autenrieth, M. Fraunholz, and C. Wolz. 2016. 'Influence of Sae-regulated and Agr-regulated factors on the escape of *Staphylococcus aureus* from human macrophages', *Cell Microbiol*, 18: 1172-83.

Nanra, J. S., S. M. Buitrago, S. Crawford, J. Ng, P. S. Fink, J. Hawkins, I. L. Scully, L. K. McNeil, J. M. Aste-Amezaga, D. Cooper, K. U. Jansen, and A. S. Anderson. 2013. 'Capsular polysaccharides are an important immune evasion mechanism for *Staphylococcus aureus*', *Hum Vaccin Immunother*, 9: 480-7.

Navidinia, Masoumeh. 2016. 'The clinical importance of emerging ESKAPE pathogens in nosocomial infections', *Jurnal of Paramedical Science*.

Negus, D., J. Burton, A. Sweed, R. Gryko, and P. W. Taylor. 2013. 'Poly-gamma-(D)-glutamic acid capsule interferes with lytic infection of Bacillus anthracis by B. anthracis-specific bacteriophages', *Appl Environ Microbiol*, 79: 714-7.

Neuhaus, F. C., and J. Baddiley. 2003. 'A continuum of anionic charge: structures and functions of D-alanyl-teichoic acids in gram-positive bacteria', *Microbiol Mol Biol Rev*, 67: 686-723.

Noble, W. C. 1967. 'Carriage of *Staphylococcus aureus* in random samples of a normal population', *J Hyg., Camb*.

O'Riordan, K., and J. C. Lee. 2004. '*Staphylococcus aureus* capsular polysaccharides', *Clin Microbiol Rev*, 17: 218-34.

Osman, K. T., L. Du, Y. He, and Y. Luo. 2009. 'Crystal structure of Bacillus cereus D-alanyl carrier protein ligase (DltA) in complex with ATP', *J Mol Biol*, 388: 345-55.

Pantaleo, Giuseppe, Bruno Correia, Craig Fenwick, Victor S. Joo, and Laurent Perez. 2022. 'Antibodies to combat viral infections: development strategies and progress', *Nature Reviews Drug Discovery*, 21: 676-96.

Park, K. H., K. Kurokawa, L. Zheng, D. J. Jung, K. Tateishi, J. O. Jin, N. C. Ha, H. J. Kang, M. Matsushita, J. Y. Kwak, K. Takahashi, and B. L. Lee. 2010. 'Human serum mannose-binding lectin senses wall teichoic acid Glycopolymer of *Staphylococcus aureus*, which is restricted in infancy', *J Biol Chem*, 285: 27167-75.

Parker, D. 2018. 'A live vaccine to *Staphylococcus aureus* infection', *Virulence*, 9: 700-02.

Pelegrin, M., M. Naranjo-Gomez, and M. Piechaczyk. 2015. 'Antiviral Monoclonal Antibodies: Can They Be More Than Simple Neutralizing Agents?', *Trends Microbiol*, 23: 653-65.

Perego, M., P. Glaser, A. Minutello, M. A. Strauch, K. Leopold, and W. Fischer. 1995. 'Incorporation of D-alanine into lipoteichoic acid and wall teichoic acid in Bacillus subtilis. Identification of genes and regulation', *J Biol Chem*, 270: 15598-606.

Pereira, M. P., and E. D. Brown. 2004. 'Bifunctional catalysis by CDP-ribitol synthase: convergent recruitment of reductase and cytidylyltransferase activities in Haemophilus influenzae and *Staphylococcus aureus*', *Biochemistry*, 43: 11802-12.

Pereira, M. P., J. W. Schertzer, M. A. D'Elia, K. P. Koteva, D. W. Hughes, G. D. Wright, and E. D. Brown. 2008. 'The wall teichoic acid polymerase TagF efficiently synthesizes poly(glycerol phosphate) on the TagB product lipid III', *Chembiochem*, 9: 1385-90.

Pidwill, G. R., J. F. Gibson, J. Cole, S. A. Renshaw, and S. J. Foster. 2020. 'The Role of Macrophages in *Staphylococcus aureus* Infection', *Front Immunol*, 11: 620339.

Pogliano, J., N. Pogliano, and J. A. Silverman. 2012. 'Daptomycin-mediated reorganization of membrane architecture causes mislocalization of essential cell division proteins', *J Bacteriol*, 194: 4494-504.

Pöhlmann-Dietze, P., M. Ulrich, K. B. Kiser, G. Doring, J. C. Lee, J. M. Fournier, K. Botzenhart, and C. Wolz. 2000. 'Adherence of *Staphylococcus aureus* to endothelial cells: influence of capsular polysaccharide, global regulator agr, and bacterial growth phase', *Infect Immun*, 68: 4865-71.

Pollard, A. J.; Perrett, K. P.; Beverley, P. C. 2009. 'Maintaining protection against invasive bacteria with protein-polysaccharide conjugate vaccines', *Nat Rev Immunol*, 9: 213-20.

Portoles, M., K. B. Kiser, N. Bhasin, K. H. Chan, and J. C. Lee. 2001. '*Staphylococcus aureus* Cap5O has UDP-ManNAc dehydrogenase activity and is essential for capsule expression', *Infect Immun*, 69: 917-23.

Poutrel, B., P. Rainard, and P. Sarradin. 1997. 'Heterogeneity of cell-associated CP5 expression on *Staphylococcus aureus* strains demonstrated by flow cytometry', *Clin Diagn Lab Immunol*, 4: 275-8.

Qian, Z., Y. Yin, Y. Zhang, L. Lu, Y. Li, and Y. Jiang. 2006. 'Genomic characterization of ribitol teichoic acid synthesis in *Staphylococcus aureus*: genes, genomic organization and gene duplication', *BMC Genomics*, 7: 74.

Rausch, M., J. P. Deisinger, H. Ulm, A. Muller, W. Li, P. Hardt, X. Wang, X. Li, M. Sylvester, M. Engeser, W. Vollmer, C. E. Muller, H. G. Sahl, J. C. Lee, and T. Schneider. 2019. 'Coordination of capsule assembly and cell wall biosynthesis in *Staphylococcus aureus*', *Nat Commun*, 10: 1404.

Reyher, K. K., S. Dufour, H. W. Barkema, L. Des Coteaux, T. J. Devries, I. R. Dohoo, G. P. Keefe, J. P. Roy, and D. T. Scholl. 2011. 'The National Cohort of Dairy Farms--a data collection platform for mastitis research in Canada', *J Dairy Sci*, 94: 1616-26.

Ribau, A. I., J. E. Collins, A. F. Chen, and R. J. Sousa. 2021. 'Is Preoperative *Staphylococcus aureus* Screening and Decolonization Effective at Reducing Surgical Site Infection in Patients Undergoing Orthopedic Surgery? A Systematic Review and Meta-Analysis With a Special Focus on Elective Total Joint Arthroplasty', *J Arthroplasty*, 36: 752-66 e6.

Rice, L. B. 2008. 'Federal funding for the study of antimicrobial resistance in nosocomial pathogens: no ESKAPE', *J Infect Dis*, 197: 1079-81.

Rohmer, C., and C. Wolz. 2021. 'The Role of hlb-Converting Bacteriophages in *Staphylococcus aureus* Host Adaption', *Microb Physiol*, 31: 109-22.

Sabat, A. J., D. Pantano, V. Akkerboom, E. Bathoorn, and A. W. Friedrich. 2021. 'Pseudomonas aeruginosa and *Staphylococcus aureus* virulence factors as biomarkers of infection', *Biol Chem*, 402: 1565-73.

Said-Salim, B., P. M. Dunman, F. M. McAleese, D. Macapagal, E. Murphy, P. J. McNamara, S. Arvidson, T. J. Foster, S. J. Projan, and B. N. Kreiswirth. 2003. 'Global regulation of *Staphylococcus aureus* genes by Rot', *J Bacteriol*, 185: 610-9.

Sakai, T., and Y. Morimoto. 2022. 'The History of Infectious Diseases and Medicine', *Pathogens*, 11.

Saraswat, M. K., J. T. Magruder, T. C. Crawford, J. M. Gardner, D. Duquaine, M. S. Sussman, L. L. Maragakis, and G. J. Whitman. 2017. 'Preoperative *Staphylococcus aureus* Screening and Targeted Decolonization in Cardiac Surgery', *Annals of Thoracic Surgery*, 104: 1349-56.

Sau, Subatta; Lee, Chia Y. 1996. 'Cloning of Type 8 Capsule Genes and Analysis of Gene Clusters for the Production of Different Capsular Polysaccharides in *Staphylococcus aureus*', *Jurnal of Bacteriology*.

Sau, Subrata; Sun, Jiwen; Lee, Chia. Y. 1997. 'Molecular Characterization and Transcriptional Analysis of Type 8 Capsule Genes in *Staphylococcus aureus*', *Jurnal of Bacteriology*.

Schlag, M., R. Biswas, B. Krismer, T. Kohler, S. Zoll, W. Yu, H. Schwarz, A. Peschel, and F. Götz. 2010. 'Role of staphylococcal wall teichoic acid in targeting the major autolysin Atl', *Mol Microbiol*, 75: 864-73.

Schneider, T., and H. G. Sahl. 2010. 'An oldie but a goodie - cell wall biosynthesis as antibiotic target pathway', *Int J Med Microbiol*, 300: 161-9.

Seaman, P., M. Day, A. D. Russell, and D. Ochs. 2004. 'Susceptibility of capsular *Staphylococcus aureus* strains to some antibiotics, triclosan and cationic biocides', *J Antimicrob Chemother*, 54: 696-8.

Senn, L., O. Clerc, G. Zanetti, P. Basset, G. Prod'hom, N. C. Gordon, A. E. Sheppard, D. W. Crook, R. James, H. A. Thorpe, E. J. Feil, and D. S. Blanc. 2016. 'The Stealthy Superbug: the Role of Asymptomatic Enteric Carriage in Maintaining a Long-Term Hospital Outbreak of ST228 Methicillin-Resistant *Staphylococcus aureus*', *MBio*, 7: e02039-15.

Shen, Peng, Han Lin, Yikai Bao, Haofei Hong, and Zhimeng Wu. 2023. 'Synthesis and immunological study of a glycosylated wall teichoic acid-based vaccine against *Staphylococcus aureus*', *Chinese Chemical Letters*, 34: 107679.

Singh, J. K., F. G. Adams, and M. H. Brown. 2018. 'Diversity and Function of Capsular Polysaccharide in Acinetobacter baumannii', *Front Microbiol*, 9: 3301.

Singh, M., J. Chang, L. Coffman, and S. J. Kim. 2017. 'Hidden Mode of Action of Glycopeptide Antibiotics: Inhibition of Wall Teichoic Acid Biosynthesis', *J Phys Chem B*, 121: 3925-32.

Soell, M., M. Diab, G. Haan-Archipoff, A. Beretz, C. Herbelin, B. Poutrel, and J. P. Klein. 1995. 'Capsular polysaccharide types 5 and 8 of *Staphylococcus aureus* bind specifically to human epithelial (KB) cells, endothelial cells, and monocytes and induce release of cytokines', *Infect Immun*, 63: 1380-6.

Soldo, B., V. Lazarevic, H. M. Pooley, and D. Karamata. 2002. 'Characterization of a Bacillus subtilis thermosensitive teichoic acid-deficient mutant: gene mnaA (yvyH) encodes the UDP-N-acetylglucosamine 2-epimerase', *J Bacteriol*, 184: 4316-20.

Soldo, Blazenka, Vladimir Lazarevic, and Dimitri Karamata. 2002. 'tagO is involved in the synthesis of all anionic cell-wall polymers in Bacillus subtilis 168aaThe EMBL accession number for the nucleotide sequence reported in this paper is AJ004803', *Microbiology*, 148: 2079-87.

Soulat, D., J. M. Jault, B. Duclos, C. Geourjon, A. J. Cozzone, and C. Grangeasse. 2006. '*Staphylococcus aureus* operates protein-tyrosine phosphorylation through a specific mechanism', *J Biol Chem*, 281: 14048-56.

Stapleton, Paul D., and Peter W. Taylor. 2002. 'Methicillin Resistance in *Staphylococcus aureus*: Mechanisms and Modulation', *Science Progress*, 85: 57-72.

Stogios, P. J., and A. Savchenko. 2020. 'Molecular mechanisms of vancomycin resistance', *Protein Sci*, 29: 654-69.

Sumrall, E. T., A. P. Keller, Y. Shen, and M. J. Loessner. 2020. 'Structure and function of Listeria teichoic acids and their implications', *Mol Microbiol*, 113: 627-37.

Sun, J., D. Qian, R. Zhou, R. Tang, L. Guan, Y. Ye, Y. Pu, and M. Yu. 2022. 'Effects of preoperative *Staphylococcus aureus* screening and targeted decolonization bundle protocols in cardiac surgery: a nine-year review of a regional cardiovascular center in China', *J Thorac Dis*, 14: 4741-50.

Suzuki, T. 2011. 'A new target for *Staphylococcus aureus* associated with keratitis', *Cornea*, 30 Suppl 1: S34-40.

Swoboda, J. G., J. Campbell, T. C. Meredith, and S. Walker. 2010. 'Wall teichoic acid function, biosynthesis, and inhibition', *Chembiochem*, 11: 35-45.

Takahashi, K., K. Kurokawa, P. Moyo, D. J. Jung, J. H. An, L. Chigweshe, E. Paul, and B. L. Lee. 2013. 'Intradermal immunization with wall teichoic acid (WTA) elicits and augments an anti-WTA IgG response that protects mice from methicillin-resistant *Staphylococcus aureus* infection independent of mannose-binding lectin status', *PLoS One*, 8: e69739.

Tamminga, Sara M., Simon L. Völpel, Kim Schipper, Thilo Stehle, Yvonne Pannekoek, and Nina M. van Sorge. 2022. 'Genetic diversity of *Staphylococcus aureus* wall teichoic acid glycosyltransferases affects immune recognition', *Microbial Genomics*, 8.

Teymournejad, O., and C. P. Montgomery. 2021. 'Evasion of Immunological Memory by *S. aureus* Infection: Implications for Vaccine Design', *Front Immunol*, 12: 633672.

Thakker, Manoj; Park, Jin-Sir; Carey, Vincent; Lee, Jean C. 1998. '*Staphylococcus aureus* Serotype 5 Capsular Polysaccharide Is Antiphagocytic and Enhances Bacterial Virulence in a Murine Bacteremia Model', *Infect Immun*.

Tipton, K. A., C. Y. Chin, M. Farokhyfar, D. S. Weiss, and P. N. Rather. 2018. 'Role of Capsule in Resistance to Disinfectants, Host Antimicrobials, and Desiccation in Acinetobacter baumannii', *Antimicrob Agents Chemother*, 62.

Tiwari, K. B., C. Gatto, S. Walker, and B. J. Wilkinson. 2018. 'Exposure of *Staphylococcus aureus* to Targocil Blocks Translocation of the Major Autolysin Atl across the Membrane, Resulting in a Significant Decrease in Autolysis', *Antimicrob Agents Chemother*, 62.

Tonello, F., and I. Zornetta. 2012. 'Bacillus anthracis factors for phagosomal escape', *Toxins (Basel)*, 4: 536-53.

Ulluwishewa, D., L. Wang, C. Pereira, S. Flynn, E. Cain, S. Stick, F. J. Reen, J. P. Ramsay, and F. O'Gara. 2016. 'Dissecting the regulation of bile-induced biofilm formation in *Staphylococcus aureus*', *Microbiology (Reading)*, 162: 1398-406.

van Dalen, R.; Peschel, A.; van Sorge, N. M. 2020. 'Wall Teichoic Acid in *Staphylococcus aureus* Host Interaction', *Trends Microbiol*, 28: 985-98.

van Dalen, Rob, Jacinto S. De La Cruz Diaz, Matevž Rumpret, Felix F. Fuchsberger, Nienke H. van Teijlingen, Jonas Hanske, Christoph Rademacher, Teunis B. H. Geijtenbeek, Jos A. G. van Strijp, Christopher Weidenmaier, Andreas Peschel, Daniel H. Kaplan, and Nina M. van Sorge. 2019. 'Langerhans Cells Sense *Staphylococcus aureus* Wall Teichoic Acid through Langerin To Induce Inflammatory Responses', *MBio*, 10: e00330-19.

van Dalen, Rob, Michèle M. Molendijk, Sara Ali, Kok P. M. van Kessel, Piet Aerts, Jos A. G. van Strijp, Carla J. C. de Haas, Jeroen Codée, and Nina M. van Sorge. 2019. 'Do not discard *Staphylococcus aureus* WTA as a vaccine antigen', *Nature*, 572: E1-E2.

van Hal, S. J., S. O. Jensen, V. L. Vaska, B. A. Espedido, D. L. Paterson, and I. B. Gosbell. 2012. 'Predictors of mortality in *Staphylococcus aureus* Bacteremia', *Clin Microbiol Rev*, 25: 362-86.

Ventola, C. L. 2015. 'The antibiotic resistance crisis: part 1: causes and threats', *P t*, 40: 277-83.

Wang, H., J. J. Wilksch, R. A. Strugnell, and M. L. Gee. 2015. 'Role of Capsular Polysaccharides in Biofilm Formation: An AFM Nanomechanics Study', *ACS Appl Mater Interfaces*, 7: 13007-13.

Wanner, S.; Schade, J.; Keinhorster, D.; Weller, N.; George, S. E.; Kull, L.; Bauer, J.; Grau, T.; Winstel, V.; Stoy, H.; Kretschmer, D.; Kolata, J.; Wolz, C.; Broker, B. M.; Weidenmaier, C. 2017. 'Wall teichoic acids mediate increased virulence in *Staphylococcus aureus*', *Nat Microbiol*, 2: 16257.

Weidenmaier, C., J. F. Kokai-Kun, S. A. Kristian, T. Chanturiya, H. Kalbacher, M. Gross, G. Nicholson, B. Neumeister, J. J. Mond, and A. Peschel. 2004. 'Role of teichoic acids in *Staphylococcus aureus* nasal colonization, a major risk factor in nosocomial infections', *Nat Med*, 10: 243-5.

Weidenmaier, C., and J. C. Lee. 2016. 'Structure and Function of Surface Polysaccharides of *Staphylococcus aureus*', *Curr Top Microbiol Immunol*.

Weidenmaier, C., R. M. McLoughlin, and J. C. Lee. 2010. 'The zwitterionic cell wall teichoic acid of *Staphylococcus aureus* provokes skin abscesses in mice by a novel CD4+ T-cell-dependent mechanism', *PLoS One*, 5: e13227.

Weidenmaier, C., and A. Peschel. 2008. 'Teichoic acids and related cell-wall glycopolymers in Gram-positive physiology and host interactions', *Nat Rev Microbiol*, 6: 276-87.

Wertheim, H. F., D. C. Melles, M. C. Vos, W. van Leeuwen, A. van Belkum, H. A. Verbrugh, and J. L. Nouwen. 2005. 'The role of nasal carriage in *Staphylococcus aureus* infections', *Lancet Infect Dis*, 5: 751-62.

WHO-ECDC. 2022. 'Joint-WHO-ECDC-AMR-report'.

WHO. 2023. 'Health promotion and disease prevention through population-based interventions, including action to address social determinants and health inequity',

Accessed 27.01.2023. https://www.emro.who.int/about-who/public-health-functions/health-promotion-disease-prevention.html.
Williams, R. E. O. 1963. 'Healthy carriage of *Staphylococcus aureus*: its prevalence and importance'.
Winstel, V., G. Xia, and A. Peschel. 2014. 'Pathways and roles of wall teichoic acid glycosylation in *Staphylococcus aureus*', *Int J Med Microbiol*, 304: 215-21.
Wojcik-Bojek, U., B. Rozalska, and B. Sadowska. 2022. '*Staphylococcus aureus*-A Known Opponent against Host Defense Mechanisms and Vaccine Development-Do We Still Have a Chance to Win?', *Int J Mol Sci*, 23.
Wood, B. McKay, John P. Santa Maria, Leigh M. Matano, Christopher R. Vickery, and Suzanne Walker. 2018. 'A partial reconstitution implicates DltD in catalyzing lipoteichoic acid d-alanylation', *Journal of Biological Chemistry*, 293: 17985-96.
Wu, X., J. Han, G. Gong, M. A. G. Koffas, and J. Zha. 2021. 'Wall teichoic acids: physiology and applications', *FEMS Microbiol Rev*, 45.
Wu, X., S. J. Kwon, D. Kim, J. Zha, M. Mora-Pale, and J. S. Dordick. 2018. 'Unprotonated Short-Chain Alkylamines Inhibit Staphylolytic Activity of Lysostaphin in a Wall Teichoic Acid-Dependent Manner', *Appl Environ Microbiol*, 84.
Xia, G., R. M. Corrigan, V. Winstel, C. Goerke, A. Grundling, and A. Peschel. 2011. 'Wall teichoic Acid-dependent adsorption of staphylococcal siphovirus and myovirus', *J Bacteriol*, 193: 4006-9.
Xia, G., L. Maier, P. Sanchez-Carballo, M. Li, M. Otto, O. Holst, and A. Peschel. 2010. 'Glycosylation of wall teichoic acid in *Staphylococcus aureus* by TarM', *J Biol Chem*, 285: 13405-15.
Xia, G., and A. Peschel. 2008. 'Toward the pathway of *S. aureus* WTA biosynthesis', *Chem Biol*, 15: 95-6.
Xiao, X., and D. S. Dimitrov. 2007. 'Monoclonal antibodies against viruses and bacteria: a survey of patents', *Recent Pat Antiinfect Drug Discov*, 2: 171-7.
Ye, J., and X. Chen. 2022. 'Current Promising Strategies against Antibiotic-Resistant Bacterial Infections', *Antibiotics (Basel)*, 12.
Zecconi, A., and F. Scali. 2013. '*Staphylococcus aureus* virulence factors in evasion from innate immune defenses in human and animal diseases', *Immunol Lett*, 150: 12-22.
Zhang, Y. H., C. Ginsberg, Y. Yuan, and S. Walker. 2006. 'Acceptor substrate selectivity and kinetic mechanism of Bacillus subtilis TagA', *Biochemistry*, 45: 10895-904.

Chapter I

The following chapter is part of the accepted research article:

"*Staphylococcus epidermidis* clones express *Staphylococcus aureus*-type wall teichoic acid to shift from a commensal to pathogen lifestyle".

The original article can be found under: doi: 10.1038/s41564-021-00913-z.

The published version was only formatted to fit the layout of this Thesis. The content is congruent to the peer-reviewed original.

Staphylococcus epidermidis clones express *Staphylococcus aureus*-type wall teichoic acid to shift from a commensal to pathogen lifestyle

Xin Du[1,2,3], Jesper Larsen[4], Min Li[5], Axel Walter[1,3], Christoph Slavetinsky[1,2,3,6], Anna Both[7], Patricia M. Sanchez Carballo[8,9], Marc Stegger[4], Esther Lehmann[1,2,3], Yao Liu[5], Junlan Liu[5], Jessica Slavetinsky[1,2,3], Katarzyna A. Duda[10], Bernhard Krismer[1,2,3], Simon Heilbronner[1,2,3], Christopher Weidenmaier[1,2,11], Christoph Mayer[1,3], Holger Rohde[7], Volker Winstel[1,2,12,13] and Andreas Peschel[1,2,3] ✉

1. Interfaculty Institute of Microbiology and Infection Medicine, University of Tübingen, Tübingen, Germany.
2. German Center for Infection Research (DZIF), partner site Tübingen, Tübingen, Germany.
3. Cluster of Excellence EXC2124 Controlling Microbes to Fight Infection, Tübingen, Germany.
4. Statens Serum Institut, København, Denmark.
5. Renji Hospital, School of Medicine, Shanghai Jiaotong University, Shanghai, China.
6. Pediatric Gastroenterology and Hepatology, University Children's Hospital Tübingen, Eberhard Karls University Tübingen, Tübingen, Germany.
7. Institute of Medical Microbiology, Virology and Hygiene, University Medical Center Hamburg–Eppendorf, Hamburg, Germany.
8. Division of Clinical Infectious Diseases, Research Center Borstel, Leibniz Lung Center, Borstel, Germany.
9. German Center for Infection Research (DZIF), Borstel, Germany.
10. Junior Research Group of Allergobiochemistry, Research Center Borstel, Leibniz Lung Center, Airway Research Center North (ARCN), German Center for Lung Research (DZL), Borstel, Germany.
11. Present address: Finch Therapeutics, Boston, MA, USA.
12. Present address: Research Group Pathogenesis of Bacterial Infections, TWINCORE, Centre for Experimental and Clinical Infection Research, a Joint Venture between the Hannover Medical School and the Helmholtz Centre for Infection Research, Hannover, Germany.
13. Present address: Institute of Medical Microbiology and Hospital Epidemiology, Hannover Medical School, Hannover, Germany.

✉e-mail: andreas.peschel@uni-tuebingen.de

Most clonal lineages of Staphylococcus epidermidis are commensals present on human skin and in the nose. However, some globally spreading healthcare-associated and methicillin-resistant *S. epidermidis* (HA-MRSE) clones are major causes of difficult-to-treat implant or bloodstream infections. The molecular determinants that alter the lifestyle of *S. epidermidis* have remained elusive, and their identification might provide therapeutic targets. We reasoned that changes in surface-exposed wall teichoic acid (WTA) polymers of *S. epidermidis*, which potentially shape host interactions, may be linked to differences between colonization and infection abilities of different clones. We used a combined epidemiological and functional approach to show that while commensal clones express poly-glycerolphosphate WTA, *S. epidermidis* multilocus sequence type 23, which emerged in the past 15 years and is one of the main infection-causing HA-MRSE clones, contains an accessory genetic element, *tarIJLM*, that leads to the production of a second, *Staphylococcus aureus*-type WTA (poly-ribitolphosphate (RboP)). Production of RboP-WTA by *S. epidermidis* impaired in vivo colonization but augmented endothelial attachment and host mortality in a mouse sepsis model. *tarIJLM* was absent from commensal human sequence types but was found in several other HA-MRSE clones. Moreover, RboP-WTA enabled *S. epidermidis* to exchange DNA with *S. aureus* via siphovirus bacteriophages, thereby creating a possible route for the inter-species exchange of methicillin resistance, virulence and colonization factors. We con- clude that *tarIJLM* alters the lifestyle of *S. epidermidis* from commensal to pathogenic and propose that RboP-WTA might be a robust target for preventive and therapeutic interventions against MRSE infections.

Introduction

The major opportunistic pathogen Staphylococcus epidermidis is a core member of human skin and upper airway microbiomes and, at the same time, causes difficult-to-treat healthcare-associated (HA) infections, including bloodstream and implant-associated infections1,2. A major percentage of the invasive *S. epidermidis* clones are resistant to methicillin (MRSE) and other antibiotics1,3,4. The species *S. epidermidis* comprises a large num- ber of clonal lineages that differ with regard to the human body parts they colonize and the ability to invade and persist in sterile tissues2,5,6. The molecular basis of the different habitat preferences and corresponding capacities to bind to specific host surfaces have remained largely unknown. The evolution of staphylococcal species and strains is shaped by the susceptibility to individual groups of bacteriophages, which use the species- or strain-specific struc- ture of wall teichoic acid (WTA) to detect and bind to appropriate bacterial host cells7,8. Phages are also the major vehicles for horizon- tal gene transfer (HGT) in staphylococci, governing the evolution of new clonal lineages9. Phages facilitate, for instance, the exchange of staphylococcal cassette chromosome mec (SCCmec) elements conferring methicillin resistance10,11, *Staphylococcus aureus* patho- genicity islands (SaPIs)12,13 or accessory adhesion factor genes such as sasX14. While mechanisms of intra-species phage-mediated HGT are well documented15, it has remained elusive how the exchange of genetic material between *S. aureus* and *S. epidermidis* or other coagulase-negative staphylococci (CoNS) is accomplished. It has remained particularly enigmatic how such transducing phages can traverse the WTA-specific HGT boundaries between individual staphylococcal species, which produce either poly-ribitolphosphate (RboP)-WTA (most *S. aureus*) or poly-glycerolphosphate (GroP)-WTA (*S. epidermidis* and many other CoNS).

We have previously shown that certain WTA biosynthesis genes reside on genomic elements that seem to move between different Staphylococcus species. The rare *S. aureus* lineage sequence type 395 (ST395), for instance, has acquired the *tagNDF* genes to pro- duce GroP-WTA and it shares susceptibility to specific transducing phages with GroP-WTA-containing CoNS15. Along this line, we hypothesized that some *S. epidermidis* strains may have gained the capacity to exchange DNA via typical *S. aureus* phages. We found that the production of RboP-WTA is not restricted to *S. aureus* but that several prominent HA-MRSE clones produce RboP-WTA in addition to GroP-WTA. In contrast, the RboP-WTA-specific *tarIJLM* genes were absent from human nasal and skin isolates, which had critical consequences for *S. epidermidis* differential phage binding, nasal colonization and bloodstream infection.

Results

Some *S. epidermidis* isolates can be transduced by Φ11 and contain an accessory *tarIJLM* gene cluster. A collection of *S. epidermidis* isolates was screened for their capacity to take up a SaPI via the archetypical *S. aureus* siphophage Φ11, which binds to RboP-WTA15. SaPIbov1, a SaPI isolated from a bovine *S. aureus* iso- late16, has previously been reported to integrate into *S. aureus* and *S. epidermidis* genomes at the same genomic position in the guano- sine monophosphate synthase (gmpS) gene17. The vast majority of the tested isolates could not be transduced by Φ11 with SaPIbov1, which is in agreement with the absence of the RboP-WTA receptor structure at the *S. epidermidis* surface. However, some isolates could be transduced (Table 1 and Fig. 1a). These isolates were also distinguished from other *S. epidermidis* clones by their capacity to bind Φ11 in addition to the GroP-WTA-specific Φ187 (ref. 15) (Extended Data Fig. 1a,b), which suggests that they express the Φ11 receptor. The genome of one of the Φ11-transducible *S. epidermidis*, E73, was sequenced and found to belong to ST23, which has emerged in recent years as one of the frequent HA-MRSE clones3,4. It contained the genes for the synthesis of the WTA linkage unit (*tagOADB*) and the GroP-WTA polymerase gene *tagF*18, which are present in virtu- ally all *S. epidermidis* genomes. Surprisingly, E73 and all other avail- able *S. epidermidis* genomes also contained a gene cluster (*tarIJL1*; Fig. 1b) encoding homologues of *S. aureus* proteins responsible for RboP synthesis (TarI and TarJ) and polymerization (TarL)18,19. Since RboP-WTA has never been documented to be produced by *S. epidermidis*, we assumed that these genes may be non-functional or silent. Indeed, expression of *tarL1* was very low or undetectable in the *S. epidermidis* laboratory strains RP62A, 1457 and ATCC12228, as well as in our clinical *S. epidermidis* isolates E6, E45 and E73. *tarL1* expression was at the detection limit at various growth conditions, including broth, synthetic nasal medium20 and human serum (Fig. 1c and Extended Data Fig. 2), which suggests that *tarIJL1* is non-functional or cannot be expressed. Notably, E73 contained a second putative RboP-WTA gene cluster (*tarIJLM2*), which also encodes a homologue of the *S. aureus* RboP-WTA glycosyl transferase TarM21. *tarL2* was efficiently expressed in isolates E6, E45 and E73 at all tested growth conditions (Fig. 1c and Extended Data Fig. 2). All Φ11-transducible isolates contained *tarIJLM2* except for one clone, which carried another *tarIJLM2*-related accessory gene cluster (Table 1), which indicates that the rare capacity to acquire foreign DNA from *S. aureus* may depend on the presence of *tarIJLM*.

Table 1 | Presence of *tarL2* and susceptibility to **Φ**11-mediated SaPibov1 transduction in infection-derived isolates from *S. epidermidis* strain collections

Strain collection	Number of strains: total	*tarL2*-positive	transduction by **Φ**11	*tarL2*-positive sequence types (number)
SaPibov1				ST5 (2), ST10 (1), ST23 (4), ST87 (3)
Nose	155	0	0	
Skin	144	0	0	
Infection	72	10 (13.9%)	7 (9.7%)[a]	
Hamburg				ST10 (1), ST23 (3), ST87 (2)
Nose	37	0	0	
Infection	75	6 (8.0%)	3 (4.0%)[a]	
Shanghai				ST2 (5)[b], ST23 (1), single-locus ST23 variant (3)
Nose	206	0	0	
Skin	138	0	0	
Infection	130	9 (6.9%)	6 (4.6%)[a]	
total	957	25 (2.6%)	16 (1.7%)[a]	

[a]Even isolates that were negative in the SaPIbov1 transduction assay bound to phage Φ11 (Extended Data Fig. 1a). Potential reasons for the lack of detectable SaPIbov1 transduction include a specific restriction barrier or CRISPR–Cas systems. [b]One of these ST2 isolates was positive for *tarIJLM3* and Φ11 transduction.

***tarIJLM*-encoding *S. epidermidis* strains produce both GroP- and RboP-WTA.** WTA was isolated from the *tarIJLM2*-negative *S. epidermidis* laboratory strains RP62A, ATCC12228 and 1457 and was found to contain only GroP-WTA, as expected, which confirms that tarIJL1 is probably non-functional. In contrast, WTA of E73 contained two types of WTA: GroP-WTA and RboP-WTA (Fig. 2a and Extended Data Fig. 3). Strain 1457 transformed with a *tarIJLM2*-expressing plasmid produced both GroP- and RboP-WTA (Fig. 2b and Extended Data Fig. 3) and could be transduced by Φ11 (Fig. 2c and Extended Data Fig. 1c), thereby confirming that *tarIJLM2* confers the capacity to produce RboP-WTA and enables *S. epidermidis* to exchange DNA with *S. aureus* via RboP-WTA-binding phages. Moreover, deletion of *tarIJLM2* in strain

E73 (ST23) or E1 (ST87) abolished RboP-WTA production and transduction by Φ11 as well as binding by Φ11. These phenotypes were restored by complementation with a plasmid-encoded *tarIJLM2* copy (Fig. 2b,c and Extended Data Figs. 1d,e and 3c). The E73 Δ*tarIJLM2* mutant (E73Δ*tarIJLM2*) showed the same growth behaviour and micro- scopic appearance as the parental strain (Extended Data Fig. 4b,c), which indicates that the genes have no essential roles in basic cellular processes.

E73Δ*tarIJLM2* had a similar phosphate amount in its cell wall as the parental strain, which indicates that the mutant cells prob- ably replaced RboP-WTA by increasing the level of GroP-WTA (Extended Data Fig. 4a). The impact of *tarIJLM* on interactions with GroP-WTA-specific phages was studied using the previously described phages ΦPH15 (ref. 22) and Φ187 (ref. 15), plus a previously uncharacterized bacteriophage ΦE72 that was isolated from *S. epidermidis* E72. E73Δ*tarIJLM2* had an increased capacity to bind the three phages compared with the E73 wild type and the complemented mutant (Fig. 2d), which supports our finding that E73 still produces GroP-WTA, albeit at reduced amounts as a consequence of simultaneous RboP-WTA production.

***tarIJLM* is found exclusively in HA-MRSE isolates.** To assess the prevalence and distribution of *tarIJLM2* among *S. epidermidis* clones, three large collections of *S. epidermidis* isolates from human arm skin (282 isolates) and nasal cavity (398 isolates) of healthy humans or from clinically relevant infections (277 isolates) from Tübingen, from Hamburg and from Shanghai were screened for the presence of tarL2 by PCR (Table 1). Only isolates that were identical in more than two samples from sterile tissues of the same participant on different days were included in the infection iso- late collection to exclude contaminating skin strains. Twenty-four isolates, exclusively derived from infections, were tarL2-positive. They belonged to the HA clones ST2, ST5, ST10, ST23 and ST87 (refs. 3,4,23–28), and three previously unknown single-locus variants of ST23. *tarIJLM2* was found in all 11 ST23 and all 5 ST87 isolates, and in 2 out of 4 ST10 isolates (Table 2). Moreover, the cluster was present in 10% and 6% of the ST2 and ST5 isolates, respectively, which represent the two most common HA-MRSE clones3,4,25,26,28. In contrast, none of the nasal or skin *S. epidermidis* isolates from any of the collections was tarL2-positive, which indicates that the additional gene cluster may be associated with poor arm skin and nose colonization but strong invasion capacities. The only minor deviation from this rule was that we detected *tarIJLM2* in an additional ST10 isolate from Tübingen (E42), which was found only in a single blood culture and therefore did not meet our definition of a clinical isolate (Supplementary Table 1). It was therefore excluded from further functional analyses.

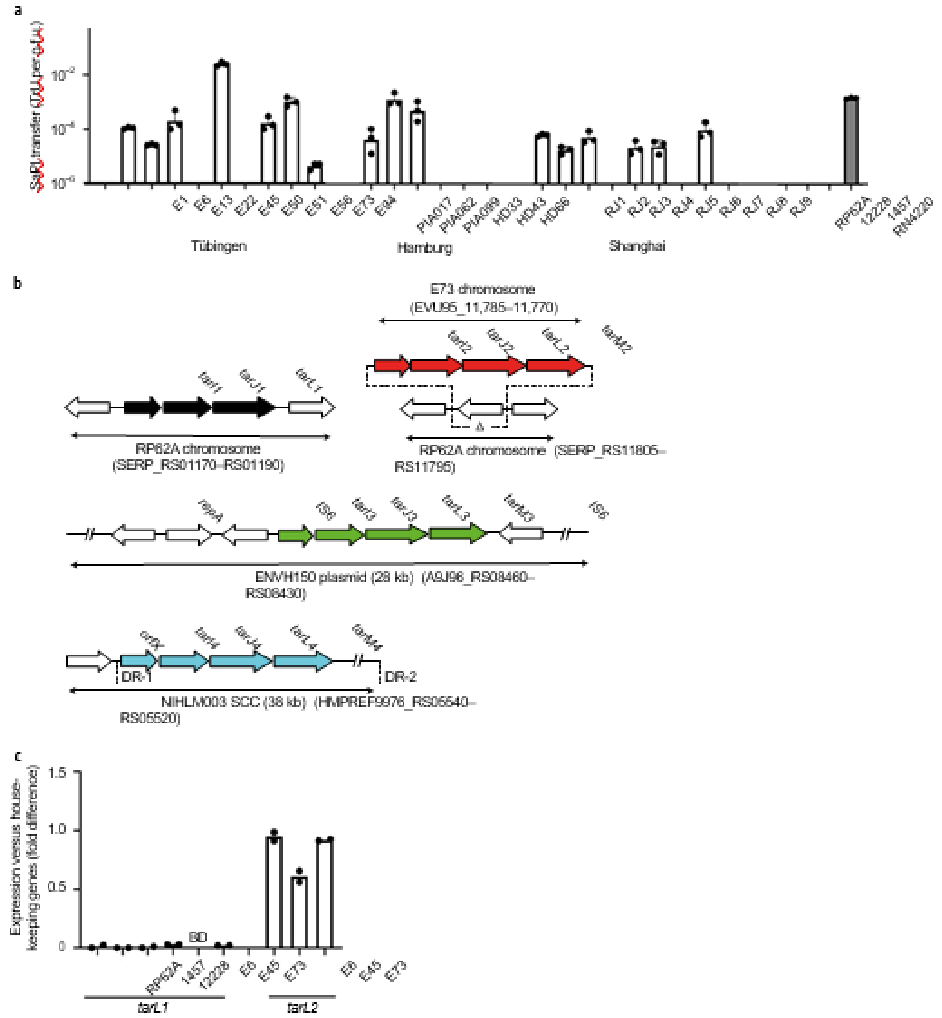

Fig. 1 | Some *S. epidermidis* genomes encode *tarIJLM* gene clusters, permitting transduction by *S. aureus* phage Φ11. a, Some infection-derived *S. epidermidis* isolates from Tübingen, from Hamburg and from Shanghai can be transduced with SaPIbov1 by Φ11. TrU per p.f.u. values indicate the ratio of transduction units (TrU, the number of transductants in 1 ml phage lysate) to p.f.u. (the number of phage plaques formed on RboP-WTA-producing *S. aureus* laboratory strain RN4220) given as the mean ± s.d. of three independent experiments. Strains without a bar had not yielded any transductant. The origin and properties of the isolates are described in Supplementary Table 1. RP62A, ATCC12228 (12228) and 1457 are *S. epidermidis* laboratory strains and only produce GroP-WTA. b, Potential RboP-WTA biosynthesis gene clusters found in the genomes of all (tarIJL1) or certain *S. epidermidis* STs (*tarIJLM2*–4). The genetic location is shown in representative strains RP62A (ST10), E73 (ST23), ENVH150 (ST2) and NIHLM003 (ST218). The direct repeat sequences (DR-1 and DR-2) flanking the SCC element in NIHLM003 are indicated. The genomic location of *tarIJLM5* genes in isolate SNUC_2569 could not be determined due to their presence on two short contigs with no flanking sequences. The figure is not drawn to scale. c, While *tarL2* is efficiently transcribed in the *tarIJLM2*-positive isolates E6, E45 and E73, tarIJL1 is not or only very weakly expressed in all tested *S. epidermidis* strains during growth in TSB after 6 h of growth as analysed by qPCR. The control strains RP62A, 1457 and 12228 lack *tarIJLM2* and were negative in the PCR assay. Values represent means of two independent experiments. They were normalized for strongly and constitutively expressed housekeeping genes gyrB, rho and tpiA. BD, below detection limit.

The identification of *tarIJLM2* in clinical isolates belonging to well-known hospital-adapted lineages but not in commensal isolates prompted us to determine the distribution of homologous genes in an international collection from two sources. An analysis of a previously described global collection of 227 *S. epidermidis* isolates from 96 hospitals in 24 countries3 showed that *tarIJLM2* was present in all 50 ST23 isolates, 1 out of 131 ST2 isolates and both ST87 iso- lates from the ST5/ST87 clade (Fig. 2e and Table 2). In addition, *tarIJLM2* was identified in four of the 497 *S. epidermidis* genomes present in the NCBI Reference Sequence Database, including three ST23 isolates and one ST87 isolate (Fig. 2e and Table 2). *tarIJLM2* was not detected in any of the genomes from other, predominantly commensal, STs, which provides support that it occurs exclusively in HA ST2, ST5, ST10, ST23 and ST87 isolates (Fig. 2e and Table 2). The *tarIJLM2* cluster replaced a chromosomal gene of unknown function found in most *S. epidermidis* genomes (Fig. 1b). It was integrated into the same chromosomal region between two con- served genes in all *tarIJLM2*-positive *S. epidermidis* isolates from our strain collections and the international collection (Fig. 1b). The genes flanking *tarIJLM2 i*n these isolates were also present in the chromosome of the *tarIJLM2*-negative *S. epidermidis* laboratory strain RP62A, but here they flanked another gene with no homology to *tarIJLM* (Fig. 1b). Analysis of the *tarIJLM2*-negative *S. epidermidis* isolates from the global collection (174 out of 227 isolates) showed that the region in RP62A was conserved in 82% (143 out of 174) of the genomes. The absence of mobile genetic elements (for example, insertion sequences (ISs)) between *tarIJLM2* and the flanking genes indicates that the missing gene might have been replaced by *tarIJLM2* in a process called homology-facilitated illegitimate recombination29.

Three other *tarIJLM2*-related gene clusters are found in HA-MRSE clones. Analysis of our strain collections and the international strain collection revealed the existence of three other *tarIJLM2*-related gene clusters, which were designated *tarIJLM3* to *tarIJLM5* (Figs. 1b and 2e, Table 2, Extended Data Fig. 5 and Supplementary Table 1). *tarIJLM3* was detected in a clinical ST2 isolate from Shanghai and in three isolates from the international collection, including two clinical ST2 isolates from Germany and the United States and a *tarIJLM2*-positive ST23 isolate. *tarIJLM4* was detected in three isolates from the international collection, including a ST2 isolate and two clinical isolates from the United States belonging to ST5 and ST218. Finally, *tarIJLM5* was found in a bovine ST100 isolate from Canada. Isolates RJ8 and DAR1907 (both ST2) bearing *tarIJLM3*, and US06 (ST5) bearing *tarIJLM4*, were analysed and found to express both, RboP- and GroP-WTA (Extended Data Fig. 6). Moreover, RJ8 and US06 bound and acquired SaPIbov1 from phage Φ11, thereby con- firming that the gene clusters are functional and have similar roles as *tarIJLM2*.

The *tarIJLM* genes from the different clusters shared 66–89% nucleotide sequence identities, and the corresponding *tarL2*, *tarL3*, *tarL4* and *tarL5* genes were more similar to the *S. aureus tarL* than the *S. epidermidis tarL1* gene (Extended Data Fig. 5a). These findings suggest that the *tarIJLM* gene clusters in *S. epidermidis* originated through HGT from an unknown donor rather than by gene duplication and diversification of the *S. epidermidis tarIJL1* cluster. This hypothesis is further supported by the patchy distribution of *tarIJLM* variants in the *S. epidermidis* phylogenetic tree (Fig. 2e and Extended Data Fig. 5b) and by our finding that both *tarIJLM3* and *tarIJLM4* are located on mobile genetic elements (Fig. 1b).

The *tarIJLM3* gene cluster was located on a 29-kb unannotated plasmid in the ST2 isolate DAR1907, and on 23- and 28-kb annotated contigs of unknown genomic origin in the other isolates. These contigs contained the *repA* plasmid replication gene and shared 100% nucleotide sequence identities with the plasmid sequence from DAR1907, which indicates that they are probably of plasmid origin (Fig. 1b). Of note, the *tarIJLM3* gene cluster was flanked by two pseudogenes homologous to IS elements belonging to the IS6 family (Fig. 1b).

Analysis of the contig containing the *tarIJLM4* gene cluster in the ST218 isolate NIHLM003 showed that it was carried on a 38-kb SCC element, which was integrated at a unique site at the 3′-end of *orfX* (referred to as integration site sequence (ISS)). It contained the ccrA2B2 genes encoding site-specific recombinases30, and was flanked by direct repeat sequences containing the ISS. The contigs containing *orfX* and the *tarIJLM4* gene cluster from isolate VCU013 (ST2) and US06 (ST5) shared 100% nucleotide sequence identities with the first 12 and 8 kb of the SCC element from NIHLM003, respectively. Apart from the SCCmec element, the ST2 and ST5 isolates each contained a mec and ccr gene complex characteristic of a type-III (3A) and type-IV (2B) SCCmec element, respectively, but they were present on different contigs and it was therefore not possible to determine their location in relation to the SCC element. We were also unable to determine the genomic location of the *tarIJLM5* gene cluster in the bovine ST100 isolate SNUC_2569 due to its presence on two short contigs with no flanking sequences. We have currently no indications for frequent mobility of any of the *tarIJLM* clusters, which suggests that they might have evolved a long time ago, potentially originating from the core-genome-encoded tar genes of *S. aureus*.

***tarIJLM* gene clusters are found in the genomes of other CoNS species.** The different *tarIJLM* gene variants (Fig. 1b) were used as queries in BLASTN searches against non-*S. epidermidis* genomes present in the NCBI Reference Sequence Database. The contigs containing the *S. epidermidis tarIJLM3* gene cluster shared 98% identity with a 7-kb region on a 33-kb contig from a bovine *Staphylococcus warneri* isolate SNUC_194 (accession number NZ_ PZFE00000000) (Supplementary Table 1), including the *tarIJLM3* gene cluster and flanking IS6-like pseudogenes. The presence of the *repA* gene on the *S. warneri* contig indicated a plasmid origin. The remaining part of the *S. warneri* contig showed little homology

to the *tarIJLM3*-carrying plasmid-like contigs from *S. epidermidis*, which provides support for mobilization of the *tarIJLM3* cluster between plasmids from different Staphylococcus species. Analysis of the contigs containing the *tarIJLM4* gene cluster showed that the left extremity of the SCC element shared 98% identity with a 5-kb region at the right extremity of a contig from an isolate belonging to an as yet uncharacterized *Staphylococcus species*, HMSC069E07 (accession number NZ_LTPB01000000) (Supplementary Table 1). The contig contained the left ISS and the *tarIJL4* gene cluster. Of note, *tarM* was not present in any of the contigs from this isolate. The *ccrA2B2* genes were located on a separate contig. The *tarIJLM5* gene cluster present in the bovine ST100 isolate, SNUC_2569, was identified on a 14-kb SCC element in an isolate belonging to another uncharacterized *Staphylococcus species*, HMSC061F01 (accession number NZ_LTNM01000000) (Supplementary Table 1). The SCC element contained the ccrA4B4 genes and was preceded by a 23-kb SCC element, which was integrated into the 3′-end of *orfX* and contained the ccrA1B1 genes. Besides the *tarIJLM5* gene cluster, the two SCC elements showed little homology to other contigs from SNUC_2569. The tarIJL5 genes, but not *tarM*, were also present in SCC elements in three bovine *Staphylococcus hominis* isolates: SNUC_3404, SNUC_5746 and SNUC_5748 (accession numbers NZ_PZHY00000000, NZ_PZHW00000000 and NZ_
QXVQ00000000, respectively) (Supplementary Table 1).

In contrast to the other *tarIJLM* gene clusters, we did not find evidence of the presence of *tarIJLM2* homologues outside *S. epidermidis*. Nonetheless, our data support the hypothesis that the *tarIJLM* gene clusters were derived from other *Staphylococcus species* through exchange of genetic material. Furthermore, the identification of the *tarIJLM3* and *tarIJLM5* gene clusters in bovine *S. warneri* and *S. epidermidis* isolates, respectively, suggests the existence of an animal reservoir.

Table 2 | Presence of *tarIJLM* in major HA-MRSE clones isolated from infections

Clone	Hamburg	Shanghai	tübingen	international collection[f]	All
	Number of clones with *tarIJLM*/total number				Percentage with *tarIJLM*
ST2	0/18	5/22[a]	0/10	4/362[a]	2.18
ST5	0/12	0/9	2/13	1/54[b]	3.41
ST10	1/1	0/2	1/1	0/2	33.3
ST23	3/3	4/4[e]	4/4	53/53[c]	100
ST87	2/2	0/0	3/3	3/3	100
Several sporadic STs	0/39 (21 different STs)	0/93 (23 different STs)	0/41 (24 different STs)	2/250[d]	1.01

Positive isolates contained *tarlJLM2* unless otherwise noted. [a]One ST2 isolate from Shanghai and two ST2 isolates from the international collection contained *tarIJLM3*, while one ST2 isolate from the international collection contained *tarIJLM4*. [b]One ST5 isolate from the international collection contained *tarIJLM4*. [c]One ST23 isolate from the international collection contained both *tarIJLM2* and *tarIJLM3*. [d]In the international collection, one ST218 isolate contained *tarIJLM4* while one ST100 isolate contained *tarIJLM5*. [e]One ST23 isolate and three single-locus ST23 variants. [f]The international collection included 497 *S. epidermidis* genomes present in the NCBI Reference Sequence Database (accessed 3 July 2018), a global collection of 227 *S. epidermidis* isolates originating from 96 institutions across 24 countries[3]. For some of these isolates, it is not clear whether they are from infections.

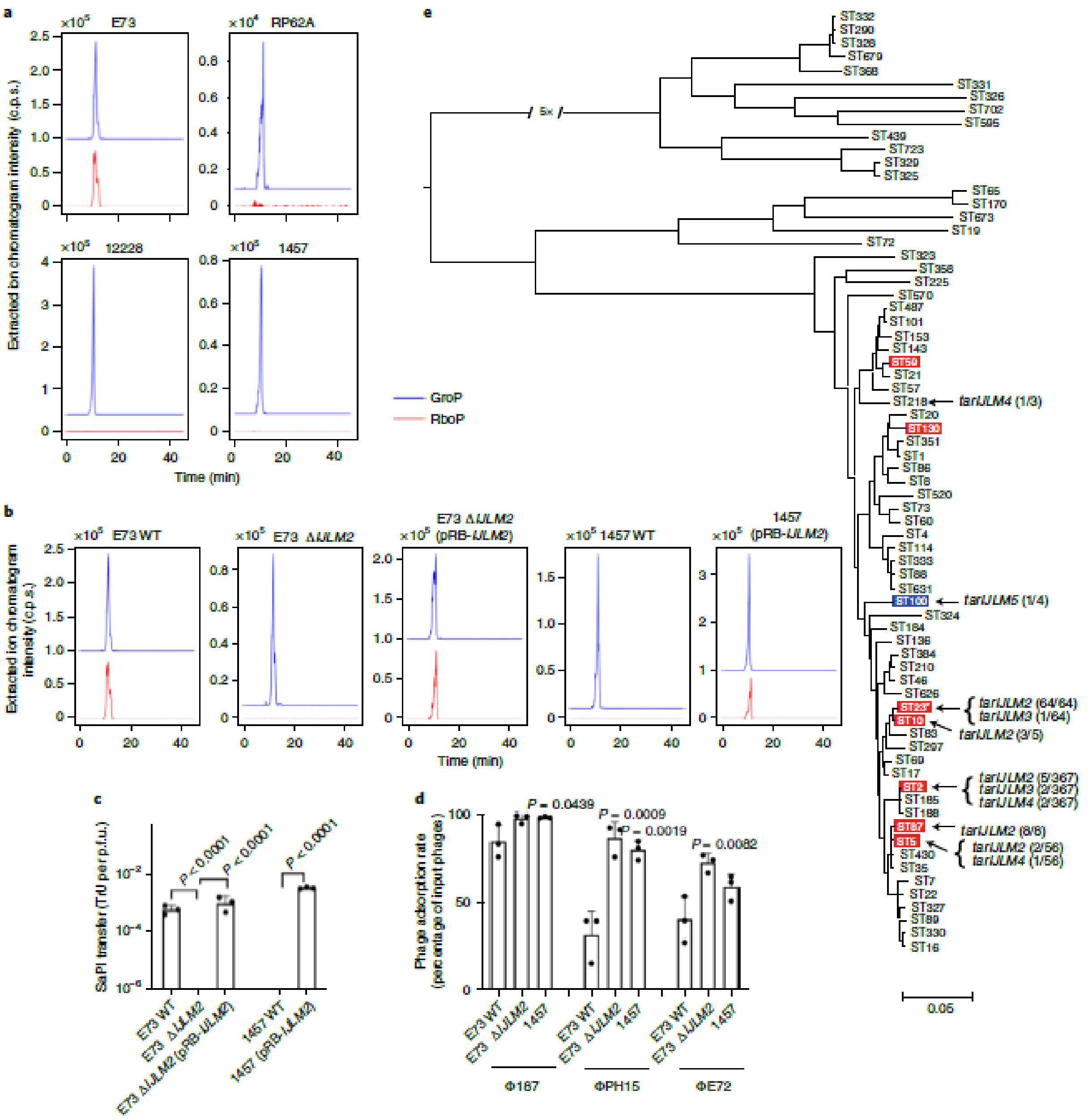

Fig. 2 | *tarIJLM* genes are responsible for RboP-WtA synthesis in *S. epidermidis* and are found in HA-MRSE clones. a, All tested *S. epidermidis* strains contain GroP (blue lines, [M + H]+ = 173.022), but only the *tarIJLM2*-positive E73 has also RboP (red line, [M + H]+ = 233.042) as WTA constituents. Counts per second (c.p.s.) measured by LC–MS are shown. b, Disruption of *tarIJLM2* abolishes RboP-WTA production in strain E73, while transformation of strain 1457 with the *tarIJLM2*-expressing plasmid pRB-IJLM2 confers RboP-WTA production. c, Expression of *tarIJLM2* enables *S. epidermidis* to accept SaPIbov1 from transducing *S. aureus* phage Φ11. Data are expressed as the mean ± s.d. Significant differences of E73 wild type (WT) versus E73 ΔIJLM2 ($P < 0.0001$) and E73 ΔIJLM2 (pRB-IJLM2) versus E73 ΔIJLM2 ($P < 0.0001$) were calculated by one-way analysis of variance (ANOVA) with Dunnett's post-test (two-sided). Significant difference of 1457 (pRB-IJLM2) versus 1457 WT ($P = 0.0000000024$) was calculated by unpaired t-test. Strains without a bar had not yielded any transductant. d, Inactivation of *tarIJLM2* in *S. epidermidis* E73 leads to increased binding of the GroP-WTA-specific phages Φ187, ΦPH15 and ΦE72. Values represent the mean ± s.d. of three independent experiments in c and d.

Significant differences versus E73 WT (P ≤ 0.05) were calculated by one-way ANOVA with Dunnett's post-test (two-sided). e, *tarIJLM2*–5 are almost exclusively found in *S. epidermidis* clones that are predominantly HA (red) or livestock-associated (blue)25 and have probably been repeatedly imported by HGT. Since the definition of *S. epidermidis* healthcare-association is ambiguous, only clones implicated with the healthcare system in at least three independent studies3,4,18,20,21,23,24 were labelled red. ST218 has also sporadically been found to cause infections23. Maximum-likelihood phylogeny of 71 *S. epidermidis* isolates representing major STs was inferred from an alignment of 87,048 core genome SNPs. The isolates represent different multilocus STs among 497 *S. epidermidis* genomes present in the NCBI Reference Sequence Database (accessed 3 July 2018), a global collection of 227 *S. epidermidis* isolates originating from 96 institutions across 24 countries3 and 25 *tarIJLM*-positive clinical *S. epidermidis* isolates collected in this study (Supplementary Table 2). The number of isolates carrying different variants of *tarIJLM* (Supplementary Table 1) together with the total number of genomes within each ST are indicated. ST23, which includes three previously unknown single-locus variants, is marked with an asterisk. Phylogenetic reconstruction was carried out using the maximum-likelihood program PhyML with a GTR model of nucleotide substitution, and support for the nodes was assessed using aBayes (Methods). The length of the broken branch was reduced by fivefold. The tree was midpoint rooted. The scale bar denotes substitutions per variable sites.

RboP-WTA impairs *S. epidermidis* epithelial binding and colonization. The absence of *tarIJLM2*-positive *S. epidermidis* from human arm skin and nose raised the question of whether RboP-WTA may impair the capacity of *S. epidermidis* to bind epithelial surfaces. E73 wild type and E73Δ*tarIJLM2* did not differ in their capacity to bind to the matrix protein fibronectin (Fig. 3a), which indicates that RboP-WTA did not change the general adhesive properties of E73. However, E73Δ*tarIJLM2* bound twofold better to the human airway epithelial A549 cell line and to primary human nasal epithelial cells (HNEpCs) than the parental strain (Fig. 4a,b). This interaction was blocked by the scavenger-receptor-specific ligand polyinositol31,32 (Extended Data Fig. 7a), which suggests that GroP-WTA may pro- mote the binding to epithelial receptors better than RboP-WTA. Similarly, the GroP-WTA-expressing *S. epidermidis* 1457 bound significantly better to A549 cells than the same strain expressing *tarIJLM2* (Extended Data Fig. 7b). These data reflect previous findings on the crucial role of the WTA structure for *S. aureus* to bind scavenger receptors on nasal epithelia32. E73Δ*tarIJLM2* also exhibited a 2.1-fold increased nasal colonization capacity compared with the parental strain in a mouse model when inoculated alone or in competition with the parental strain (Fig. 4c,d). This result provides support for the capacity of *tarIJLM2* to interfere with nasal epithelial binding and may explain the absence of *tarIJLM*-positive isolates from the human nose.

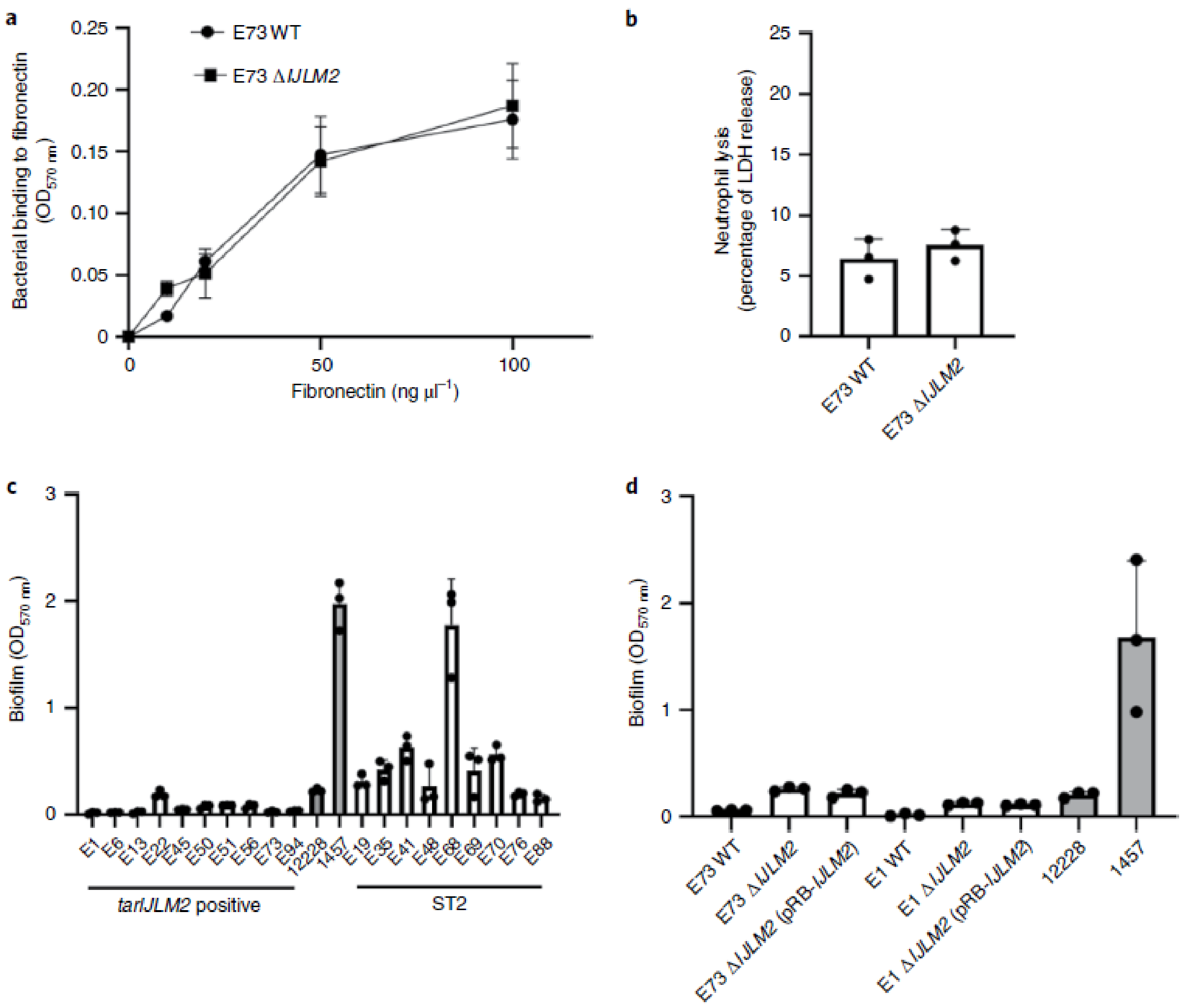

Fig. 3 | RboP-WtA production does not affect the fibronectin binding, cytotoxic or biofilm-forming capacity of *S. epidermidis*. a, Dose-dependent binding of E73 WT and E73 Δ*IJLM2* to microtitre plates coated with the indicated fibronectin concentrations. b, *S. epidermidis* E73 and E73 Δ*IJLM2* culture filtrates do not differ in their ability to lyse human neutrophils, as measured by the release of lactate dehydrogenase (LDH). c, In contrast to typical ST2 strains, *tarIJLM*-positive ST5 (E51 and E56), ST10 (E22), ST23 (E6, E13, E50 and E73) and ST87 (E1, E45 and E94) isolates do not produce a notable biofilm on polystyrene microtitre plates, although some of them contained the *icaADBC* locus (E6, E13, E50 and E73) required for synthesis of the biofilm-promoting intercellular adhesion glycopolymer38. d, Knockout of *tarIJLM2* does not alter biofilm formation by *S. epidermidis* E73 (ST23) or E1 (ST87). The laboratory *S. epidermidis* strains ATCC12228 (biofilm negative) and 1457 (biofilm positive) were included as control strains. The mean ± s.d. of three independent experiments are shown (a–d).

RboP-WTA production increases the virulence of *S. epidermidis*. The exclusive association of *tarIJLM2* with *S. epidermidis* isolates from infections raised the question of whether the altered WTA may increase HA-MRSE virulence. E73 and E73Δ*tarIJLM2* had the same low degree of cytotoxicity for human cells (Fig. 3b). ST2 clones are known for their particular capacity to form biofilms on plastic surfaces, which is believed to contribute to their invasive- ness33–35. Several ST2 isolates from our collection indeed formed biofilms on polystyrene plates (Fig. 3c). However, none of the *tarIJLM2*–positive ST10, ST23 or ST87 isolates produced a notable biofilm compared with the biofilm-negative and -positive model strains ATCC12228 (ref. 36) and 1457 (ref. 37), respectively, although some of them contained the *icaADBC* locus that is required for synthesis of the biofilm-promoting intercellular adhesin glycopolymer38. Moreover, the biofilm-forming capacity of E73 (ST23) and E1 (ST87) was not altered by deletion of *tarIJLM2* (Fig. 3d). Thus, the altered WTA of *tarIJLM*-bearing isolates does not seem to affect the intrinsically low capacity of *S. epidermidis* ST10, ST23 and ST87 to form biofilms, which suggests that there may be another reason for the increased invasiveness of RboP-WTA-expressing clones. Since WTA composition has been found to shape the ability of *S. aureus* to adhere to endothelial cells39, it was tempting to assume that RboP-WTA is overrepresented among invasive *S. epidermidis* to promote endothelial cell interactions. In contrast to airway epithelial cells, human endothelial cells were significantly less effectively bound by E73Δ*tarIJLM2* compared with the parental and complemented mutant strains (Fig. 4e). Conversely, the exclusively GroP-WTA-expressing strain 1457 bound 1.7-fold better to endothelial cells following ectopic expression of *tarIJLM2* (Extended Data Fig. 7c).

Together, these findings suggest that RboP-WTA promotes the ability of *S. epidermidis* to persist in the bloodstream. In line with this assumption, significantly lower numbers of E73Δ*tarIJLM2* cells were found in the bloodstream of intravenously infected mice compared with the parental strain, and this ratio was similar when mutant and parental strains were simultaneously injected into the same animals (Fig. 4f,g). Following binding to endothelial cells, *S. epidermidis* can leave the vasculature to form abscesses in peripheral organ tissues. In agreement with their stronger ability to bind endothelial cells, E73 wild-type cells were more abundant in the kidneys of intravenously infected mice compared with E73Δ*tarIJLM2* cells (Fig. 4h). Moreover, mice infected with the mutant exhibited strongly reduced mortality compared with the wild-type strain (Fig. 4i). Thus, RboP-WTA renders *S. epidermidis* more virulent in invasive infections, presumably by increasing its capacity to interact with blood vessel walls.

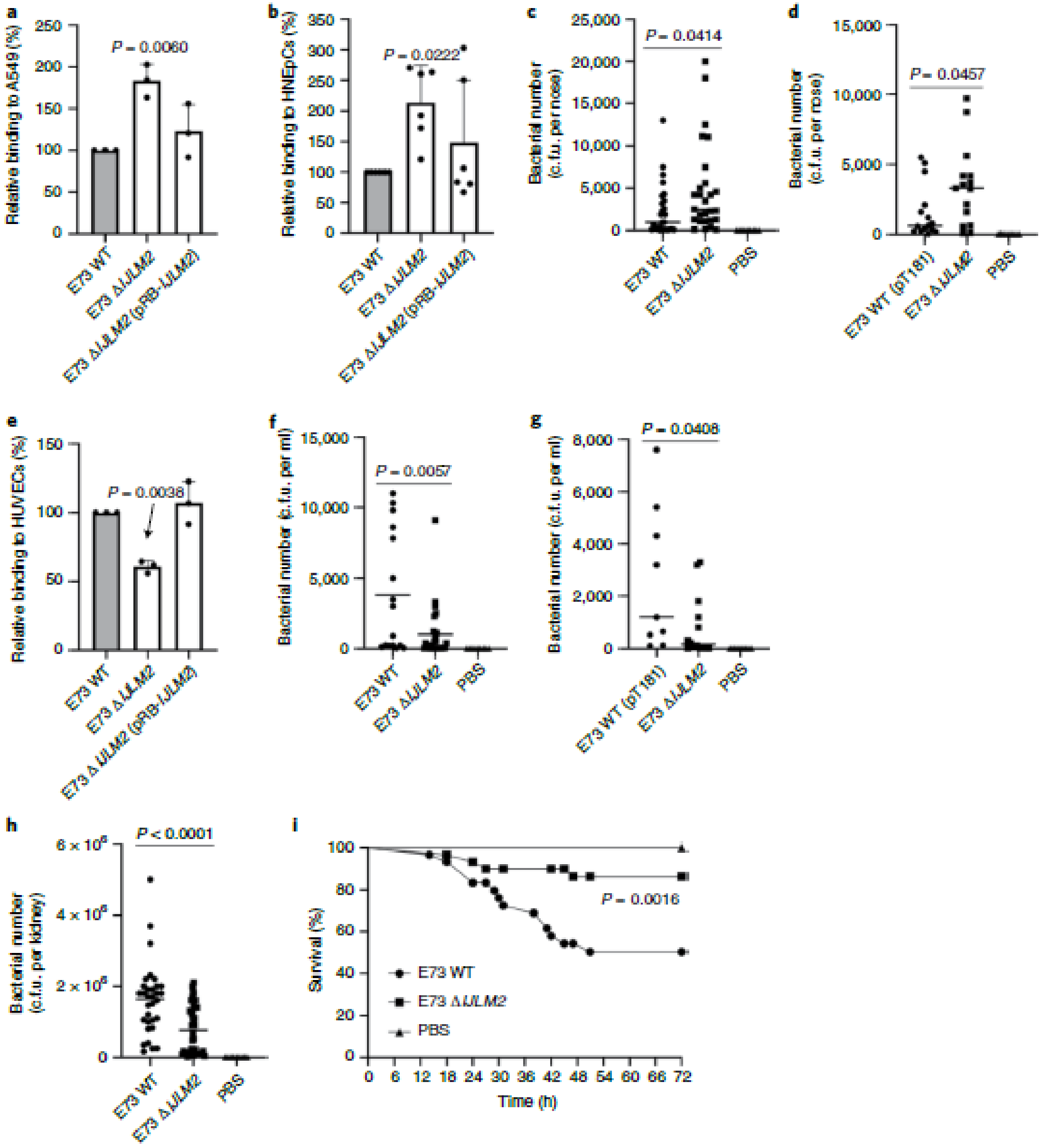

Fig. 4 | RboP-WtA impairs colonization but increases infection capacities of *S. epidermidis*. a–d, RboP-WTA production decreases *S. epidermidis* binding to the human airway epithelial cell line A549 (a) and to primary HNEpCs (b). The E73Δ*tarIJLM2* mutant colonized mouse noses significantly better than the WT when the two strains were used to inoculate separate animals (c) or the same animals as a 1:1 mixture (d). e, RboP-WTA production promotes *S. epidermidis* binding to HUVECs. f,g, Blood of E73Δ*tarIJLM2*-infected mice contained lower c.f.u. compared with WT-infected mice at 72 h post-infection in a bacteraemia model when the two strains were used to infect separate animals (f) or the same animals as a 1:1 mixture (g). h, RboP-WTA production leads to significantly increased numbers of bacteria in the kidneys of intravenously infected mice (P = 0.000022). i, Strain E73 is attenuated for virulence after deletion of *tarIJLM2*, as shown in survival curves from a mouse bacteraemia model using individual bacterial strains. The mean ± s.d. of three independent experiments are shown in a, b and e. Dot plots with medians are shown in c, d and f–h, with each dot representing one sample from each mouse. Significant differences (P ≤ 0.05) were calculated by one-way ANOVA with Dunnett's post-test (two-sided) in a, b and e (versus WT), by unpaired t-test in c, d and f–h or log-rank (Mantel–Cox) test in i.

Discussion

WTA is essential for efficient attachment to epithelial cells and for nasal colonization by *S. aureus*40 since it facilitates binding to scavenger receptors that interact with zwitterionic bacterial polymers such as WTA32,41. However, the diversity and specificity of scavenger receptors on nasal epithelial and potentially on endothelial cells have remained elusive41. Our study indicated that the type of WTA is crucial for *S. epidermidis* interactions with human epithelial and endothelial cells and that RboP- and GroP-WTA differ in their impact on the adhesive properties for different human cell types, thereby shaping the colonization and invasion capacities of several HA-MRSE clones. WTA is essential for *S. aureus* nasal colonization in addition to several surface-anchored proteins40,42,43. Our study suggests that GroP-WTA may promote nasal colonization even more efficiently than RboP-WTA, which is reflected by the higher prevalence of commensal *S. epidermidis* in the human nose (almost 100%) compared to *S. aureus* (~30% of the population)44,45. The fact that RboP-WTA-producing HA-MRSE strains do not seem to colonize human noses and skin of the arms raises the question of which niches they may use as their major reservoirs. An in-depth characterization of potential habitats on other human body sites or in specific HA environments may help find such niches, whose colonization may not be impaired or may even be promoted by the production of RboP-WTA.

The various HA-MRSE clones seem to use different virulence strategies. While ST2 isolates usually are strong biofilm formers but contain only rarely *tarIJLM* gene clusters, all known ST23 and ST87 isolates bear *tarIJLM* but appear to be poor biofilm formers. Future studies will show if these differences in bacterial properties may be reflected by different courses of infection. Future infection-control regimes will rely on biomarkers in pathogen genomes that will enable the stratification of risks associated with colonization or infection by a specific pathogen clone46. The *tarIJLM* cluster rep- resents one of the few *S. epidermidis* determinants with a strong link to invasiveness and virulence, although it is used only by a subfraction of the invasive HA-MRSE clones. Nevertheless, it may be included as an indicator in surveillance programmes of this globally important pathogen. It is worth noting that a tarIJL cluster is also found in an epidemic lineage of the opportunistic pathogen Staphylococcus capitis, which causes severe infection outbreaks among newborns47. Protein-conjugated RboP-WTA represents a promising antigen for future preventive or therapeutic vaccines against *S. aureus*48. Our study suggests that such vaccines could also protect against RboP-WTA-producing HA-MRSE and other CoNS clones. Development of an anti-Staphylococcus vaccine remains a major challenge though. A detailed understanding of the structure and variability of surface antigens will be essential for success48.

Methods

Bacterial strains and growth conditions. *S. epidermidis* laboratory strains RP62A, ATCC12228 and 1457 were used as controls for WTA analytical and phenotypic experiments. *S. aureus* strains RN4220 and PS187 were used as phage propagation and as test strains for phage binding and transduction experiments. *S. aureus* JP1794 (ref. 49) and PS187-H VW1 (ref. 15) were used as donor strains for SaPI particle propagation as described below. Escherichia coli DC10B was used as the cloning host. RN4220 and PS187ΔsauUSIΔhsdR50 were used as donor strains for plasmid transduction. *S. epidermidis* and *S. aureus* strains were cultivated in tryptic soy broth (TSB) medium or Mueller–Hinton broth (MHB), unless otherwise noted, and incubated at 37 °C on an orbital shaker. E. coli strains were cultivated in lysogeny broth (LB). Media were supplemented with appropriate antibiotics (tetracycline (5 μg ml−1), chloramphenicol (10 μg ml−1) or ampicillin (100 μg ml−1)). *S. epidermidis* isolates were obtained from clinical specimens or from nasal (anterior nasal mucosa of both nostrils) or skin (elbow pit of both arms) swabs from healthy volunteers. Bacteria were plated on blood agar plates immediately after swabbing, Colonies were analysed by matrix-assisted laser desorption–ionization time-of-flight (MALDI–TOF) mass spectrometry (MS) for species determination. Because many *S. epidermidis* isolates from clinical samples are known to result from contaminating skin bacteria, strict criteria were used for the definition of true clinical isolates. These included the repeated isolation of the same strain at two different days and the origin from a typical infection site such as a blood culture or infected implant.

SaPI transfer and phage-adsorption assays. SaPI-transfer experiments were performed according to standard procedures15. Briefly, approximately 8.0 × 107 cells of a recipient strain grown overnight were mixed with 100 μl of lysates obtained from *S. aureus* strain JP1794 or PS187-H VW1 bearing the tetracycline-resistance marker-labelled SaPIbov1 (~1.0 × 106 p.f.u. ml−1), incubated for 15 min at 37 °C, diluted and plated on tetracyclin-containing TSB agar to count transductant colonies.

The adsorption efficiency of Φ11, Φ187, ΦPH15 and ΦE72 was determined as previously described with minor modifications15. Briefly, adsorption rates were analysed using a multiplicity of infection (m.o.i.) of 0.1. The adsorption rate was elucidated by determining the number of unbound phages in the supernatant and dividing the number of bound phages by the number of input phages.

The *S. epidermidis* phage phiE72 was isolated by incubating the clinical *S. epidermidis* isolate E72 with 5 μg ml−1 mitomycin C overnight at 30 °C, adding the culture supernatant to agar plates with lawns of the laboratory strain *S. epidermidis* 1457. Phage plaques were isolated and used to infect strain 1457 again to generate phage lysates. The genome of ΦE72 was sequenced, which showed that ΦE72 is a previously unknown member of the siphovirus phage family. The ability of ΦE72 to infect *S. epidermidis* strain 1457, which produces only GroP-WTA, showed that ΦE72 recognizes GroP-WTA.

Whole-genome sequencing. Whole-genome sequences were generated for the 25 *tarIJLM*-positive *S. epidermidis* isolates collected in this study (Table 1 and Supplementary Table 1). Bacterial DNA was extracted from mechanically or lysostaphine-lysed bacterial cells and quantified using a DNeasy Blood and Tissue kit (Qiagen) and a Qubit 3.0 Fluorometer (Invitrogen), respectively. Libraries were prepared with a Nextera XT DNA library prep kit (Illumina) or a NEBNext Ultra library prep kit (New England Biolabs) after shearing the DNA to fragments of 300 bp on a Bioruptor Pico instrument (Diagenode), and then sequenced on a MiSeq platform (Illumina) with 2 × 251 bp using a MiSeq Reagent kit v2 or on a NextSeq platform with 2 × 150 bp using a NextSeq 500/550 v2 kit. Velvet (v.1.2.10)51 or SPAdes (v.3.11.1)52 was used to generate de novo assemblies. *S. epidermidis* E73 was also sequenced using the PacBio Sequel platform. DNA was sheared to 10-kb fragments using g-TUBEs (Covaris). SMRTbell libraries were constructed using standard procedures (Pacific Biosciences). The genome was de novo assembled using the Hierarchical Genome Assembly Process (HGAP4) workflow in SMRT Link (v.5.1.0.26411; Pacific Biosciences). A second de novo assembly was made based on Illumina sequencing, and the combination of the sequence contigs resulted in the final genome, which was confirmed by mapping the Illumina reads to the final assembly. The circular chromosome was annotated using the NCBI Prokaryotic Genome Annotation Pipeline.

Sequence analyses. The *tarIJLM2* genes in E73 (Fig. 1b) were used as queries in BLASTN searches against 497 *S. epidermidis* genomes present in the NCBI Reference Sequence Database (accessed 3 July 2018), a global collection of 227 *S. epidermidis* isolates originating from 96 healthcare institutions across 24 countries1, and the 25 *S. epidermidis* isolates collected in this study (Table 1). Multilocus sequence typing (MLST) was performed by comparing contigs with the *S. epidermidis* MLST database53. SCCmec typing was carried out with SCCmecFinder (v.1.2)54. IS elements were classified according to transposase gene similarity by using BLAST analysis with the ISfinder database55.

Phylogenetic analyses. Mapping of sequence reads and single-nucleotide polymorphism (SNP) calling were carried out using the Northern Arizona SNP pipeline (v.1.0.0)56. In brief, sequence reads were mapped against the *S. epidermidis* ST2 reference isolate BPH0662 (GenBank accession number NC_017673) using the Burrows–Wheeler Alignment tool57. SNP calling was achieved using the GATK Unified Genotyper58,59 with the following parameters: ≥10× mapping coverage; ≥90% unambiguously base calls; and insertions and deletions were ignored. SNPs contained in repeats, as determined by NUCmer60,61, were excluded. Next, phages in BPH0662 were identified with PHASTER62, and SNPs residing within these were manually removed from the alignment, whereafter Gubbins (v.2.3.4)63 was used to remove recombination tracts. The MUSCLE algorithm64 was used to construct multiple sequence alignments for each of the *tarIJLM* genes and to calculate pairwise nucleotide identities. A subset of *tarIJLM* genes (Fig. 1b) representing the diversity observed within *S. epidermidis* was used as queries in BLASTN searches against non-*S. epidermidis* genomes present in the NCBI Reference Sequence Database (accessed 29 October 2018). Phylogenetic reconstruction was carried out using the maximum-likelihood program PhyML (v.3.0) with a GTR model of nucleotide substitution65,66. Support for the nodes was assessed using aBayes67.

Specific PCR screening for different types of *tarL* genes. Isolates were screened for different variants of *tarL* genes by PCR amplification using the primers listed in Supplementary Table 3. The following thermocycler conditions for amplification were used: 98 °C for 2 min, 98 °C for 30 s, 55 °C for 30 s, 72 °C for 1 min, 72 °C for 10 min, 32 cycles. The PCR products were confirmed by sequencing (Eurofins).

Cell wall and WTA isolation. Cell walls and WTA were isolated as previously described40. Briefly, bacteria were grown overnight in TSB supplemented with 0.25% glucose. Bacterial cells were disintegrated with a FastPrep-24 instrument (MP Biomedicals). Lysates were incubated overnight with DNase I (40 units per ml; Roche) and RNase A (80 units per ml; Sigma) at 37 °C, sonicated and washed with sodium dodecyl sulfate. WTA was then released from cell walls by treatment with 5% trichloroacetic acid dialysed against pyrogen-free water (Ambion), and quantified by phosphate assay as previously described40. To quantify the WTA amount per cell, 300 µl cell wall suspension was mixed with 300 µl 1 M NaOH and incubated at 60 °C with constant shaking at 600 r.p.m. After 2 h, the phosphate content in supernatants of this mixture was measured as described above. The same amount of 300 µl cell wall was dried in a Speedvac concentrator and weighted to determine the phosphate amount per cell wall dry mass.

WTA chromatography and MS analysis. The composition of pure WTA samples was determined by methanolysis of the samples with 0.5 m HCl/MeOH at 85 °C for 45 min followed by peracetylating twice using acetic anhydride and pyridine (1:1, v/v) at 85 °C for 10 min and detection by gas–liquid chromatography (GLC) and GLC–MS. The systems used were an Agilent Technologies 7890A instrument equipped with a HP-5MS capillary column (30 m × 0.25 mm, film thickness 0.25 µm) and applying a temperature gradient of 150 °C (kept for 3 min) to 250 °C at 3 °C min−1 for GLC or an Agilent Technologies 7890A instrument equipped with a dimethylpolysiloxane column (Agilent, HP Ultra 1, 12 m × 0.2 mm, film thickness 0.33 µm) and 5975C series MSD detector with electron impact ionization (EI) mode under autotuned condition at 70 eV applying a temperature gradient of 70 °C (kept for 1.5 min) to 110 °C at 60 °C min−1 and then to 320 °C at 5 °C min−1. For the WTA sample of E73 wild type, the absolute configuration was determined by GLC by comparison with authentic standards of the acetylated (S)-2-butanol glycoside derivative after butanolysis (2 M HCl, (S)-2-butanol at 85 °C for 2 h) and acetylation as previously described68. The same system was used for detection, applying a temperature gradient of 120 °C (kept for 3 min) to 320 °C at 3 °C min−1. Identification of the WTA polymer type was performed using an Ultimate 3000RS HPLC system (Dionex) coupled to a micrOTOFII electrospray-ionization (ESI) TOF mass spectrometer (Bruker). For HPLC, a Gemini C18 column (150 × 4.6 mm, 110 Å, 5 µM, Phenomenex) was used at 37 °C with a flow rate of 0.2 ml min−1. A 5-min equilibration step with 100% buffer A (0.1% formic acid, 0.05% ammonium formate) was applied, followed by a linear gradient of 0 to 40% buffer B (acetonitrile) for 30 min. A final washing step with 40% buffer B for 5 min and a re-equilibration step (100% buffer A) for 5 min completed the method. Samples were ionized via ESI in positive-ion mode. Exact masses in positive-ion mode for GroP [M + H]+ = 173.022 m/z and RboP [M + H]+ = 233.042 m/z were presented as extracted ion chromatograms with Data Analysis (Bruker). Base peak chromatograms were used for sample normalization.

Nuclear magnetic resonance microscopy. Experiments were carried out in D2O at 300 K. All one-dimensional (1H and 13C) and two-dimensional homonuclear (COSY, TOCSY and ROESY) and heteronuclear (HSQC-DEPT and HMBC) experiments were recorded with a Bruker AvanceII 700 MHz spectrometer (operating frequencies of 700.43 MHz for 1H nuclear magnetic resonance (NMR), and 176.13 MHz for 13C NMR) using standard Bruker software. COSY, TOCSY and ROESY were recorded using datasets (t1 by t2) of 4,096 by 512 points, and four scans (E73 wild type, 1457 wild type and 1457 (pRB-*IJLM2*)), two scans (E73 Δ*tarIJLM2*) or one scan (E73 Δ*tarIJLM2* (pRB-IJLM2)) were acquired for each t1 value in the case of COSY, eight scans (E73 wild type, E73 Δ*tarIJLM2*, E73 Δ*tarIJLM2* (pRB-IJLM2) and 1457 (pRB-*IJLM2*)) or 16 scans (1457 wild type) in the case of TOCSY and eight scans in the case of ROESY. The TOCSY experiment was carried out in the phase-sensitive mode with mixing times of 120 ms. The 1H–13C correlations were measured in the 1H-detected mode via HSQC-DEPT with proton decoupling in the 13C domain acquired using datasets of either 4,096 by 512 points (16 scans for each t1 value in the case of E73 Δ*tarIJLM2* and E73Δ*tarIJLM2* (pRB-*IJLM2*); 48 scans for each t1 in the case of 1457 wild type and 1457 (pRB-*IJLM2*) or 4,096 by 1,024 points (32 scans for each t1 in the case of E73 wild type). The HMBC spectra were acquired using datasets of 4,096 by 512 points and either 32 scans (E73 Δ*tarIJLM2* and 1457 wild type), 36 scans (E73Δ*IJLM2*(pRB-*IJLM2*)), 104 scans (E73 wild type) or 128 (1457(pRB-*IJLM2*)) for each t1 value. Chemical shifts are reported relative to external acetone (1H, 2.225; 13C, 31.50).

Molecular genetic methods. For the construction of the Δ*tarIJLM2* mutant in *S. epidermidis* E73, the pBASE6-erm/lox1 shuttle vector was used according to standard procedures69. For mutant complementation experiments, plasmid pRB474 was used70. The primers for knockout and complementation plasmid construction are listed in Supplementary Table 3. Plasmid transduction to *S. epidermidis* strains was performed using Φ11 with *S. aureus* RN4220 as the donor strain or Φ187 as the transduction phage with *S. aureus* PS187 as the donor strain according to the method by Winstel et al.50.

RNA isolation and qRT–PCR. Bacterial cultures grown overnight in TSB were diluted in fresh TSB, PBS with 50% pooled heat-inactivated human serum from healthy donors, or synthetic nasal medium (SNM3, containing 0.2 mM bipyridine)20 and grown at 37 °C and 180 r.p.m. Bacteria were collected after 6 h (exponential growth phase) and immersed in RNAprotect bacteria reagent (Qiagen), and washed and resuspended in RLT lysis buffer, followed by mechanical lysis with a bead-beating homogenizer (Precellys). RNA was extracted from the lysate with a RNeasy Mini kit (Qiagen), transcribed into complementary DNA with iScript reverse transcriptase (Bio-Rad), and quantitative PCR with reverse transcription (RT–qPCR) was performed on a LightCycler480 instrument (Roche). Transcription levels of tarL1 and tarL2 were normalized against the expression of the constitutively transcribed gyrB, rho and tpiA housekeeping genes. PCR set-up, cycling conditions and assays for housekeeping genes were as previously described29. Each experiment was performed in biological and technical duplicates. qPCR results were analysed in LightCycler 480 SW 1.5.1. and GenEx software (multiD).

Semiquantitative biofilm assay. *S. epidermidis* biofilm formation was analysed using 96-well Nunc delta microtitre plates as previously described71 with the following modifications. After incubation at 37 °C for 24 h, the cells were washed gently three times in PBS and then stained with 0.1% crystal violet solution. The stain was washed off gently under slowly running water and plates were dried. Finally, 5% acetic acid was added to the wells to dissolve the stain. The absorbance was measured at 570 nm using a MicroELISA autoreader (Bio-Rad).

Adherence of *S. epidermidis* to immobilized fibronectin. Nunc delta microtitre plates were coated with fibronectin (Sigma) in carbonate-coating buffer (15 mM Na2CO3, 35 mM NaHCO3, pH 9.6). and incubated overnight at 4 °C. BSA (5 mg ml−1 in PBS) was added and incubated for 2 h at 37 °C. The plates were then washed three times with PBS. A bacterial cell suspension (A600 nm = 1.0 in PBS) was added and incubated for 1.5 h at 37 °C. Plates were washed three times with PBS and bound cells were fixed with formaldehyde (25% v/v) for 30 min followed by staining with crystal violet (0.5% v/v, 100 µl per well) for 1 min. After three washes with PBS, acetic acid (5% v/v) was added (100 µ per well) for 10 min at room temperature. The absorbance was measured at 570 nm.

Fluorescein isothiocyanate labelling of *S. epidermidis* cells. Overnight-grown *S. epidermidis* cultures were diluted in fresh MHB and grown at 37 °C to logarithmic growth phase (OD600 nm = 1.0). Bacteria were then collected, washed three times with PBS labelled with fluorescein isothiocyanate (FITC; 0.1 mg ml−1) for 1 h at 37 °C and washed three times with

PBS, resuspended in RPMI medium (Sigma) and stored at −80 °C. The concentration of FITC-labelled bacteria was determined using a Neubauer chamber.

Cell culture. A549 human bronchial epithelial cells (American Type Culture Collection (ATCC) CCL-185) were grown in DMEM (Gibco-BRL) supplemented with 100 μg ml−1 streptomycin, 100 U ml−1 penicillin, 10% heat-inactivated fetal bovine serum and 2 mM glutamine. Human umbilical vein endothelial cells (HUVECs) cryopreserved from pooled donors were purchased from PromoCell (C-12203) and grown in endothelial cell growth medium (PromoCell). Primary human nasal epithelial cells (HNEpCs) cryopreserved from normal human nasal mucosa of pooled donors were purchased from PromoCell (C-12620) and grown in airway epithelial cell growth medium. All cells used here were grown at 37 °C under 5% CO2. A549, HUVECs and HNEpCs were used until passage nine, seven and five, respectively.

Lysis of human neutrophils. Lysis of human neutrophils by culture filtrates of *S. epidermidis* was analysed as previously described72. Briefly, *S. epidermidis* strains were cultivated for 18 h in TSB medium. The culture supernatant was sterilized by filtration. After 1:5 dilution with RPMI, 100 μl culture filtrate was mixed with 100 μl human neutrophil suspension containing 105 cells, isolated by standard procedure72, and incubated for 1 h at 37 °C. The ability of bacteria to cause cell lysis was quantified by measuring the release of cytoplasmic lactate dehydrogenase (LDH) (Cytotoxicity Detection kit, Roche Diagnostics).

Interaction of *S. epidermidis* with epithelial or endothelial cells. The capacity of *S. epidermidis* to adhere to epithelial or endothelial cells was analysed as previously described40. Briefly, approximately 1 × 106 A549 cells, HNEpCs or HUVECs were seeded onto ibiTreat slides (Ibidi) to form confluent cell monolayers. Cells were grown at 37 °C under 5% CO2 in appropriate cell culture media. The cells were washed twice with DMEM (A549) or DMEM-F12 (HUVECs and HNEpCs) and inoculated with FITC-labelled bacteria at a m.o.i. of 100 for 1 h at 37 °C under 5% CO2. To mimic the liquid flow in nose and bloodstream, peristaltic pumps (Amersham) were used during infection (30 min) with FITC-labelled bacteria at a flow rate of 1 ml h−1 at 0.3 dynes cm−2. The nuclei and cytoskeletons of the cells were stained with 4′,6-diamidino-2-phenylindole and phalloidin tetramethylrhodamine B isothiocyanate, respectively. Bacteria were fixed using 3.5% paraformaldehyde (PFA) in PBS at room temperature. PFA was removed and wells were coated with 1 ml PBS. No morphological changes of bacterial or human cells were observed after this procedure. Bacteria adhering to epithelial or endothelial cells were counted using a confocal microscope. To assess whether scavenger receptors are involved in the cell binding process, A549 cells were pre-incubated for 30 min with different concentrations of the polyanionic scavenger receptor ligand poly I (Sigma). After washing with DMEM, cells were used in binding assays with FITC-labelled bacteria as described above.

Mouse experiments. Female 4–6-week-old BALB/c mice, kept at a temperature of 20–25 °C, relative humidity of 40–70% and light–dark alternation times of 12–14/12–10 h, and bacterial cells grown in TSB to mid-exponential growth phase (OD 600 nm = 1.0), washed, and resuspended in sterile PBS, were used for all animal experiments.

For the nasal colonization model, 27 mice per bacterial strain were given water containing kanamycin (25 μg ml−1) for 3 days before infection. The inoculum, which contained 1010 colony forming units (c.f.u.) in 10 μl PBS or PBS alone, was pipetted slowly onto the nares of anaesthetized mice without touching the skin with the pipette tip. Three days after inoculation, mice were euthanized, nasal regions were wiped externally with 70% ethanol and the nasal tissues were homogenized in 0.5 ml of TSB. The total number of *S. epidermidis* c.f.u. per nose was assessed by plating 100 μl diluted nasal suspensions on TSA with 5% sheep blood and enumerating colonies after overnight growth at 37 °C.

To study the capacity of strain E73 and its mutant E73ΔIJLM2 to compete with each other during nasal colonization, E73 was transformed with plasmid pT181 rendering the strain resistant to tetracycline to allow its discrimination from the tetracyclin-susceptible E73ΔIJLM2. The two strains grew equally well in TSB medium and the plasmid was almost 100% maintained in E73 over 72 h even without antibiotic selection (equal c.f.u. on antibiotic-selective and nonselective plates) (Extended Data Fig. 8). The two strains were mixed 1:1 in PBS. A total of 10 μl of the suspension containing 1010 c.f.u. of or 10 μl PBS alone were used to colonize the mouse nares as described above. Homogenized tissue samples were plated on TSA with 5% sheep blood with or without tetracycline (25 μg ml−1) for strain distinction and determination of c.f.u.

For the bacteraemia model, 30 anaesthetized mice per bacterial strain received 1011 c.f.u. of E73 wild type or mutant in 0.1 ml PBS or PBS alone by retro-orbital injection via the right eye. After inoculation, general animal health condition and disease advancement were regularly monitored for up to 72 h. Evaluation of animal morbidity was based on the following criteria: hunched posture, activity levels, ruffled fur and laboured breathing. All surviving mice were euthanized at 72 h post-infection. The blood and kidney samples were plated on TSA with 5% sheep blood to measure c.f.u. of *S. epidermidis* in blood.

To study the capacity of strain E73 wild type (pT181) and its mutant E73ΔIJLM2 to compete with each other during systemic infection, 1:1 mixture of the two strains with 1011 c.f.u. in 100 μl PBS or 100 μ PBS alone were used to infect mice by retro-orbital injection as described above. The mortality was monitored, and blood samples were obtained after 72 h and plated on TSA with 5% sheep blood with or without tetracycline (25 μg ml−1) for strain distinction and determination of c.f.u. in blood.

Statistical analysis. Statistical analysis was performed using the Prism 8.0 package (GraphPad Software). P values of ≤0.05 were considered significant.

Ethics statement. Bacterial samples from human volunteers were collected after written informed consent and approval by the institutional review boards of the Universities of

Tübingen (577/2015A) and Shanghai Jiaotong University (protocol 2017001). Isolates from Hamburg were obtained in accordance with Section 12 of the Hamburg Hospital Law (HmbKHG). All mouse work was performed in China, which was approved by the Ethics Committee of Renji Hospital, School of Medicine, Shanghai Jiaotong University.

Reporting Summary.

Further information on research design is available in the Nature Research Reporting Summary linked to this article.

Data availability

The whole-genome sequence data from this study were deposited in the NCBI Sequence Read Archive; the accession numbers can be found in Supplementary Table 1. Source data are provided with this paper. Additional information can be obtained from the corresponding author upon reasonable request.

Received: 9 November 2020; Accepted: 20 April 2021;
Published online: 24 May 2021

References

1. Becker, K., Heilmann, C. & Peters, G. Coagulase-negative staphylococci. Clin. Microbiol. Rev. 27, 870–926 (2014).
2. Byrd, A. L., Belkaid, Y. & Segre, J. A. The human skin microbiome. Nat. Rev. Microbiol. 16, 143–155 (2018).
3. Lee, J. Y. H. et al. Global spread of three multidrug-resistant lineages of Staphylococcus epidermidis. Nat. Microbiol. 3, 1175–1185 (2018).
4. Li, M., Wang, X., Gao, Q. & Lu, Y. Molecular characterization of Staphylococcus epidermidis strains isolated from a teaching hospital in Shanghai, China. J. Med. Microbiol. 58, 456–461 (2009).
5. Meric, G. et al. Disease-associated genotypes of the commensal skin bacterium Staphylococcus epidermidis. Nat. Commun. 9, 5034 (2018).
6. Heilmann, C., Ziebuhr, W. & Becker, K. Are coagulase-negative staphylococci virulent?. Clin. Microbiol. Infect. 25, 1071–1080 (2019).
7. Weidenmaier, C. & Peschel, A. Teichoic acids and related cell-wall glycopolymers in Gram-positive physiology and host interactions. Nat. Rev. Microbiol. 6, 276–287 (2008).
8. Moller, A. G., Lindsay, J. A. & Read, T. D. Determinants of phage host range in Staphylococcus species. Appl. Environ. Microbiol. 85, e00209-19 (2019).

9. Chen, J. et al. Genome hypermobility by lateral transduction. Science 362, 207–212 (2018).

10. Haaber, J., Penades, J. R. & Ingmer, H. Transfer of antibiotic resistance in *Staphylococcus aureus*. Trends Microbiol. 25, 893–905 (2017).

11. Lee, A. S. et al. Methicillin-resistant *Staphylococcus aureus*. Nat. Rev. Dis. Primers 4, 18033 (2018).

12. Penades, J. R. & Christie, G. E. The phage-inducible chromosomal islands: a family of highly evolved molecular parasites. Annu. Rev. Virol. 2, 181–201 (2015).

13. Meric, G. et al. Ecological overlap and horizontal gene transfer in *Staphylococcus aureus* and Staphylococcus epidermidis. Genome Biol. Evol. 7, 1313–1328 (2015).

14. Li, M. et al. MRSA epidemic linked to a quickly spreading colonization and virulence determinant. Nat. Med. 18, 816–819 (2012).

15. Winstel, V. et al. Wall teichoic acid structure governs horizontal gene transfer between major bacterial pathogens. Nat. Commun. 4, 2345 (2013).

16. Fitzgerald, J. R. et al. Characterization of a putative pathogenicity island from bovine *Staphylococcus aureus* encoding multiple superantigens. J. Bacteriol. 183, 63–70 (2001).

17. Maiques, E. et al. Role of staphylococcal phage and SaPI integrase in intra- and interspecies SaPI transfer. J. Bacteriol. 189, 5608–5616 (2007).

18. Brown, S., Santa Maria, J. P. Jr. & Walker, S. Wall teichoic acids of Gram-positive bacteria. Annu. Rev. Microbiol. 67, 313–336 (2013).

19. Winstel, V., Xia, G. & Peschel, A. Pathways and roles of wall teichoic acid glycosylation in *Staphylococcus aureus*. Int. J. Med. Microbiol. 304, 215–221 (2014).

20. Krismer, B. et al. Nutrient limitation governs *Staphylococcus aureus* metabolism and niche adaptation in the human nose. PLoS Pathog. 10, e1003862 (2014).

21. Xia, G. et al. Glycosylation of wall teichoic acid in *Staphylococcus aureus* by TarM. J. Biol. Chem. 285, 13405–13415 (2010).

22. Dean, B. A., Williams, R. E., Hall, F. & Corse, J. Phage typing of coagulase- negative staphylococci and micrococci. J. Hyg. (Lond.) 71, 261–270 (1973).

23. Miragaia, M. et al. Comparison of molecular typing methods for characterization of Staphylococcus epidermidis: proposal for clone definition. J. Clin. Microbiol. 46, 118–129 (2008).

24. Sivadon, V. et al. Partial atlE sequencing of Staphylococcus epidermidis strains from prosthetic joint infections. J. Clin. Microbiol. 47, 2321–2324 (2009).

25. Mertens, A. & Ghebremedhin, B. Genetic determinants and biofilm formation of clinical Staphylococcus epidermidis isolates from blood cultures and indwelling devises. Eur. J. Microbiol. Immunol. 3, 111–119 (2013).

26. Sharma, P. et al. Multilocus sequence typing for interpreting blood isolates of Staphylococcus epidermidis. Interdiscip. Perspect. Infect. Dis. 2014, 787458 (2014).
27. Post, V. et al. Comparative genomics study of Staphylococcus epidermidis isolates from orthopedic-device-related infections correlated with patient outcome. J. Clin. Microbiol. 55, 3089–3103 (2017).
28. Both, A. et al. Distinct clonal lineages and within-host diversification shape invasive Staphylococcus epidermidis populations. PLoS Pathog. 17, e1009304 (2021).
29. Weiser, J. et al. Sub-inhibitory tigecycline concentrations induce extracellular matrix binding protein Embp dependent Staphylococcus epidermidis biofilm formation and immune evasion. Int. J. Med. Microbiol. 306, 471–478 (2016).
30. Wang, L. & Archer, G. L. Roles of CcrA and CcrB in excision and integration of staphylococcal cassette chromosome mec, a *Staphylococcus aureus* genomic island. J. Bacteriol. 192, 3204–3212 (2010).
31. Jiang, Y., Oliver, P., Davies, K. E. & Platt, N. Identification and characterization of murine SCARA5, a novel class A scavenger receptor that is expressed by populations of epithelial cells. J. Biol. Chem. 281, 11834–11845 (2006).
32. Baur, S. et al. A nasal epithelial receptor for *Staphylococcus aureus* WTA governs adhesion to epithelial cells and modulates nasal colonization. PLoS Pathog. 10, e1004089 (2014).
33. Widerstrom, M., McCullough, C. A., Coombs, G. W., Monsen, T. & Christiansen, K. J. A multidrug-resistant Staphylococcus epidermidis clone (ST2) is an ongoing cause of hospital-acquired infection in a Western Australian hospital. J. Clin. Microbiol. 50, 2147–2151 (2012).
34. Ziebuhr, W. et al. Nosocomial infections by Staphylococcus epidermidis: how a commensal bacterium turns into a pathogen. Int. J. Antimicrob. Agents 28, S14–S20 (2006).
35. Du, X. et al. Molecular analysis of Staphylococcus epidermidis strains isolated from community and hospital environments in China. PLoS ONE 8, e62742 (2013).
36. Zhang, Y. Q. et al. Genome-based analysis of virulence genes in a non-biofilm-forming Staphylococcus epidermidis strain (ATCC 12228). Mol. Microbiol. 49, 1577–1593 (2003).
37. Mack, D., Siemssen, N. & Laufs, R. Parallel induction by glucose of adherence and a polysaccharide antigen specific for plastic-adherent Staphylococcus epidermidis: evidence for functional relation to intercellular adhesion. Infect. Immun. 60, 2048–2057 (1992).
38. Otto, M. Staphylococcal biofilms. Microbiol. Spectr. https://doi.org/10.1128/microbiolspec.GPP3-0023-2018 (2018).

39. Weidenmaier, C. et al. Lack of wall teichoic acids in *Staphylococcus aureus* leads to reduced interactions with endothelial cells and to attenuated virulence in a rabbit model of endocarditis. J. Infect. Dis. 191, 1771–1777 (2005).
40. Weidenmaier, C. et al. Role of teichoic acids in *Staphylococcus aureus* nasal colonization, a major risk factor in nosocomial infections. Nat. Med. 10, 243–245 (2004).
41. Schade, J. & Weidenmaier, C. Cell wall glycopolymers of Firmicutes and their role as nonprotein adhesins. FEBS Lett. 590, 3758–3771 (2016).
42. Weidenmaier, C. et al. Differential roles of sortase-anchored surface proteins and wall teichoic acid in *Staphylococcus aureus* nasal colonization. Int. J. Med. Microbiol. 298, 505–513 (2008).
43. Foster, T. J. Surface proteins of Staphylococcus epidermidis. Front. Microbiol. 11, 1829 (2020).
44. Zipperer, A. et al. Human commensals producing a novel antibiotic impair pathogen colonization. Nature 535, 511–516 (2016).
45. Iwase, T. et al. Staphylococcus epidermidis Esp inhibits *Staphylococcus aureus* biofilm formation and nasal colonization. Nature 465, 346–349 (2010).
46. Ladner, J. T., Grubaugh, N. D., Pybus, O. G. & Andersen, K. G. Precision epidemiology for infectious disease control. Nat. Med. 25, 206–211 (2019).
47. Wirth, T. et al. Niche specialization and spread of Staphylococcus capitis involved in neonatal sepsis. Nat. Microbiol. 5, 735–745 (2020).
48. van Dalen, R. et al. Do not discard *Staphylococcus aureus* WTA as a vaccine antigen. Nature 572, E1–E2 (2019).
49. Tormo, M. A. et al. *Staphylococcus aureus* pathogenicity island DNA is packaged in particles composed of phage proteins. J. Bacteriol. 190, 2434–2440 (2008).
50. Winstel, V., Kuhner, P., Rohde, H. & Peschel, A. Genetic engineering of untransformable coagulase-negative staphylococcal pathogens. Nat. Protoc. 11, 949–959 (2016).
51. Zerbino, D. R. & Birney, E. Velvet: algorithms for de novo short read assembly using de Bruijn graphs. Genome Res. 18, 821–829 (2008).
52. Bankevich, A. et al. SPAdes: a new genome assembly algorithm and its applications to single-cell sequencing. J. Comput. Biol. 19, 455–477 (2012).
53. Thomas, J. C. et al. Improved multilocus sequence typing scheme for Staphylococcus epidermidis. J. Clin. Microbiol. 45, 616–619 (2007).
54. Kaya, H. et al. SCC mecFinder, a web-based tool for typing of staphylococcal cassette chromosome mec in *Staphylococcus aureus* using whole-genome sequence data. mSphere https://doi.org/10.1128/mSphere.00612-17 (2018).

55. Siguier, P., Perochon, J., Lestrade, L., Mahillon, J. & Chandler, M. ISfinder: the reference centre for bacterial insertion sequences. Nucleic Acids Res. 34, D32–D36 (2006).
56. Sahl, J. W. et al. NASP: an accurate, rapid method for the identification of SNPs in WGS datasets that supports flexible input and output formats. Micro. Genom. 2, e000074 (2016).
57. Li, H. & Durbin, R. Fast and accurate long-read alignment with Burrows– Wheeler transform. Bioinformatics 26, 589–595 (2010).
58. McKenna, A. et al. The Genome Analysis Toolkit: a MapReduce framework for analyzing next-generation DNA sequencing data. Genome Res. 20, 1297–1303 (2010).
59. DePristo, M. A. et al. A framework for variation discovery and genotyping using next-generation DNA sequencing data. Nat. Genet. 43, 491–498 (2011).
60. Delcher, A. L., Phillippy, A., Carlton, J. & Salzberg, S. L. Fast algorithms for large-scale genome alignment and comparison. Nucleic Acids Res. 30, 2478–2483 (2002).
61. Kurtz, S. et al. Versatile and open software for comparing large genomes. Genome Biol. 5, R12 (2004).
62. Arndt, D. et al. PHASTER: a better, faster version of the PHAST phage search tool. Nucleic Acids Res. 44, W16–W21 (2016).
63. Croucher, N. J. et al. Rapid phylogenetic analysis of large samples of recombinant bacterial whole genome sequences using Gubbins. Nucleic Acids Res. 43, e15 (2015).
64. Edgar, R. C. MUSCLE: multiple sequence alignment with high accuracy and high throughput. Nucleic Acids Res. 32, 1792–1797 (2004).
65. Guindon, S. & Gascuel, O. A simple, fast, and accurate algorithm to estimate large phylogenies by maximum likelihood. Syst. Biol. 52, 696–704 (2003).
66. Guindon, S. et al. New algorithms and methods to estimate maximum-likelihood phylogenies: assessing the performance of PhyML 3.0. Syst. Biol. 59, 307–321 (2010).
67. Anisimova, M., Gil, M., Dufayard, J. F., Dessimoz, C. & Gascuel, O. Survey of branch support methods demonstrates accuracy, power, and robustness of fast likelihood-based approximation schemes. Syst. Biol. 60, 685–699 (2011).
68. Gerwig, G. J., Kamerling, J. P. & Vliegenthart, J. F. Determination of the absolute configuration of mono-saccharides in complex carbohydrates by capillary G.L.C. Carbohydr. Res. 77, 10–17 (1979).
69. Geiger, T. et al. The stringent response of *Staphylococcus aureus* and its impact on survival after phagocytosis through the induction of intracellular PSMs expression. PLoS Pathog. 8, e1003016 (2012).
70. Bruckner, R. A series of shuttle vectors for Bacillus subtilis and Escherichia coli. Gene 122, 187–192 (1992).

71. Wang, L. et al. SarZ is a key regulator of biofilm formation and virulence in Staphylococcus epidermidis. J. Infect. Dis. 197, 1254–1262 (2008).
72. Kretschmer, D., Rautenberg, M., Linke, D. & Peschel, A. Peptide length and folding state govern the capacity of staphylococcal beta-type phenol-soluble modulins to activate human formyl-peptide receptors 1 or 2. J. Leukoc. Biol. 97, 689–697 (2015).

Acknowledgements

We thank M. Marschal for clinical *S. epidermidis* strains and strain information; F. Oesterhelt for the help with microscopy; R. Stemmler, P. Kühner and L. Li for phage propagation and WTA isolation; K. Jakob and H. Käßner for technical support with NMR spectroscopy and chemical composition analysis; R. Rosenstein and D. Gerlach for helpful discussions; A. Tooming-Klunderud for PacBio sequencing of strain E73;
A. Schneider for help with LC–MS analysis of strain E73 WTA; J. Y. H. Lee for sending us the strain US06; D. A. Robinson for sending us the strain DAR1907; and J. Doškař for sending us the phage ΦPH15. This work was financed by grants from the Deutsche Forschungsgemeinschaft (DFG) SFB766 to C.W., C.M. and A.P.; TRR34 to C.W. and A.P.; TRR156 (project ID 246807620) to A.P.; PE 805/7-1 to A.P.; the German Center of
Infection Research to B.K., S.H., C.W. and A.P.; the National Natural Science Foundation of China 81861138043 to M.L.; and the Damp Foundation (HAPDICS project 2013-19) to H.R. B.K., S.H., C.M. and A.P. were supported by infrastructural funding from the Cluster of Excellence EXC 2124 'Controlling Microbes to Fight Infections' (project ID 390838134) from the DFG.

Author contributions

X.D. conceived the study and performed and analysed most of the bacteriological, molecular and cell culture experiments. J. Larsen performed most of the bioinformatics experiments (with support from M.S.). M.L., A.B. and H.R. collected and typed the *S. epidermidis* strains. M.L. provided important intellectual support and performed the animal experiments with the help of Y.L. and J. Liu. The WTA structure was analysed via MS by A.W. and C.M. and via NMR microscopy by P.M.S.C. and
K.A.D. C.S., E.L., J.S. and C.W. contributed to the cell culture experiments. B.K. and
S.H. helped with the design of the cloning experiments. V.W. and A.P. conceived and supervised the study.

Competing interests

The authors declare no competing interests.

Additional information

Extended data is available for this paper at https://doi.org/10.1038/s41564-021-00913-z.

Supplementary information The online version contains supplementary material available at https://doi.org/10.1038/s41564-021-00913-z.

Correspondence and requests for materials should be addressed to A.P.

Peer review information Nature Microbiology thanks Victor Torres, Wilma Ziebuhr and the other, anonymous, reviewer(s) for their contribution to the peer review of this work. Peer reviewer reports are available.

Reprints and permissions information is available at www.nature.com/reprints.

Publisher’s note Springer Nature remains neutral with regard to jurisdictional claims in published maps and institutional affiliations.

Extended Data

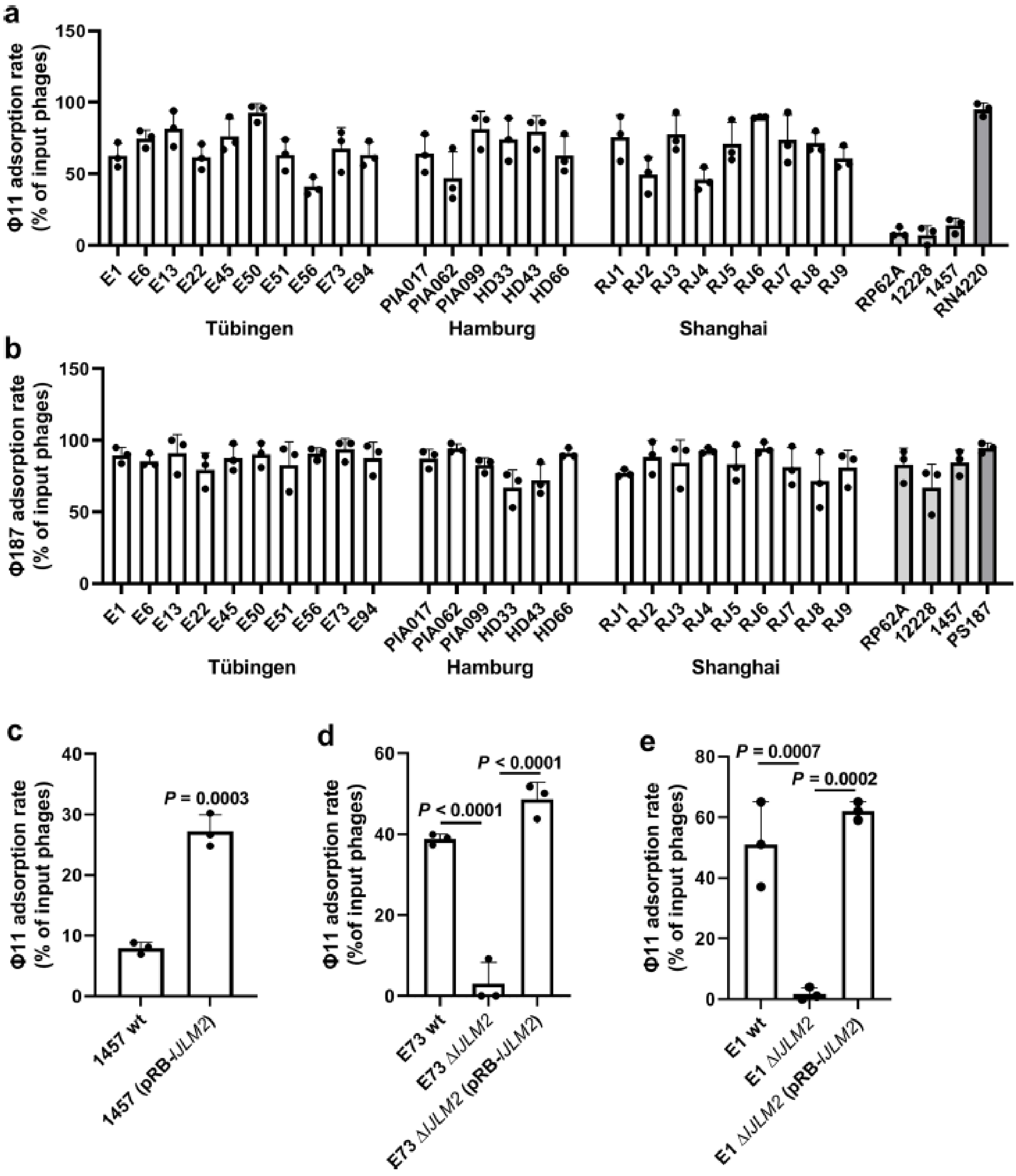

Extended Data Fig. 1 | Phage adsorption assay confirms presence of the RboP-WtA phage receptor on *tarIJLM2*-positive *S. epidermidis* isolates. The binding rate of RboP-WTA specific phage Φ11 (a, c, d, e) and of GroP-WTA specific Φ187 (b) to the indicated strains is shown. RP62A, ATCC12228, and 1457 are *S. epidermidis* laboratory strains (light gray), only expressing GroP-WTA. *S. aureus* strains RN4220 or PS187 (dark gray) express RboP-WTA or GroP-WTA, respectively. Means ± s.d. of three independent experiments are shown. One-way ANOVA with Dunnett’s post-test (two-sided) was used to analyze significant differences vs. mutant in (d) and (e). Unpaired t-test was used to analyze significant differences between wt and the hybrid strain in (c).

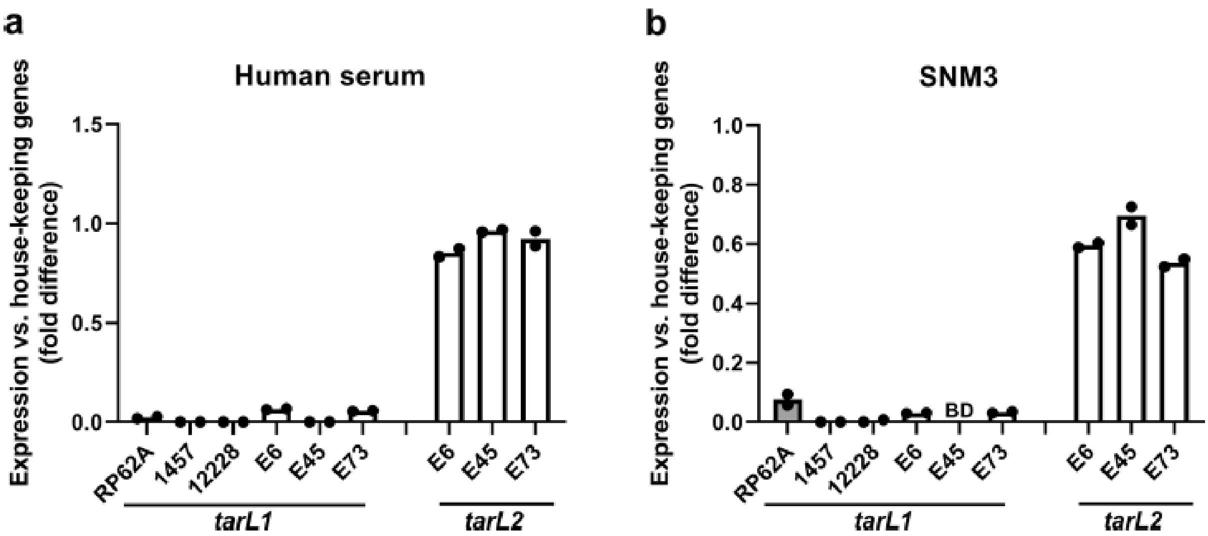

Extended Data Fig. 2 | While *tarL2* is efficiently transcribed in the *tarIJLM2*-positive isolates E6, E45, and E73, tarL1 is not or only very weakly expressed in all tested *S. epidermidis* strains during growth in human serum (a) or synthetic nasal medium 3 (SNM3) (b). The control strains RP62A, 1457, and 12228 lack *tarIJLM2* and were negative in the PCR reaction. Values represent means of two independent experiments. They were normalized for strongly and constitutively expressed housekeeping genes *gyrB*, *rho*, and *tpiA*. BD, below detection limit.

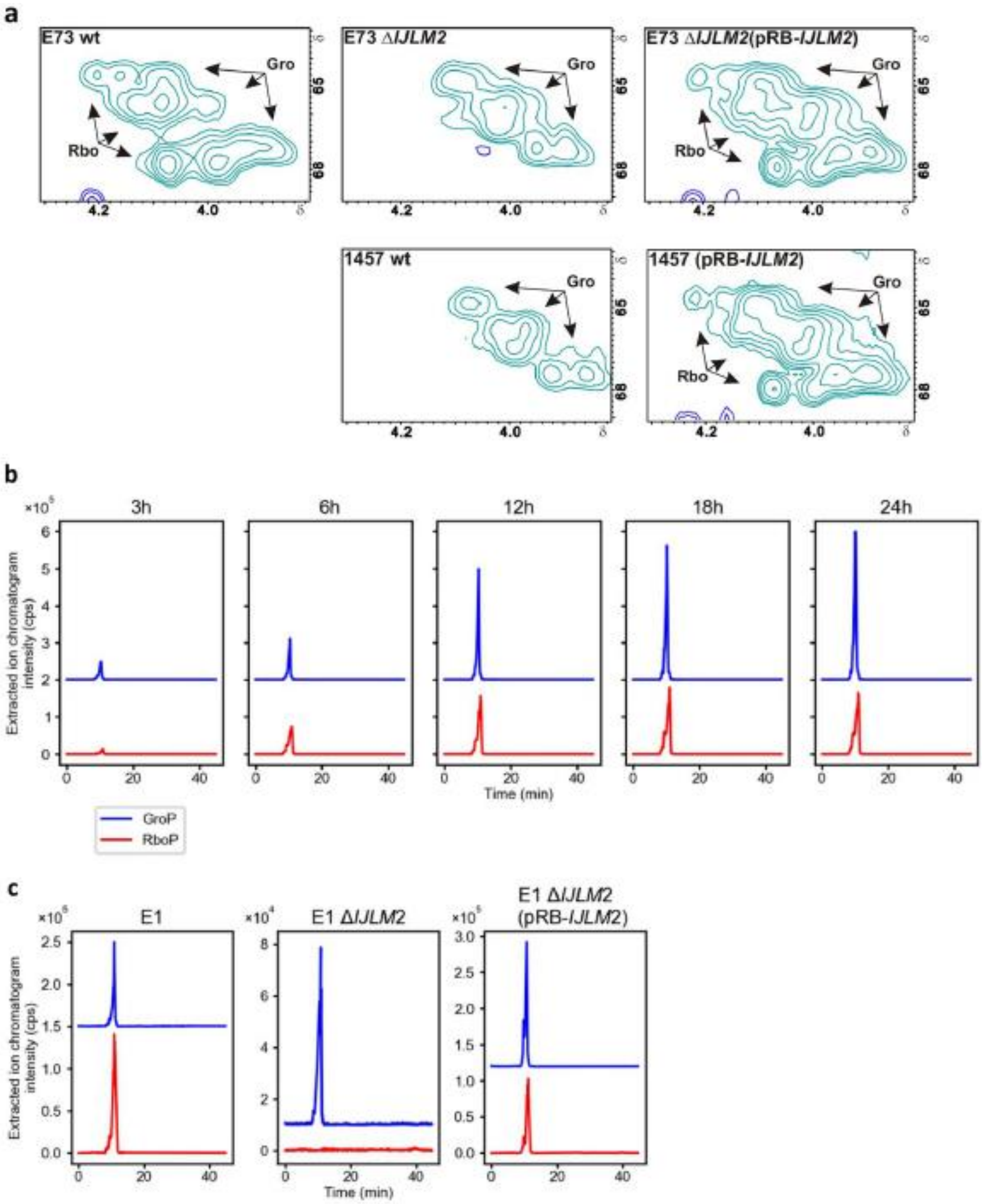

Extended Data Fig. 3 | NMR and MS spectroscopy confirm that WtA from *tarIJLM2*-positive *S. epidermidis* strains contains both, glycerol (gro) and ribitol (Rbo), while WtA of *tarIJLM2*-lacking strains contains only gro. a, Part of the HSQC-DEPT spectra of the methylene region of Rbo/Gro in the poly-RboP/GroP of the indicated WTA samples are shown. Signals corresponding to different substitutions of the polymers are shifted depending on the substitution. The presence of poly-RboP is clearly seen in the case of the WTA samples E73 wild type (wt), E73ΔIJLM2 (pRB-IJLM2), and 1457 (pRB-IJLM2) with signals at d 4.13;4.09/65.7, 4.07;3.98/67.8 and 4.20;4.16/64.7 (H/C), which are absent in the case of the other WTA samples. b, S. epidermidis E73 produces both, GroP (blue lines, [M + H]+ = 173.022 m/z) and RboP (red line, [M + H]+ = 233.042 m/z) in different growth phase as shown by LC-MS. c, another *tarIJLM2*-positive *S. epidermidis* E1 also produces both, GroP (blue lines, [M + H]+ = 173.022 m/z) and RboP (red line, [M + H]+ = 233.042 m/z) as shown by LC-MS.

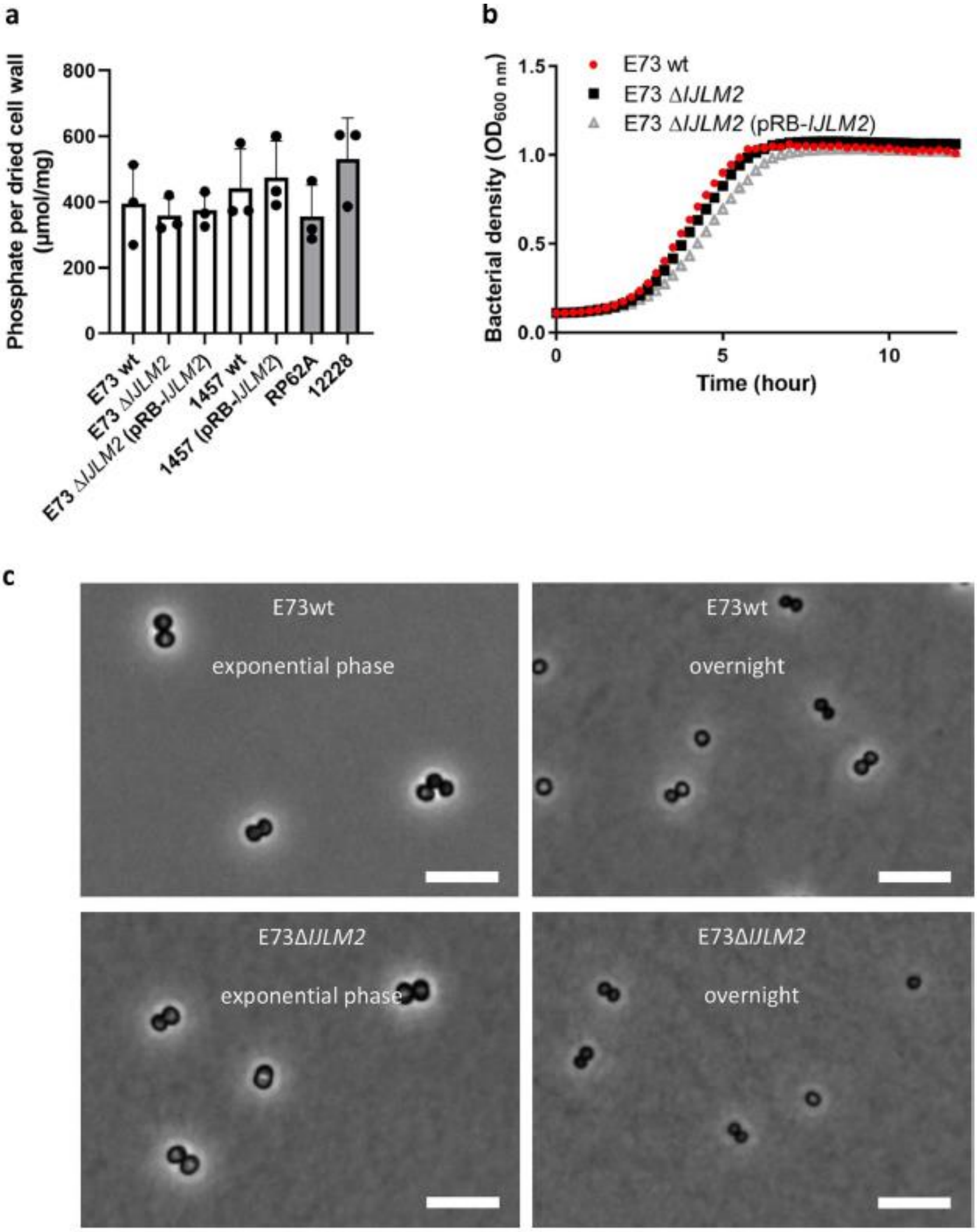

Extended Data Fig. 4 | RboP-WtA production does not increase the overall WtA amounts and does not affect *S. epidermidis* growth behavior or microscopic appearance. a, Total WTA phosphate amount per cell wall dry weight of the indicated *S. epidermidis* strains. Means ± s.d. of three independent experiments are shown. None of the minor differences is significant. b, Growth curves of S*. epidermidis* E73 with or without *tarIJLM2* in TSB. Means of three independent experiments are shown. c, Microscopic images of E73 with or without tarIJLM2. Scale bars: 5 µm.

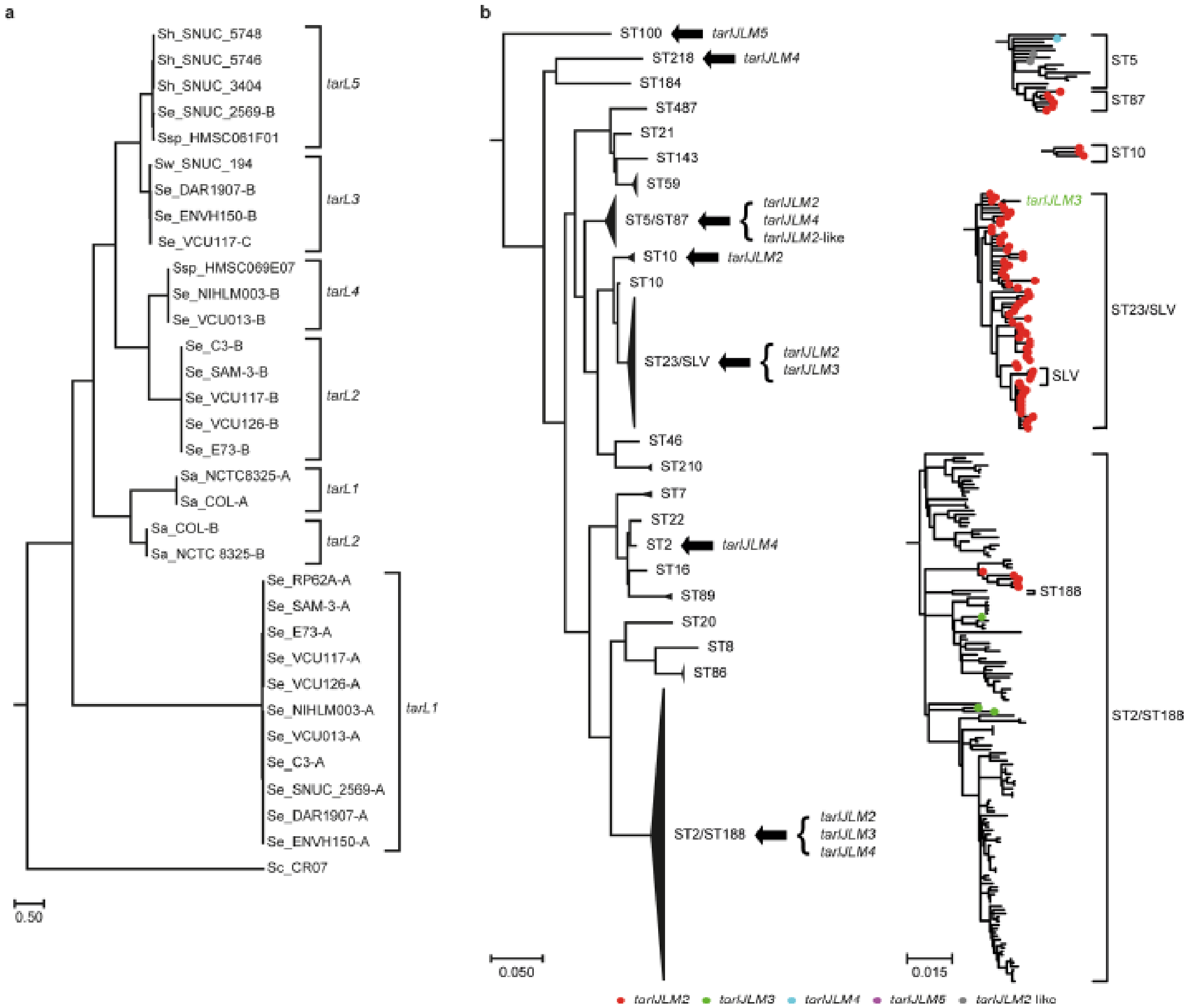

Extended Data Fig. 5 | Detailed phylogenetic distribution of *tarIJLM2*-5 among selected *S. epidermidis* clones and evolutionary relation of *tarL* from different gene clusters. a, Maximum-likelihood phylogeny of 33 *tarL* genes from representative *S. epidermidis* (Se) and *S. aureus* (Sa) isolates and other *Staphylococcus spp*. isolates that carried *tarIJL* with or without *tarM*, including *S. warneri* (Sw), *S. hominis* (Sh), *S. capitis* (Sc), and uncharacterised *Staphylococcus species* (Ssp) (Source Data). The *tarL2* gene found in *S. epidermidis* is more closely related to the two *tarL* genes in *S. aureus* than to *S. epidermidis tarL1*. The S. *epidermidis tarL3*, *tarL4*, and *tarL5* genes, but not *tarL2*, were also found in other *Staphylococcus species*. Phylogenetic reconstruction was carried out using the maximum-likelihood program PhyML with a GTR model of nucleotide substitution, and support for the nodes was assessed using aBayes (see Methods). The tree was midpoint rooted. The scale bar denotes substitutions per variable sites. b, Maximum-likelihood phylogeny of 261 *S. epidermidis* isolates, comprising 25 *tarIJLM*-positive *S. epidermidis* isolates collected in this study, nine *tarIJLM*-positive S. epidermidis genomes from in the NCBI Reference Sequence Database (accessed July 3 2018), and a global collection of 227 *S. epidermidis* isolates originating from 96 healthcare institutions across 24 countries3 was inferred from an alignment of 39,298 single-nucleotide polymorphisms (Supplementary Table 2). Four *tarIJLM*-negative isolates (BPH0677, BPH0704, BPH0737, and SEI) were manually removed from the phylogeny due to their extreme divergence, and clades containing isolates with the same or closely related STs were collapsed to reduce complexity. The *tarIJLM2* genes in E73 (Fig. 1b) were used as queries in BLASTN searches. The multilocus sequence types (STs) are indicated. Phylogenetic reconstruction was carried out using the maximum-likelihood program PhyML with a GTR model of nucleotide substitution, and support for the nodes was assessed using aBayes (see Methods). The tree was rooted according to work of Lee et al.3 The scale bar denotes substitutions per variable sites. Expanded subtrees illustrate the phylogenetic relationships of isolates belonging to ST5/ST87, ST10, ST23/single-locus variant (SLV), and ST2/ST188. The presence of *tarIJLM2*-5 is indicated in colors. A single ST23 isolate, VCU117, carried both, *tarIJLM2* and *tarIJLM3*.

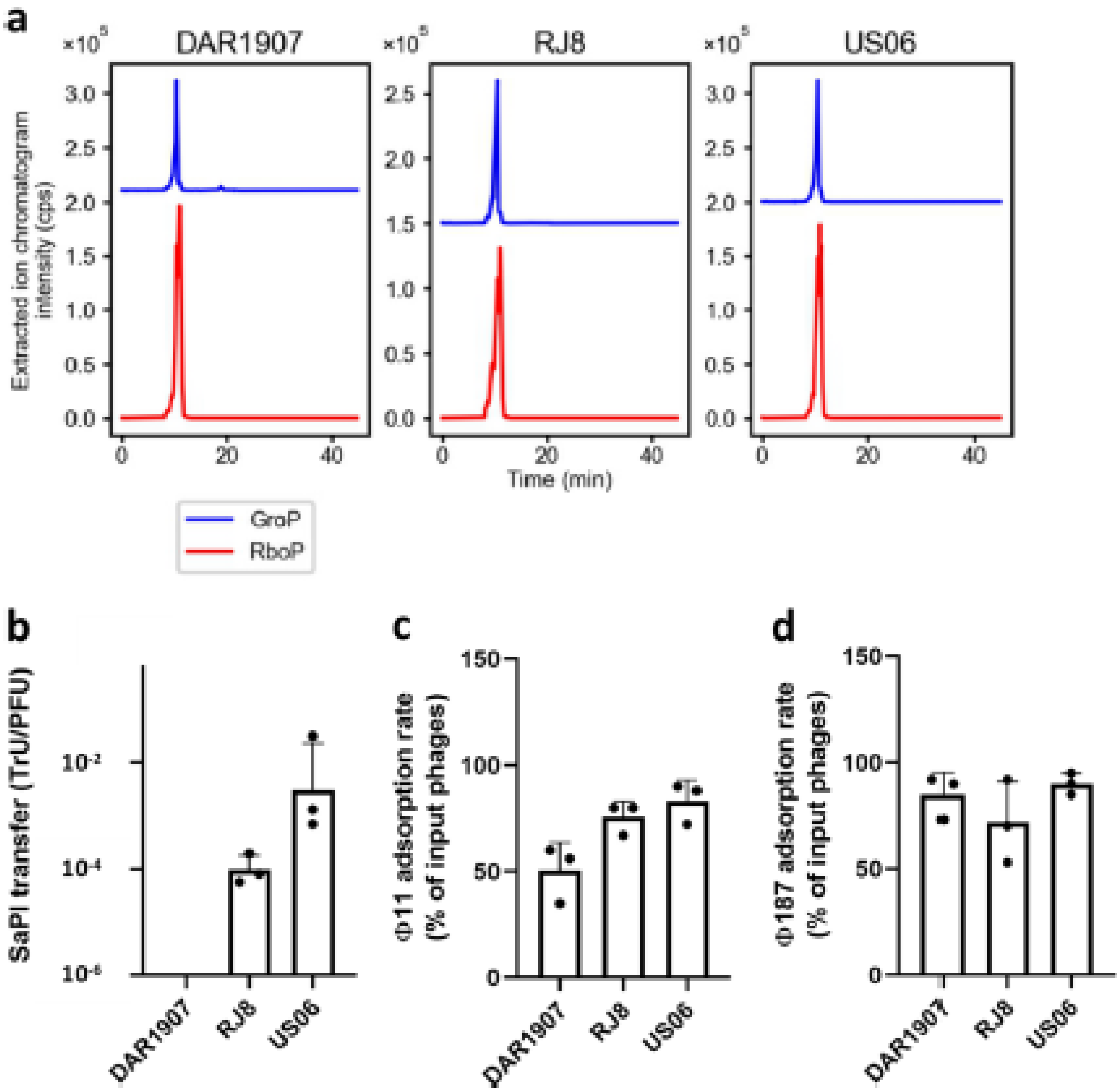

Extended Data Fig. 6 | the gene cluster *tarIJLM3* and *tarIJLM4* lead to RboP-WtA synthesis in HA-MRSE St2 and St5 strains. a, The tested *tarIJLM3*-positive (DAR1907 and RJ8, both ST2) and *tarIJLM4*-positive *S. epidermidis* strains (US06, ST5) contain both, GroP (blue lines, [M + H]+ = 173.022) and RboP (red line, [M + H]+ = 233.042) as WTA constituents; counts per second (CPS) measured by LC-MS are shown. b, Transduction with SaPIbov1 via Φ11. c, The binding rate of RboP-WTA-specific phage Φ11. d, The binding rate of GroP-WTA-specific phage Φ187. Means ± s.d. of three independent experiments are shown in (b-d).

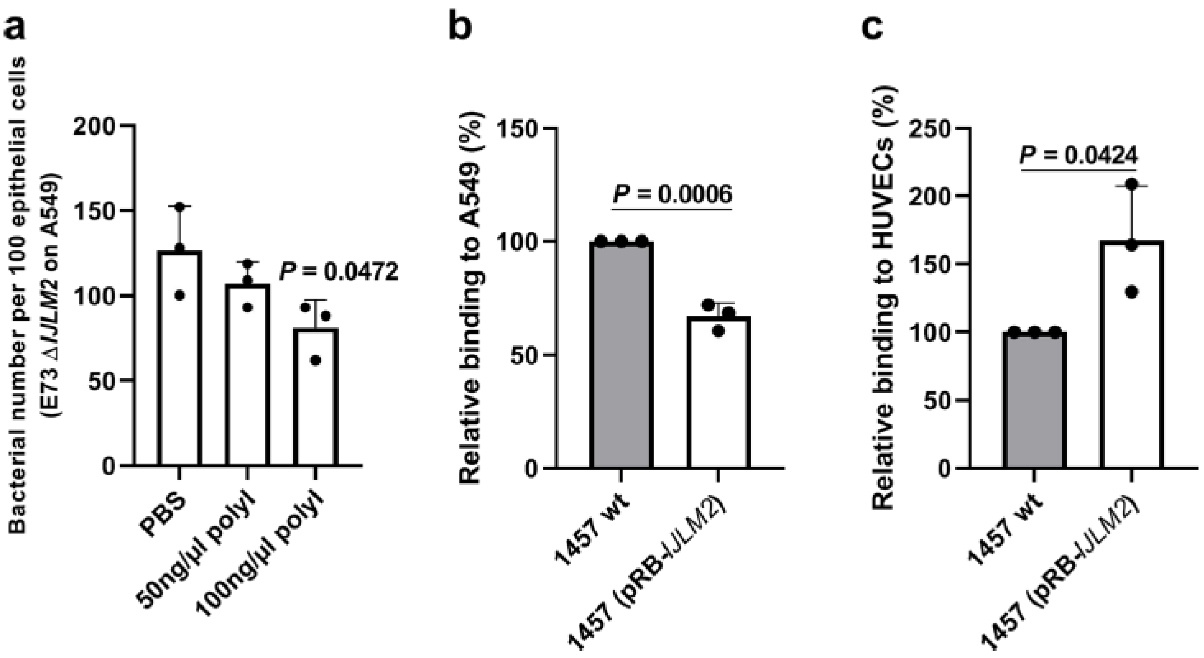

Extended Data Fig. 7 | RboP-WtA impairs *S. epidermidis* 1457 binding to A549 but promotes its binding to HuVECs. a, The scavenger receptor inhibitor polyinosinic acid (poly-I) inhibits the increased binding of *S. epidermidis* E73Δ*IJLM2* to A549. b, RboP-WTA production in the GroP-WTA S. epidermidis 1457 decreases its binding to the human airway epithelial cell line A549 but promotes its binding to HUVECs (c). Means ± s.d. of three independent experiments are shown in (a-c). One-way ANOVA with Dunnett's post-test (two-sided) was used to analyze significant differences vs. PBS condition in
(a). Significant differences (P ≤ 0.05) were calculated by unpaired t-test between wt and the hybrid strain in (b) and (c).

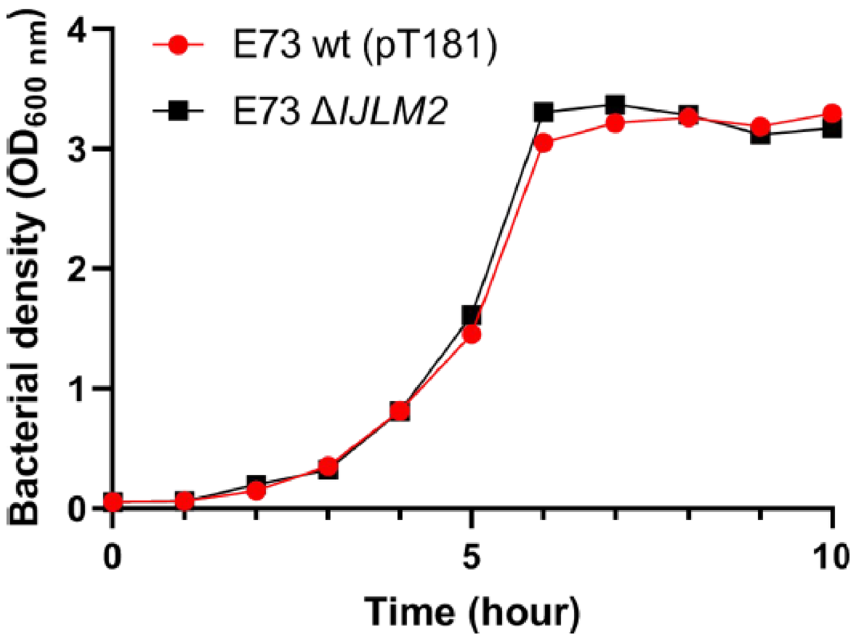

Extended Data Fig. 8 | the presence of plasmid pt181 does not affect the growth behavior of *S. epidermidis* E73 wild type (wt) compared to E73Δ*IJLM2*. The indicated bacterial strains were grown in TSB medium. Means of two independent experiments are shown.

Chapter II

The following chapter is part of the accepted research article:

"Influence of *Staphylococcus aureus* strain background on Sa3int phage life cycle switches".

The original article can be found under: doi: 10.3390/v14112471.

The published version was only formatted to fit the layout of this Thesis. The content is congruent to the peer-reviewed original.

Influence of *Staphylococcus aureus* strain background on Sa3int phage life cycle switches

Carina Rohmer[1,3†], Ronja Dobritz[1†], Dilek Tuncbilek-Dere[2,4], Esther Lehmann[1], David Gerlach[5], Shilpa E. George[1], Taeok Bae[6], Kay Nieselt[2,4] and Christiane Wolz[1,2,*]

1. Interfaculty Institute of Microbiology and Infection Medicine, University of Tübingen; Germany
2. Cluster of Excellence EXC 2124 “Controlling Microbes to Fight Infections”, University of Tübingen, Germany
3. Fraunhofer Institute for Interfacial Engineering and Biotechnology IGB, Stuttgart, Germany Institute for Bioinformatics and Medical Informatics, University of Tübingen, Germany
4. Department of Microbiology, University of Würzburg, Germany
5. Department of Microbiology and Immunology, Indiana University School of Medicine-Northwest, Gary, IN 46408, US

* Correspondence: christiane.wolz@med.uni-tuebingen.de;
Tel.: +49 7071 297464; Fax: +49 7071 295165

† These authors contributed equally to this work.

Abstract: *Staphylococcus aureus* asymptomatically colonizes the nasal cavity of mammals, but it is also a leading cause of life-threatening infections. Most human nasal isolates carry Sa3 phages, which integrate into the bacterial *hlb* gene encoding a sphingomyelinase. The virulence factor-encoding genes carried by the Sa3-phages are highly human-specific and most animal strains are Sa3 negative. Thus, both insertion and excision of the prophage could potentially confer a fitness advantage to *S. aureus*. Here we analysed the phage life cycle of two Sa3 phages, Φ13 and ΦN315, in different phage cured *S. aureus* strains. Based on phage transfer experiments, strains could be classified into low (8325-4, SH1000, USA300c) and high (MW2c, Newman-c) transfer strains. High transfer strains promoted the replication of phages whereas phage adsorption, integration, excision or *recA* transcription was not significant different between strains. RNASeq analyses of replication deficient lysogens revealed no strain specific differences in the CI/Mor regulatory switch region. However, lytic genes were significantly upregulated in the high transfer strain MW2c Φ13 compared to strain 8325-4 Φ13. By transcriptional start site prediction, new promoter-regions within the lytic modules were identified which are likely targeted by specific host factors. Such host-phage interaction probably accounts for the strain specific differences in phage replication and transfer frequency. Thus, the genetic make-up of the host strains may determine the rate of phage

mobilization, a feature that might impact the speed at which certain strains can achieve host adaptation.

Keywords: Phage, virulence, induction, gene regulation, Staphylococcus, hemolysin

Introduction

Staphylococcus aureus is a major human pathogen but also colonizes and infects different animal species [1-5]. Transmission of *S. aureus* between humans and livestock is of particular concern as *S. aureus* isolates from farmed animals are often antibiotic resistant [6]. Adaptation to the different mammalian hosts occurs largely through acquisition/loss of mobile genetic elements. *S. aureus* has jumped between species many times, resulting in the dynamic gain and loss of host-specific adaptive genes many of which are prophage encoded [5,7-9]. Most prominent is the repeated loss of the temperate Sa3int phages upon jump of *S. aureus* from humans to different animals [10]. In several instances, the animal-adapted strain was transmitted back to humans where it often reacquired Sa3int phages, emphasizing their important role in human colonization [1,8-12]. Up to 96% of human nasal isolates were observed to carry Sa3int phages integrated into the *hlb* locus, which encodes ß-hemolysin (Hlb), also named ß-toxin [13]. These phages carry genes that encode human-specific immune evasion factors [14] and other potential virulence factors [10]. The observation that Hlb is always functional after phage excision and that this process also occurs during human infections resulting in Hlb positive subpopulations [15], indicates that under certain infec-tious conditions Hlb is essential for bacterial survival.

Temperate staphylococcal phages belong to the family of *Siphoviridae*. The genomes of siphoviruses are typically organized into six functional modules: lysogeny, DNA replication, packaging, head, tail, and lysis. The evolution of phage lineages is driven by the lateral gene transfer of interchangeable genetic elements (modules), which consist of functionally related genes [8,13,16-19]. *S. aureus*-infecting siphoviruses have been classified according to polymorphisms of the integrase gene (*int*) [13,16,17,20]. The *int* type dictates chromosomal integration at cognate *attB* sites and is closely associated with the virulence gene content of the prophage [13]. However, due to the mosaic nature of *S. aureus* siphoviruses the distinct phage modules can show high homology between different Sa-Int phages. E.g., several open reading frames (ORFs) from the prototypic Sa3int phage Φ13 are homologous to those of PVL (Pan-ton-Valentine leucocidin)-encoding Sa2int phages.

The molecular interactions between the *S. aureus* host and its temperate phages are largely unknown. The large number of phage genes encoding hypothetical proteins highlights how little is known about temperate phages and their influence on bacterial lifestyle switches. Likewise, we largely ignore which host factors influence the lysogenic-lytic cycle switch of temperate phages. Previous analysis of Sa2int phages revealed that the inducibility of the very same prophage can be significantly different when analyzed in diverse host genetic backgrounds [21]. Mobilization of the Sa2mw prophage from *S. aureus* strain MW2 or Newman was 100 fold higher than that from strain 8325-4.

Here, we investigated whether strain specific features also impact the life cycle of Sa3int phages. For this, we constructed and integrated Sa3int phages into different phage-cured *S. aureus* strains (8325-4, SH1000, USA300c, Newman-c and MW2c). We focused on two prototypic Sa3int phages, namely Φ13 and ΦN315. Φ13 is derived from the *S. aureus* reference strain 8325 of clonal complex (CC) 8. ΦN315 is derived from the methicillin resistant strain N315 (CC5) and carries the *tarP* gene encoding for an alternative glycosyltransferase [22]. The strain background was found to impact phage transfer and replication. RNAseq analysis hint to specific interaction of host factors with phage regulatory region located in the lytic module of the phage.

Materials and Methods

Growth conditions

Unless otherwise stated, single-lysogens of *S. aureus* carrying Φ13kan (Tang et al., 2017) or ΦN315tet were used. *S. aureus* cells were grown in Tryptic Soy Broth (TSB) (Oxoid), 37°C, 180 rpm. Precultures were supplemented with the appropriate antibiot-ics: kanamycin (KanA, 50 µg ml-1), tetracycline (Tet, 3 µg ml-1), erythromycin (Erm, 10 µg ml-1), chloramphenicol (Chloro, 10 µg ml-1), streptomycin (Strep, 500 µg ml-1).

Strain construction

Strains are listed in Supplementary Table S1, oligonucleotides in Supplementary Table S2.

Selection of strep resistant strains

S. aureus isolates were grown in TSB to OD600 = 0.7 and supplemented with Strep (500 µg ml-1). After 4 hours of growth, serial dilutions were plated on TSB agar plates supplemented with Strep (500 µg ml-1). Resistant colonies were sub-cultured and growth compared to the parental strain. Only streptomycin-resistant clones that were not impaired in growth were used in this study.

Generation of phage cured USA300 (USA300c)

Native prophages (Sa2int and Sa3int) of *S. aureus* strain USA300 were deleted using plasmid pKOR1 as described for *S. aureus* Newman (Bae et al., 2006). In brief: a 2 kb DNA-fragment containing the respective *attB* sequences were PCR-amplified with the following primers (for Sa2int prophage: primer627 and primer628; for Sa3int prophage: primer434 and primer435) and inserted into pKOR1 and mutagenesis performed as described.

Generation of phage lysates and lysogens

Phage lysates of Φ13kan or ΦN315tet were obtained after mitomycin C (MMC, 500 ng ml-1) induction of 8325-4 Φ13kan or N315-ΦN315tet in liquid culture (OD600 = 0.7). After 2 h, 37°C additional mitomycin C (500 ng ml-1) was added and supernatant collected after further incubation for 1 h (37°C). Supernatants were filtered (0.45 µm pore size (Merck)) and phage titer enumerated by plaque assay. Single-lysogens were obtained by incubation of 106 phages with phage-cured *S. aureus* strains (10 ml) from exponential growth phase (OD600 = 0.7) for 4 h, 37°C. Selection of lysogens was per-formed on TSA-plates containing KanA (50 µg ml-1) or Tet (3 µg ml-1), respectively. Single-lysogens were sub-cultivated four times and phage integration at the cognate *att* site within *hlb* verified by loss of β-hemolysin production and PCR using oligonu-cleotides hlb675 and Sa3intfor.

Construction of phage ΦN315tet

Phage ΦN315 was labelled with a *tet* resistance cassette. *TetK* was amplified from plasmid pT181 using primer pair Tet2-F BamHI and Tet2-R BamHI. ΦN315 IEC specific overhangs were amplified using primer pair IEC:tet A+B and C +D. The three resulting fragments were fused using overlap extension PCR, ligated into plasmid pBASE6 (Geiger et al., 2012) and cloned into E. coli DC10B. The vector was subsequently transferred into *S. aureus* N315 using electroporation and mutagenesis per-formed as described (Geiger et al., 2012). The mutation was verified by PCR and resulted in replacement of phage encoded *chp* and *scn* with the *tet* cassette.

Construction of phage Φ13kan-Δrep

Left and right flanking regions of prophage encoded replication factor (SAOU-HSC_02217) were amplified via PCR using oligonucleotides PiMAYrepdelrev/ repdelrev and repdelfor/ PiMAYrepdelfor (Supplementary Table S2) and cloned into shuttle vector piMAY (Monk et al., 2012) by Gibson assembly in E. coli DC10B. The vector was transferred from E. coli DC10B into 8325-4 Φ13kan and MW2c Φ13kan via electroporation and mutagenesis performed as previously described (Monk et al., 2012). Gene deletion was verified by sequencing of PCR amplicons spanning the mutation site. Further, lysogens were checked for β-hemolysin negative phenotype on blood agar plates.

Phage transfer assay

Cultures of donor strains (single lysogens) and recipients (phage-cured, streptomycin resistant) were grown to exponential phase (OD600 = 0.7), mixed at a ratio of 1:1, and co-cultivated for 4 h, 37°C, 180 rpm. Single and mixed cultures were diluted in PBS and colony forming units (CFU) determined on blood agar plates (Oxoid) and TSA agar plates containing single antibiotics (KanA 50 µg ml-1, Tet 3 µg ml-1, Strep 500 µg ml-1) and double antibiotics (KanA 50 µg ml-1, Strep 500 µg ml-1 or Tet 3 µg ml-1, Strep 500 µg ml-1), respectively. Phage transfer frequency was determined by CFU grown on double antibiotic containing plates divided by CFU grown on TSA plates containing streptomycin 500 µg ml-1. Single colonies were analyzed for loss of Hlb synthesis and phage integration by PCR. All tested double resistant colonies carried the *hlb* converting phage. Spontaneous resistance was monitored by plating donor and recipient strains on selective agar plates and was many magnitudes lower than the observed transfer rates.

Lysogenization assay

Phage-cured derivatives of *S. aureus* isolates were grown to exponential growth phase (OD600 = 0.7) and 108 bacteria per ml were infected with phages to a multiplicity of infection (MOI) of 0.1 or MOI 0.01 followed by incubation for 20 min or 4 h, 37°C, 180 rpm. CFU was determined on blood agar plates and TSA agar plates containing either KanA or Tet for selection of lysogens. Single colonies were picked on blood agar plate to verify loss of ß-hemolysin activity. Lysogenization frequency was determined by CFU on antibiotic-containing plates divided by total CFU on blood plates.

Plaque-assay

Phage titer was determined by agar overlay method using strain LS1 as indicator strain. Indicator strains were grown to OD600 = 0.1 in TSB. 100 µl bacterial culture was mixed with 3 ml liquid phage soft agar (Casaminoacids 3 g l-1, Yeast Extract 3 g l-1, NaCl 5.9 g l-1, Agar 7.5 g l-1) and poured on TSA-plate. After solidification, dilutions of sterile-filtered phage lysates were dropped on the lawn and incubated at 37°C to enumerate plaque forming units (PFU).

Phage adsorption assay

Phage adsorption assays were performed as described [23] with slight modifications. In brief, 100 µl (3x106 phages) were incubated with 3 x108 bacteria in 1 ml TSB for 10 minutes at room temperature under non-shaking condition. Bacteria were pelleted (5000 x g, 5 min), supernatant filtered (0.45 µm pore size (Labsolute)) and used for PFU determination.

Prophage spontaneous induction or induction using mitomycin C

Single-lysogens were grown to exponential growth phase (OD600 = 0.7) and split into 10 ml aliquots. Aliquots were further incubated with and without subinhibitory concentrations of mitomycin C (300 ng ml-1) for 1 h. Supernatants were filtered (0.45 µm pore size (Merck)), PFU enumerated and stored at -20°C for qPCR. For absolute quantification of free phage DNA 100 µl of phage lysates were incubated with Proteinase K (100 µg ml-1, AppliChem) for 1 h at 55°C, followed by heat inactivation at 95°C for 10 min. Phage DNA was quantified by quantitative PCR (qPCR) using SYBR Green qPCR Kit (QIAGEN) and primers circlefor and circlerev spanning the reconstituted *attP* site of the phage. For quantification standard molecules were obtained by PCR using primers phi13circlefor and phi13circlerev. The amplicons were purified, and DNA concentration determined using A260. For quantification of excised phages within bacteria, *attP* and the chromosomal *recA* (recAF1 and recA661) were quantified using bacterial pellets. Bacteria were mechanically lysed using zirconia/silica beads in high speed homogenizer (6500 rpm, Fastprep). Lysed pellets were boiled for 10 min in water bath and stored at -20°C. 1 µl of a 1:100 dilution (RNase-free water, Ambion) was used for qPCR.

Northern blot analysis and preparation of RNA-probes

Bacteria were grown to OD600 = 0.7 followed by 1 h incubation at 37°C with or without mitomycin C (300 ng ml-1). In brief, bacterial pellet was resuspended in TRIzol (Thermo Fisher Scientific) and mechanically lysed using zirconia/silica beads in a high speed homogenizer. For Northern blot analysis RNA was isolated as recommended by TRIzol manufacturer. Transcripts on Northern blots were hybridized with digoxigenin-labelled DNA probes generated by PCR (Supplementary Table S2). RNA probes were generated with specific primer pairs containing T7 promoter for in vitro transcription. In vitro transcription was performed with MEGAshortskript T7 kit following instructions with the exception that a nucleotide mix from Roche containing DIG-11-UTP was used for labeling of fragments with digoxigenin. For RNA-seq analysis RNA from the aqueous phase was further purified using the ExpressArt® RNA ready Add-on Kit for TRIzol extraction (AmpTec) with the following modifications. After loading the sample on an RNAready column, RNA was washed additionally with inhibitor removal buffer (5 M guanidine-HCl, 20 mM Tris-HCl pH 6.6, 37 % (v/v) EtOH). DNase digest of the sample was directly performed on the column.

TagRNAseq and RNAseq

RNA aliquots were subjected to tagRNA-seq [24]. Experiments were conducted by Vertis Biotechnologie AG. Library preparation on rRNA depleted RNA samples was performed as follows: first Illumina TruSeq sequencing adapter (CTGAAGCT) was ligated to RNAs containing a 5´monophosphate end (resulting from processing events and thereby represent so-called processed start sites - PSS) followed by treatment with TEX (Terminator Exonuclease, Lucigen) to remove unligated 5´P-ends. Next, RNA 5´Polyphosphatase (5´PP, Lucigen) was used to convert triphosphate groups at 5´-RNA ends to monophosphate 5´-RNA ends. Formed monophosphate ends were then tagged by ligation of a second Illumina TruSeq sequencing adapter (TAATGCGC) (represent-ing transcription start sites - TSS). After fragmentation, an oligonucleotide adapter was ligated to the 3´ end of RNA fragments and cDNA synthesis performed using M-MLV reverse transcriptase. cDNA was PCR amplified within 16 cycles using high fidelity DNA polymerase. cDNA was purified using Agencourt AMPure XP Kit (Beck-man Coulter Genomics). Last, the cDNA pool was single-read sequenced on an Illumina NextSeq 500 system using 75 bp read length. Output read data were assigned to three different sets based on the tags from sequencing: read-files assigned to either transcriptional start site (TSS), read-files assigned to processed start site (PSS), unas-signed read-files. The first two sets were used for transcription start site analysis, the latter was used for expression analysis.

Differential expression analysis of phage-encoded genes using tagRNA-seq

The reference genome of *S. aureus* 8325 (NCBI (NC_007795.1) was manually phage-cured, Φ13kan genome integrated and the sequence manually SNP-corrected based on resequencing of the 8325 strain [25]. Raw data files of reads (unassigned) were trimmed using CLC genomics workbench (QIAGEN). Trimmed reads were mapped against the reference genome, and then normalized for library depth and gene length, resulting in datasets containing expression values (RPKM-values).

Raw data and processed files containing RPKM-values are available at https://www.ncbi.nlm.nih.gov/geo/query/acc.cgi?acc=GSE214523. Expression values were used for differential expression using the Wald test for statistical analysis. Significance was set to FDR-value of <0.05 and log2 fold change of lower than -1 or higher +1. From resulting datasets of the whole genome, the prophage genome was extracted and analyzed (Supplementary Table S4). Read mapping was visualized to the Φ13 genome using Integrated Genome Viewer.

Determination of TSSs

To prepare the raw read data for TSS identification, reads were preprocessed, mapped and a coverage per base was computed. For this, the RNA-seq analysis pipe-line READemption version 0.5.0 [26] was used,. All read samples were mapped to the respective reference sequence with the subcommand align, which integrates the map-per segemehl version 0.3.4 (Hoffmann et al., 2009). For the mapping, the following parameters were used: (--adapter AGATCGGAAGAGCACACGTCTGAACTCCAG-TCAC, --processes 4, --segemehl_accuracy 95, --segemehl_evalue 5.0, --poly_a_clipping, --min_phred_score 20 --fastq, --progress). The subcommand coverage calculates one position based coverage files, also called wiggle files, resulting in three file sets: the unnormalized raw wiggle files, files normalized by the total number of mapped reads (TNOAR) and multiplied by one million (mil_normalized), and files normalized by the total number of mapped read and multiplied by the lowest number of mapped reads taking all libraries in consideration (min_normalized). The min_normalized wiggle files were used for TSS calling. The TSS identification using the normalized wiggle files of the tagRNA-seq reads was conducted with TSSpredator 1.1 (Bischler et al., 2015; Dugar et al., 2013). For all of the TSSpredator runs, the preset de-fault parameters were used, except that matching replicates was set to 2. TSSpredator expects two types of reads, one from the so-called enriched library and one from the so-called normal or unenriched library. For the tagRNA-seq data, we used the TSS la-belled reads as the enriched libraries, and the PSS labelled reads as the normal, control libraries. The experimental setup of this study used three strains and compared two conditions. Therefore, TSSpredator was run both with the strain-setup and condition-setup, to analyze this data. For the cross-condition analysis each strain was considered separately. For the cross-strain analysis TSSpredator expects wiggle files normalized across all input libraries as input. For this, the lowest number of aligned reads over all replicates regarding both conditions was calculated and then each library was multiplied by this minimum. From each TSSpredator run the resulting MasterTables for each condition were combined manually and the phage region was extracted (Sup-plementary Table S3). For the cross-condition analysis each strain was considered sep-arately, resulting in three MasterTables. A detailed description of TSSpredator parameters, TSS classes and output files can be taken from the user manual available at https://tsspredator20-rtd.readthedocs.io/en/latest/index.html

Statistical analysis

Statistical analyses were performed using GraphPad Prism software. Differences between two groups were evaluated using Student’s t test. For multiple comparisons, statistical analysis was performed using one-way ANOVA (parametric) or Krus-kal-Wallis test (non-parametric), with Bonferroni test for parametric samples, or Dunn’s test for non-parametric samples as a post-hoc test. Differences at $p<0.05$ were considered significant. All statistical analysis methods are based on independent bio-logical replicates.

Results

Sa3int phage transfer during co-cultivation depends on the bacterial host strain

The Sa3int phage Φ13 is derived from the *S. aureus* reference strain 8325. This strain was previously cured of all phages and the phage cured derivative 8325-4 is widely used as a prototypic *S. aureus* strain in many genetic studies. To facilitate the analysis of the phage life cycle a kanamycin (*kan*) resistance cassette was introduced at the 3´end of Φ13 [27]. To compare phage transfer/acquisition in different bacterial strains Φ13kan lysogens were generated in different phage-free host strains: 8325-4, SH1000, MW2c, Newman-c, USA300c (Supplementary Table S1). Phage transfer was monitored after 4 h of co-culture of the Φ13kan single-lysogens with the isogenic, streptomycin (strep)-resistant and phage-free recipient under non-inducing conditions (Figure 1A). A high transfer rate was observed for strain MW2c and strain Newman-c as enumerated by double resistance. Newly generated lysogens were Hlb-negative on blood agar plates and phage integration into the *hlb* gene was verified by PCR using integration specific oligonucleotides. Significantly lower phage transfer rates were observed for the 8325-4 or USA300c strain pairs as compared to Newman-c or MW2c. During the analyses we observed that strain 8325-4 strain tended to aggregate during the incubation period. An *rsbU* repaired derivative of 8325-4 (strain SH1000) was de-scribed to form less aggregates [28]. To rule out any artifacts due to clumping we also generated an SH1000 Φ13kan lysogen. This strain indeed did not aggregate but still showed a significantly lower phage transfer rate compared to Newman-c or MW2c. In summary, we could confirm that the host background significantly influences phage lifecycle and pinpoint high (Newman-c and MW2-c) and low (8325-4, SH1000 and USA300) phage transfer strains (Figure 1A).

To analyze whether the strain background similarly determine the transfer rate of other phages we included phage ΦN315 derived from strain N315 into the analysis. The phage was labeled with a *tet* resistance cassette and mobilized into the same set of phage cured strains. Phage transfer rate was lower compared to Φ13kan (Figure 1B). However, again strain Newman-c and MW2c exhibited higher phage transfer com-pared to the low transfer strains SH1000 and USA300.

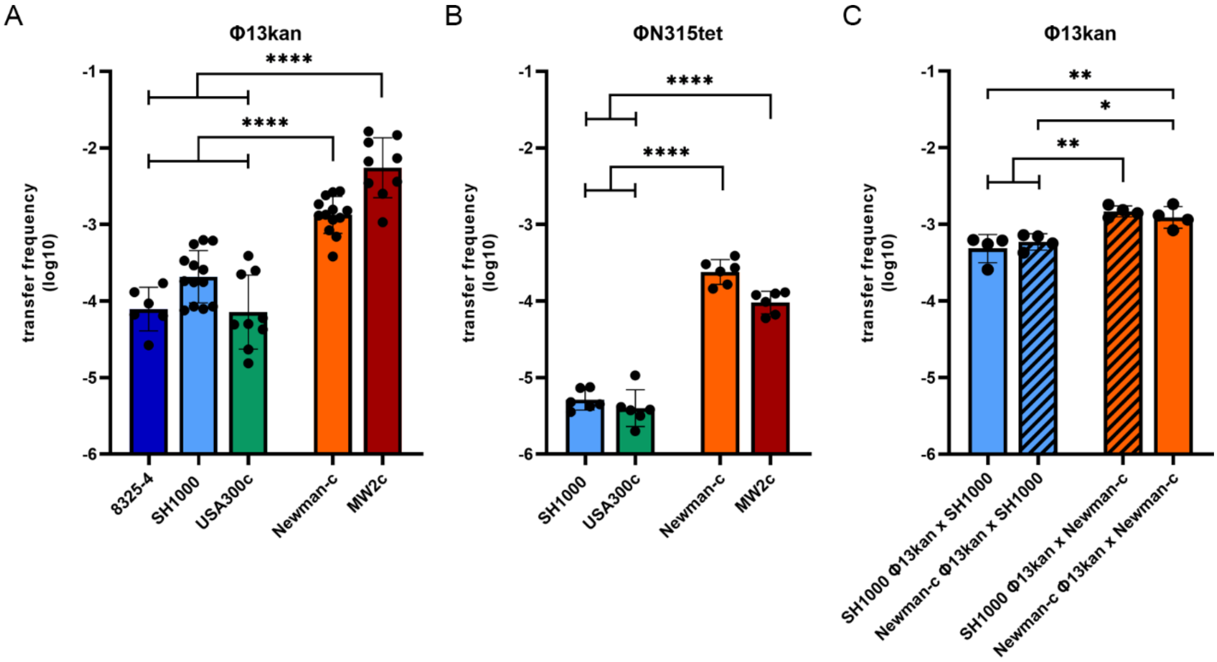

Figure 1. Phage transfer frequency of Φ13kan (A, C) or ΦN315tet (B) is strain dependent. Lysogens were mixed with isogenic, phage-cured, streptomycin-resistant recipients 8325-4 (dark blue), SH1000 (light blue), USA300c (green), Newman-c (orange) or MW2c (dark red) at a 1:1 ratio (4 h coculture in tryptic soy broth) (A, B) or with non-isogenic recipients (C). Phage transfer frequency was determined by calculating the ratio of CFU of double-resistant colonies (kanamycin/streptomycin for Φ13kan or tetracycline/streptomycin for ΦN315tet, respectively) divided by CFU on streptomycin (representing recipient). Values are independent biological replicates referring to mean ± SD. Statistical analysis was performed on log-transformed data using one-way ANOVA.

Strain-dependent differences in Sa3int phage transfer are determined by the recipient

Strain 8325-4, SH1000, USA300 and Newman are assigned to the same CC 8 with no obvious restriction barrier [29]. MW2 belongs to CC1 and gene transfer between CC8 and CC1 strains is restricted due to different restriction/modification systems. Accordingly, phage transfer between CC8 strains and MW2 was found to be severely impaired (Supplementary Figure S1). We next analyzed whether transfer between low (SH1000) and high (Newman-c) transfer strains of the same CC is determined by the donor or by the recipient strain (Figure 1C). Strain Newman as recipient showed high-er phage acquisition when incubated with either SH1000 Φ13kan or Newman-c Φ13kan. Strain SH1000 showed lower phage acquisition even when incubated with high transfer strain Newman-c Φ13kan. Thus, the different phage transfer rate among strains depends on the recipient.

Phage adsorption does not account for strain dependent phage integration

We speculated that strain-dependent phage transfer may be the result of differential phage adsorption. Wall-teichoic acids (WTA) function as conserved phage receptor for *S. aureus* phages [8]. This could be verified for Φ13kan since phage adsorption was not detectable in the WTA deficient strain USA300 Δ*tagO* (Supplementary Figure S2). All tested wild type strains showed high phage adsorption with only minor differences between strains. Small differences in phage adsorption did not correlate with the observed strain dependent differences in lysogenicity efficiency. Thus, processes following initial phage adsorption are responsible for strain-specific differences in phage transfer and replication.

Strain dependent Sa3 lysogenization and replication

We next analyzed whether the various bacterial recipients differed in phage integration and/or replication rate. Newman-c lysogens were treated with mitomycin to induce prophage excision, and phage titer was enumerated by plaque assay. Phages were incubated with recipient strains and phage integration enumerated by the phage resistance marker. After 20 min co-incubation of Φ13kan with recipient strains a simi-lar fraction of SH1000 and Newman-c bacteria became lysogens (Figure 2A, B). This indicates that phage integration is equally efficient in both strains. However, after prolonged incubation (4 h) significantly more Φ13kan (Figure 2C) and ΦN315tet (Figure 2D) lysogens were recovered in the high transfer strain Newman-c compared to the low transfer strain SH1000. We assumed that this is due to enhanced phage replication in strain Newman-c. To monitor phage replication free phage titers were enumerated after the 4 h incubation period. Significantly higher phage replication of both phages (Φ13kan and ΦN315tet) was observed after phage infection of strain New-man-c compared to strain SH1000 (Figure 2E, F). The phage titer of Φ13kan increased 650 fold in strain Newman-c and only 55 fold in strain SH1000.

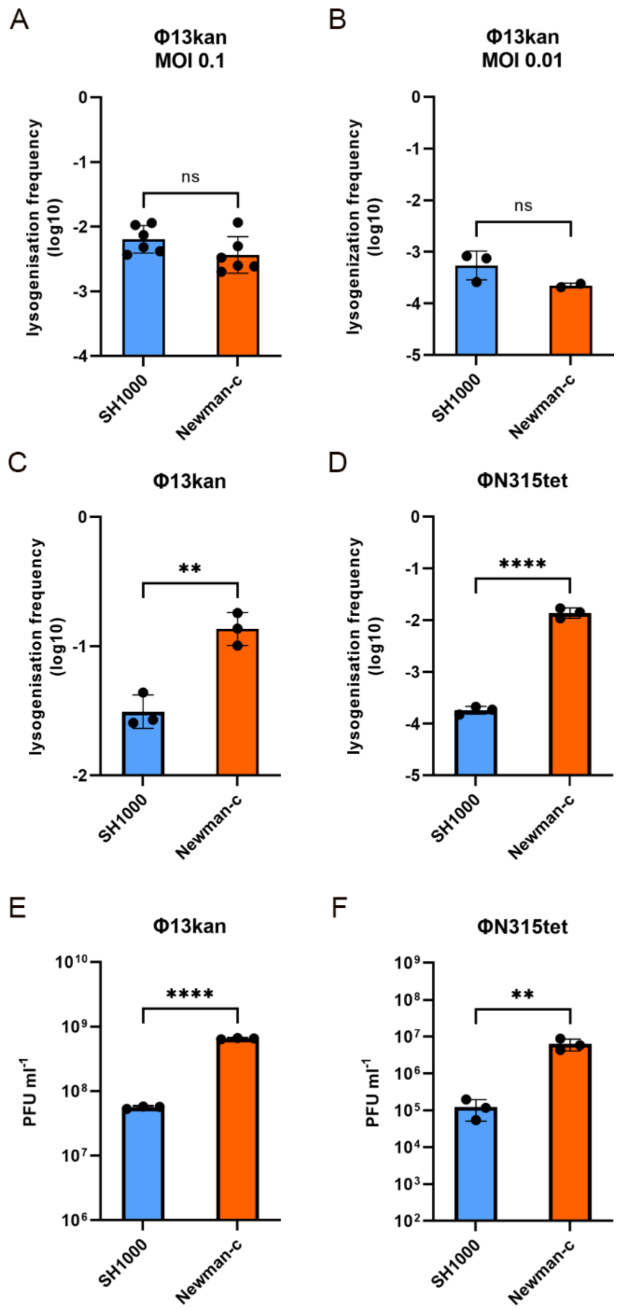

Figure 2. Strain dependent lysogenization and replication of Φ13kan and ΦN315tet. Lysogenization of phage-cured SH1000 (blue) and Newman-c (orange) with Φ13kan (A,B,C,E) or ΦN315-tet (D,F) during exponential growth. Phages and phage-cured recipient bacteria were co-cultured to investigate lysogenization rates. Co incubation was performed for 20 min at 37°C and MOI of 0.1 (A) or 0.01 (B), or for 4 h at 37°C and MOI of 0.01 (C-F). Lysogenization rates were determined by CFU on TSA-plates containing kanamycin or tetracyclin (representing lysogenized colonies)/CFU on blood-agar plates. Replication of Φ13kan (E) and ΦN315tet (F) was determined by enumerating phage particles in sterile filtrated supernatant by plaque assay 4 h post phage infection. Values are independent biological replicates referring to mean ± SD. Statistical analysis was performed using t-test (A,B) and one-way ANOVA of log-transformed data (C-F). Data are back-transformed for visualization of phage titers (E,F).

Thus, prior phage replication the integration efficiency seems not to differ between strains. However, in the high transfer strain Newman-c phage replication is enhanced. The higher phage replication in turn increases the chance of phage integration as seen in the later time points of infection.

Phage gene expression is dependent on the host strain background

Most of the genes carried by Φ13 encode proteins of unknown functions. Recently, a regulatory switch region was identified in Φ13 genome [30]. The region is composed of a CI coding repressor gene (*cI*) and a divergently transcribed mor (modulator of re-pression) gene. We monitored transcription of lysogenic genes presumably initiating from the *cI* promoter and of the lytic genes initiating from mor by Northern blot analysis in MW2c- and 8325-4 Φ13kan lysogens (Figure 3A). As expected, transcription of lytic genes (*mor*) was only detected after mitomycin treatment. One major transcript was detected representing co-expression of mor with downstream lytic genes. Several additional bands were also visible indicating processing of the transcript. The expression of these lytic genes was mainly detectable in the MW2-c Φ13kan strain. This is consistent with higher replication observed in high phage transfer strain, i.e., Newman (Figure 2E). Higher phage replication in MW2 background could be verified by quantification of phage copy numbers after mitomycin treatment via qPCR (Figure 3B). Phage replication also explains why expression of genes within the lysogenic module such as *cI* and *orfC* was also increased after mitomycin treatment. Thus, multi-copy effect after phage replication impedes the interpretation of these results.

Φ13 is likely induced following DNA damage-mediated RecA activation and sub-sequent CI autocleavage [30]. We speculated that MW2 might be more sensitive to RecA activation/SOS response compared to 8325-4. Therefore, we compared the induction of the SOS gene *recA* (preceded by a canonical LexA binding motif) in both strains. No difference in mitomycin-induced *recA* expression was observed between strains. In summary, the Northern blot analysis supported the hypothesis that RecA-independent bacterial factors promote phage replication in high transfer strains.

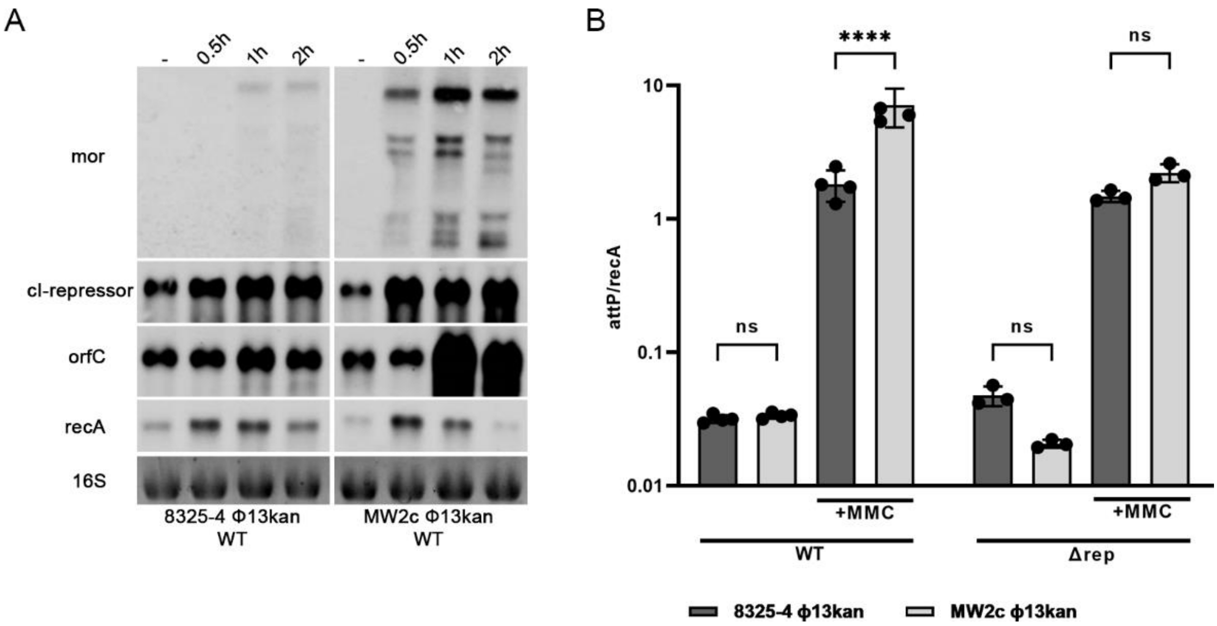

Figure 3. Phage replication is strain dependent. Transcriptional analysis of phage related genes (*cI*, *mor*, *orfC*) and chromosomally encoded *recA* under non-inducing and phage inducing conditions (A). 8325-4 Φ13kan and MW2c Φ13kan were grown to OD600 = 0.7 and treated with mitomycin for 0.5 h, 1 h, or 2 h) or without mitomycin (1h). RNA was hybridised with digoxygenin labelled DNA probes. Phage induction/replication in wild type (8325-4 Φ13kan, MW2c Φ13kan) and replication deficient derivatives (Δ*rep*) under non-inducing and phage inducing (1h mitomycin, MMC) conditions (B). Phage excision/replication was enumerated as the ratio of excised, circularized phage copies (*attP*) per copy of bacterial chromosome (*recA*) as quantified by qPCR.

Induction of Φ13kan-Δrep is not strain dependent

To exclude multicopy effects we constructed replication deficient mutants (Φ13kan-Δ*rep*) in different bacterial strain backgrounds. In such mutants the phage can excise but not replicate (Figure 3B). No phage particles were detectable by plaque assays. Calculation of the excised prophage genomes per bacterial cell was performed by absolute quantification of *attP* in relation to *recA* (as proxy for bacterial genome copy numbers) via qPCR. After mitomycin treatment, roughly one excised phage copy per bacterial genome was produced with no significant differences between strains. This indicates that phage induction is not significantly different between strains.

Transcriptional start site prediction of Φ13kan-Δrep

Besides the CI/Mor regulatory switch region additional regulatory elements on the phage genome are likely involved in the phage-host cross talk. So far, such putative regulatory elements and additional phage promoters are ill defined. Therefore, we aimed to dissect phage transcriptional units in the replication deficient lysogens 8325-4 Φ13kan-Δ*rep* and MW2c

Φ13kan-Δ*rep* using tagRNA-seq [24] followed by comparative analysis with putative TSSs as predicted by TSSpredator [31] (Figure 4, Supplementary Table S3).

We detected a total of 57 transcriptional start sites. For prediction at least two replicates had to agree on the position of a TSS. The expression of corresponding genes is shown in Figure 4 and Supplementary Table S3. In general, transcription followed the expected orientation, namely leftwards in the lysogenic module and rightwards in the lytic/structural modules.

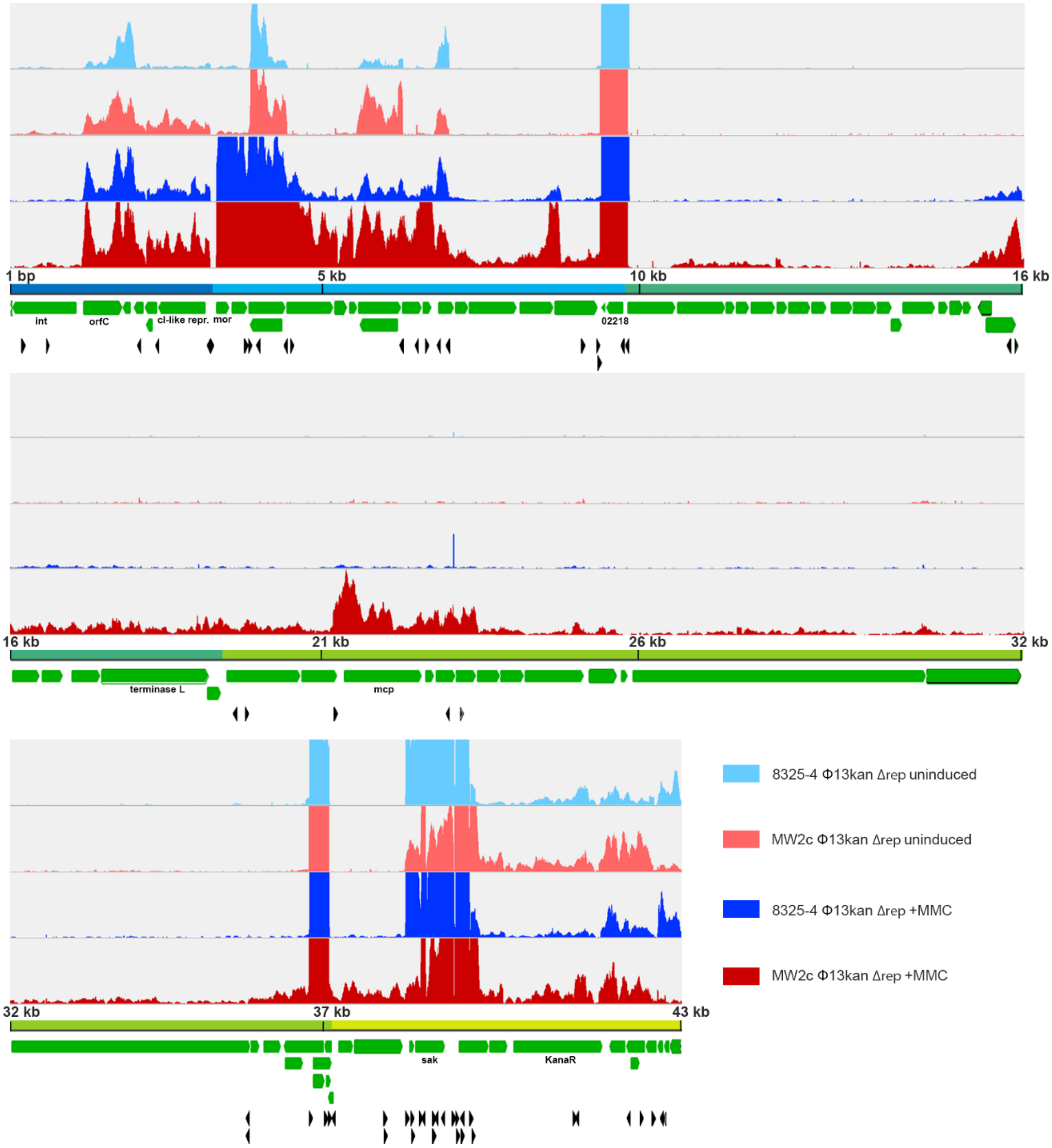

Figure 4. Visualization of predicted and enriched TSS and transcriptional profile of extracted Φ13 prophage region. Reads mapping to the phage genome are visualized for MW2c- and 8325-4 Φ13kan-Δ*rep* strains under uninduced (light red and light blue, respectively) and induced (1h mitomycin C treatment; dark red and dark blue) conditions from a representative sample out of 3 replicates. The maximum for the Y-axis in each panel is 200 counts. Protein coding genes are depicted in green and

predicted TSS (Table S3) by black arrowheads. Module organization of the genome is indicated by colour scheme shown in Figure 6A.

The analysis also revealed several noncontiguous operons (operons containing a gene(s) that is transcribed in the opposite direction to the rest of the operon) (Figure 4, Supplementary Table S3) which were only recently acknowledged to play a role in gene regulation [32]. For instance, a single gene transcript (S861) located next to ant (putative anti-repressor, SAOUHSC_02229) is part of a lytic transcript but is also transcribed in anti-sense direction towards the lysogenic module (SAOUHSC_02232) (Supplementary Table S4). A noncontiguous operon was also detected in the lysogenic module. *orfC* located between *int* and the putative phage repressor ci is transcribed opposite to the expected lysogenic direction (Figure 5A). CI transcription is initiated between *mor* and *cI* from the predicted promoter identified previously [30] (Figure 5). Northern blot analysis using strand specific RNA probes confirmed that a transcript spanning *cI* and *orfC* is simultaneously detectable with a smaller *orfC* transcript starting from the opposite strand (Figure 5B).

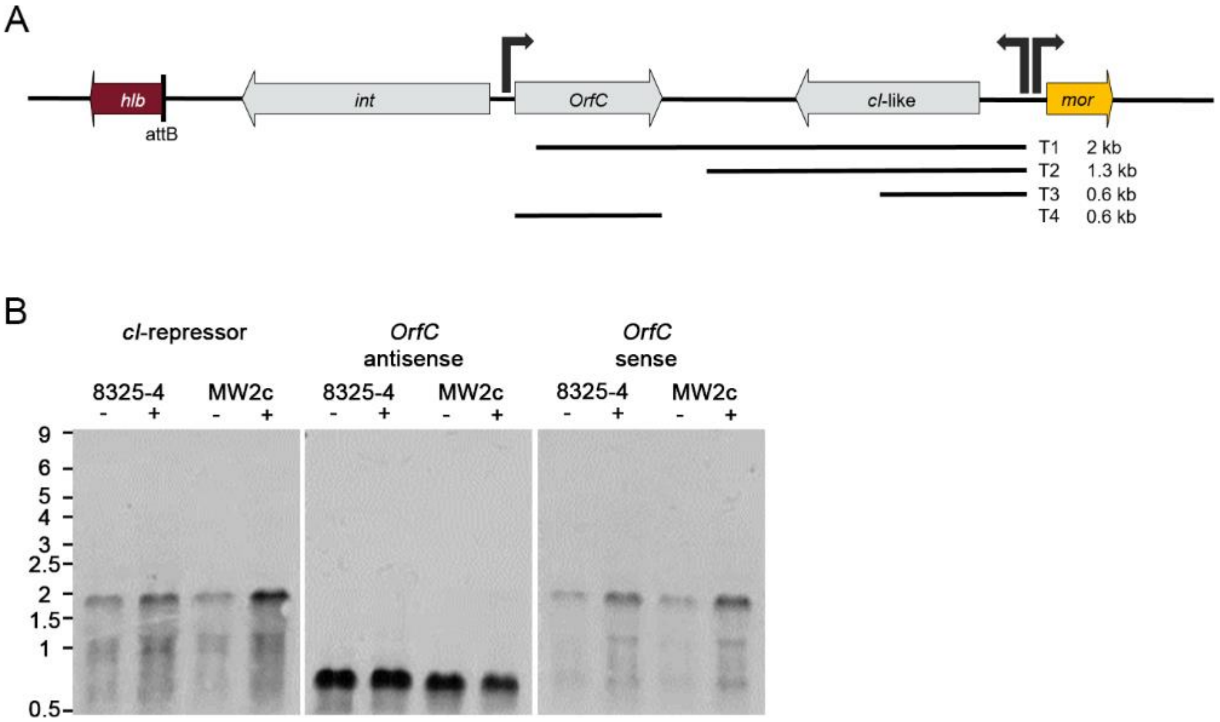

Figure 5. Transcriptional organization of the lysogenic modules of Φ13. Schematic representation of the lyosegenic module (A) of Φ13. Transcriptional units were visualized by hybridization of total RNA with digoxigenin labeled RNA probes. Replication deficient derivatives (Δ*rep*) of 8325-4 Φ13kan and MW2c Φ13kan were grown to OD600 = 0.7 and treated with (+) or without (-) mitomycin (1 h).

Thus, transcriptional regulation of phage genes seems highly complex and gene expression is controlled at several levels. While most of the 57 TSSs were common to both strain backgrounds, strain-specific TSSs were also identified. 14 of the predicted TSS are specific to 8325-4 Φ13kan (5 TSS: uninduced, 8 TSS: +MMC, 1 TSS: both conditions) and 14 TSS to MW2c Φ13kan (1 TSS: uninduced, 12 TSS: +MMC, 1 TSS: both conditions).

Strain-dependent gene expression of Φ13kan-Δrep

Phage gene expression of Φ13kan-Δrep in 8325-4 and MW2c background was quantified by RNA-seq under non-induced and induced (1 h, mitomycin treatment) conditions (Supplementary Table S4). Under uninduced conditions only 9 phage genes were differential expressed between both strains (Figure 6B). OrfC was expressed at higher levels in the 8325-background compared to the MW2-background. This is also evident in the Northern blot analysis of the Φ13kan-Δrep mutant (Figure 5B). The noncontiguous genes SAOUHSC_02232 and SAOUHSC_02218 were also more highly expressed in the 8325-4 background. Interestingly, these two genes of unknown function are transcribed in lysogenic direction although localized within the lytic phage region. Additionally, IEC genes showed higher expression in 8325 compared to MW2 (e.g., *sak*, coding for staphylokinase and the TA-system sprGF1/sprF1). The expression of *sak* was previously reported to be dependent on the host strain background with ex-pression being lower in MW2 compared to RN6390 (a derivative of 8325) background (Wirtz et al., 2009). This is in agreement with previous work showing that Sa3int-encoded virulence genes are expressed independent from phage lifecycle [10]. *Mcp* is the only gene that was found to be significantly more highly expressed in strain MW2c than in 8325-4 under non-inducing conditions.

We next compared strain dependent phage gene expression after mitomycin treatment (1 h) revealing a more profound difference in phage gene expression be-tween the two strains. Most of the prophage genes either in 8325 (40 out of 73) and MW2 (56 out of 73) were significantly upregulated after mitomycin C treatment (Supplementary Table S4). However, upregulation was more pronounced in the MW2 background. 35 prophage-encoded genes were expressed at significantly higher levels in MW2 compared to 8325 background (Figure 6C). Interestingly, no differences in the expression of *cI* and *mor* was observed between strains. Instead, most differences appeared in later genes assigned to regulation (blue), replication/packaging (dark green) and structural module (light green). Several TSSs were predicted within the lytic module, assuming that expression of gene modules is dependent on different promoters (Figure 4 and Supplementary Table S3, S4) which are subject to strain specific regulation.

Thus, the expression of lytic genes of prophage Φ13kan-Δ*rep* is more pronounced in the MW2 background compared to 8325 and probably accounts for the higher phage particle number observed in the MW2 background.

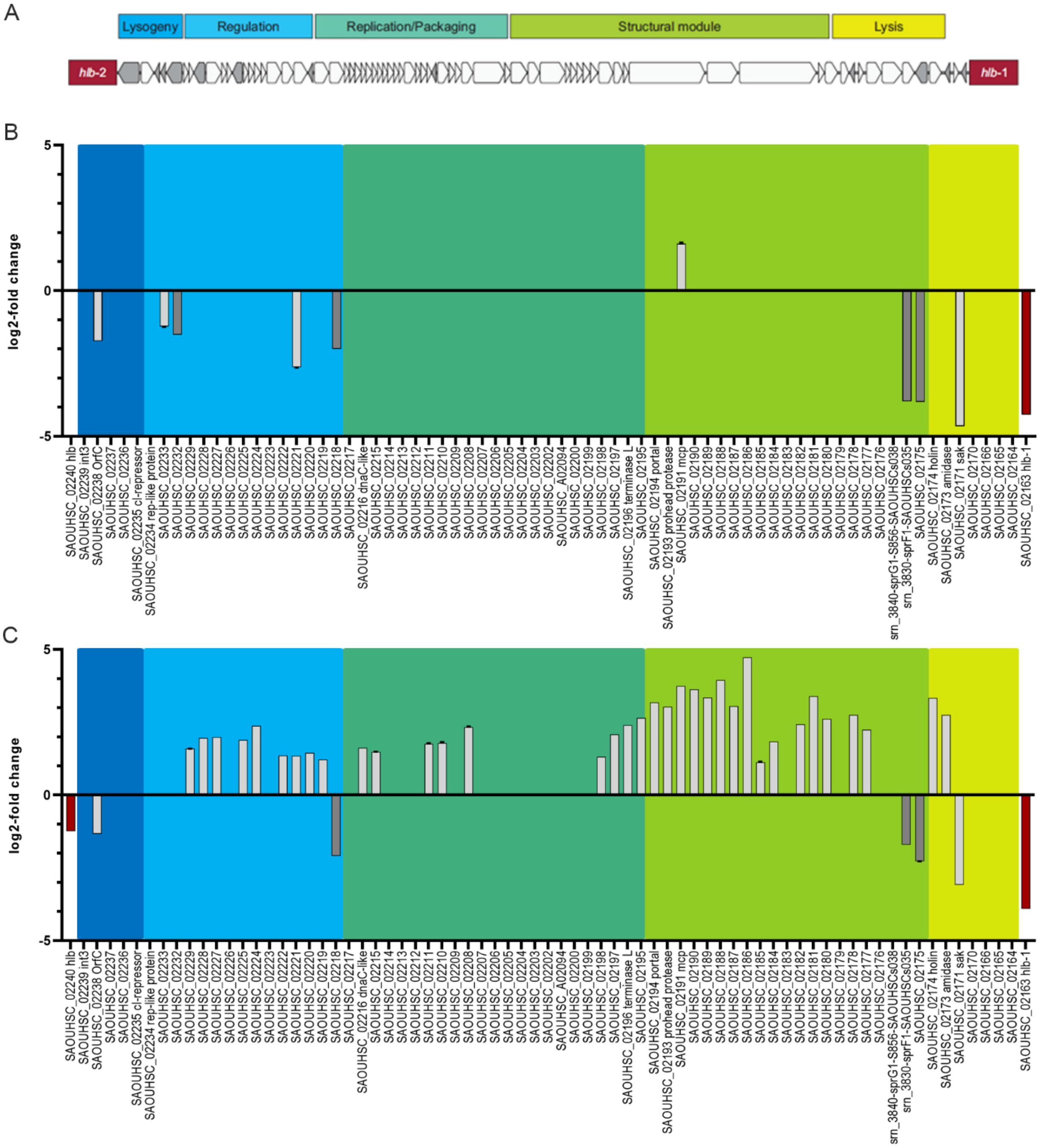

Figure 6. Comparison of Φ13kan-Δ*rep* gene expression between MW2- and 8325-background under uninduced conditions (B) and after mitomycin induction (C). Only genes with significant differences in gene expression are shown (FDR-value <0,05; log2fold change >+1 and <-1). Negative values represent higher expression in 8325 background, positive values represent higher expression in MW2 background.

Discussion

Here we could show that the lifecycle of *S. aureus* prophage is influenced by bacterial host factors. Replication of the *hlb* converting phages Φ13 and ΦN315 was significantly enhanced in the Newman and MW2 strains compared to derivatives of the 8325 lineage or USA300. The higher replication rate correlated with higher spontaneous phage transfer events during co-culture. A similar dependence of phage replication on the host background was previously shown for unrelated pvl-carrying ΦSa2mw phage [21]. The strain dependency is not due to differences in phage absorption (Supplementary Figure S2), phage integration (Figure 2), excision or *recA* transcription (Figure 3). Interference with other phages could also be ruled out since all experiments were per-formed in single-lysogens.

To get more insights into the molecular mechanisms of the predicted phage-host interaction we performed tagRNA-seq and determined the TSSs located on the Φ13kan-Δ*rep* phage and compared expression of phage genes in 8325-4 and MW2c background. The decision between phage lifestyles is made by phage-encoded genetic switches best studied in phage λ of Escherichia coli. The transcriptional repressors CI and Cro can repress each other and compete for the same operator. Phage repressor CI represses transcription of lytic genes, whereas Cro relieves repression thus facilitating the lytic life cycle. A CI/Cro like switch region can be identified in ΦN315 and ΦSa2mw2. However, in Φ13 the switch region is composed of an autocleavable CI re-pressor and a Mor homologue [30,33]. We confirmed the previously identified promoter regions as well as mitomycin sensitivity of Φ13. The CI repressor, which is ex-pressed from the lysogenic promoter PR, represses the lytic promoter initiating *mor* expression. The small repressor MOR, first identified in lactococcal phages, functions as an anti-repressor of CI by protein-protein interaction but on its own does not directly influence transcription [33-35]. Thus, *S. aureus* phages can carry either CI/Mor (Φ13) or CI/Cro like switches (ΦN315, ΦSa3mw) but nevertheless show similar strain dependency. It is thus unlikely that the proposed host factors influencing phage life cycle target the canonical switch regions. Indeed, expression of *cI* and *mor* genes was not significantly different between strains. Analysis of promoter fusions in B. subtilis also indicated that the decision switching by the minimal switch region of Φ 13 does not require *S. aureus* specific host factors [30]. This is also in line with the observation that phage integration/excision seems to be independent of the strain background and likely only determined by RecA activity.

Nevertheless, replication and gene expression were elevated in the MW2 strain background, suggesting specific regulation downstream of the switch region. The TSS analysis points to many additional promoter regions that could be subject to gene regulation. The phage derived mRNA landscape is further complicated by additional RNA processing sites. RNA processing might also be tightly controlled and functionally important [36,37]. Additionally, sRNAs or post-transcriptional regulation via e.g., anti-termination [38] may be involved. Moreover, our analysis revealed several non-contiguous operons. Such a genetic arrangement was proposed to lead to mutual regulation of the expression of overlapping transcripts and to provide an additional strategy for coordinating the expression of functionally related genes within an operon [32].

Some TSSs were detected only in one strain background. Genes coding for structural phage proteins are more highly expressed in MW2 than in 8325-4. Thus, these TSSs are likely targets for host-dependent regulation. Post excision regulation of phage replication and assembly, processes that are important to finalize the phage lytic phase, may also be a crucial determinant of the lysogenic-lytic cycle switch. Thus, under certain circumstances the phages may just excise leading to reconstitution of the intact *hlb* gene in absence of complete phage assembly and host cell lysis. Such a pro-cess is reminiscent of the recently described process termed active lysogeny [39]. *L. monocytogenes* strain 10403S harbors a prophage in its *comK* gene. During infection of macrophage cells, the prophage lytic pathway is induced but the phage lytic response is arrested, preventing the expression of the late genes. A phage encoded LlgA transcription regulator (LlgA) and a DNA replicase are proposed to support the phage adaptive behavior [40]. No LlgA homologue could be identified but functionally simi-lar elements may be present in the *S. aureus* phages. The data strongly indicate that host factors interfere with such putative regulatory phage regions. Recently discussed xenogenic silencing factors might be involved in such a balance [41]. They promote tolerance of foreign genetic material and may play an important role in maintaining the lysogenic state. Those discovered so far are small, nucleoid-associated proteins that recognize and bind AT-rich DNA stretches (H-NS in Proteobacteria, MvaT/U in *Pseudomonas species*, Rok in *Bacillus subtilis* and Lsr2 in Actinobacteria). Of note, none of these factors is present in *S. aureus*. The phage encoded virulence genes are known to be under the control of bacterial virulence regulatory systems such as the quorum sensing system, Agr or the SaeRS two-component system [20]. From genome comparison between the low and high transfer strains no obvious difference in known regulatory circuits such as quorum sensing or transcriptional factors was evident. Nevertheless, our data indicate that also phage structural genes are tightly controlled although the mechanism remains to be determined.

Epidemiological data strongly indicate that Sa3int phages have co-evolved with the *S. aureus* host to facilitate the adaptation of the species to the human host. Adaptation is likely mediated by the phage-encoded virulence factors, which are specific to humans (Rohmer & Wolz, 2021). Of note, most *S. aureus* strains lack major phage defense systems such as CRISPR/Cas, cyclic-oligonucleotide-based anti-phage signaling systems (Millman et al., 2020b) or phage-resistance mediating retrons (Millman et al., 2020a). This indicates that the species has likely evolved to tolerate phages and that the phages, to a large extent, are probably beneficial to the bacterial host. However, the phages remain highly mobile to relieve expression of the interrupted *hlb* gene when needed, e.g., during infection [15,42]. This may occur either in the form of “active lysogeny” or prophage loss. Such switches must be controlled through firm molecular interactions between bacterial and phage factors. The postulated bacterial factors are highly strain specific, and certain *S. aureus* strains may be more prone than others to support either a lysogenic or a lytic life cycle. Thus, the genetic make-up of the host strains may determine the rate of phage mobilization during infection, a feature that might determine the speed at which certain strains can achieve host adaptation.

Supplementary Materials: The following supporting information can be downloaded at: www.mdpi.com/xxx/s1, Figure S1: Phage transfer between CC8 and CC1; Figure S2: Phage adsorption; Table S1: Strains used in this study; Table S2: Oligonucleotides used in this study; Table S3: TSS prediction and corresponding gene expression; Table S4: Differential gene expression analysis of extracted prophage genomic region.

Author Contributions: Conceptualization, C.R., R.D. and C.W.; methodology, C.R., R.D., E.L., D.G., S.E.G.; software, D.T.D., K.N.; validation, C.R., R.D., D.T.D, K.N. and C.W.; formal analysis, C.R., R.D., D.T.D.; investigation, C.R., R.D., D.T.D., D.G., T.B.; writing—original draft preparation, C.R., R.D., C.W.; writing—review and editing, C.R., R.D., C.W., K.N.; visualization, C.R., R.D.; supervision, C.W.; project administration, C.W.; funding acquisition, C.W. All authors have read and agreed to the published version of the manuscript.

Funding: This work was funded by Deutsche Forschungsgemeinschaft, GRK1708 to CW and CR (Project 174858087), Schwerpunktprogramm Spp2330 to CW (Project 464612409) and by infra-structural funding from the Deutsche Forschungsgemeinschaft (DFG), Cluster of Excellence EXC 2124 “Controlling Microbes to Fight Infections” (Project 390838134).

Data Availability Statement: RNAseq raw data and processed files containing RPKM-values are available at https://www.ncbi.nlm.nih.gov/geo/query/acc.cgi?acc=GSE214523.

Acknowledgments: We thank Nataly Korn und Vittoria Bisanzio for technical assistance and Libera Lo Presti for scientific discussions and editing of the manuscript, and Jeffrey J. Power for bioinformatic support.

Conflicts of Interest: The authors declare no conflict of interest.

References

1. Matuszewska, M.; Murray, G.G.R.; Harrison, E.M.; Holmes, M.A.; Weinert, L.A. The Evolutionary Genomics of Host Specificity in *Staphylococcus aureus*. Trends Microbiol 2020, 28, 465-477, doi:10.1016/j.tim.2019.12.007.

2. Balasubramanian, D.; Harper, L.; Shopsin, B.; Torres, V.J. *Staphylococcus aureus* pathogenesis in diverse host environments. Pathog Dis 2017, 75, doi:10.1093/femspd/ftx005.
3. Turner, N.A.; Sharma-Kuinkel, B.K.; Maskarinec, S.A.; Eichenberger, E.M.; Shah, P.P.; Carugati, M.; Holland, T.L.; Fowler, V.G., Jr. Methicillin-resistant *Staphylococcus aureus*: an overview of basic and clinical research. Nat Rev Microbiol 2019, 17, 203-218, doi:10.1038/s41579-018-0147-4.
4. Sakr, A.; Bregeon, F.; Mege, J.L.; Rolain, J.M.; Blin, O. *Staphylococcus aureus* Nasal Colonization: An Update on Mechanisms, Epidemiology, Risk Factors, and Subsequent Infections. Front Microbiol 2018, 9, 2419, doi:10.3389/fmicb.2018.02419.
5. Haag, A.F.; Fitzgerald, J.R.; Penades, J.R. *Staphylococcus aureus* in Animals. Microbiol Spectr 2019, 7, doi:10.1128/microbiolspec.GPP3-0060-2019.
6. Richardson, E.J.; Bacigalupe, R.; Harrison, E.M.; Weinert, L.A.; Lycett, S.; Vrieling, M.; Robb, K.; Hoskisson, P.A.; Holden, M.T.G.; Feil, E.J.; et al. Gene exchange drives the ecological success of a multi-host bacterial pathogen. Nat Ecol Evol 2018, 2, 1468-1478, doi:10.1038/s41559-018-0617-0.
7. McCarthy, A.J.; Witney, A.A.; Lindsay, J.A. *Staphylococcus aureus* temperate bacteriophage: carriage and horizontal gene transfer is lineage associated. Front Cell Infect Microbiol 2012, 2, 6, doi:10.3389/fcimb.2012.00006.
8. Ingmer, H.; Gerlach, D.; Wolz, C. Temperate Phages of *Staphylococcus aureus*. Microbiol Spectr 2019, 7, doi:10.1128/microbiolspec.GPP3-0058-2018.
9. Chaguza, C.; Smith, J.T.; Bruce, S.A.; Gibson, R.; Martin, I.W.; Andam, C.P. Prophage-encoded immune evasion factors are critical for *Staphylococcus aureus* host infection, switching, and adaptation. Cell Genomics 2022, doi:10.1016/j.xgen.2022.100194.
10. Rohmer, C.; Wolz, C. The Role of *hlb*-Converting Bacteriophages in *Staphylococcus aureus* Host Adaption. Microb Physiol 2021, 31, 109-122, doi:10.1159/000516645.
11. Bouiller, K.; Bertrand, X.; Hocquet, D.; Chirouze, C. Human Infection of Methicillin-Susceptible *Staphylococcus aureus* CC398: A Review. Microorganisms 2020, 8, doi:10.3390/microorganisms8111737.
12. Sung, J.M.; Lloyd, D.H.; Lindsay, J.A. *Staphylococcus aureus* host specificity: comparative genomics of human versus animal isolates by multi-strain microarray. Microbiology (Reading) 2008, 154, 1949-1959, doi:10.1099/mic.0.2007/015289-0.
13. Goerke, C.; Pantucek, R.; Holtfreter, S.; Schulte, B.; Zink, M.; Grumann, D.; Broker, B.M.; Doskar, J.; Wolz, C. Diversity of prophages in dominant *Staphylococcus aureus* clonal lineages. J Bacteriol 2009, 191, 3462-3468, doi:10.1128/JB.01804-08.
14. van Wamel, W.J.; Rooijakkers, S.H.; Ruyken, M.; van Kessel, K.P.; van Strijp, J.A. The innate immune modulators staphylococcal complement inhibitor and chemotaxis inhibitory

protein of *Staphylococcus aureus* are located on beta-hemolysin-converting bacteriophages. J Bacteriol 2006, 188, 1310-1315, doi:10.1128/JB.188.4.1310-1315.2006.
15. Goerke, C.; Wirtz, C.; Fluckiger, U.; Wolz, C. Extensive phage dynamics in *Staphylococcus aureus* contributes to adaptation to the human host during infection. Mol Microbiol 2006, 61, 1673-1685, doi:10.1111/j.1365-2958.2006.05354.x.
16. Deghorain, M.; Van Melderen, L. The Staphylococci phages family: an overview. Viruses 2012, 4, 3316-3335, doi:10.3390/v4123316.
17. Kahankova, J.; Pantucek, R.; Goerke, C.; Ruzickova, V.; Holochova, P.; Doskar, J. Multilocus PCR typing strategy for differentiation of *Staphylococcus aureus* siphoviruses reflecting their modular genome structure. Environ Microbiol 2010, 12, 2527-2538, doi:10.1111/j.1462-2920.2010.02226.x.
18. Oliveira, H.; Sampaio, M.; Melo, L.D.R.; Dias, O.; Pope, W.H.; Hatfull, G.F.; Azeredo, J. Staphylococci phages display vast genomic diversity and evolutionary relationships. BMC Genomics 2019, 20, 357, doi:10.1186/s12864-019-5647-8.
19. Zhou, W.; Wen, H.; Li, Y.; Gao, Y.; Zheng, X.; Yuan, L.; Zhu, G.; Yang, Z. Whole-Genome Analysis Reveals That Bacteriophages Promote Environmental Adaptation of *Staphylococcus aureus* via Gene Exchange, Acquisition, and Loss. Viruses 2022, 14, doi:10.3390/v14061199.
20. Xia, G.; Wolz, C. Phages of *Staphylococcus aureus* and their impact on host evolution. Infect Genet Evol 2014, 21, 593-601, doi:10.1016/j.meegid.2013.04.022.
21. Wirtz, C.; Witte, W.; Wolz, C.; Goerke, C. Transcription of the phage-encoded Panton-Valentine leukocidin of *Staphylococcus aureus* is dependent on the phage life-cycle and on the host background. Microbiology (Reading) 2009, 155, 3491-3499, doi:10.1099/mic.0.032466-0.
22. Gerlach, D.; Guo, Y.; De Castro, C.; Kim, S.H.; Schlatterer, K.; Xu, F.F.; Pereira, C.; Seeberger, P.H.; Ali, S.; Codee, J.; et al. Methicillin-resistant *Staphylococcus aureus* alters cell wall glycosylation to evade immunity. Nature 2018, 563, 705-709, doi:10.1038/s41586-018-0730-x.
23. Xia, G.; Corrigan, R.M.; Winstel, V.; Goerke, C.; Grundling, A.; Peschel, A. Wall teichoic Acid-dependent adsorption of staphylococcal siphovirus and myovirus. J Bacteriol 2011, 193, 4006-4009, doi:10.1128/JB.01412-10.
24. Innocenti, N.; Golumbeanu, M.; Fouquier d'Herouel, A.; Lacoux, C.; Bonnin, R.A.; Kennedy, S.P.; Wessner, F.; Serror, P.; Bouloc, P.; Repoila, F.; et al. Whole-genome mapping of 5' RNA ends in bacteria by tagged sequencing: a comprehensive view in *Enterococcus faecalis*. RNA 2015, 21, 1018-1030, doi:10.1261/rna.048470.114.

25. Berscheid, A.; Sass, P.; Weber-Lassalle, K.; Cheung, A.L.; Bierbaum, G. Revisiting the genomes of the *Staphylococcus aureus* strains NCTC 8325 and RN4220. Int J Med Microbiol 2012, 302, 84-87, doi:10.1016/j.ijmm.2012.01.002.
26. Forstner, K.U.; Vogel, J.; Sharma, C.M. READemption-a tool for the computational analysis of deep-sequencing-based transcriptome data. Bioinformatics 2014, 30, 3421-3423, doi:10.1093/bioinformatics/btu533.
27. Tang, Y.; Nielsen, L.N.; Hvitved, A.; Haaber, J.K.; Wirtz, C.; Andersen, P.S.; Larsen, J.; Wolz, C.; Ingmer, H. Commercial Biocides Induce Transfer of Prophage Phi13 from Human Strains of *Staphylococcus aureus* to Livestock CC398. Front Microbiol 2017, 8, 2418, doi:10.3389/fmicb.2017.02418.
28. Haaber, J.; Leisner, J.J.; Cohn, M.T.; Catalan-Moreno, A.; Nielsen, J.B.; Westh, H.; Penades, J.R.; Ingmer, H. Bacterial viruses enable their host to acquire antibiotic resistance genes from neighbouring cells. Nat Commun 2016, 7, 13333, doi:10.1038/ncomms13333.
29. Moller, A.G.; Lindsay, J.A.; Read, T.D. Determinants of Phage Host Range in Staphylococcus Species. Appl Environ Microbiol 2019, 85, doi:10.1128/AEM.00209-19.
30. Kristensen, C.S.; Varming, A.K.; Leinweber, H.A.K.; Hammer, K.; Lo Leggio, L.; Ingmer, H.; Kilstrup, M. Characterization of the genetic switch from phage 13 important for *Staphylococcus aureus* colonization in humans. Microbiologyopen 2021, 10, e1245, doi:10.1002/mbo3.1245.
31. Dugar, G.; Herbig, A.; Forstner, K.U.; Heidrich, N.; Reinhardt, R.; Nieselt, K.; Sharma, C.M. High-resolution transcriptome maps reveal strain-specific regulatory features of multiple Campylobacter jejuni isolates. PLoS Genet 2013, 9, e1003495, doi:10.1371/journal.pgen.1003495.
32. Saenz-Lahoya, S.; Bitarte, N.; Garcia, B.; Burgui, S.; Vergara-Irigaray, M.; Valle, J.; Solano, C.; Toledo-Arana, A.; Lasa, I. Noncontiguous operon is a genetic organization for coordinating bacterial gene expression. Proc Natl Acad Sci U S A 2019, 116, 1733-1738, doi:10.1073/pnas.1812746116.
33. Pedersen, M.; Neergaard, J.T.; Cassias, J.; Rasmussen, K.K.; Lo Leggio, L.; Sneppen, K.; Hammer, K.; Kilstrup, M. Repression of the lysogenic PR promoter in bacteriophage TP901-1 through binding of a CI-MOR complex to a composite OM-OR operator. Sci Rep 2020, 10, 8659, doi:10.1038/s41598-020-65493-0.
34. Rasmussen, K.K.; Palencia, A.; Varming, A.K.; El-Wali, H.; Boeri Erba, E.; Blackledge, M.; Hammer, K.; Herrmann, T.; Kilstrup, M.; Lo Leggio, L.; et al. Revealing the mechanism of repressor inactivation during switching of a temperate bacteriophage. Proc Natl Acad Sci U S A 2020, 117, 20576-20585, doi:10.1073/pnas.2005218117.

35. Pedersen, M.; Hammer, K. The role of MOR and the CI operator sites on the genetic switch of the temperate bacteriophage TP901-1. J Mol Biol 2008, 384, 577-589, doi:10.1016/j.jmb.2008.09.071.
36. Lacoux, C.; Fouquier d'Herouel, A.; Wessner-Le Bohec, F.; Innocenti, N.; Bohn, C.; Kennedy, S.P.; Rochat, T.; Bonnin, R.A.; Serror, P.; Aurell, E.; et al. Dynamic insights on transcription initiation and RNA processing during bacterial adaptation. RNA 2020, 26, 382-395, doi:10.1261/rna.073288.119.
37. Marincola, G.; Schafer, T.; Behler, J.; Bernhardt, J.; Ohlsen, K.; Goerke, C.; Wolz, C. RNase Y of *Staphylococcus aureus* and its role in the activation of virulence genes. Mol Microbiol 2012, 85, 817-832, doi:10.1111/j.1365-2958.2012.08144.x.
38. Yin, Z.; Kaelber, J.T.; Ebright, R.H. Structural basis of Q-dependent antitermination. Proc Natl Acad Sci U S A 2019, 116, 18384-18390, doi:10.1073/pnas.1909801116.
39. Feiner, R.; Argov, T.; Rabinovich, L.; Sigal, N.; Borovok, I.; Herskovits, A.A. A new perspective on lysogeny: prophages as active regulatory switches of bacteria. Nat Rev Microbiol 2015, 13, 641-650, doi:10.1038/nrmicro3527.
40. Pasechnek, A.; Rabinovich, L.; Stadnyuk, O.; Azulay, G.; Mioduser, J.; Argov, T.; Borovok, I.; Sigal, N.; Herskovits, A.A. Active Lysogeny in Listeria monocytogenes is a bacteria-phage adaptive response in the mammalian environment. Cell Rep 2020, 32, 107956, doi:10.1016/j.celrep.2020.107956.
41. Pfeifer, E.; Hunnefeld, M.; Popa, O.; Frunzke, J. Impact of xenogeneic silencing on phage-host interactions. J Mol Biol 2019, 431, 4670-4683, doi:10.1016/j.jmb.2019.02.011.
42. Goerke, C.; Matias y Papenberg, S.; Dasbach, S.; Dietz, K.; Ziebach, R.; Kahl, B.C.; Wolz, C. Increased frequency of genomic alterations in *Staphylococcus aureus* during chronic infection is in part due to phage mobilization. J Infect Dis 2004, 189, 724-734, doi:10.1086/381502.

Chapter III

The following chapter is part of the dissertation of Jessica Slaventinsky (née Schade) in form of an earlier version of this manuscript ready for submission.

The former version was published as

The following chapter was rewritten based on the mentioned manuscript and is thus in parts congruent to it.
The published version of this manuscript may diverge from the version below.

Wall teichoic acids mediate *Staphylococcus aureus* binding to scavenger receptor LOX-1 on endothelial cells

Jessica Slavetinsky[1], Esther Lehmann[1], Christoph Slavetinsky[1], Lisa Gritsch[1], Rob van Dalen[1], Dorothee Kretschmer[1], Lisa Bleul[1], Christiane Wolz[1,2], Christopher Weidenmaier, Andreas Peschel[1,2,3]

1. Interfaculty Institute of Microbiology and Infection Medicine
2. Cluster of Excellence EXC 2124 “Controlling Microbes to Fight Infections”, University of Tübingen
3. German Center for Infection Research (DZIF), Partner Site Tübingen, Tübingen, Germany

Keywords

Staphylococcus aureus; wall teichoic acid; scavenger receptor; endocarditis; sepsis

Corresponding author: Prof. Dr. Andreas Peschel, Dr. Christopher Weidenmaier
E-mail: andreas.peschel@uni-tuebingen.de

Abstract

Staphylococcus aureus is a major bacterial pathogen and leading cause for severe endovascular infections. The mechanisms that allow *S. aureus* to adhere to the endothelial lining and to disseminate into the underlying tissue are not fully understood. Wall teichoic acid (WTA) has been described as non-proteinaceous cell-surface component mediating adhesion to host cells. Here we show that purified WTA specifically bind to recombinant scavenger receptor LOX-1. Adhesion of *S. aureus* to LOX-1 transfected cell line as well as to LOX-1 expressing human primary endothelial cells was WTA-dependent. Increased expression of LOX-1 as well as WTA correlated with increased adhesion of *S. aureus* to primary endothelial cells. Competitive inhibitors (PolyI), specific antibodies (LOX-1-mAB) and ligands (oxLDL) of LOX-1 reduced adhesion of *S. aureus* to endothelial cells to the level of the WTA-deficient Δ*tagO* mutant. In sum, we identified LOX-1 as a novel receptor for *S. aureus* WTA that mediates endothelial adhesion.

Introduction

Staphylococcus aureus is one of the most prevalent bacterial pathogens isolated from patients with endovascular infections (Hoerr 2018; Nappi et al. 2022). It frequently disseminates from the bloodstream into the underlying tissue and organs. Upon dissemination *S. aureus* causes acute and chronic infections such as endocarditis, septic arthritis or osteomyelitis (Lowy 1998; Tong et al. 2015; Dayan et al. 2016; Pollitt et al. 2018; Turner et al. 2019). The onset and progression of endovascular infections is regulated by a series of complex interactions between circulating bacteria and the vascular lining and initiated by *S. aureus* adhesion to the endothelium (Nappi et al. 2022). Subsequent dissemination from the bloodstream is followed by metastatic infections of the organs (Surewaard et al. 2016). For a long time, research on *S. aureus*-endothelium interaction has focused on protein adhesins such as the microbial surface components recognizing adhesive matrix molecules (MSCRAMMs) (Patti et al. 1994; Foster and Hook 1998; Hoerr et al. 2018). The MSCRAMMs FnbPA and FnbPB, for example, bind endothelial cells via fibronectin-integrin interactions, which can trigger uptake of *S. aureus* into endothelial cells and contribute to the ability of *S. aureus* to cause infective endocarditis (Edwards et al. 2010; Edwards and Massey 2011).

We have previously shown that, besides protein adhesins, also the non-proteinaceous wall teichoic acid (WTA) polymers contribute to the binding of *S. aureus* to epithelial and endothelial cells and aggravate pathogenesis of infections (Weidenmaier et al. 2005; Baur et al. 2014; Wanner 2017). WTA is an important cell surface determinant and virulence factor of *S. aureus* and many other Gram-positive bacteria (Kohler, Weidenmaier, and Peschel 2009; van Dalen 2020). It is a major surface antigen of *S. aureus* and governs important host defense processes such as activation of complement system, of Langerhans cells, and of T-cells and the susceptibility to antimicrobial host peptides and lipids (van Dalen 2020). *S. aureus* WTA is comprised of a polyribitolphosphate backbone with secondary *N*-acetylglucosamine (GlcNAc) and D-alanine modifications (van Dalen 2020) and has a characteristic zwitterionic charge profile due to the combination of the negatively charged phosphates in the backbone and the positively charged D-alanine modification (Weidenmaier, McLoughlin, and Lee 2010; Winstel et al. 2015; Weidenmaier and Lee 2016). Overexpression of WTA biosynthesis genes lead to a WTA^{high} phenotype resulting in increased virulence of the respective *S. aureus* strains in an abscess model in a T-cell dependent fashion. The WTA^{high} phenotype has been linked to highly virulent *S. aureus* isolates, such as community-acquired methicillin-resistant *S. aureus* (CA-MRSAs) and proposed as mechanism to increase their invasiveness while typical healthcare-associated MRSA (HA-MRSA) usually exhibit WTA^{low} properties (Wanner 2017). We could previously show that WTA-coated microspheres bind endothelial cells in a dose-dependent manner, whereas a WTA-deficient *S. aureus* mutant (*ΔtagO*) showed reduced adhesion to human endothelial cells and attenuated virulence in endovascular infections when compared to the parental strain (Weidenmaier et al. 2005). However, the endothelial receptor responsible for WTA-mediated *S. aureus* attachment has remained unknown.

S. aureus uses WTA also to bind to epithelial cells as a prerequisite for continued nasal colonization (Baur et al. 2014). We have previously demonstrated that WTA binds to the epithelial scavenger receptor SREC-1, which is required for *S. aureus* colonization in a cotton rat model of nasal colonization (Baur et al. 2014). Scavenger receptors form a heterogeneous class of surface proteins that interact with a variety of endogenous and exogeneous molecules (Pombinho, Sousa, and Cabanes 2018). Some have been found to facilitate binding of bacteria, albeit, with largely unknown ligand specificities and unclear relevance (Taban et al. 2022). SREC-1 was the first scavenger receptor reported to bind *S. aureus* WTA. SREC-1 facilitates epithelial adhesion. However, possible binding partners on endothelial cells are yet to be identified. We speculate endothelial scavenger receptors might be responsible WTA-mediated binding of *S. aureus* to the endothelium. The lectin-like class-E scavenger receptor LOX-1 is expressed on endothelial cells (Morawietz et al. 2001) and has been shown to bind Gram-positive (*S. aureus*) and Gram-negative bacteria (*Escherichia coli*) (Shimaoka et al. 2001). Still, the molecular ligand for LOX-1 on the *S. aureus* surface and the relevance for endothelial binding has remained elusive.

We hypothesized that WTA mediates attachment of *S. aureus* to endothelial cells via LOX-1 and assessed this possibility using purified LOX-1, LOX-1 transfected cell lines, and specific inhibitors of LOX-1. Our results demonstrate that WTA-LOX-1 interactions are crucial for *S. aureus* binding to endothelial cells.

Results

The scavenger receptor LOX-1 binds *S. aureus* WTA

To assess if WTA might be the bacterial ligand for LOX-1, we first designed an in-vitro interaction assay. WTA isolated from *S. aureus* (USA300 JE2) was immobilized on latex beads and incubated with the soluble LOX-1. We observed that Cy3-labeled LOX-1 bound to the WTA-coated beads (figure 1A). Binding increased with the amount of WTA used for coating indicating that LOX-1 binds *S. aureus* WTA.

To analyze a potential role of WTA as LOX-1 ligand for *S. aureus* cell adhesion, we transduced Chinese Hamster Ovary (CHO-k1) cells with the human LOX-1 gene to generate a LOX-1-expressing cell line named CHO-LOX-1, as described previously for CHO-SREC-1 (Baur et al. 2014) (supplemental figure 1). We compared adhesion of *S. aureus* USA300 JE2, a WTA-high clone (Wanner 2017), and the WTA-deficient isogenic Δ*tagO* mutant to CHO-LOX-1 and the parental cell line that does not express scavenger receptors. There was no difference in the residual LOX-1-independent adhesion to CHO-k1 between USA300 JE2 and USA300 JE2 Δ*tagO*. In contrast, adhesion of USA300 JE2 to CHO-LOX-1 was significantly increased, while it remained unchanged for the Δ*tagO* mutant. The complemented mutant USA300 JE2 Δ*tagO* p*tagO* showed the same adhesion behavior as USA300 JE2 (Figure 1B).

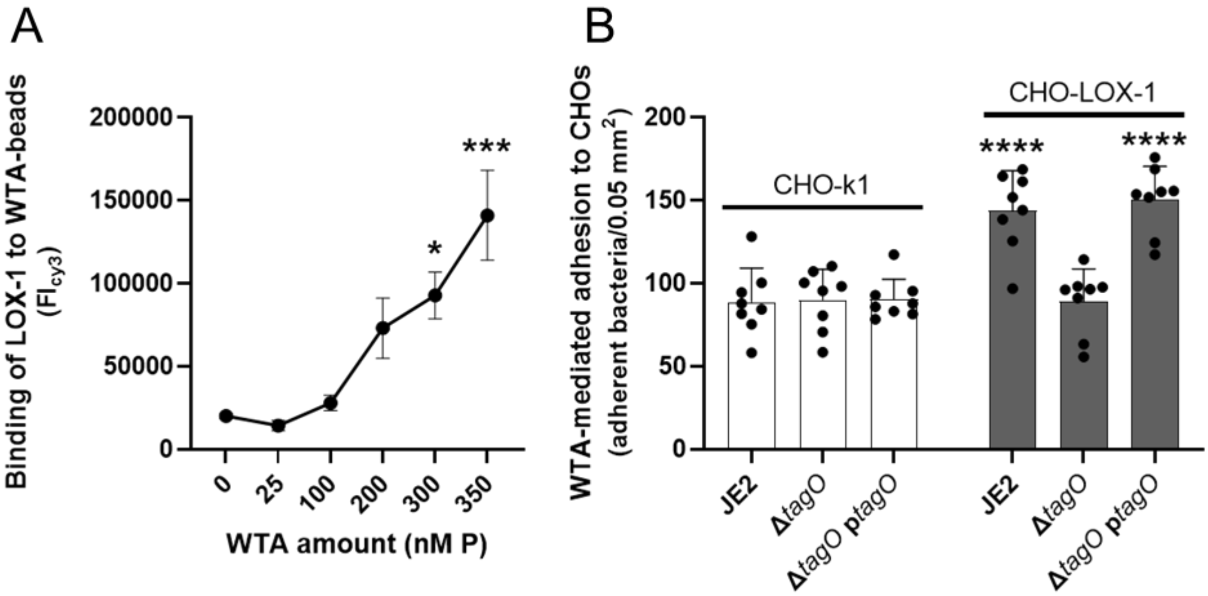

Figure 2: Interaction of LOX-1 with *S. aureus* WTA. (A) Immobilized WTA bind LOX-1 in a dose-dependent manner. Amine-modified latex beads were coated with WTA from USA300 JE2 at increasing concentrations (given in amounts of organic phosphate (P)). Interaction of WTA with Cy3 labeled LOX-1 was quantified by absolute fluorescence (FI_{cy3}). Data represent means ± SD of three independent experiments. Significance of differences vs. 0 mM phosphate were calculated by one-way analysis of variance (ANOVA) with Dunnett's test for multiple comparison. (B) Adhesion assays were performed with FITC-labelled bacteria. CHO-k1 and CHO-LOX-1 were incubated with USA300 JE2, USA300 JE2 Δ*tagO,* or USA300 JE2 Δ*tagO* p*tagO*. Numbers of adherent bacteria per 0.5 mm^2 of confluent cell layers were counted. Data represents means ± SD of eight independent experiments. Significance of differences were calculated compared to adhesion of USA300 JE2 to CHO-k1 by two-way ANOVA with Tukey's correction for multiple comparison. (*$p < 0.05$; **$p < 0.01$; ***$p < 0.001$; ****$p < 0.0001$)

LOX-1 facilitates WTA-dependent adhesion of *S. aureus* to endothelial cells

After demonstrating WTA-dependent interaction of *S. aureus* with the receptor LOX-1 in CHO cells, we assessed if LOX-1 also supports binding of *S. aureus* to primary endothelial cells using human umbilical vein endothelial cells (HUVECs), pooled from multiple donors. To study how variations of WTA amounts may affect endothelial binding we used the WTA^{low} *S. aureus* strain SA113 and its derivate with plasmid p*tarH,* which overexpresses the WTA transporter TarH resulting in a WTA^{high} phenotype. Adhesion of the WTA^{high} strains SA113 p*tarH* and USA300 JE2 to HUVECs was significantly higher compared to the WTA^{low} strain SA113 (figure 2A). Together these data indicate a crucial and dose-dependent role of WTA in the capacity of *S. aureus* to adhere to HUVECs. LOX-1 expression can be upregulated on endothelial cells by stimulation with the LOX-1 ligand oxLDL (Pirillo et al. 2011; Pirillo et al. 2012). As described by Pirillo et al. LOX-1 expression on HUVECs was increased by treatment with 50 µg/ml oxLDL for 12 hours (supplemental figure 2). In parallel, adhesion of SA113 increased upon oxLDL stimulation. In contrast, the WTA-deficient SA113 Δ*tagO* mutant did not change binding behavior upon oxLDL stimulation while the complemented mutant SA113 Δ*tagO* p*tagO* reverted to wild-type adhesion phenotype (figure 2B).

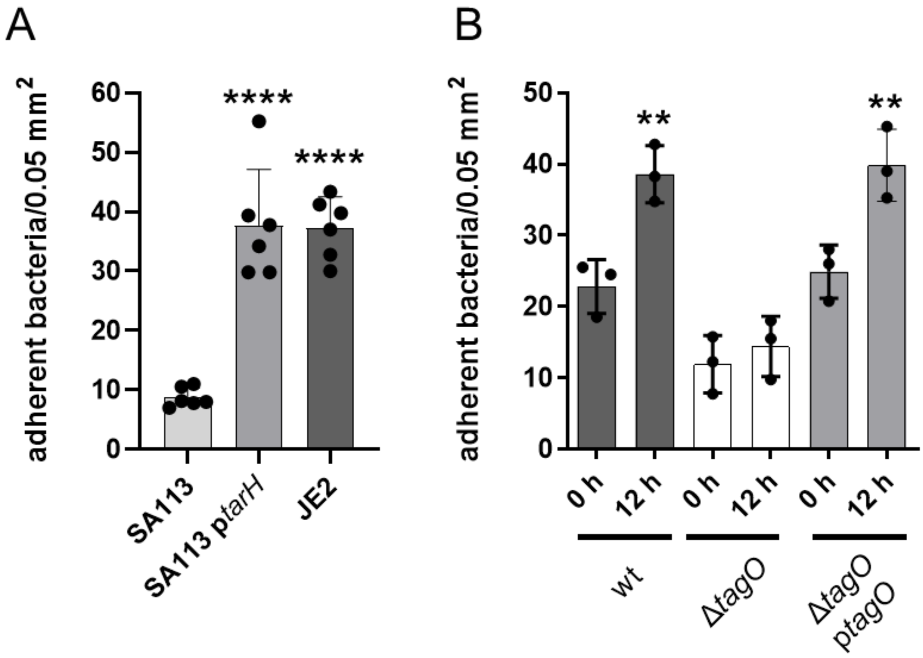

Figure 3: *S. aureus* adhesion to endothelial cells increases upon LOX-1 upregulation. *S. aureus* adhesion can be increased by upregulation of expression of either WTA or LOX-1. (A) HUVECs were infected with SA113, SA113 p*tarH* and USA300 JE2. Data represents means ± SD of 6 independent experiments. Significances of differences vs. SA113 were calculated by one-way ANOVA with Dunnett's test for multiple comparison. (B) Induction of LOX-1 expression in HUVECs by pre-incubation with 50 µg/ml oxLDL. Bacterial counts of five random 0.05 mm^2 fields per replicate were counted. Significant differences vs. respective 0 h value were calculated by one-way ANOVA with Tukey's correction for multiple comparison. (*p < 0.05; **p < 0.01; ***p < 0.001; ****p < 0.0001).

Blocking of LOX-1 inhibits WTA-mediated *S. aureus* adhesion to endothelial cells

The polyanionic glycopolymer poly inositol (poly-I) is known as a competitive inhibitor of LOX-1 (Palkama 1993). In order to confirm the WTA dependent binding of *S. aureus* to HUVECs via LOX-1 we analyzed the capacity of poly-I to block the WTA-dependent binding of *S. aureus* to HUVECs (Figure 3). Adhesion of SA113 as well as of SA113 Δ*tagO* p*tagO* to HUVECs could be blocked by pre-incubation of HUVECs with poly-I in a dose-dependent manner leading to a similarly low binding level as for the WTA-deficient SA113 *tagO* mutant (figure 3A). In contrast, the binding of SA113 *tagO* was not affected by poly-I. Likewise, the endogenous LOX-I ligand oxLDL (figure 3B) and a monoclonal anti-LOX-1 antibody (figure 3C) also blocked binding of WTA-expressing but not of WTA-deficient *S. aureus* to HUVECs. Thus, WTA-dependent binding of *S. aureus* to HUVECs is largely mediated by LOX-1.

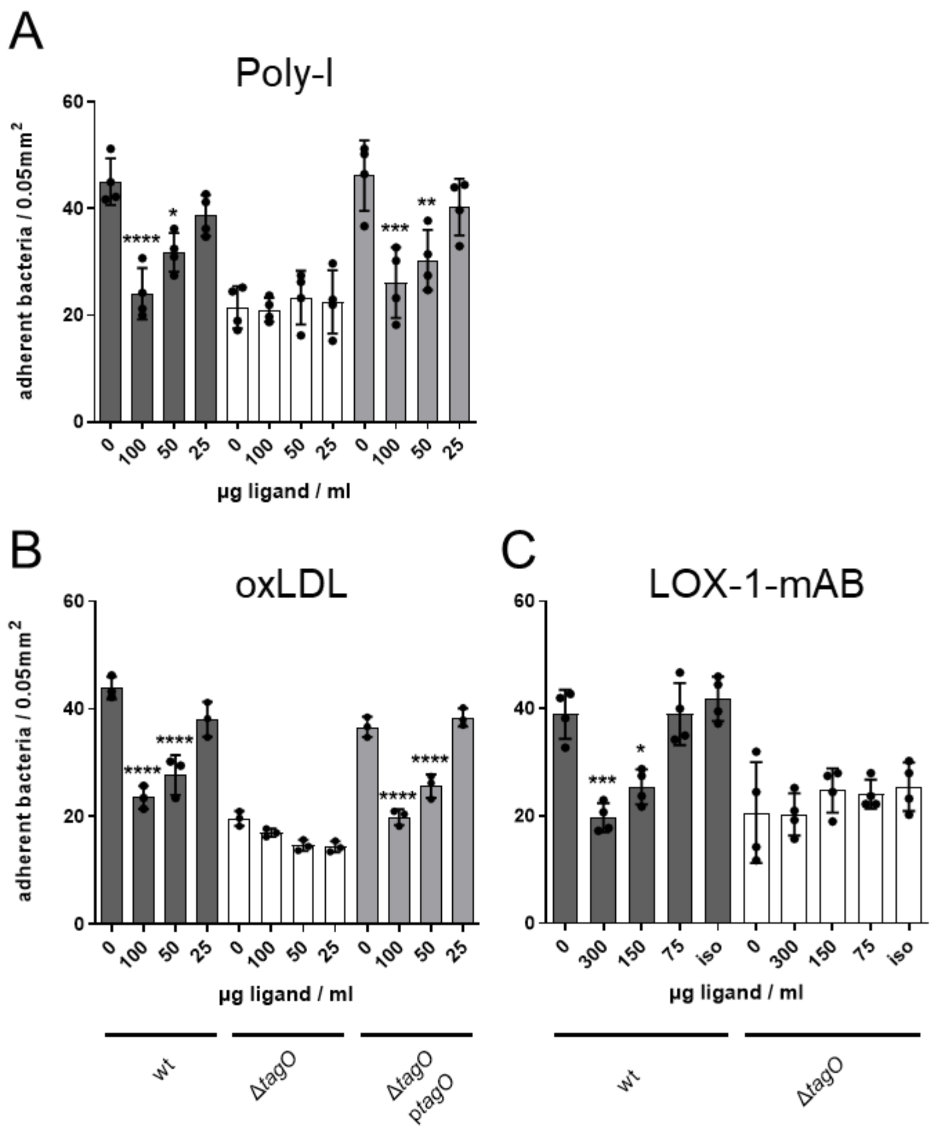

Figure 4: Pre-blocking of LOX-1 reduces *S. aureus* binding to HUVECs in a WTA-dependent manner. Microscopic evaluation of five random 0.05-mm^2 fields of confluent HUVEC layers. (A) HUVECs were pre-incubated with increasing concentrations of poly-I. (n=4) (A), oxLDL. (n=3) (B), or anti-hLOX-1 antibody (n=4) (C). Data represents means ± SD of 3 to 4 independent experiments. Differences were calculated by one-way ANOVA with Tukey test for multiple comparison vs. respective HUVECs preincubated with buffer only. (*p < 0.05; **p < 0.01; ***p < 0.001; ****p < 0.0001).

Discussion

Scavenger receptors contribute to bacterial infection and antibacterial host defense in multiple ways (Pombinho, Sousa, and Cabanes 2018). The multitude if different receptors, expressing cell types, and host or bacterial ligands has complicated their functional analysis. Accordingly, our knowledge of scavenger receptor functions is still rudimental (Mukhopadhyay and Gordon 2004; Komai et al. 2017; Pombinho, Sousa, and Cabanes 2018). We demonstrate here that LOX-1 on endothelial cells, in addition to SREC-1 on epithelial cells, can bind WTA and mediates binding of *S. aureus* to scavenger-receptor expressing host cells.

Mammalian cells express several types of scavenger receptors that bind surface molecules of different bacteria and elicit proinflammatory cellular responses. The oxidative burst generated by activated phagocytes does not only damage intruding bacteria but also host molecules such as the lipid and protein moieties of low-density lipoproteins leading to the generation of oxLDL, which is also an important ligand for many of the scavenger receptors (Pombinho, Sousa, and Cabanes 2018). Some bacteria, however, exploit the affinity of scavenger receptors for bacterial surface molecules for effective adhesion to scavenger-receptor expressing host cells (Shimaoka et al. 2001; Baur et al. 2014). Accordingly, the pathogens *Yersina pestis*, *Porphyromonas gingivalis*, and *S. aureus* have been found to bind to human cells in a scavenger-receptor dependent fashion but the exact bacterial ligands for interactions have remained mostly elusive (Baur et al. 2014; Yang et al. 2015; Dalen et al. 2019; Li et al. 2020). LOX-1 binds multiple structurally unrelated macromolecules including oxLDL (Oka et al. 1998; Marsche et al. 2001; Apostolov et al. 2009), advanced glycation end products (AGE) (Jono et al. 2002), activated platelets, bacteria, apoptotic or aged cells, heat shock proteins (Sawamura et al. 1997; Chen, Zhang, and Du 2008; Apostolov et al. 2009), and synthetic polymers such as poly-I (Palkama 1993). The lectin-like carbohydrate-binding domain of LOX-1 in the so-called “basic spine” of the receptor is enriched in positively charged amino acids (Nakano et al. 2012). This domain appears to be responsible for the promiscuity binding capacities of LOX-1, which may rely on affinity for poly-anionic glycosylated compounds (Murphy et al. 2006; Moriwaki et al. 1998; Chen, Zhang, and Du 2008). These preferences resemble those of SCREC-1, which does not share, however, sequence similarities with LOX-1. The fact that oxLDL competed with *S. aureus* WTA for binding to LOX-1 indicates that these two types of ligands are bound by the same or by adjacent parts of LOX-1. In addition to endothelial cells, LOX-1 is also expressed on macrophages, platelets, cardiomyocytes, and smooth muscle cells (Sawamura et al. 1997; Chen, Zhang, and Du 2008; Apostolov et al. 2009), where it may have additional functions in *S. aureus* pathogenesis.

Further scavenger receptors including langerin and macrophage galactose-type Lectin (MGL), and the soluble C-type lectin mannose-binding lectin (MBL) have been shown to specifically bind *S. aureus* WTA (Park et al. 2010; van Dalen, De La Cruz Diaz, et al. 2019; Mnich et al. 2019). However, these interactions do not support host cell adhesion but lead instead to immune cell or complement activation. The human pulmonary collectin SP-D is known to interact with lipoteichoic acids (LTA) (Palaniyar, Nadesalingam, and Reid 2002), which exhibit a different structure but similar polyanionic properties as WTA (Fischer 1994).

WTA-mediated binding seems to play a major role, which may be even stronger *in vivo* when proinflammatory signals cause upregulation of LOX-1 on endothelial cells. The prominent role of WTA-LOX-1 interactions in *S. aureus* binding to endothelial cells may contribute the increased virulence of WTA^{high} strains such as the USA300 lineage. Interestingly, upregulation of LOX-1 expression on the endothelial lining is also crucial for the pathogenesis of atherosclerosis (Morawietz et al. 2001; Sawamura et al. 1997) as the resulting increase in

oxLDL binding leads to overall endothelial dysfunction, increased foam cell and platelet aggregation culminating in aggravated local inflammation (Barreto et al. 2021). This dysbiosis might explain why bacterial infections can contribute to the initiation and progression of atherosclerosis (Ielapi et al. 2021) through interaction with the damaged endothelium and plaques themselves (Boumegouas et al. 2022). Blocking of oxLDL-LOX-1 interaction by monoclonal antibodies has been found to reduce LOX-1-induced plaque formation and damage to the vascular lining in atherosclerosis models (Guo et al. 2022). Since we found that monoclonal anti-LOX-1 antibodies also reduced *S. aureus* binding to endothelial cells, LOX-1-targeting interventions may also become helpful for the prevention and therapy of *S. aureus* blood-stream infections. The recent development of synthetic LOX-1 inhibitors and neutralizing antibodies (Joaquim Barreto 2021) may provide the basis for such approaches.
The preferences of LOX-1 for WTA from other pathogens in addition to *S. aureus* remains a to be explored in the future. Nevertheless, emerging *Staphylococcus epidermidis* clones with increased virulence have recently been found to bind better to endothelial cells because they produce *S. aureus*-type WTA (Du et al. 2021). Thus, LOX-1-WTA interactions may play crucial roles in infections caused by several pathogens. LOX-1-directed interventions may therefore become of general importance against endovascular bacterial infections.

Methods

Bacterial strains and growth conditions

All bacterial strains, plasmids, and oligonucleotides used in this study are described in Supplementary table 1-3. Bacteria were cultivated in B-Medium (5 g/L yeast extract (Ohly Kat, Deutsches Hefewerk) + 10 g/L Soy Peptone (A3SC, ORGANO TECHNIE) + 5 g/L NaCl + 1 g/L glucose + 0.8 g/L K_2HPO_4) (for cell wall or WTA isolation and infection experiments) or in TSB (tryptic soy broth) medium (Oxoid/Difco Laboratories) and incubated at 37°C and 200 rpm. All strains were kept on blood agar plates to monitor Agr-dependent toxin production. Resistant bacteria were additionally kept on TSA (tryptic soy agar) and cultivated in media supplemented with the appropriate antibiotics (ampicillin [10 µg/ml], erythromycin [2.5 µg/ml], chloramphenicol [10 µg/ml]).
S. aureus USA300 JE2 is a clinically relevant CA-MRSA clone with a naturally WTA^{high} phenotype (Wanner 2017). A markerless Δ*tagO* mutant was generated in this strain background by Gibson cloning of the two flanking regions of *tagO* into the mutagenesis vector pBASE6, following mutagenesis as described elsewhere (Bae and Schneewind 2006). For complementation of USA300 JE2 Δ*tagO,* plasmid pRB*tagO* was constructed by cloning the USA300 JE2 *tagO* gene into the shuttle vector pRB474 analogous to (Weidenmaier et al. 2004). The mutant genotypes were confirmed by PCR and controlled for *agr* activity and toxin production (Cheung, Duong, and Otto 2012; Adhikari, Arvidson, and Novick 2007), coagulase

activity (Biomerieux STAPH-ASE (Ref 55181)), and deposition of anti-WTA-Fabs (clones 4461 and 4497 patent (Driguez et al. 2017)) as described previously (van Dalen, Molendijk, et al. 2019). *S. aureus* SA113 (ATCC 35556) is a frequently used laboratory strain (Novick 1991). The WTA deficient mutant SA113 Δ*tagO* as well as the complementation SA113 Δ*tagO* pRB*tagO* have been previously described (Weidenmaier et al. 2004). Increased expression of the WTA biosynthesis gene *tarH* leads to a WTA^{high} phenotype in SA113 pRB*tarH* (Wanner 2017).

Labeling of bacteria

Bacteria were grown to mid-logarithmic phase in TSB (Oxoid), washed three times, and resuspended in PBS. They were labeled with 0.1 mg/ml of fluorescein isothiocyanate (FITC) (Sigma) at 4°C for 1 h, washed three times with PBS, and resuspended in cell culture media (IMDM, Gibco for blocking assays, or DMEM-F12, Gibco for adhesion assays). Bacterial cell numbers were determined using a Neubauer counting chamber.

WTA extraction and purification

The procedure for WTA isolation was modified from Peschel et al. 1999 (Peschel et al. 1999). Briefly, *S. aureus* was grown overnight in B-Medium containing 0.2% glucose. Bacteria were disrupted by mechanical forces using a FastPrep-24™ (MP Biomedicals) and glass beads (Sigma, 425-600µm). After centrifugation the lysate was DNase/RNase digested and treated with 2% SDS. The sonication step during SDS treatment was omitted. SDS was completely removed by multiple PBS washes and WTA was released from the peptidoglycan by treatment with 5% trichloroacetic acid and separated by centrifugation. The amounts of phosphorus in the WTA samples were determined as described previously (Chen, Toribara, and Warner 1965) using a phosphate standard solution (Sigma, P3869).

Direct Interaction-Assay

WTA from USA300 JE2 was isolated and immobilized on amine-modified latex beads with increasing concentrations as described previously (Baur et al. 2014). Briefly, amine-modified polystyrene latex beads (Sigma, L1030-1ML) were washed 2 times with 20 ml PBS (without $MgCl_2$ and $CaCl_2$; Gibco)) (200 rpm, 20 min, 4°C) and then resuspended in 15 ml PBS. 100 µl of the bead solution was mixed with 100 µl of appropriate dilutions of WTA solution, incubated at 4°C for 30 min with gentle shaking. Recombinant penta-his-tagged human LOX-1/ORL1 (R&D Systems, Ref 1798-LX) was labeled using a Cy3 HIS-tag dye (HIS Lite Cy3 Bis NTA-Ni Complex, AAT Bioquest) according to the manufacturer's instruction. 100 µl of WTA-coated beads were transferred to a 96-well plate (flat bottom, Greiner) and incubated with 100 µl Cy3-

labelled LOX-1 at room temperature for 1 h at 300 rpm. This procedure was followed by 3 washing steps with 200 µl PBS (Gibco) and centrifugation at 4000 rpm for 2 min at 4°C. Finally, 200 µl PBS were pipetted into each well and absolute Cy3 fluorescence was measured in a fluororeader (Clariostar).

Cell lines and growth conditions

All cell lines and primary cells used in this study are described in Supplementary table 4. HUVECs were cultured in endothelial cell growth medium (Promocell) and used up to passage number six. CHO cells were cultured in DMEM-F12 with 10% heat-inactivated FCS plus 1% penicillin-streptomycin solution (Gibco) up to passage number ten. Culturing of the cells and incubation during the experiments were performed at 37°C under 5% CO_2 and 95% relative humidity.

CHO cells expressing LOX-1

To generate CHO-K1 cells expressing LOX-1 (LOX-1-CHO), the lentiviral vector pReceiver-Lv130 (GeneCopoeia). was used. The vector included the orl-1 nucleotide sequence, the mCherry nucleotide sequence, and the puromycin resistance cassette under control of the strong constitutive overexpression promotor of *Cytomegalovirus* CMV. Lentivirus particles were produced in 239T cells co-transfected with helper plasmids (psPAX2 *gag/pol*, pMD2.G *env*) and pReceiver-Lv130. CHO-K1 cells were infected with lentivirus particles and transfectants were selected with 4,5µg/ml of puromycin for 5 passages. Puromycin-resistant cells were seeded in 96-well plate (1 cell/well) to create a single cell-derived cell line. The strength of LOX-1 expression was correlated with the brightness of mCherry reporter protein and evaluated by confocal microcopy (supplemental figure 1). The cell lines with the brightest signals were selected for further experiments.

Adhesion Assays

HUVECs were seeded at a density of 1 to 3x 10^6/channel in channel slides (ibidi µ-Slide VI 0.4) and allowed to attach overnight. Prior to inoculation with FITC-labeled bacteria the cells were washed with DMEM-F12 (Gibco). For the USA300 JE2 panel, pilot experiments (MOI ranging from 5 to 100) confirmed an optimal window of resolution for 1 h at MOI 10 (data not shown). After incubation for 1 h the channels were washed 2 times with pre-warmed DMEM and 1 time with pre-warmed PBS. Cells were then fixed with 4% PFA in 1x PBS for 20 min at RT, and permeabilized with 0.1% Triton X-100 in PBS for 10 min at room temperature. DNA was stained with DAPI (ThermoFisher, [1 µg/ml]) for 20 min at room temperature and the actin cytoskeleton was stained with phalloidin-TRITC (ThermoFisher, [2.5 µg/ml]) for 30 min at room temperature. Adhesion was evaluated by bacterial count of five random fields of view per replicate using a confocal laser scanning microscope (cLSM) on a Zeiss LSM710 NLO. Adhesion assays with CHO cells followed the same principle as described for HUVECs, with the difference that CHOs were cultured in DMEM-F12 containing 10% heat-inactivated FCS and 1% penicillin-streptomycin solution (Gibco) and seeded at a density of $2x10^6$/channel. Experiments were performed at a MOI of 10 for 1 h, as described above for the adhesion assays with HUVECs. The number of adherent bacteria to CHO cells was determined by confocal microcopy on a Zeiss LSM710 NLO.

Adhesion inhibition with scavenger receptor inhibitors, monoclonal antibodies, or oxLDLs, LOX-1 immunoflurescence

For all blocking assays as well as for induction of LOX-1 expression via oxLDL, HUVECs were seeded to 24-well culture plates at 1×10^5/well and grown at until confluency. Confluent HUVEC monolayers were washed twice with RPMI (Thermo Fisher). For the blocking assays, cells were then preincubated for 30 min with the respective inhibitor and washed once with RPMI before inoculation with FITC-labeled bacteria.
To assess the impact of scavenger receptors on *S. aureus* adhesion to HUVECs, the polynucleotide poly-I (Sigma) was used. HUVECs were preincubated with 25 µg/ml, 50 µg/ml or 100 µg/ml of the inhibitor. For specific blocking of the receptor LOX-1, HUVECs were preincubated with an anti-hLOX-1 antibody (R&D systems, MAB1798). The antibody was used at concentrations of 300 µg/ml, 150 µg/ml or 75 µg/ml to block *S. aureus* adhesion. To test competition with the endogenous ligand of LOX-1, oxLDL was purchased (Thermo Fisher, Ref L34357). HUVECs were preincubated with oxLDL at concentrations of 25 µg/ml, 50 µg/ml or 100 µg/ml. Adhesion to HUVECs was dependent on the MOI, incubation time, and the bacterial strain background. For the SA113 panel, pilot experiments (MOI ranging from 5 to 100) confirmed an optimal window of resolution for 1 h incubation at an MOI of 30. After incubation for 1 h the wells were washed three times with RPMI and fixed with 4% paraformaldehyde in PBS. No morphological changes in HUVECs were observed after this procedure. The number of adherent bacteria/0.1 mm^2 was determined using a confocal laser scanning microscope (Zeiss 710 NLO). Experiments were performed in biological triplicates or quadruplicates and up to 10 random fields of view were counted in each well.
For microscopic detection of LOX-1 expression, Cells were washed three times with PBS and blocked for 10 min with 1% BSA in PBS followed by incubation with a polyerythtitol-conjugated anti-hLOX-1-mAB (Miltenyi Biotec, Ref 130-122-110; 1:50) in PBS with 1% BSA for 1 h. After washing with PBS, the slides were fixed with 4% paraformaldehyde (PFA) for 30 min. PFA was then replaced by PBS. Antibody deposition was analyzed by means of confocal fluorescence

microscopy (Zeiss LSM 710 NLO) and bacterial adhesion assay was performed as described above.

Statistical analysis

For statistical analysis we used Graphpad Prism (Graphpad Prism Software 9.1.2) and appropriated statistical methods as indicated in the figure legends. $P < 0.05$ was considered significant. All statistical analyses are based on independent biological replicates.

Supplemental tables and figures

Supplemental table 1. List of strains

Bacterial strain	Description	Reference
S. aureus		
USA300 JE2	CA-MRSA, USA300 LAC cured of all 3 native plasmids	(Nuxoll et al. 2012)
USA300 JE2 Δ*tagO*	*tagO* deletion, WTA deficient mutant	This Work
USA300 JE2 Δ*tagO* pRB*tagO*	Complementation of Δ*tagO* (pRB473+tagO)	This Work
SA113	Laboratory strain ATCC 35556, derivative of NCTC8325	(Iordanescu and Surdeanu 1976)
SA113 *tarH*	*tarH* overexpression (pRB474+*tarH)*, WTA high phenotype	(Wanner 2017)
SA113 Δ*tagO*	*tagO* deletion, WTA deficient mutant	(Weidenmaier et al. 2004)
SA113 Δ*tagO* pRB*tagO*	Complementation of Δ*tagO* (pRB473+*tagO)*	(Weidenmaier et al. 2004)
RN4220	Restriction-deficient derivate of 8325-4, verification of agr activity (cross streak)	(Kreiswirth et al. 1983)
E. coli		
DC10B	Cloning strain, DNA cytosine methyltransferase mutant	(Monk et al. 2012)

Supplemental table 2. List of Vectors

Vectors and Plasmids	Description	Reference
pReceiver-Lv130	Lentiviral vector encoding for LOX-1(*orl-1*)-mCherry fusion protein and a puromycin resistance cassette under the control of the CMV promoter	GeneCopoeia
psPAX2 gag/pol	helper plasmid, production of lentiviral particles	GeneCopoeia
pMD2.G env	helper plasmid, production of lentiviral particles	GeneCopoeia
pBASE6	tetracyclin inducible suicide mutagenesis plasmid	(Geiger et al. 2012)
pCG472	pBASE6 for generation of USA300 JE2 Δ*tagO*	This Work
pRB474	pRB474, a chloramphenicol-resistant derivative of pRB374	(Jankovic, Egeter, and Bruckner 2001), (Brückner 1992)

pRB474+tagO	shuttle vector, complementation USA300 JE2 Δ*tagO*	This Work

Supplemental table 3. List of Oligonukleotides

Primer	extentionSEQUENCE	Use
tagOGibMutfor	ctcatcgcagtgcagcggAATAATGATAGCACAT CATTTTGT	generation of USA300 JE2 Δ*tagO*
tagOGibMutrev	ccgggtaccgagctccggGCATTTATTGCTGCA ATAAA	generation of USA300 JE2 Δ*tagO*
tagOlinkMutfor	aggtgaataaGGAATGAAAGCATAGCTGTAT GGG	generation of USA300 JE2 Δ*tagO*
tagOlinkMutrev	ctttcattccTTATTCACCTTCATCGATATT	generation of USA300 JE2 Δ*tagO*
tagocontrolfor	TCCTTTAATTGACCACTAGCT	control PCR
tagocontrolrev	AAGTACACGTTTATGGCAGT	control PCR
tagOGibcomplfor	gctggcggccgctgcatgTGTCATTAGTTTACAT ATAAAA	complementation USA300 JE2 ΔtagO
tagOGibcomplrev	taactctttccgcaaaggAATATCAATTGCGTATT ATTAAACGACA	complementation USA300 JE2 ΔtagO
tagOGibcomplfor2	gctggcggccgctgcatgTGTCATTAGTTTACAT ATAA	complementation USA300 JE2 ΔtagO
tagOGibcomplrev2	tattaactctttccgcaaaggAATATCAATTGCGTA TTATTAAACG	complementation USA300 JE2 ΔtagO
473 Eco	CCTCAAGCTAGAGAGTCATTACCCC	digest control pRB474
473 Hind	CTGGATTTGTTCAGAACGCTCGG	digest control pRB474

Supplemental table 4. List of Cell lines

Cell lines	Description	Reference
239T cells	production of lentiviral particles	GeneCopoeia
CHO-K1	Chinese Hamster Ovary Cells	DSMZ (AC110)
CHO LOX-1	CHOs transfected to express LOX-1/ORL1	This work
HUVECs	primary Human Umbilical Vein Endothelial Cells	PromoCell (C-12203)

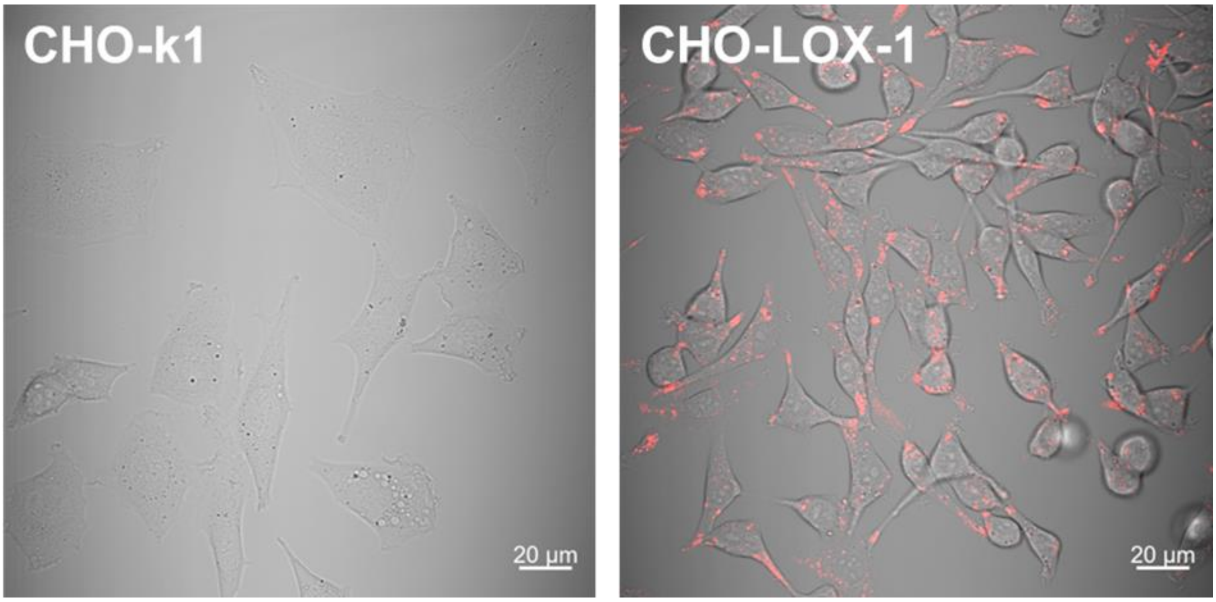

Supplemental figure 1. Microscopic conformation of LOX-1 expression in CHO-LOX-1 cell line. CHO-LOX-1 was generated via lentiviral transduction. Plasmid (pReceiver-Lv130) carries a human LOX-1-mCherry fusion protein, and for selection a puromycin resistance cassette under the control of the CMV promoter (GeneCopoeia). Single cell lines were generated in microtiter plates (seeding one cell per well). The cell line with the brightest signal for LOX-1 (see above, red: mCherry fusion protein) was selected for further experiments (cLSM: Zeiss LSM710 NLO).

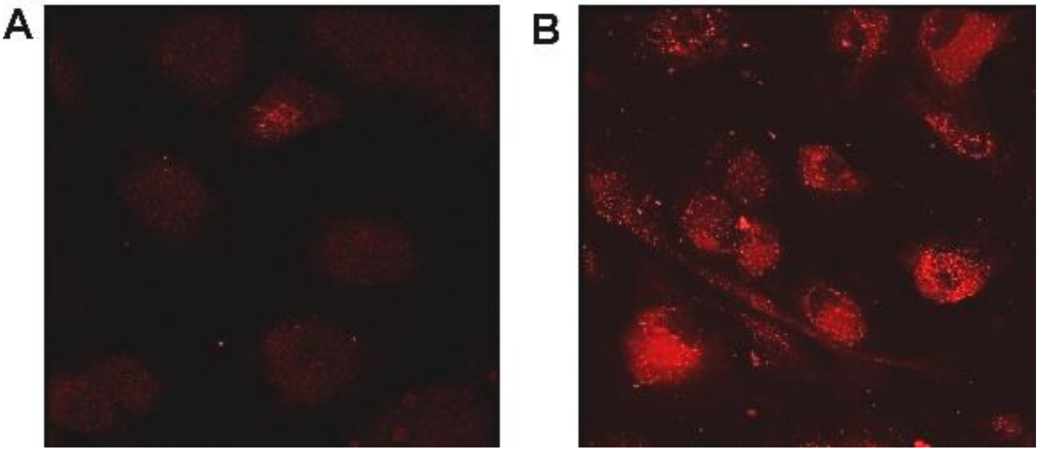

Supplemental figure 2 Microscopic conformation of LOX-1 expression after induction with oxLDL. LOX-1 expression was induced as formally described (Pirillo et al. 2011; Pirillo et al. 2012) by 12h pre-incubation of HUVECs with 50µg/ml oxLDL and visualized by immunofluorescence (cLSM: Zeiss LSM710 NLO). red: anti-LOX-1*APC mAB (Miltenyi Biotec, Ref 130-122-110).

References

Adhikari, R. P., S. Arvidson, and R. P. Novick. 2007. 'A nonsense mutation in agrA accounts for the defect in agr expression and the avirulence of Staphylococcus aureus 8325-4 traP::kan', *Infect Immun*, 75: 4534-40.

Apostolov, E. O., S. V. Shah, D. Ray, and A. G. Basnakian. 2009. 'Scavenger receptors of endothelial cells mediate the uptake and cellular proatherogenic effects of carbamylated LDL', *Arterioscler Thromb Vasc Biol*, 29: 1622-30.

Bae, T., and O. Schneewind. 2006. 'Allelic replacement in Staphylococcus aureus with inducible counter-selection', *Plasmid*, 55: 58-63.

Barreto, J., S. K. Karathanasis, A. Remaley, and A. C. Sposito. 2021. 'Role of LOX-1 (Lectin-Like Oxidized Low-Density Lipoprotein Receptor 1) as a Cardiovascular Risk Predictor: Mechanistic Insight and Potential Clinical Use', *Arterioscler Thromb Vasc Biol*, 41: 153-66.

Baur, S., M. Rautenberg, M. Faulstich, T. Grau, Y. Severin, C. Unger, W. H. Hoffmann, T. Rudel, I. B. Autenrieth, and C. Weidenmaier. 2014. 'A nasal epithelial receptor for Staphylococcus aureus WTA governs adhesion to epithelial cells and modulates nasal colonization', *PLoS Pathog*, 10: e1004089.

Boumegouas, M., M. Raju, J. Gardiner, N. Hammer, Y. Saleh, A. Al-Abcha, A. Kalra, and G. S. Abela. 2022. 'Interaction between bacteria and cholesterol crystals: Implications for endocarditis and atherosclerosis', *PLoS One*, 17: e0263847.

Brückner, R. 1992. 'A series of shuttle vectors for Bacillus subtilis and Escherichia coli', *Gene*, 122: 187-92.

Chen, P. S. , T. Y. Toribara, and Huber Warner. 1965. 'Microdetermination of Phosphorus', *Analytical Chemistry*, 28, NO. 11.

Chen, X. P., T. T. Zhang, and G. Du. 2008. 'Advanced glycation end products serve as ligands for lectin-like oxidized low-density lipoprotein receptor-1(LOX-1): biochemical and binding characterizations assay', *Cell Biochemistry and Function*, 26: 760-70.

Cheung, G. Y., A. C. Duong, and M. Otto. 2012. 'Direct and synergistic hemolysis caused by Staphylococcus phenol-soluble modulins: implications for diagnosis and pathogenesis', *Microbes Infect*, 14: 380-6.

Dalen, Rob van, Jacinto S. De La Cruz Diaz, Matevž Rumpret, Felix F. Fuchsberger, Nienke H. van Teijlingen, Jonas Hanske, Christoph Rademacher, Teunis B. H. Geijtenbeek, Jos A. G. van Strijp, Christopher Weidenmaier, Andreas Peschel, Daniel H. Kaplan, Nina M. van Sorge, Angelika Gründling, and Tarek Msadek. 2019. 'Langerhans Cells Sense <i>Staphylococcus aureus</i> Wall Teichoic Acid through Langerin To Induce Inflammatory Responses', *MBio*, 10: e00330-19.

Dayan, G. H., N. Mohamed, I. L. Scully, D. Cooper, E. Begier, J. Eiden, K. U. Jansen, A. Gurtman, and A. S. Anderson. 2016. 'Staphylococcus aureus: the current state of disease, pathophysiology and strategies for prevention', *Expert Rev Vaccines*, 15: 1373-92.

Driguez, Pierre-Alexandre, Nathalie Guillo, Bachra Rokbi, Noëlle Mistretta, and Philippe Talaga. 2017. "Immunogenic Compositions Against S. aureus." In. WO: Sanofi Pasteur.

Du, X., J. Larsen, M. Li, A. Walter, C. Slavetinsky, A. Both, P. M. Sanchez Carballo, M. Stegger, E. Lehmann, Y. Liu, J. Liu, J. Slavetinsky, K. A. Duda, B. Krismer, S. Heilbronner, C. Weidenmaier, C. Mayer, H. Rohde, V. Winstel, and A. Peschel. 2021. 'Staphylococcus epidermidis clones express Staphylococcus aureus-type wall teichoic acid to shift from a commensal to pathogen lifestyle', *Nat Microbiol*, 6: 757-68.

Edwards, A. M., and R. C. Massey. 2011. 'How does Staphylococcus aureus escape the bloodstream?', *Trends Microbiol*, 19: 184-90.

Edwards, A. M., J. R. Potts, E. Josefsson, and R. C. Massey. 2010. 'Staphylococcus aureus host cell invasion and virulence in sepsis is facilitated by the multiple repeats within FnBPA', *PLoS Pathog*, 6: e1000964.

Fischer, W. 1994. 'Lipoteichoic Acid and Lipids in the Membrane of Staphylococcus-Aureus', *Medical Microbiology and Immunology*, 183: 61-76.

Foster, T. J., and M. Hook. 1998. 'Surface protein adhesins of Staphylococcus aureus', *Trends Microbiol*, 6: 484-8.

Geiger, T., P. Francois, M. Liebeke, M. Fraunholz, C. Goerke, B. Krismer, J. Schrenzel, M. Lalk, and C. Wolz. 2012. 'The stringent response of Staphylococcus aureus and its impact on survival after phagocytosis through the induction of intracellular PSMs expression', *PLoS Pathog*, 8: e1003016.

Guo, X., Y. Guo, Z. Wang, B. Cao, C. Zheng, Z. Zeng, and Y. Wei. 2022. 'Reducing the Damage of Ox-LDL/LOX-1 Pathway to Vascular Endothelial Barrier Can Inhibit Atherosclerosis', *Oxid Med Cell Longev*, 2022: 7541411.

Hoerr, V., M. Franz, M. W. Pletz, M. Diab, S. Niemann, C. Faber, T. Doenst, P. C. Schulze, S. Deinhardt-Emmer, and B. Loffler. 2018. 'S. aureus endocarditis: Clinical aspects and experimental approaches', *Int J Med Microbiol*.

Hoerr, V.; Franz, M.; Pletz, M. W.; Diab, M.; Niemann, S.; Faber, C.; Doenst, T.; Schulze, P. C.; Deinhardt-Emmer, S.; Löffler, B. 2018. 'S. aureus endocarditis: Clinical aspects and experimental approaches', *International Journal of Medical Microbiology*, 308: 640-52.

Ielapi, N., F. Caprino, B. Malizia, A. Sisinni, L. Ssempijja, M. Andreucci, N. Licastro, and R. Serra. 2021. 'Infection, Infectious Agents and Vascular Disease'.

Iordanescu, S., and M. Surdeanu. 1976. 'Two Restriction and Modification Systems in *Staphylococcus aureus* NCTC8325', *J Gen Microbiol*.

Jankovic, I., O. Egeter, and R. Bruckner. 2001. 'Analysis of catabolite control protein A-dependent repression in Staphylococcus xylosus by a genomic reporter gene system', *J Bacteriol*, 183: 580-6.

Jono, T., A. Miyazaki, R. Nagai, T. Sawamura, T. Kitamura, and S. Horiuchi. 2002. 'Lectin-like oxidized low density lipoprotein receptor-1 (LOX-1) serves as an endothelial receptor for advanced glycation end products (AGE)', *FEBS Lett*, 511: 170-4.

Kohler, T., C. Weidenmaier, and A. Peschel. 2009. 'Wall teichoic acid protects Staphylococcus aureus against antimicrobial fatty acids from human skin', *J Bacteriol*, 191: 4482-4.

Komai, K., T. Shichita, M. Ito, M. Kanamori, S. Chikuma, and A. Yoshimura. 2017. 'Role of scavenger receptors as damage-associated molecular pattern receptors in Toll-like receptor activation', *Int Immunol*, 29: 59-70.

Kreiswirth, B. N., S. Lofdahl, M. J. Betley, M. O'Reilly, P. M. Schlievert, M. S. Bergdoll, and R. P. Novick. 1983. 'The toxic shock syndrome exotoxin structural gene is not detectably transmitted by a prophage', *Nature*, 305: 709-12.

Li, Q., J. Liu, W. Liu, Y. Chu, J. Zhong, Y. Xie, X. Lou, and X. Ouyang. 2020. 'LOX-1 Regulates P. gingivalis-Induced Monocyte Migration and Adhesion to Human Umbilical Vein Endothelial Cells', *Front Cell Dev Biol*, 8: 596.

Lowy, Franklin D. 1998. 'Staphylococcus aureus infections', *The New England Jurnal of Medicine*.

Marsche, G., S. Levak-Frank, O. Quehenberger, R. Heller, W. Sattler, and E. Malle. 2001. 'Identification of the human analog of SR-BI and LOX-1 as receptors for hypochlorite-modified high density lipoprotein on human umbilical venous endothelial cells', *FASEB J*, 15: 1095-7.

Mnich, Malgorzata E., Rob van Dalen, David Gerlach, Astrid Hendriks, Guoqing Xia, Andreas Peschel, Jos A. G. van Strijp, and Nina M. van Sorge. 2019. 'The C-Type Lectin Receptor MGL senses N-acetylgalactosamine on the unique Staphylococcus aureus ST395 Wall Teichoic Acid', *Cellular Microbiology*: e13072.

Monk, I. R., I. M. Shah, M. Xu, M. W. Tan, and T. J. Foster. 2012. 'Transforming the untransformable: application of direct transformation to manipulate genetically Staphylococcus aureus and Staphylococcus epidermidis', *MBio*, 3.

Morawietz, H., N. Duerrschmidt, B. Niemann, J. Galle, T. Sawamura, and J. Holtz. 2001. 'Induction of the oxLDL receptor LOX-1 by endothelin-1 in human endothelial cells', *Biochem Biophys Res Commun*, 284: 961-5.

Moriwaki, H., N. Kume, T. Sawamura, T. Aoyama, H. Hoshikawa, H. Ochi, E. Nishi, T. Masaki, and T. Kita. 1998. 'Ligand specificity of LOX-1, a novel endothelial receptor for oxidized low density lipoprotein', *Arterioscler Thromb Vasc Biol*, 18: 1541-7.

Mukhopadhyay, S., and S. Gordon. 2004. 'The role of scavenger receptors in pathogen recognition and innate immunity', *Immunobiology*, 209: 39-49.

Murphy, J. E., D. Tacon, P. R. Tedbury, J. M. Hadden, S. Knowling, T. Sawamura, M. Peckham, S. E. Phillips, J. H. Walker, and S. Ponnambalam. 2006. 'LOX-1 scavenger receptor mediates calcium-dependent recognition of phosphatidylserine and apoptotic cells', *Biochem J*, 393: 107-15.

Nakano, S., M. Sugihara, R. Yamada, K. Katayanagi, and S. Tate. 2012. 'Structural implication for the impaired binding of W150A mutant LOX-1 to oxidized low density lipoprotein, OxLDL', *Biochim Biophys Acta*, 1824: 739-49.

Nappi, F., G. Martuscelli, F. Bellomo, S. S. Avtaar Singh, and M. R. Moon. 2022. 'Infective Endocarditis in High-Income Countries', *Metabolites*, 12.

Novick, R. P. 1991. 'Genetic systems in staphylococci', *Methods Enzymol*, 204: 587-636.

Nuxoll, Austin S., Steven M. Halouska, Marat R. Sadykov, Mark L. Hanke, Kenneth W. Bayles, Tammy Kielian, Robert Powers, and Paul D. Fey. 2012. 'CcpA Regulates Arginine Biosynthesis in Staphylococcus aureus through Repression of Proline Catabolism', *PLoS Pathog*, 8: e1003033.

Oka, K., T. Sawamura, K. Kikuta, S. Itokawa, N. Kume, T. Kita, and T. Masaki. 1998. 'Lectin-like oxidized low-density lipoprotein receptor 1 mediates phagocytosis of aged/apoptotic cells in endothelial cells', *Proc Natl Acad Sci U S A*, 95: 9535-40.

Palaniyar, N., J. Nadesalingam, and K. B. Reid. 2002. 'Pulmonary innate immune proteins and receptors that interact with gram-positive bacterial ligands', *Immunobiology*, 205: 575-94.

Palkama, T.; Majuri, M.-L.; Mattila, P.; Hurme, M.; Renkonen, R. 1993. 'Regulation of endothelial adhesion molecules by ligands binding to the scavenger receptor', *Clin Exp Immunol*.

Park, K. H., K. Kurokawa, L. Zheng, D. J. Jung, K. Tateishi, J. O. Jin, N. C. Ha, H. J. Kang, M. Matsushita, J. Y. Kwak, K. Takahashi, and B. L. Lee. 2010. 'Human serum mannose-binding lectin senses wall teichoic acid Glycopolymer of Staphylococcus aureus, which is restricted in infancy', *J Biol Chem*, 285: 27167-75.

Patti, J. M., B. L. Allen, M. J. McGavin, and M. Hook. 1994. 'MSCRAMM-mediated adherence of microorganisms to host tissues', *Annu Rev Microbiol*, 48: 585-617.

Peschel, A., M. Otto, R. W. Jack, H. Kalbacher, G. Jung, and F. Gotz. 1999. 'Inactivation of the dlt operon in Staphylococcus aureus confers sensitivity to defensins, protegrins, and other antimicrobial peptides', *J Biol Chem*, 274: 8405-10.

Pirillo, A., A. Reduzzi, N. Ferri, H. Kuhn, A. Corsini, and A. L. Catapano. 2011. 'Upregulation of lectin-like oxidized low-density lipoprotein receptor-1 (LOX-1) by 15-lipoxygenase-modified LDL in endothelial cells', *Atherosclerosis*, 214: 331-7.

Pirillo, A., P. Uboldi, N. Ferri, A. Corsini, H. Kuhn, and A. L. Catapano. 2012. 'Upregulation of lectin-like oxidized low density lipoprotein receptor 1 (LOX-1) expression in human endothelial cells by modified high density lipoproteins', *Biochem Biophys Res Commun*, 428: 230-3.

Pollitt, E. J. G., P. T. Szkuta, N. Burns, and S. J. Foster. 2018. 'Staphylococcus aureus infection dynamics', *PLoS Pathog*, 14: e1007112.

Pombinho, R., S. Sousa, and D. Cabanes. 2018. 'Scavenger Receptors: Promiscuous Players during Microbial Pathogenesis', *Crit Rev Microbiol*, 44: 685-700.

Sawamura, T., N. Kume, T. Aoyama, H. Moriwaki, H. Hoshikawa, Y. Aiba, T. Tanaka, S. Miwa, Y. Katsura, T. Kita, and T. Masaki. 1997. 'An endothelial receptor for oxidized low-density lipoprotein', *Nature*, 386: 73-77.

Shimaoka, T., N. Kume, M. Minami, K. Hayashida, T. Sawamura, T. Kita, and S. Yonehara. 2001. 'LOX-1 supports adhesion of Gram-positive and Gram-negative bacteria', *J Immunol*, 166: 5108-14.

Surewaard, B. G., J. F. Deniset, F. J. Zemp, M. Amrein, M. Otto, J. Conly, A. Omri, R. M. Yates, and P. Kubes. 2016. 'Identification and treatment of the Staphylococcus aureus reservoir in vivo', *J Exp Med*, 213: 1141-51.

Taban, Q., P. T. Mumtaz, K. Z. Masoodi, E. Haq, and S. M. Ahmad. 2022. 'Scavenger receptors in host defense: from functional aspects to mode of action', *Cell Commun Signal*, 20: 2.

Tong, S. Y., J. S. Davis, E. Eichenberger, T. L. Holland, and V. G. Fowler, Jr. 2015. 'Staphylococcus aureus infections: epidemiology, pathophysiology, clinical manifestations, and management', *Clin Microbiol Rev*, 28: 603-61.

Turner, N. A., B. K. Sharma-Kuinkel, S. A. Maskarinec, E. M. Eichenberger, P. P. Shah, M. Carugati, T. L. Holland, and V. G. Fowler, Jr. 2019. 'Methicillin-resistant Staphylococcus aureus: an overview of basic and clinical research', *Nat Rev Microbiol*, 17: 203-18.

van Dalen, R.; Peschel, A.; van Sorge, N. M. 2020. 'Wall Teichoic Acid in Staphylococcus aureus Host Interaction', *Trends Microbiol*, 28: 985-98.

van Dalen, Rob, Jacinto S. De La Cruz Diaz, Matevž Rumpret, Felix F. Fuchsberger, Nienke H. van Teijlingen, Jonas Hanske, Christoph Rademacher, Teunis B. H. Geijtenbeek, Jos A. G. van Strijp, Christopher Weidenmaier, Andreas Peschel, Daniel H. Kaplan, and Nina M. van Sorge. 2019. 'Langerhans Cells Sense Staphylococcus aureus Wall Teichoic Acid through Langerin To Induce Inflammatory Responses', *MBio*, 10: e00330-19.

van Dalen, Rob, Michèle M. Molendijk, Sara Ali, Kok P. M. van Kessel, Piet Aerts, Jos A. G. van Strijp, Carla J. C. de Haas, Jeroen Codée, and Nina M. van Sorge. 2019. 'Do not discard Staphylococcus aureus WTA as a vaccine antigen', *Nature*, 572: E1-E2.

Wanner, S.; Schade, J.; Keinhorster, D.; Weller, N.; George, S. E.; Kull, L.; Bauer, J.; Grau, T.; Winstel, V.; Stoy, H.; Kretschmer, D.; Kolata, J.; Wolz, C.; Broker, B. M.; Weidenmaier, C. 2017. 'Wall teichoic acids mediate increased virulence in Staphylococcus aureus', *Nat Microbiol*, 2: 16257.

Weidenmaier, C., J. F. Kokai-Kun, S. A. Kristian, T. Chanturiya, H. Kalbacher, M. Gross, G. Nicholson, B. Neumeister, J. J. Mond, and A. Peschel. 2004. 'Role of teichoic acids in Staphylococcus aureus nasal colonization, a major risk factor in nosocomial infections', *Nat Med*, 10: 243-5.

Weidenmaier, C., and J. C. Lee. 2016. 'Structure and Function of Surface Polysaccharides of Staphylococcus aureus', *Curr Top Microbiol Immunol*.

Weidenmaier, C., R. M. McLoughlin, and J. C. Lee. 2010. 'The zwitterionic cell wall teichoic acid of Staphylococcus aureus provokes skin abscesses in mice by a novel CD4+ T-cell-dependent mechanism', *PLoS One*, 5: e13227.

Weidenmaier, C., A. Peschel, Y. Q. Xiong, S. A. Kristian, K. Dietz, M. R. Yeaman, and A. S. Bayer. 2005. 'Lack of wall teichoic acids in Staphylococcus aureus leads to reduced interactions with endothelial cells and to attenuated virulence in a rabbit model of endocarditis', *J Infect Dis*, 191: 1771-7.

Winstel, V., P. Kuhner, F. Salomon, J. Larsen, R. Skov, W. Hoffmann, A. Peschel, and C. Weidenmaier. 2015. 'Wall Teichoic Acid Glycosylation Governs Staphylococcus aureus Nasal Colonization', *MBio*, 6: e00632.

Yang, K., C. G. Park, C. Cheong, S. Bulgheresi, S. Zhang, P. Zhang, Y. He, L. Jiang, H. Huang, H. Ding, Y. Wu, S. Wang, L. Zhang, A. Li, L. Xia, S. S. Bartra, G. V. Plano, M. Skurnik, J. D. Klena, and T. Chen. 2015. 'Host Langerin (CD207) is a receptor for Yersinia pestis phagocytosis and promotes dissemination', *Immunol Cell Biol*, 93: 815-24.

Chapter IV

The following chapter is part of a manuscript ready for submission.

The published version of this manuscript may diverge from the version below.

Capsular polysaccharides obstruct the function of wall-teichoic acid in *Staphylococcus aureus*

Esther Lehmann[1,2], Rob van Dalen[1,2], Lisa Gritsch[1,2], Christoph Slavetinsky, Natalya Korn[1,2], Carina Rohmer[1], Andreas Peschel[1,2], Christopher Weidenmaier, Christiane Wolz[1,2]

1. **Interfaculty Institute of Microbiology and Infection Medicine**
2. **Cluster of Excellence EXC 2124 “Controlling Microbes to Fight Infections”, University of Tübingen**

Keywords

WTA, CP, Capsule, Staphylococcus, virulence, abscess

Corresponding author: Phone: +49 7071 2974648. Fax: +49 7071 295165.

E-mail: christiane.wolz@uni-tuebingen.de

Abstract

The cell envelope of *Staphylococcus aureus* contains two major secondary cell wall glycopolymers: the capsular polysaccharide (CP) and wall teichoic acid (WTA). Both the CP and the WTA are attached to the cell wall and play distinct roles in *S. aureus* colonization, pathogenesis, and bacterial evasion of the host immune defences. Here we analysed whether CP interferes with WTA mediated virulence in strains with natural, heterogeneous expression of CP, CP deficient strains and strains with high CP expression. WTA-mediated phage adsorption, specific antibody deposition as well as cell adhesion were negatively correlated with the amount of CP expressed. WTA but not CP enhanced bacterial burden in a mouse abscess model, while CP overexpression resulted in intermediate virulence. In summary, CP protects the bacteria from WTA dependent opsonization and phage binding. Such protection comes with the cost of diminished adherence to host cells. Our findings indicate that the CP expression shields WTA. The highly regulated and mostly heterogeneous expression of CP has probably evolved as bet hedging strategy to ensure the survival and optimal physiological adaptation of a subpopulation in changing environments.

Introduction

The bacterial cell envelope is a multi-layered structure that mediates specific interactions with the changing environments encountered during infection or colonization. The surface of *Staphylococcus aureus* is highly glycosylated, and is mainly composed of peptidoglycan (PG), cell wall-anchored - often glycosylated - proteins and the secondary cell wall glycopolymers (SCWGs) wall teichoic acid (WTA) and capsular polysaccharide (CP). Both WTA and CP are covalently linked to the C-6 hydroxyl of MurNAc of PG (Chan et al. 2013; Chan et al. 2014). *S. aureus* WTA is composed of 30-50 ribitol-phosphate (RboP) repeating units that are modified with D-alanine and GlcNAc (Brown 2013; Weidenmaier and Lee 2016). WTA has multiple functions in cell wall turnover, cellular physiology, phage interaction, host cell adhesion, antibiotic resistance as well as immune regulation (Weidenmaier and Lee 2016; Weidenmaier and Peschel 2008; Keinhörster, George, et al. 2019; Ingmer, Gerlach, and Wolz 2019; van Dalen 2020). High quantities of WTA, as found in the clinically highly relevant, methicillin resistant USA300 lineage, have been linked to increased virulence (Wanner 2017). In addition, as the primary staphylococcal phage receptor, WTA is also of critical importance for *S. aureus* genetic plasticity, since horizontal gene transfer in *S. aureus* is driven largely by phage transduction. The GlcNAc modifications of WTA are important for interaction with some, but not all, *S. aureus*-targeting phages (Ingmer, Gerlach, and Wolz 2019; Xia et al. 2011).

CP serotypes 5 and 8 are the two main CP serotypes produced by *S. aureus* (O'Riordan and Lee 2004; Keinhörster, George, et al. 2019). The proteins involved in CP5 or CP8 biosynthesis, *O*-acetylation, transport and regulation are encoded by *cap5A-P* or *cap8A-P* operons, respectively. The structures of CP5 and CP8 are very similar, both consisting of trisaccharide repeating units of D-*N*-acetyl mannosaminuronic acid, L-*N*-acetyl fucosamine, and D-*N*-acetyl fucosamine. The difference between the serotypes lies in the linkages between the sugars and the site of *O*-acetylation of the mannosaminuronic acid residues (Fournier et al., 1984, 1987; Moreau et al., 1990; Jones, 2005). CP expression depends on the local conditions encountered during particular types of infections (O'Riordan and Lee 2004; Tuchscherr et al. 2010; Keinhörster, George, et al. 2019). CP enhanced virulence in murine models of bacteremia (Thakker et al. 1998; Watts et al. 2005), septic arthritis (Nilsson et al. 1997), and surgical wound infection (McLoughlin et al. 2006). Moreover, acapsular *S. aureus* derived from chronic infections can regain capsule expression after passage through the bloodstream in a bacteraemia mouse model (Suligoy et al. 2020). However, CP reduced virulence in mammary gland infections (Tuchscherr et al. 2005) and in catheter-induced endocarditis (Baddour et al. 1992; Nemeth and Lee 1995). Furthermore, loss of CP expression has been frequently reported in *S. aureus* isolates from chronic infections (e.g. osteomyelitis, mastitis, cystic fibrosis or atopic dermatitis) indicating that loss of CP expression is of advantage under these conditions (Herbert et al. 1997; Lattar et al. 2009; Tuchscherr et al. 2010; Key et al. 2022). Interestingly, the highly virulent USA300 lineage is capsule deficient due to conserved mutations in the *cap5* locus (Boyle-Vavra et al., 2015). The seemingly contradictory role of CP to either enhance or diminish virulence is likely reflected by the highly heterogeneous expression of CP. At the population level, the CP has an unique expression pattern tightly linked to the growth phase of the bacterium (Keinhörster, George, et al. 2019). *Cap* expression is repressed during exponential growth, starts heterogeneously in late exponential phase and reaches its maximum during stationary phase while still being bistable. The heterogenous synthesis of CP entails a highly complex regulation of *cap* expression and the interplay between several regulatory circuits and environmental conditions. The alternative Sigma factor B (SigB) and the extended region upstream of the SigB consensus sequence within the *cap* promotor (P_{cap}) both have mainly repressive function. Mutation of this region and modification of the SigB binding motif result in strains with increased and mostly homogenous CP expression (Keinhörster, George, et al. 2019).

We hypothesize that the striking highly heterogeneous pattern of CP expression is beneficial for the *S. aureus* population. The CP-positive population may allow immune evasion due the antiphagocytic properties of CP (Thakker et al. 1998; Nanra et al. 2013), whereas the CP-negative population may favour adhesion. It has been postulated that the CP likely masks underlying cell-wall structures such as the cell-wall attached clumping factor A (Pöhlmann-Dietze et al. 2000; Risley et al. 2007). Here, we show that CP also obstructs the major functions of WTA. We analysed *S. aureus* isogenic mutants without CP, with heterogenous CP and with high CP expression to show that CP significantly reduces WTA-dependent adhesion, phage absorption and IgG deposition.

Methods

Bacterial strains, phages, and growth conditions

All bacterial strains, phages and eukaryotic cells are listed in supplemental table 1, supplemental table 2 and table 5, respectively. Bacteria were cultivated overnight in TSB (tryptic soy broth, Oxoid/Difco Laboratories) (37°C, 200 rpm). Resistant bacteria were grown with appropriate antibiotics (ampicillin [10 µg/ml], erythromycin [2.5 µg/ml], chloramphenicol [10 µg/ml], kanamycin [50 µg/ml]) during pre-culture.

Strain construction

Plasmids and oligonucleotides used in this study are listed in supplemental table 3 and supplemental table 4, respectively. A markerless Δ*tagO* mutant was generated in *S. aureus* USA300 JE2, a clinically relevant CA-MRSA clone (Wanner 2017), by Gibson cloning of the two flanking regions of *tagO* into the mutagenesis vector pBASE6, followed by mutagenesis

as described elsewhere (Bae and Schneewind 2006). The left and right flank were amplified using primer pairs tagOGibMutfor / tagOGibMutrev and tagOlinkMutfor / tagOlinkMutrev.
int (SAOUHSC_02239) of phi13kan was mutated (450 bp internal deletion) using the mutagenesis vector pIMAY (Monk et al., 2012). Briefly, right and left *int* flanking regions were amplified using primer pairs pCG849i1gibfor/pCG849i1gibrev and pCG849i2gibfor/ pCG849i2gibrev, and linked via PCR. The fragment was cloned into shuttle vector pIMAY by Gibson assembly, cloned into *E. coli* DC10B and transferred into USA300cΦ13kan by electroporation. Mutagenesis was performed as previously described (Monk et al. 2012). Deletion of the N-terminal part of *int* in USA300cΦ13kan-Δ*int* was verified via PCR. To obtain Φ13kan-Δ*int* (which is unable to excise from the bacterial chromosome), we complemented USA300cΦ13kan-Δ*int* with its native integrase using pCG32 (Mainiero et al. 2010). pCG32 was transduced from RN4220 into USA300cΦ13kan-Δ*int* using Φ11. Φ13kan-Δ*int* was induced from USA300cΦ13kan-Δ*int,* pCG32 with mitomycin C (500 ng/ml). All strains were verified on blood agar plates for Agr activity and ß-toxin production.

PFU determination via plaque-assay

Phage titer was determined by agar overlay method as described previously (Kropinski et al. 2009) using *S. aureus* strains RN4220 (for Φ11 and ΦK) or LS1 (for Φ13kΔ*int*) as indicator strains. Briefly, indicator strains were grown to OD_{600} = 0.1 in TSB. 100 µl of bacterial cultures were mixed with 3 ml liquid soft agar (TSA + 0.75% agar (BD)) and poured on a NB2-plate (Nutrient Broth No. 2 (Oxoid) + 0.75% agar (BD) + 2.72 mM $CaCl_2$; pH 7.5). After solidification, 10 µl of dilutions of sterile filtered (0.45 µm membrane filter (Labsolute)) phage lysates were spotted on the lawn. Plates were incubated at 37°C overnight and plaque forming units (PFU) determined.

Phage adsorption assay

Phage adsorption assays were performed at an MOI (multiplicity of infection) of 0.01, according to (Xia et al., 2011) with slight modifications. Briefly, 10^8 bacteria from an overnight culture were incubated with 10^6 phages in a total volume of 1 ml TSB with 2.72 mM $CaCl_2$ for 10 min, at room temperature, under non-shaking conditions. Bacteria were pelleted (5000 x g, 5 min), the supernatant was sterile filtered (0.45 µm membrane filter (Labsolute)) and used for PFU determination.

Antibody deposition

Antibody deposition to whole *S. aureus* cells was performed analogous to Hendriks et al. (Hendriks et al. 2021) employing an anti-α-1,4-GlcNAc-WTA Fab (clone 4461) (Driguez et al. 2017), to avoid epitope independent interaction with staphylococcal protein A. In brief, bacterial **overnight cultures** were adjusted by OD_{600} to $1.25*10^6$ cells in 1x PBS (phosphate-buffered saline) + 0.1% BSA (bovine serum albumin; Sigma A7906) and incubated with 4461-Fab at 10 µg/ml – 0.1 µg/ml in 3-fold serial dilution steps for 30 min at 4°C. After washing once with PBS + 0.1% BSA, bacteria were incubated with 1:1000 diluted PE-conjugated F(ab')2-anti-human-kappa-light-chain (Invitrogen, PA1-74408) in PBS + 0.1% BSA (20 min, 4°C). Unbound antibodies were removed and bacteria were fixed in 1% paraformaldehyde (PFA) in PBS for 15 min. The fixative was removed and bacteria were resuspended in a total volume of 150 µl PBS for flow cytometric analysis. Flow cytometry data was acquired on a FACSFortessa (BD) using FACSDiva (BD). Per sample, 10,000 events were measured within the set gate. All data were analyzed using FlowJo 10 (FlowJo, LLC).

FITC-labeling of bacteria

Bacterial overnight cultures grown in TSB (Oxoid) were washed three times, resuspended in 1x PBS and labeled with 0.1 mg/ml of fluorescein isothiocyanate (FITC) (Sigma) at 4°C for 1 h. Labeled bacteria were washed three times with 1x PBS, and resuspended in DMEM-F12 (Gibco). Labelled bacteria were stored at -20°C. Bacterial cell numbers were determined using a Neubauer counting chamber.

Cell culture and adhesion assays

Human umbilical vein endothelial cells (HUVECs) from pooled donors (Promocell) were cultured in endothelial cell growth medium (Promocell) and used up to passage number six. Culturing of the cells and incubation during the experiments were performed at 37°C under 5% CO2 and 95% rH. During experimental procedures HUVECs were kept in DMEM-F12 (Gibco).

Adhesion assays were performed under static conditions with HUVECs and FITC-labeled bacteria. Briefly, HUVECs were seeded at a density of 1 to $3x10^6$/channel in channel slides (ibidi µ-Slide VI 0.4) and incubated to attach overnight at 37°C, 5% CO_2 and 95% rH. Prior to infection, HUVECs were washed once with pre-warmed DMEM-F12 (Gibco). For the USA300 JE2 panel, pilot experiments confirmed an optimal window of resolution of 1 h at MOI 10 (data not shown). For the Newman panel we confirmed an optimal window of resolution of 2 h at MOI 10 (data not shown). After infection, the channels were washed twice with pre-warmed DMEM-F12 and once with pre-warmed 1x PBS (Gibco). Cells were fixed with 4% PFA in 1x PBS (Gibco) for 20 min at RT, and permeabilized with 0.1 % Triton X-100 in 1x PBS for 10 min at RT. DNA was stained with DAPI (ThermoFisher, [1 µg/ml]) for 20 min at RT, the actin cytoskeleton was stained with Phalloidin-TRITC (ThermoFisher, [2.5 µg/ml]) for 30 min at RT. The number of adherent bacteria to HUVECs was determined by confocal microscopy on a Zeiss LSM710 NLO.

Ethics statement

Animal experiments were performed in strict accordance with the German regulations of the Society for Laboratory Animal Science (GV-SOLAS) and the European Health Law of the Federation of Laboratory Animal Science Associations (FELASA). The protocol was approved by the Regierungspräsidium Tübingen (permit no. IMIT 01/20G).

Abscess model

Procedure was altered from (Wanner 2017). Briefly, eight weeks old female C57BL/6JRccHsd mice were obtained from Envigo and housed with up to five animals per cage in individually ventilated cages (IVCs). Bacterial suspensions from overnight cultures were adjusted to a CFU of 10^5 in 100 µl and mixed with an equal volume of dextran beads (Cytodex-1 microcarriers; Sigma) to gain a final concentration of 0.5% cytodex-1 beads per 200 µl. Mice were anesthetized using an isoflurane-oxygen mixture (cp-pharma) and injected subcutaneously in each flank with 0.2 ml of the *S. aureus*-beads suspensions. Mice were tightly monitored and euthanized after two days of bacterial challenge. The abscesses were excised and homogenized in 1 ml 1x PBS containing protease inhibitor (Roche) according to the manufacturer's instructions. Serial dilutions of the homogenates were plated in technical duplicates on TSA plates. Results were analyzed as the log CFU of bacteria/abscess.

WTA isolation and purification

WTA isolation was modified from Peschel et al. 1999 (Peschel et al. 1999). Briefly, *S. aureus* was grown overnight in B-Medium (5 g/L yeast extract (Ohly Kat, Deutsches Hefewerk) + 10 g/L Soy Peptone (A3SC, ORGANO TECHNIE) + 5 g/L NaCl + 1 g/L glucose + 0.8 g/L K_2HPO_4) with additional 0.2% glucose. Bacteria were disrupted by mechanical forces using a FastPrep-24™ (MP Biomedicals) and glass beads (Sigma, 425-600µm). After sedimentation by centrifugation the lysate was DNase/RNase (Sigma) digested and treated with 2% SDS. WTA was released from the peptidoglycan by treatment with 5% trichloroacetic acid and separated by centrifugation. The amounts of phosphorus in the WTA samples was determined as described previously in Chen et al. (Chen, Toribara, and Warner 1965) against a phosphate standard solution (Sigma, P3869). The pellet was dried via vacuum centrifugation (Speedvac) and the amount of peptidoglycan was determined by pellet weight. The amount of WTA was displayed as [nmol $_{\text{WTA}}$/g $_{\text{cell wall}}$].

Statistical analysis

For statistical analysis we used Graphpad Prism (Graphpad Prism Software 9.1.2) and appropriate statistical methods as indicated in the figure legends. $P < 0.05$ was considered to be significant. All statistical analysis is based on independent biological replicates.

Results

WTA abundance is unaffected by CP production.

Although WTA and CP are synthesized by dedicated biosynthesis enzymes encoded by separate gene clusters, these pathways are entangled to a large extent. Both WTA and CP rely on the universal UDP-GlcNAc building blocks, the universal lipid II (UDP) carrier and mutual enzymes from the LPC family for attachment to the PG. We speculated that the synthesis of WTA and CP might therefore be coordinated, and set out to determine first whether the WTA content of the cell wall is affected by the ability of the bacteria to produce CP. We therefore used a set of *S. aureus* mutants with varying CP synthesis capacities. *S. aureus* strain USA300 JE2 is naturally CP-deficient as a result of three point mutations within *capD*, *capE* and the *cap* SigB consensus motif (Boyle-Vavra et al. 2015). These three mutations have been cured in USA300-cr, resulting in a mutant with the canonical heterogeneous CP expression in stationary phase (Keinhörster, George, et al. 2019). USA300-high is a derivative of USA300-cr that homogeneously expresses CP in stationary phase. This was achieved by deletion of the repressive upstream region and mutation of the SigB binding motif of the *cap* promotor region. We measured the total WTA abundance per dry cell wall weight in the two strains with the largest difference in CP production, namely CP-less USA300 and USA300-high (figure 1). WTA was extracted from stationary stationary phase cultures to ensures CP expression. The WTA abundance did not differ significantly between these two strains. We therefore concluded that any effect that CP production might have on WTA-mediated functions stems from limited accessibility of WTA, rather than attenuated WTA biosynthesis.

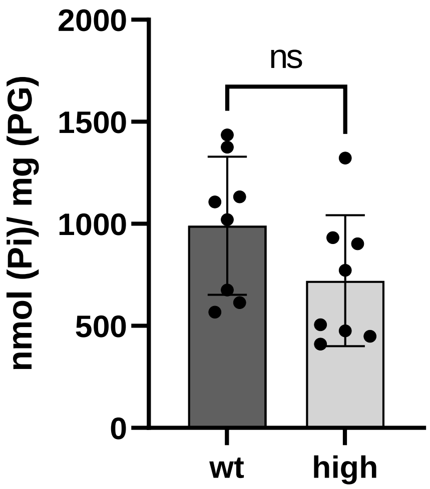

Figure 1. Impact of CP expression on WTA abundance. WTA of USA300 (wt) and USA300-high was isolated and quantified from stationary phase cultures to ensure CP production. The WTA abundance was approximated by phosphate (Pi) concentration in nmol per mg cell wall (PG).

Represented are data with mean and SD of eight independent biological replicates. Statistical analysis was performed by unpaired t test. There are no significant differences vs. USA300 wt.

CP expression reduces phage adhesion.

To assess whether the CP affected WTA-mediated phage absorption, strains with varying degree of CP, as well as the WTA-deficient USA300-Δ*tagO* mutant, were incubated with representative phages: Φ11 (siphovirus, shown to recognize α-1,4-GlcNAc-, β-1,4-GlcNAc- and partially β-1,3-GlcNAc-RboP-WTA (Xia et al. 2011; Ingmer, Gerlach, and Wolz 2019)), ΦK (myovirus, shown to recognize RboP-WTA (Xia et al. 2011)) and Φ13*int* (siphovirus, unknown phage receptor). Since Φ13 phages produce turbid plaques that are difficult to enumerate, we partially deleted the phage integrase gene *int*, resulting in clear plaque formation. After adsorption, the number of unbound phages was determined in a double agar overlay plaque assay, with low numbers of unbound phages translating to high phage adsorption (figure 2). No absorption was detected in the Δ*tagO* mutant, confirming the dominant role of WTA as phage receptor. Phage adsorption negatively correlated with the CP expression level. For all three phages, the highest adsorption was observed to the CP negative USA300 wildtype and adsorption to CP positive strains USA300-cr and USA300-high was significantly decreased. For both Φ11 and Φ13kΔ*int*, absorption to USA300-high was as low as to the WTA-deficient Δ*tagO* mutant (figure 2A and 2C), indicating that high CP expression efficiently blocks access of all three phages to their WTA receptor.

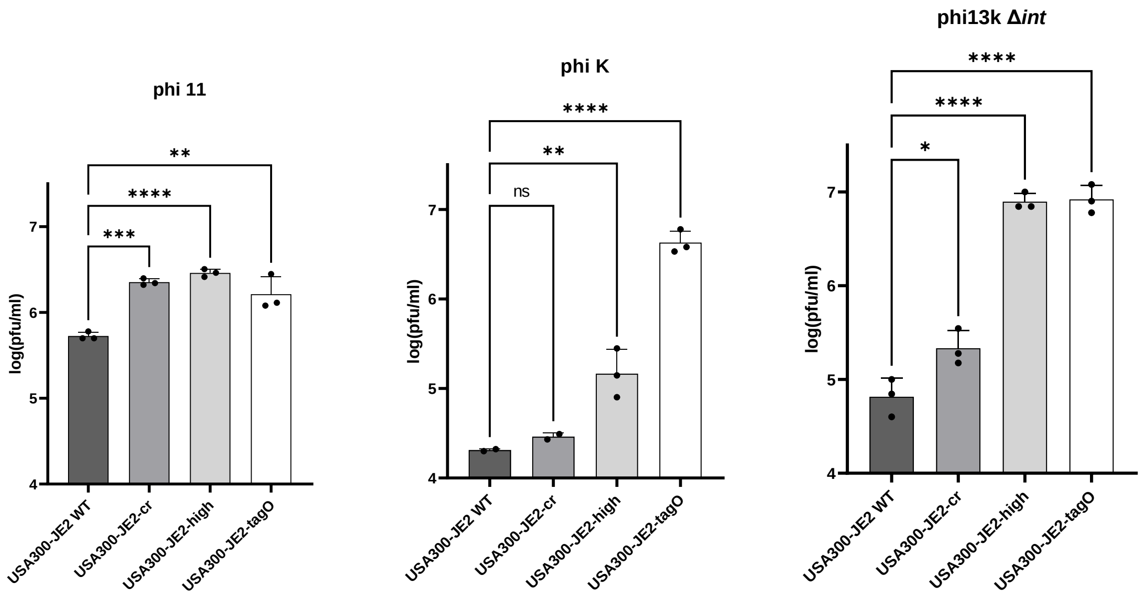

Figure *2.* Phage adsorption in the presence of CP. Enumeration of plaque forming units (PFU) after adsorption (MOI 0.01, 10 min) to *S. aureus* cell wall mutants, by double agar overlay plaque assay. USA300: CP-deficient; USA300-cr: heterogeneous CP expression; USA300-high: homogeneous high

CP expression; USA300 Δ*tagO*: WTA deficient. Increased phage adsorption translates to reduced numbers of unbound phages.
Represented are log-transformed data with mean and SD of three independent experiments. Statistical analysis was performed by one-way analysis of variance (ANOVA) with Dunnett's test for multiple comparison. Significant differences vs. USA300 wt are indicated by one (P<0.05), two (P<0.01), three (p<0.001), or four (P<0.0001) asterisks (*).

CP expression reduces binding of WTA-specific antibodies.

An estimated 70% of *S. aureus*-reactive IgG is directed towards WTA GlcNAc (Lehar et al. 2015). We analyzed whether CP impedes access of these antibodies to WTA. To avoid interaction of antibodies with the *S. aureus* antibody-binding protein SpA, we used anti-α-1,4-GlcNAc-F(ab') fragments (Di Carluccio et al. 2022) in a flow cytometry-based immunofluorescent staining experiment. Antibody deposition on USA300 wt increased in a dose dependent manner, reaching saturation at 3 µg/ml. Deposition was clearly impaired in the Δ*tagO* mutant and in the CP high strain (figure 3A).

CP expression is highly growth-phase dependent and bacteria from exponential phase are mostly CP negative. Accordingly, CP-dependent inhibition of antibody deposition correlated with the growth phase. Significant reduction of WTA staining was seen only in bacteria from late exponential or stationary growth phase cultures (figure 3B). These results indicate that CP production limits accessibility of antibodies to WTA, the dominant antibody target of *S. aureus*.

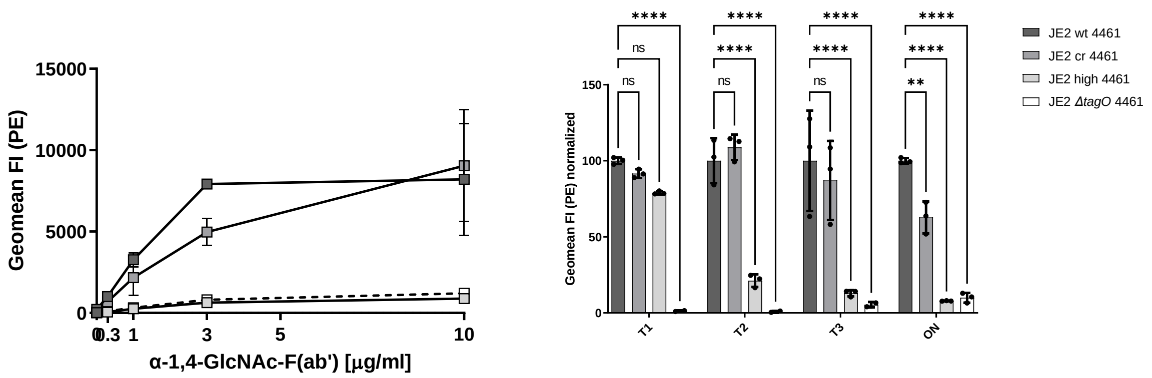

Figure 3. **Anti-WTA-antibody deposition is dependent on CP expression.** Binding of human α-1,4-GlcNAc-F(ab') to *S. aureus* cell wall mutants (USA300 JE2 wt, USA300 JE2 cr, USA300 JE2 high and USA300 JE2 Δ*tagO*), measured by flow cytometry using PE-conjugated human kappa light chain as secondary antibody. (A) Dose-response curve with 0 µg/ml, 0.3 µg/ml, 1 µg/ml, 3 µg/ml and 10 µg/ml α-1,4-GlcNAc-F(ab'). Data displayed as geometrical mean of the PE fluorescent intensity. (B) α-1,4-GlcNAc-F(ab') deposition at 3 µg/ml in synchronized cultures. T1: early exponential, T2: late exponential, T3: early stationary, T4: late stationary growth. Data displayed as geometrical mean of the PE fluorescent intensity normalized to the wildtype in the respective growth phase.
The mean and SD of three independent experiments are shown. Statistical analysis was performed by two-way ANOVA with Dunnett's test for multiple comparison. Significant differences vs. USA300 JE2 wild type are indicated by one (P<0.05), two (P<0.01), three (p<0.001), or four (P<0.0001) asterisks (*).

CP expression reduces WTA dependent adhesion to endothelial cells.

Pöhlmann-Dietze et al., 20002 have shown that CP expression in *S. aureus* Newman inhibits bacterial binding to endothelial cells indicating that CP inhibits adhesion by masking cell wall adhesins (Pöhlmann-Dietze et al. 2000). In strain Newman the major adhesins FNBA and FNBB are truncated (Grundmeier et al. 2004) and WTA might function as major cell-wall adhesin in this strain background. Endothelial cell adhesion using Δ*tagO* and a sortase deficient mutant *srtA::erm* confirmed that endothelial cell adhesion is mainly mediated via WTA. The adhesion was significantly impaired in a CP overexpressing strain Newman-high (Keinhörster, Salzer, et al. 2019), supporting that CP masks WTA accessibility. Also in strain USA300 adhesion was predominantly WTA dependent and negatively correlated to CP expression. These observations supported our hypothesis that CP impedes WTA specific binding to endothelial cells.

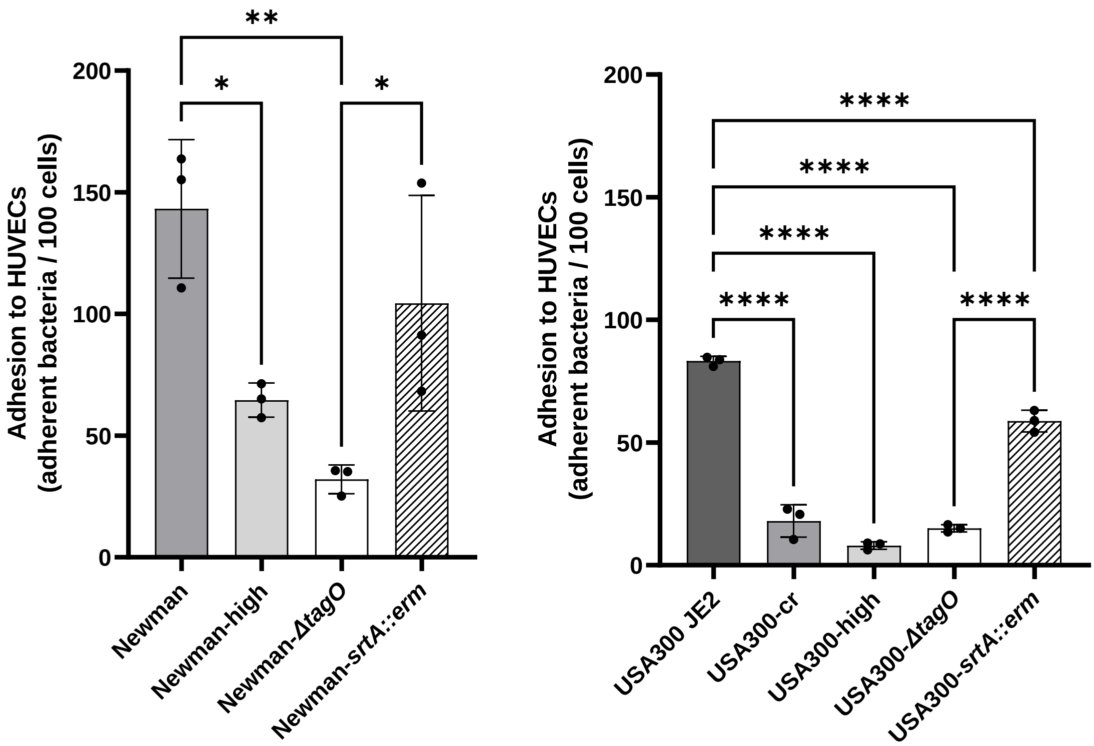

Figure 4. Impact of CP expression on endothelial adhesion. Adhesion of FITC-labelled USA300, USA300-cr, USA300-high, USA300 ΔtagO and USA300 srtA::erm (MOI 10, 1h) or Newman, Newman-high, Newman ΔtagO and Newman srtA::erm (MOI 10, 2h) to HUVECs. Adherent bacteria were microscopically evaluated in five random fields of view per replicate. Data displayed as number of adherent bacteria per 100 HUVECs. The mean and SD of three independent experiments are shown. Statistical analysis was performed by one-way ANOVA with Tukey's test for multiple comparison. Significant differences are indicated by one (P<0.05), two (P<0.01), three (p<0.001), or four (P<0.0001) asterisks (*).

CP expression reduces abscess formation in USA300.

Previously, high WTA expression was shown to increase the bacterial burden in a mouse skin abscess model (Wanner 2017). We hypothesized that CP production may affect this WTA-mediated phenotype. We therefore used an identical *in vivo* model and induced abscess formation in the flanks of C57BL/6J mice by injection of *S. aureus* mixed with cytodex beads (figure 5). After 48h, we observed a significantly reduced bacterial burden when mice were inoculated with USA300 Δ*tagO* as compared to USA300 wt, confirming the pivotal role of WTA for abscess formation. The bacterial burden of USA300-cr did not differ from that of USA300 wt. High expression of CP resulted in an intermediate phenotype with a tendency towards lower bacterial burden compared to wild type and no significant difference to the WTA-deficient USA300 Δ*tagO* mutant. These results indicate that in this infection model WTA, but not CP, is important for bacterial virulence, and hint towards a limiting effect of CP with regards to WTA-mediated virulence in skin abscess formation.

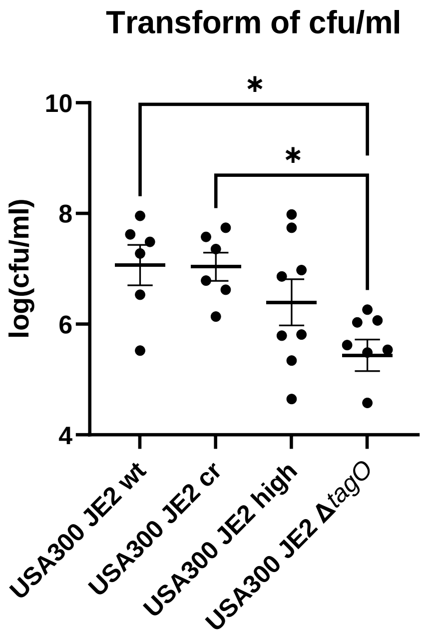

Figure 5. Impact of CP on WTA-mediated virulence in skin abscess formation. Abscess formation was induced by 10^5 colony-forming units (CFU) of USA300 WT, USA300-cr, USA300-high and USA300 Δ*tagO*). Bacteria were mixed with cytodex beads and injected subcutaneous into the flanks of C57BL/6J mice (two abscesses per mouse). After 48 h, the mice were euthanized, the abscesses excised, homogenized and the bacterial burden was determined by dilution plating. Data are represented as a dot-blot with mean and SEM of the log-transformed cfu count. Each dot represents a single abscess. Statistical analysis was performed by one-way ANOVA with Dunnett's test for multiple comparison. Significant differences are indicated by one (P<0.05), or two (P<0.01) asterisks (*).

Discussion

The central role of *S. aureus* SCWGs in virulence and host adaptation has become increasingly evident in the past decade (Weidenmaier and Lee 2016). In this study, we show that CP impedes WTA functionality such as phage absorption, cell adhesion and antibody deposition. *S. aureus* WTA was previously shown to mediate adhesion to epithelial cells (Baur et al. 2014), Langerhans cells (van Dalen, De La Cruz Diaz, et al. 2019) and endothelial cells (Weidenmaier et al. 2005)(manuscript in preparation), via recognition of host receptors SREC-1, Langerin and LOX-1 respectively. Here we confirmed that WTA is the major adhesin mediating binding of *S. aureus* to endothelial cells. This could be shown for the FnbAB deficient strain Newman as well as for the CP negative strain USA300. In both strain background adhesion was highly dependent on WTA but less influenced by cell-wall attached adhesins. Interestingly, some emerging *S. epidermidis* lineages express *S. aureus*-type WTA which coincides with increased endothelial binding (Du et al. 2021). Overexpression of CP significantly decreased adhesion in both strains confirming that CP masks WTA accessibility. The results also confirm that mutations within the *cap* operon as present in the USA300 lineage enhance the binding to endothelial cells similar to artificial *cap* mutation in strain Newman (Pöhlmann-Dietze et al. 2000).

WTA is the major phage receptor in *S. aureus* and other firmicutes (Leprince and Mahillon 2023). However, in many other species including *Lactococcus lactis* CP functions as predominant phage receptor (Bertozzi Silva, Storms, and Sauvageau 2016). Here, we show that CP in *S. aureus* modulates phage absorption by impeding the binding of phages to WTA. A similar observation was made previously in *Bacillus anthracis*, where shielding of phage absorption by CP was also demonstrated (Negus et al. 2013). Previous observations regarding the role of CP in phage absorption in *S. aureus* were often non-conclusive and only the “macro-capsules” encoded by a different gene cluster was shown to interfere with phage absorption (Wilkinson and Holmes 1979). Results concerning the more prevalent CP5 and CP8 micro-capsule are less clear (Sompolinsky et al. 1985; Witte 1975). This might be explained by the observation that CP expression only occurs in a subpopulation of bacteria, specifically in stationary growth phase (George et al. 2015). Thus, phage inhibitory effects of CP in exponentially growing bacteria might be undetectable.

It was shown previously that when bacteria were grown under conditions of optimal capsule expression, capsule protected from opsonophagoctyic killing in the presence of either complement or antibodies (Cunnion, Lee, and Frank 2001; Thakker et al. 1998). WTA is not only recognized by phages but also a major antigen of *S. aureus*. About 70 % of all natural antibodies directed against *S. aureus* recognize WTA (Lehar et al. 2015). These antibodies are able to induce complement activation (Jung et al. 2012) and phagocytosis by neutrophils

(Lehar et al. 2015; Dalen et al. 2019). We here demonstrate that enhanced CP production blocks opsonization by specific monoclonal anti-WTA-F(ab') fragments (Driguez et al. 2017). This effect is likely even underestimating the *in vivo* blocking capacity of CP, as the F(ab') constructs used in this study were approximately three-fold smaller than full-sized IgG.
On the other hand, under *in vivo* conditions effective antibody opsonization of *S. aureus* would be further reduced by the activity of Staphylococcal Protein A (SpA)*,* an important immune evasion protein of *S. aureus* that hinders effective opsonization through Fc-dependent antibody binding. In our assays, SpA effects were omitted by the use of F(ab') constructs. The impact of CP expression on opsonization *in vivo* remains to be answered. However, our results highlight the capacity of CP to shield opsonins (Kuipers et al. 2016) specifically WTA, form being targeted by antibodies. Since there is very little evidence of effective antibody deposition to CP-positive cells during natural infection, its relative impact on opsonization by antibodies would need to be addressed. This might also yield further insight into the emergence of the highly clinically relevant CP-deficient lineages. Interestingly, in early serotyping assays agglutination of *S. aureus* in the presence of teichoic acid antiserum was used as negative control to identify CP deficient *S. aureus* isolates (Fournier 1984). Until now, this observation was never evaluated in the context of CP-WTA interactions.

The USA300 lineage is known for its high prevalence in skin and soft tissue infections, which has partially been ascribed to its WTA^{high} phenotype (Wanner 2017). Interestingly, CP expression in *S. aureus* was also shown to promote subcutaneous abscess formation (Portoles et al. 2001). Portoles and colleagues investigated abscess formation in a CP heterogenous background. Here we could confirm the role of WTA, whereas CP overexpression does not promote abscess formation. Rather, the USA300-high strain displayed a phenotype more similar to the significantly attenuated WTA-deficient mutant. This might indicate that CP even dampens virulence through the WTA shielding effect and further strengthens the notion that by retaining WTA functionality in a part of the population, heterogeneity in CP expression is important for *S. aureus* adaptation to the host

In summary, CP expression masks WTA to protect the bacteria from opsonization with antibodies and infection by phages. The latter can be both beneficial and possibly deadly for the bacteria. However, CP-dependent masking of bacterial adhesion to e.g., endothelial cells might be a disadvantage for the bacteria. Thus, the highly heterogenous and tightly regulated CP expression has likely evolved to ensure that part of the population can fulfill the other essential function. Although the regulation of CP synthesis is heavily studied (Keinhörster, Salzer, et al. 2019), it is still unclear under which *in vivo* conditions CP is expressed. Thus, there might be unforeseen implications of CP expression *in vivo*. Interestingly, there is some evidence in murine infection models that even the non-encapsulated USA300 may produce CP in certain *in vivo* conditions (Mohamed et al. 2019)

Supplemental tables and figures

Supplemental table 5. **List of bacterial strains.**

Bacterial strain	Description	Reference
S. aureus		
USA300 JE2	CA-MRSA, USA300 LAC cured of all 3 native plasmids, natural CP5 deficient	(Nuxoll et al. 2012)
USA300 JE2 cr	Mutations in CP-operon have been reversed, CP5 expression	(Keinhörster, Salzer, et al. 2019)
USA300 JE2 high	Modification of Pcap SigB-binding-site, CP5 overexpression	(Keinhörster, Salzer, et al. 2019)
USA300 JE2 Δ*tagO*	*tagO* deletion, WTA deficient mutant	LOX manuskript
USA300 JE2 *srtA*::erm	Transposon insertion in *srtA*, mutant deficient for all major cell wall proteins	This work
Newman	HA-MRSA, CP5	(Duthie and Lorenz 1952)
Newman high	Modification of Pcap SigB-binding-site, CP5 overexpression	(Keinhörster, George, et al. 2019)
Newman Δ*tagO*	*tagO* deletion, WTA deficient mutant	
Newman-132	CP deficient mutant	(Jansen et al. 2013)
RN4220	Restriction-deficient derivate of 8325-4, indicator strain, phage propagation	(Kreiswirth et al. 1983)
LS1	Mouse arthritis/osteomyelitis strain, Indicator strain for Φ13kΔ*int*	(Bremell et al. 1990)
E. coli		
DC10B	Cloning strain, DNA cytosine methyltransferase mutant	(Monk et al. 2012)

Supplemental table 6. List of bacteriophages.

Phages	Description	Reference
Φ11	siphovirus, receptor: α-1,4-GlcNAc-, β-1,4-GlcNAc- and partially β-1,3-GlcNAc-RboP-WTA	
ΦK	myovirus, receptor: RboP-WTA	
Φ13k	siphoviurs, unknown phage receptor	(Tang et al. 2017)
Φ13k Δ*int*	siphoviurs, unknown phage receptor	This work
ΦN315tet	siphoviurs, unknown phage receptor	(Rohmer et al. 2022)

Supplemental table 7. List of Plasmids and Vectors

Plasmids	Description	Reference
pBASE6	tetracyclin inducible suicide mutagenesis plasmid	(Geiger et al. 2012)
pCG472	pBASE6 for generation of USA300 JE2 Δ*tagO*	This work

Supplemental table 8. List of oligonucleotides.

Primer	extentionSEQUENCE	Use
tagOGibMutfor	ctcatcgcagtgcagcggAATAATGATA GCACATCATTTTGT	generation of USA300 JE2 Δ*tagO*
tagOGibMutrev	ccgggtaccgagctccggGCATTTATTG CTGCAATAAA	generation of USA300 JE2 Δ*tagO*
tagOlinkMutfor	aggtgaataaGGAATGAAAGCATAG CTGTATGGG	generation of USA300 JE2 Δ*tagO*
tagOlinkMutrev	ctttcattccTTATTCACCTTCATCGA TATT	generation of USA300 JE2 Δ*tagO*
tagocontrolfor	TCCTTTAATTGACCACTAGCT	control PCR
tagocontrolrev	AAGTACACGTTTATGGCAGT	control PCR

Supplemental table 9. List of eukaryotic cells.

Cell lines	Description	Company
HUVECs	primary Human Umbilical Vein Endothelial Cells	PromoCell (C-12203)

Acknowledgement:

This work was funded by Deutsche Forschungsgemeinschaft, Spp2330 to CWo (Project 464612409), SFB766, Projectnummer 32152271 to CWo and CWe and by infrastructural funding from the Deutsche Forschungsgemeinschaft (DFG), Cluster of Excellence EXC 2124 “Controlling Microbes to Fight Infections” (Project 390838134). Personal Funding was awarded to EL in form of a Promotionsstipendium nach dem Landesgraduiertenförderungsgesetz. We thank Cosima Hirt and Dorothee Kretschmer for assistance and scientific discussion regarding the animal experiments. We thank Simon Heilbronner for help with the ethics proposal and Libera Lo Presti for scientific discussions and editing of the manuscript.

References

Baddour, L. M., C. Lowrance, A. Albus, J. H. Lowrance, S. K. Anderson, and J. C. Lee. 1992. '*Staphylococcus aureus* microcapsule expression attenuates bacterial virulence in a rat model of experimental endocarditis', *J Infect Dis*, 165: 749-53.

Bae, T., and O. Schneewind. 2006. 'Allelic replacement in Staphylococcus aureus with inducible counter-selection', *Plasmid*, 55: 58-63.

Baur, S., M. Rautenberg, M. Faulstich, T. Grau, Y. Severin, C. Unger, W. H. Hoffmann, T. Rudel, I. B. Autenrieth, and C. Weidenmaier. 2014. 'A nasal epithelial receptor for Staphylococcus aureus WTA governs adhesion to epithelial cells and modulates nasal colonization', *PLoS Pathog*, 10: e1004089.

Bertozzi Silva, J., Z. Storms, and D. Sauvageau. 2016. 'Host receptors for bacteriophage adsorption', *FEMS Microbiol Lett*, 363.

Boyle-Vavra, S., X. Li, M. T. Alam, T. D. Read, J. Sieth, C. Cywes-Bentley, G. Dobbins, M. Z. David, N. Kumar, S. J. Eells, L. G. Miller, D. J. Boxrud, H. F. Chambers, R. Lynfield, J. C. Lee, and R. S. Daum. 2015. 'USA300 and USA500 clonal lineages of

Staphylococcus aureus do not produce a capsular polysaccharide due to conserved mutations in the cap5 locus', *MBio*, 6.

Bremell, T., S. Lange, L. Svensson, E. Jennische, K. Gröndahl, H. Carlsten, and A. Tarkowski. 1990. 'Outbreak of spontaneous staphylococcal arthritis and osteitis in mice', *Arthritis Rheum*, 33: 1739-44.

Brown, Stephanie.; Santa Maria, John P. Jr.; Walker, Suzanne. 2013. 'Wall teichoic acids of gram-positive bacteria', *Annual review of microbiology*, 67: 313-36.

Chan, Y. G., M. B. Frankel, V. Dengler, O. Schneewind, and D. Missiakas. 2013. 'Staphylococcus aureus mutants lacking the LytR-CpsA-Psr family of enzymes release cell wall teichoic acids into the extracellular medium', *J Bacteriol*, 195: 4650-9.

Chan, Y. G., H. K. Kim, O. Schneewind, and D. Missiakas. 2014. 'The capsular polysaccharide of Staphylococcus aureus is attached to peptidoglycan by the LytR-CpsA-Psr (LCP) family of enzymes', *J Biol Chem*, 289: 15680-90.

Chen, P. S. , T. Y. Toribara, and Huber Warner. 1965. 'Microdetermination of Phosphorus', *Analytical Chemistry*, 28, NO. 11.

Cunnion, K. M., J. C. Lee, and M. M. Frank. 2001. 'Capsule production and growth phase influence binding of complement to Staphylococcus aureus', *Infect Immun*, 69: 6796-803.

Di Carluccio, C., P. Soriano-Maldonado, F. Berni, C. J. C. de Haas, A. R. Temming, A. Hendriks, S. Ali, A. Molinaro, A. Silipo, N. M. van Sorge, M. J. van Raaij, J. D. C. Codee, and R. Marchetti. 2022. 'Antibody Recognition of Different Staphylococcus aureus Wall Teichoic Acid Glycoforms', *ACS Cent Sci*, 8: 1383-92.

Driguez, Pierre-Alexandre, Nathalie Guillo, Bachra Rokbi, Noëlle Mistretta, and Philippe Talaga. 2017. "Immunogenic Compositions Against S. aureus." In. WO: Sanofi Pasteur.

Du, X., J. Larsen, M. Li, A. Walter, C. Slavetinsky, A. Both, P. M. Sanchez Carballo, M. Stegger, E. Lehmann, Y. Liu, J. Liu, J. Slavetinsky, K. A. Duda, B. Krismer, S. Heilbronner, C. Weidenmaier, C. Mayer, H. Rohde, V. Winstel, and A. Peschel. 2021. 'Staphylococcus epidermidis clones express Staphylococcus aureus-type wall teichoic acid to shift from a commensal to pathogen lifestyle', *Nat Microbiol*, 6: 757-68.

Duthie, E. S., and L. L. Lorenz. 1952. 'Staphylococcal coagulase; mode of action and antigenicity', *J Gen Microbiol*, 6: 95-107.

Fournier, Jean. Michel.; Vann, Willie. F.; and Karakawa, Walter. W. 1984. 'Purification and Characterization of Staphylococcus aureus Type 8 Capsular Polysaccharide', *Infect Immun*.

Geiger, T., P. Francois, M. Liebeke, M. Fraunholz, C. Goerke, B. Krismer, J. Schrenzel, M. Lalk, and C. Wolz. 2012. 'The stringent response of Staphylococcus aureus and its impact on survival after phagocytosis through the induction of intracellular PSMs expression', *PLoS Pathog*, 8: e1003016.

George, S. E., T. Nguyen, T. Geiger, C. Weidenmaier, J. C. Lee, J. Liese, and C. Wolz. 2015. 'Phenotypic heterogeneity and temporal expression of the capsular polysaccharide in Staphylococcus aureus', *Mol Microbiol*, 98: 1073-88.

Grundmeier, M., M. Hussain, P. Becker, C. Heilmann, G. Peters, and B. Sinha. 2004. 'Truncation of fibronectin-binding proteins in Staphylococcus aureus strain Newman leads to deficient adherence and host cell invasion due to loss of the cell wall anchor function', *Infect Immun*, 72: 7155-63.

Hendriks, A., R. van Dalen, S. Ali, D. Gerlach, G. A. van der Marel, F. F. Fuchsberger, P. C. Aerts, C. J. C. de Haas, A. Peschel, C. Rademacher, J. A. G. van Strijp, J. D. C. Codee, and N. M. van Sorge. 2021. 'Impact of Glycan Linkage to Staphylococcus aureus Wall Teichoic Acid on Langerin Recognition and Langerhans Cell Activation', *ACS Infect Dis*, 7: 624-35.

Herbert, S., D. Worlitzsch, B. Dassy, A. Boutonnier, J. M. Fournier, G. Bellon, A. Dalhoff, and G. Döring. 1997. 'Regulation of *Staphylococcus aureus* capsular polysaccharide type 5: CO2 inhibition *in vitro* and *in vivo*', *J Infect Dis*, 176: 431-38.

Ingmer, H., D. Gerlach, and C. Wolz. 2019. 'Temperate Phages of Staphylococcus aureus', *Microbiol Spectr*, 7.

Jansen, K. U., D. Q. Girgenti, I. L. Scully, and A. S. Anderson. 2013. 'Vaccine review: "Staphyloccocus aureus vaccines: problems and prospects"', *Vaccine*, 31: 2723-30.

Keinhörster, D., A. Salzer, A. Duque-Jaramillo, S. E. George, G. Marincola, J. C. Lee, C. Weidenmaier, and C. Wolz. 2019. 'Revisiting the regulation of the capsular polysaccharide biosynthesis gene cluster in Staphylococcus aureus', *Mol Microbiol*, 112: 1083-99.

Keinhörster, Daniela, Shilpa Elizabeth George, Christopher Weidenmaier, and Christiane Wolz. 2019. 'Function and regulation of Staphylococcus aureus wall teichoic acids and capsular polysaccharides', *Int J Med Microbiol*: 151333.

Key, Felix M., Veda D. Khadka, Carolina Romo-González, Kimbria J. Blake, Liwen Deng, Tucker C. Lynn, Jean C. Lee, Isaac M. Chiu, Maria Teresa García-Romero, and Tami D. Lieberman. 2022. 'On-person adaptive evolution of Staphylococcus aureus during atopic dermatitis increases disease severity'.

Kreiswirth, B. N., S. Lofdahl, M. J. Betley, M. O'Reilly, P. M. Schlievert, M. S. Bergdoll, and R. P. Novick. 1983. 'The toxic shock syndrome exotoxin structural gene is not detectably transmitted by a prophage', *Nature*, 305: 709-12.

Kropinski, A. M., A. Mazzocco, T. E. Waddell, E. Lingohr, and R. P. Johnson. 2009. 'Enumeration of bacteriophages by double agar overlay plaque assay', *Methods Mol Biol*, 501: 69-76.

Kuipers, A., D. A. C. Stapels, L. T. Weerwind, Y. P. Ko, M. Ruyken, J. C. Lee, K. P. M. van Kessel, and S. H. M. Rooijakkers. 2016. 'The Staphylococcus aureus polysaccharide capsule and Efb-dependent fibrinogen shield act in concert to protect against phagocytosis', *Microbiology (Reading)*, 162: 1185-94.

Lattar, S. M., L. P. Tuchscherr, R. L. Caccuri, D. Centron, K. Becker, C. A. Alonso, C. Barberis, G. Miranda, F. R. Buzzola, C. von Eiff, and D. O. Sordelli. 2009. 'Capsule expression and genotypic differences among *Staphylococcus aureus* isolates from patients with chronic or acute osteomyelitis', *Infect Immun*, 77: 1968-75.

Lehar, S. M., T. Pillow, M. Xu, L. Staben, K. K. Kajihara, R. Vandlen, L. DePalatis, H. Raab, W. L. Hazenbos, J. H. Morisaki, J. Kim, S. Park, M. Darwish, B. C. Lee, H. Hernandez, K. M. Loyet, P. Lupardus, R. Fong, D. Yan, C. Chalouni, E. Luis, Y. Khalfin, E. Plise, J. Cheong, J. P. Lyssikatos, M. Strandh, K. Koefoed, P. S. Andersen, J. A. Flygare, M. Wah Tan, E. J. Brown, and S. Mariathasan. 2015. 'Novel antibody-antibiotic conjugate eliminates intracellular S. aureus', *Nature*, 527: 323-8.

Leprince, A., and J. Mahillon. 2023. 'Phage Adsorption to Gram-Positive Bacteria', *Viruses*, 15.

Mainiero, M., C. Goerke, T. Geiger, C. Gonser, S. Herbert, and C. Wolz. 2010. 'Differential target gene activation by the Staphylococcus aureus two-component system saeRS', *J Bacteriol*, 192: 613-23.

McLoughlin, R. M., R. M. Solinga, J. Rich, K. J. Zaleski, J. L. Cocchiaro, A. Risley, A. O. Tzianabos, and J. C. Lee. 2006. 'CD4+ T cells and CXC chemokines modulate the pathogenesis of *Staphylococcus aureus* wound infections', *Proc Natl Acad Sci U S A*, 103: 10408-13.

Mohamed, N., Y. Timofeyeva, D. Jamrozy, E. Rojas, L. Hao, N. C. Silmon de Monerri, J. Hawkins, G. Singh, B. Cai, P. Liberator, S. Sebastian, R. G. K. Donald, I. L. Scully, C. H. Jones, C. B. Creech, I. Thomsen, J. Parkhill, S. J. Peacock, K. U. Jansen, M. T. G. Holden, and A. S. Anderson. 2019. 'Molecular epidemiology and expression of capsular polysaccharides in Staphylococcus aureus clinical isolates in the United States', *PLoS One*, 14: e0208356.

Monk, I. R., I. M. Shah, M. Xu, M. W. Tan, and T. J. Foster. 2012. 'Transforming the untransformable: application of direct transformation to manipulate genetically Staphylococcus aureus and Staphylococcus epidermidis', *MBio*, 3.

Nanra, J. S., S. M. Buitrago, S. Crawford, J. Ng, P. S. Fink, J. Hawkins, I. L. Scully, L. K. McNeil, J. M. Aste-Amezaga, D. Cooper, K. U. Jansen, and A. S. Anderson. 2013. 'Capsular polysaccharides are an important immune evasion mechanism for Staphylococcus aureus', *Hum Vaccin Immunother*, 9: 480-7.

Negus, D., J. Burton, A. Sweed, R. Gryko, and P. W. Taylor. 2013. 'Poly-gamma-(D)-glutamic acid capsule interferes with lytic infection of Bacillus anthracis by B. anthracis-specific bacteriophages', *Appl Environ Microbiol*, 79: 714-7.

Nemeth, J., and J. C. Lee. 1995. 'Antibodies to capsular polysaccharides are not protective against experimental *Staphylococcus aureus* endocarditis', *Infect Immun*, 63: 375-80.

Nilsson, I. M., J. C. Lee, T. Bremell, C. Ryden, and A. Tarkowski. 1997. 'The role of staphylococcal polysaccharide microcapsule expression in septicemia and septic arthritis', *Infect Immun*, 65: 4216-21.

Nuxoll, Austin S., Steven M. Halouska, Marat R. Sadykov, Mark L. Hanke, Kenneth W. Bayles, Tammy Kielian, Robert Powers, and Paul D. Fey. 2012. 'CcpA Regulates Arginine Biosynthesis in Staphylococcus aureus through Repression of Proline Catabolism', *PLoS Pathog*, 8: e1003033.

O'Riordan, K., and J. C. Lee. 2004. 'Staphylococcus aureus capsular polysaccharides', *Clin Microbiol Rev*, 17: 218-34.

Peschel, A., M. Otto, R. W. Jack, H. Kalbacher, G. Jung, and F. Gotz. 1999. 'Inactivation of the dlt operon in Staphylococcus aureus confers sensitivity to defensins, protegrins, and other antimicrobial peptides', *J Biol Chem*, 274: 8405-10.

Pöhlmann-Dietze, P., M. Ulrich, K. B. Kiser, G. Doring, J. C. Lee, J. M. Fournier, K. Botzenhart, and C. Wolz. 2000. 'Adherence of Staphylococcus aureus to endothelial cells: influence of capsular polysaccharide, global regulator agr, and bacterial growth phase', *Infect Immun*, 68: 4865-71.

Portoles, M., K. B. Kiser, N. Bhasin, K. H. Chan, and J. C. Lee. 2001. 'Staphylococcus aureus Cap5O has UDP-ManNAc dehydrogenase activity and is essential for capsule expression', *Infect Immun*, 69: 917-23.

Risley, A. L., A. Loughman, C. Cywes-Bentley, T. J. Foster, and J. C. Lee. 2007. 'Capsular polysaccharide masks clumping factor A-mediated adherence of Staphylococcus aureus to fibrinogen and platelets', *J Infect Dis*, 196: 919-27.

Rohmer, Carina, Ronja Dobritz, Dilek Tuncbilek-Dere, Esther Lehmann, David Gerlach, Shilpa Elizabeth George, Taeok Bae, Kay Nieselt, and Christiane Wolz. 2022. 'Influence of Staphylococcus aureus Strain Background on Sa3int Phage Life Cycle Switches', *Viruses*, 14.

Sompolinsky, D., Z. Samra, W. W. Karakawa, W. F. Vann, R. Schneerson, and Z. Malik. 1985. 'Encapsulation and capsular types in isolates of Staphylococcus aureus from different sources and relationship to phage types', *J Clin Microbiol*, 22: 828-34.

Suligoy, C. M., R. E. Diaz, A. K. Gehrke, N. Ring, G. Yebra, J. Alves, M. I. Gomez, S. Wendler, J. R. Fitzgerald, L. Tuchscherr, B. Loffler, D. O. Sordelli, M. N. Llana, and F. R. Buzzola. 2020. 'Acapsular Staphylococcus aureus with a non-functional agr regains capsule expression after passage through the bloodstream in a bacteremia mouse model', *Sci Rep*, 10: 14108.

Tang, Y., L. N. Nielsen, A. Hvitved, J. K. Haaber, C. Wirtz, P. S. Andersen, J. Larsen, C. Wolz, and H. Ingmer. 2017. 'Commercial Biocides Induce Transfer of Prophage Phi13 from Human Strains of Staphylococcus aureus to Livestock CC398', *Front Microbiol*, 8: 2418.

Thakker, M., J. S. Park, V. Carey, and J. C. Lee. 1998. 'Staphylococcus aureus serotype 5 capsular polysaccharide is antiphagocytic and enhances bacterial virulence in a murine bacteremia model', *Infect Immun*, 66: 5183-9.

Tuchscherr, L., B. Loffler, F. R. Buzzola, and D. O. Sordelli. 2010. 'Staphylococcus aureus adaptation to the host and persistence: role of loss of capsular polysaccharide expression', *Future Microbiol*, 5: 1823-32.

Tuchscherr, L. P., F. R. Buzzola, L. P. Alvarez, R. L. Caccuri, J. C. Lee, and D. O. Sordelli. 2005. 'Capsule-negative *Staphylococcus aureus* induces chronic experimental mastitis in mice', *Infect Immun*, 73: 7932-37.

van Dalen, R.; Peschel, A.; van Sorge, N. M. 2020. 'Wall Teichoic Acid in Staphylococcus aureus Host Interaction', *Trends Microbiol*, 28: 985-98.

van Dalen, Rob, Jacinto S. De La Cruz Diaz, Matevž Rumpret, Felix F. Fuchsberger, Nienke H. van Teijlingen, Jonas Hanske, Christoph Rademacher, Teunis B. H. Geijtenbeek, Jos A. G. van Strijp, Christopher Weidenmaier, Andreas Peschel, Daniel H. Kaplan, and Nina M. van Sorge. 2019. 'Langerhans Cells Sense Staphylococcus aureus Wall Teichoic Acid through Langerin To Induce Inflammatory Responses', *MBio*, 10: e00330-19.

Wanner, S.; Schade, J.; Keinhorster, D.; Weller, N.; George, S. E.; Kull, L.; Bauer, J.; Grau, T.; Winstel, V.; Stoy, H.; Kretschmer, D.; Kolata, J.; Wolz, C.; Broker, B. M.; Weidenmaier, C. 2017. 'Wall teichoic acids mediate increased virulence in Staphylococcus aureus', *Nat Microbiol*, 2: 16257.

Watts, A., D. Ke, Q. Wang, A. Pillay, A. Nicholson-Weller, and J. C. Lee. 2005. 'Staphylococcus aureus strains that express serotype 5 or serotype 8 capsular polysaccharides differ in virulence', *Infect Immun*, 73: 3502-11.

Weidenmaier, C., and J. C. Lee. 2016. 'Structure and Function of Surface Polysaccharides of Staphylococcus aureus', *Curr Top Microbiol Immunol*.

Weidenmaier, C., and A. Peschel. 2008. 'Teichoic acids and related cell-wall glycopolymers in Gram-positive physiology and host interactions', *Nat Rev Microbiol*, 6: 276-87.

Weidenmaier, C., A. Peschel, Y. Q. Xiong, S. A. Kristian, K. Dietz, M. R. Yeaman, and A. S. Bayer. 2005. 'Lack of wall teichoic acids in Staphylococcus aureus leads to reduced interactions with endothelial cells and to attenuated virulence in a rabbit model of endocarditis', *J Infect Dis*, 191: 1771-7.

Wilkinson, B. J., and K. M. Holmes. 1979. 'Staphylococcus aureus cell surface: capsule as a barrier to bacteriophage adsorption', *Infect Immun*, 23: 549-52.

Witte, W. 1975. 'Capsule formation in Staphylococcus aureus as a reason for nontypability by phages (author's transl)', *Zentralblatt fur Bakteriologie, Parasitenkunde, Infektionskrankheiten und Hygiene. Erste Abteilung Originale. Reihe A: Medizinische Mikrobiologie und Parasitologie*, 233: 447-51.

Xia, G., R. M. Corrigan, V. Winstel, C. Goerke, A. Grundling, and A. Peschel. 2011. 'Wall teichoic Acid-dependent adsorption of staphylococcal siphovirus and myovirus', *J Bacteriol*, 193: 4006-9.

Conclusion and Implications

As discussed in this thesis, *S. aureus* poses a significant threat to human health due to a high prevalence in the human and animal populations, possession of a broad spectrum of virulence factors, and a rapid ability to develop multi drug resistance (Wojcik-Bojek, Rozalska, and Sadowska 2022). The adaptability of *S. aureus* and its potential to switch to a pathogenic lifestyle, hinges upon its capacity to undermine effective immunity and its capacity to quickly acquire virulence genes. Counterintuitively, this might in part be due to its “commensal” lifestyle. Recent studies strongly suggest that prior exposures to *S. aureus* by colonization jeopardize immune responses to many staphylococcal antigens, thereby causing the ineffectiveness of *S. aureus* vaccines in humans (Clegg et al. 2021). Combined with the notion that a significant proportion of the human population is colonized by *S. aureus*, and virtually everyone has been exposed to it during their lifetimes, this pre-exposure represents a huge caveat in vaccine design and testing of vaccine candidates.

The cell wall of *S. aureus* plays a central role in the aforementioned immune evasion strategies and in survival in hostile environments. It is comprised predominantly of glycopolymers and glycosylated molecules, which play important roles not only in the makeup but also in the functionalization of the cell wall (Weidenmaier and Lee 2016; van Dalen 2020). In this thesis, I have highlighted multiple roles of *S. aureus* wall teichoic acids (WTA) and capsule polysaccharide (CP) for *S. aureus* virulence. However, our understanding of the molecular interactions between these glycans (e.g. their regulation, spatial organization, secondary modification) and their interaction with the environment is still incomplete.

While the regulation of WTA biosynthesis is only rudimentarily understood, it is known that WTA chain length is upregulated (via suppression of *tarK* by agr) with CP expression in stationary phase (Keinhörster, George, et al. 2019). Thus, even though the relative WTA quantity is unaffected by the CP expression status, WTA regulation (especially in conjunction with PG and CP regulation) and direct molecular WTA-CP interactions would need to be further elucidated to draw final conclusions.

While it is widely accepted that spatiotemporal separation of intracellular processes are crucial for all physiological functions and that compartmentalization of the bacterial membrane is essential for membrane protein function, our understanding of the bacterial cell wall is a rather limited. For long, the *S. aureus* cell envelop structure was depicted with CP forming a shield-like structure on top of the PG and other cell wall structures, and with the WTA protruding far into the extracellular space. In *S. aureus*, neither CP nor WTA are crosslinked, resulting in both presumably sticking outward from their anchoring point in the PG (van Dalen 2020). The basic findings of chapter IV concerning the interaction of *S. aureus* CP and WTA, highlight a need to rethink our understanding of cell envelop structure and functionalization.

Yet, the tools to study glycan-glycan interaction are very limited. Classical genetic approaches are unsuitable for deciphering glycan composition and expression (Burkholz, Quackenbush, and Bojar 2021), as they are synthesized and modified by a multitude of biosynthetic enzymes, rather than directly encoded (Drula et al. 2022). A better understanding of cell wall composition of and the interplay between these mayor cell wall components will help to understand the impact that these glycans have on the modulation of bacterial-host interactions. Given the central role that these SCWGs hold in virulence, fundamental insights into bacterial glycobiology are key, outlook and challenge for the future in order to combat *S. aureus*.

Burkholz, R., J. Quackenbush, and D. Bojar. 2021. 'Using graph convolutional neural networks to learn a representation for glycans', *Cell Rep*, 35: 109251.

Clegg, J., E. Soldaini, R. M. McLoughlin, S. Rittenhouse, F. Bagnoli, and S. Phogat. 2021. 'Staphylococcus aureus Vaccine Research and Development: The Past, Present and Future, Including Novel Therapeutic Strategies', *Front Immunol*, 12: 705360.

Drula, E., M. L. Garron, S. Dogan, V. Lombard, B. Henrissat, and N. Terrapon. 2022. 'The carbohydrate-active enzyme database: functions and literature', *Nucleic Acids Res*, 50: D571-D77.

Keinhörster, Daniela, Shilpa Elizabeth George, Christopher Weidenmaier, and Christiane Wolz. 2019. 'Function and regulation of Staphylococcus aureus wall teichoic acids and capsular polysaccharides', *Int J Med Microbiol*: 151333.

van Dalen, R.; Peschel, A.; van Sorge, N. M. 2020. 'Wall Teichoic Acid in Staphylococcus aureus Host Interaction', *Trends Microbiol*, 28: 985-98.

Weidenmaier, C., and J. C. Lee. 2016. 'Structure and Function of Surface Polysaccharides of Staphylococcus aureus', *Curr Top Microbiol Immunol*.

Wojcik-Bojek, U., B. Rozalska, and B. Sadowska. 2022. 'Staphylococcus aureus-A Known Opponent against Host Defense Mechanisms and Vaccine Development-Do We Still Have a Chance to Win?', *Int J Mol Sci*, 23.

CURRICULUM VITAE

The curriculum vitae was deleted in the online version of this publication out of Data security concerns.

Acknowledgements

An dieser Stelle würde ich gerne meinen Dank ausdrücken.
An **Prof. Dr. Andreas Peschel**, danke für die Möglichkeit meine Arbeit in deiner Gruppe zu Ende zu bringen. Es war ein ehr unkonventioneller Weg. Danke für deine Betreuung und das Erstellen des Erstgutachtens. Auch danke ich **Prof. Dr. Friedrich Götz**, für das Erstellen des Zweitgutachtens und angeregte Diskussionen in den Seminaren. Bei **Prof. Dr. Christiane Wolz** bedanke ich mich für die jahrelange Betreuung. Danke, dass ich Teil deiner wundervollen Arbeitsgruppe sein durfte. Danke auch an **Dr. Christopher Weidenmeier**. Du hast mich bestärkt diesen Weg zu gehen. Bei **Dr. Dorothee Kretschmer** bedanke ich mich für die Unterstützung bei den Tierversuchen. Danke für deine Zeit und Hilfe.

Special thanks go to **Shilpa** I learned so much from you. Thank you for your honesty when I needed a reality check and for all the G'n'T-talk-times. Liebe **Jessi** danke für deine Unterstützung, dass ich mich immer melden darf und die „Think-Tanks" mit angetauter Donauwelle und Bier/Sekt. 😊

I want to thank everyone who went with me through the turbulences along my way from **AG Weidenmeier** via **AG Wolz** to **AG Peschel**.
Tausend Dank an die unglaublichen Menschen im Institut! **Dr. Monika Schütz** und **Dr. Erwin Bohn**, danke für eure offenen Ohren. **Udo, Ulli** und **Stefan**, ohne euch wäre ich zwischen den ganzen Laborumzügen und Päckchen in die Staaten untergegangen. Ihr seid toll!
Danke an meine vielen Büro- und Labornachbarn. **Liam**, **Jan**, **Malte** (because you care), **Karo**, **Fabi**, **Ole**, **Andi, Frau Bürgermeister…** ohne euch wäre die Zeit nicht halb so schön gewesen.
Ich bedanke mich bei meinen ehemaligen Studenten. **Laura**, **Jens**, **Lea** und insbesondere auch bei **Valentin** (du wirst das rocken!) und **Lisa** (du warst die beste Hilfe die man sich wünschen kann!).
Janina, **Andrea** und **Ronja** danke für die Diskussionen und eure Unterstützung. **Naty** und **Vitty** danke, dass ich mir eure goldenen Hände ausleihen durfte. **Petra** und **Carina**: F**k it yes! Ihr seid einfach die Besten! Danke, dass ich euch meine Freunde nennen darf! Danke, dass ihr immer hinter mir und an meiner Seite steht; mal mit Rat und Tat, mal mir verrückten Ideen und ernsten Worten. Ihr seid unglaublich! Carina mein Maus-Maus danke, dass du an mich glaubst! Zu erklären, was mir das bedeutet wäre Stoff für eine weitere Doktorarbeit!
Cosima, **Gerti**, **Regine**, **Dani** und **Gisela** auf euch ist halt verlass! Ich habe euch oft viel Spontanität abverlangt danke für eure Zeit und euer offenes Ohr. Ohne Leute wie euch läuft der Laden nicht.

ACKNOWLEDGEMENTS

Ich danke **Janna** (danke für deine Kunst! „A dirty mind is a pleasure for everyone”), **Chris S.** (danke für deine Zeit, die vielen Diskussionen, Drinks und all die guten Ideen), **Darya** (danke für deine Unterstützung! Fühl dich gedrückt!), **Lea**, **Angi**, **Lara**, **Christian**, **Marco**, **Janna**, **Janes**, **Benni**, **Sofia**, **Leonie**,… Es war schön mit euch zu arbeiten.
„I was takin' a walk the other day and I seen a man, an intriguing man in the cafeteria. I decide to go over and get to know him, you know? "Hello, mister, Is Dr. **Jeff**rey John Power your real name?” He replied "Oh yes, you want to get to know me, let’s grab a drink" Is it ~~wickedness?~~ Bingo!” Thank you for routing for me! Thanks for all the Wednesdays! I’m looking forward to many more to come!

Danke **Stefan**, danke **Marco**! „Es gibt Dinge, die man nicht gemeinsam erleben kann, ohne dass man Freundschaft schließt, und sich von Geiern in die Nase beißen zu lassen ist eine davon“.

Danke an meine Aca-Bi***es, **Olli**, **Vivi**, **Tanja**, **Barb**! Auf dass wir uns nie aus den Augen verlieren.

“New Kids in tha House”. Wirklich die beste Entscheidung bei euch einzuziehen! Danke für eure Unterstützung! You keept me sane! Tausend Knutschies gehen raus an **Oxi**, **Lisa**, **Felix** und **Anna**! Bester WG der Welt!

Ich danke **meiner Familie**, die an mich glaubt und meiner Herde. Ihr seid meine Wahlfamilie! **Marlene** die Bestefreundin, die man sich wünschen kann. **Lukas**, **Jonas**, **Edu**: für immer ein Package-deal! **Sarah**, **Leonie**, ich weiß nicht, wo ich richtig abgebogen bin um Menschen wie euch zu verdienen. **Tina** und **Tias**, danke für einen Platz im Paradies. Ich kann nicht in Worte fassen wieviel mir das bedeutet! Ihr seid die Besten!

Rob, now that this is over, I officially forgive you for stealing the PhD topic that should have been mine😉. Thank you for your input, your time and help. Thank you for having my back and believing in me. Thank you for all the adventures we had together (and the ones to come); And thank you especially for believing you could drive a car through a 50 cm deep puddle of water! Thank you for being my friend, my work-hubby, my partner. Ik hau van jau!